Field theory of reversible and active network formation

by

Stanard Mebwe Pachong

Dissertation presented for the degree of Doctor of Philosophy in the Faculty of Science at Stellenbosch University

Supervisor: Prof. Kristian Müller-Nedebock

December 2017

Declaration

By submitting this dissertation electronically, I declare that the entirety of the work contained therein is my own, original work, that I am the sole author thereof (save to the extent explicitly otherwise stated), that reproduction and publication thereof by Stellenbosch University will not infringe any third party rights and that I have not previously in its entirety or in part submitted it for obtaining any qualification.

Date: December 2017

Abstract

Field theory of reversible and active network formation

S. Mebwe

Department of Physics,
Stellenbosch University,
Private Bag X1, Matieland 7602, South Africa.

Dissertation: PhD

December 2016

This dissertation presents a statistical physics analysis of randomly cross-linked polymer networks with both reversible and permanent cross-links. The theory used here is adapted from the field theory elaborated by Edwards (1988) for the permanent network and later used for a reversibly associated network by Fantoni and Müller-Nedebock (2011). The field theory automatically ensures cross linking constraints, includes the reversible link and enables the computation of the average numbers and fluctuations of cross-links in the network. The average density of cross-linkers is calculated. This contains statistical information about the behaviour of individual polymer chains and cross-linkers inside the network. For active cross-linkers moving in a preferential direction along filaments we show that the polarity of the polymer chains influences the elastic properties of the network. The response of the network under a small deformation is studied. We make use of the replica trick to calculate the free energy over the possible disorder in the system. We show that, when adding reversible cross linkers into a permanent polymer network, these make the network become softer.

We study a special case of such networks to understand the biological network called "the contractile ring". We implement the Random Phase Approximation (RPA) along with a one dimensional Langevin dynamics simulation to investigate the stability of the ring. We calculate the explicit expression for the density-density correlation function which can be tested experimentally. Results show that the motor proteins pull and push the chains leading to a constant overtaking of the chains within the ring. It turns out that the energy generated by the network to maintain the chains connected is the one responsible for the contractile behaviour of the ring. Specifically, these observations

only hold in the case of a finite periodic ring. The present consideration suggests that even in case of low ATP, the ring still contracts. The simulation and the analytical results confirm that the force generated by the motor protein sustains the polarisation current and therefore maintains the stability of the ring. On the other hand, the force generated to maintain the integrity of the ring render the ring unstable and interrupts the current flowing through it. The change of phase of the chain distribution within the ring therefore occurs due to the interplay of the two forces mentioned above.

Uittreksel

Field theory of reversible and active network formation

S. Mebwe

Fisika Departement,
Stellenbosch Universiteit,
Privaatsak X1, Matieland 7602, Suid Afrika.

Proefskrif: PhD

Desember 2016

Hierdie proefskrif is 'n aanbieding van die statistiese fisika van 'n polimeernetwerk met lukraak geplaasde kruisverbindingspunte, wat beide permanent en tydelik is. Die teorie waarvan hier gebruik gemaak word is 'n aanpassing van Edwards (1988) se veldeteoretiese formulering vir die permanente netwerk en wat later deur Fantoni en Müller-Nedebock (2011) aangewend is vir omkeerbaar geassosieerde netwerke. Die veldeteorie verseker outomaties dat die verbindings bevredig word, en sluit nie-permanente knooppunte in en laat ook die berekening van gemiddelde getalle en fluktuasies van knooppunte in die netwerk toe. Die gemiddelde digtheid van knooppunte word bereken. Dit bevat statistiese inligting omtrent die gedrag van polimeerkettings en knooppunte binnekant die netwerk. Vir aktiewe knooppunte, wat in 'n voorkeurrigting op filamente beweeg, toon ons aan dat die polariteit van die polimeerkettings die elastiese eienskappe van die netwerk beïnvloed. Die gedrag van die netwerk onder klein vervorming word ondersoek. Ons maak gebruik van die replikametode om die vrye-energie te bereken, wat gemiddel word oor die wanorde in die stelsel. Ons toon aan dat die byvoeging van nie-permanente knooppunte in 'n permanente netwerk daartoe lei dat die netwerk sagter word.

Ons ondersoek die spesiale geval van sulke netwerke om die biologiese netwerk, die sogenaamde kontraktiele ring, te verstaan. Ons maak gebruik van 'n kwadratiese kollektiewe koördinaatransformasie ("RPA") tesame met eendimensionele Langevin-dinamika simulasies om die stabiliteit van die ring te ondersoek. Ons bereken eksplisiet die digtheid-digtheid korrelasiefunksie wat eksperimenteel getoets kan word. Die resultate dui daarop dat die masjiene die filamente trek en stoot sodat filamente die hele tyd vir mekaar verbysteek. Die

energie wat deur die netwerk gestoor word, is verantwoordelik vir die saamtrekking in die ring. Spesifiek geld hierdie gevolgtrekkings vir 'n eindige ring, wat periodies verloop. Die ondersoek dui aan dat, selfs in die geval van lae ATP-konsentrasies, die ring steeds sal saamtrek. Beide simulasies en analitiese resultate bevestig dat die krag wat deur die proteïenmasjientjies gegenereer word, die polarisasiestroom in die ring onderhou en dus ook vir die stabiliteit van die ring verantwoordelik is. Verder is die krag, wat die samehangendheid van die ring produseer, verantwoordelik daarvoor dat in sommige gevalle die ring onstabiel raak en die polarisasiestroom daarin onderbreek word. Die faseoorgang van die verdeling van kettings binne die ring is dus 'n gevolg van beide bogenoemde kragte.

Acknowledgements

I would like to express my sincere gratitude to my supervisor Professor Kristian K. Müller-Nedebock For his patience, guidance, support and encouragement during the completion of this project.

I would like to say thank you to the financial sponsor: the Organisation for Women in Science for the Developing world (OWSD) without whom this work would have not be possible. To the African Institute for Mathematical Science (AIMS) Senegal for given me the opportunity to test my limits and for the help and opportunities they have provided me.

A big thank you goes to my AIMS project's supervisor Professor Jean-Francois Joanny and to Doctor Rhoda Hawkins for having introduced me to the field of biophysics. My gratitude goes to Professor Mane-Mane Jeannot for his help and support, for introducing me to research and supporting me.

A special thank you to my office mates, J. Meylahn and Doctor Mohau Mateyisi for their interesting physics discussion. To Doctor Anicia Mateyisi, for her constant help and moral support. To my friend and office mate Florence Azote, thank you for the interesting discussions and the support.

A big gratitude goes to my parents and family whom have always be by my side, for their love, prayers and support a big thank you. To my family "Ami BU" a big thank for all your love and support for all these years.

Without you God, this work would have not be possible and all the thanks are not enough to express my gratitude.

Dedications

To my parents, for their unconditional love and support. For all you have done for me: A big Thank You!

Contents

Declaration i

Abstract ii

Uittreksel iv

Acknowledgements vi

Dedications vii

Contents viii

List of Figures xi

I Introduction and background 1

1 Introduction and motivations 2

2 General background 7
2.1 Introduction 7
2.2 Basic concepts of polymer theory 7
2.3 Network formed by polymer chains: Edwards formulation 12
2.4 Example of biopolymer network: The Contractile ring 17
2.5 Conclusion 20

II Polymer network formation using field theory 22

3 Polymer network with movable and permanent cross-link 23
3.1 Introduction 23
3.2 Cross-linkage of Gaussian chains 24
3.3 Model description 28
3.4 Saddle point approximation 35
3.5 Field theory approach for network deformation 39

3.6 Conclusion . . . 45

4 Slipping link in a permanent network of polar chains 47
4.1 Introduction . . . 47
4.2 Model description . . . 48
4.3 Reversible cross-link as slipping ring . . . 49
4.4 Reversible link as motor heads attached by a spring . . . 52
4.5 Conclusion . . . 58

III Natural active network: Example of the contractile ring 59

5 Collective dynamics of the filaments inside an actomyosin network 60
5.1 Introduction . . . 60
5.2 Linear model describing the contractile ring . . . 61
5.3 The formalism . . . 68
5.4 The RPA results . . . 76
5.5 Conclusion . . . 81

6 The contractile ring model 83
6.1 Introduction . . . 83
6.2 The periodic ring model . . . 84
6.3 Correlation function . . . 86
6.4 Ring contraction . . . 87
6.5 Effective single chain dynamics: Investigation of the drift velocity 89
6.6 Polarisation current density . . . 94
6.7 Numerical simulation . . . 98
6.8 Conclusion . . . 105

IV Summary and outlook 106

7 Summary and outlook 107

Appendices 110

A Details for calculations in chapters 3 and 4 111
A.1 Solve the saddle point (SPA) equations calculation . . . 111
A.2 Calculate the density fluctuation using the generating functional method . . . 113
A.3 Details of calculation on the Network deformation . . . 115

B Details calculation on chapters 5 and 6 119

B.1 Introduction of collective variables 119
B.2 Random Phase Approximation(RPA) 125
B.3 Effective chain dynamics calculation 138

List of References **144**

List of Figures

2.1 Self avoiding chain 9
2.2 Self-consistence method: The many chains system is simplified to a single chain inside an external field created by the other chains. . 12
2.3 The four main steps of the mitosis. The cytokinesis which is the final stage of the physical division of the cell overlaps with the anaphase and telophase. The cytokinesis may start at either anaphase or telophase, depending on the cell, and it finishes shortly after the telophase process. 18

3.1 (a):The figure presents two strands of polymer chains. On the chain (1), the labels r_0 and r_1 stand for the starting end of the chain and the finishing end of the chain. x is the spatial position along the chain where the reversible cross-linker can be anchored. The total length of the chain(1) is L as well as for the chain(2). s and $L-s$ represent the distances from r_0 to the position x and from the position x to the final end of the polymer chain r_1 respectively. The same reasoning is made with the chain(2). ψ is the field placed at x and X on chain(1) and (2), respectively. (b): the cross-link of the two chains imposes the same position in space so that $\psi(r(s)) = \psi(R(S)) = \psi(x)$ 25
3.2 Reversible cross-linker made of two available seats. 28
3.3 (a): the passive cross-linker agent with functionality 3; (b): cross-link of chains (1) and (2) by the permanent (at the ends) and the reversible cross-linker along the chains. 30
3.4 $g = G(r - r(s), s)$ and $g' = G(r(s) - r', L - s)$ are used as the shorthand notation for the Green's functions, $r = r_0 = r(s_0)$ and $r' = r_L = r(s_L)$.s is the arc length of the chain, N is the number of polymer chains. Network Formation: (a)Polymeric chain. (b) Permanent cross-linker and (c) Reversible cross-linker assumed to be represented by a spring attached at each motor head. The combination of all those three components gives a network where the reversible and permanent cross-linker are seated along and at the ends of the chains respectively. 32

3.5 Example of network form with 4, 3 and 6 permanent, reversible cross-linkers and chains respectively. 34
3.6 Simple affine deformation of a network with topology m. We distinguish the o^{th} (undeformed) and the other n (deformed) replicas. The permanent (in black cross) and the reversible (blues dots) cross-linkers. $R_\varsigma = r$ is the spacial position of the permanent cross-link number ς. 40

4.1 Ring-model of network: The fields ϕ and ψ represent the passive and active cross-linkers. This latter linker is free to move toward the $(+)$ end of the chains. $r(s)$ and $R(S)$ are, respectively, the label of the chain (1) and the chain (2). $r_0 = r(s = 0)$, $r_L = r(s = L)$,$R_0 = R(S = 0)$,$R_L = R(S = L)$. $x = r(s)$ and $X = R(S)$ are the spacial positions of the motor head along the chain(1) and chain(2) with the arc lengths s and S respectively. 49
4.2 The field ϕ and ψ are for passive and active cross-linkers. $r(s)$ and $R(S)$ are respectively the positions labelled on the chain (1) and (2). $x = r(s)$ and $X = R(s)$ are the spacial positions of the motor head along the chains with s and S the arc length of each chain. The motor heads are not in the same position along the chain ie $(r(s) \neq R(S))$. $(+)$ and $(-)$ indicate the polarity orientation of the polymer chain. 53

5.1 Contractile ring as a linear periodic system. d is the width of the ring, $L = 2\,\pi\,R$ (R is the radius of the ring) is the total length of the ring, it is simply the contour area length of the ring if we suppose that the linear ring model is the ring that have been opened. 60
5.2 The motor head moves toward the $(+)$ end of the chain making the chain slide moving toward the $(-)$ end direction of the chain. (i): Parallel filaments Bundle network. (ii): Anti-parallel with their $(-)$ ends close to each other. The chains move closer to one another, the overlap distance between them increases and more motor is recruited to fit the empty space between the chains and then lead to the contraction behaviour. (iii): Anti-parallel with their $(+)$ ends close to each other. The chains repel each other leading the expansion the system. 62
5.3 Prediction of the average density of the motor head in antiparallel chains system. 63
5.4 Density-density correlation function plotted for the parameters values: $\lambda = 1, l = 2.5, n_0 = 10, \gamma = 0.9, f = 0.1, \epsilon = 0.1$. The graph shows that the peak shrinks toward the small ω direction. 77

5.5 Correlation function plotted for the parameters values: $\lambda = 1, l = 2.5, n_0 = 10, \gamma = 0.9, f = 0.1, \epsilon = 0.1$ and for different values of the frequency $\omega = 0.1, 0.5, 1$ from top to bottom respectively. The maximal peak is observed at smaller frequency value. 78
5.6 Dependence of the density-density correlation function for $\omega = 0.5$, the attractive force($\epsilon = -0.01$) and $l = 2.5, \lambda = 1, \gamma = 0.9, n_0 = 10$ and for different value of the active force $f = 0.01, 0.03, 0.04$ as indicated on the figure. 79
5.7 Plot of the correlation function dependence of the attractive networking force $\epsilon = -0.05, -0.06, -0.08$ with the other parameters $f = 0.01, \omega = 0.5, l = 2.5, \lambda = 1, \gamma = 0.9, n_0 = 10$. 80
5.8 Plot of the correlation function dependence of the networking force $\epsilon = 0.05, 0.06, 0.08$ when the sign of the networking force is swapped (from negative to positive value). The parameters are: $f = 0.01, \omega = 0.5, l = 2.5, \lambda = 1, \gamma = 0.9, n_0 = 10$. 80
5.9 Plot of the density-density correlation function equation (5.4) at different value of ϵ and f. The parameters are: $k = 0.1$, $\ell = 2.5$, $n_0 = 10$, $\gamma = 1$, $\lambda = 1$, $\omega = 0.5$. The critical values of ϵ and f must not be zero for the correlation function to keep its physical meaning. 81

6.1 The contractile ring. The green dots represent the motor myosin II. The blue and red arrows represent the actin filaments that are clockwise and anti-clockwise oriented respectively. 83
6.2 Total networking energy plotted against the radius of the ring with the parameters: $\lambda = \gamma = 1, n_0 = 10, f = 0, \epsilon = 1, N = 10, \omega = 0.5$. The plot shows that the energy increases with the radius of the ring. This means that the contraction of the ring is indeed due to the networking force. 88
6.3 Analytic polarisation current density. Parameters are: $f = 1, N = 20, L = 1, l = 0.2, \lambda = 1, \gamma = 1$. We observe a decrease of the current through the ring with the increase of the networking force. The critical value of the networking force is given in equation (6.46). ϵ_{cr} on the plot indicates where the plot starts changing phase. . . . 97
6.4 Trajectories of a sample of seven chains confined in a ring of circumference L. Parameters are: $N = 7, f = 0.1, \epsilon = 0.1, \lambda = 1, \gamma = 0.9, n_0 = 10, \ell = 0.2, L = 1.0$ The signs + and − in the legend represent the orientation of each chain. 100
6.5 Density-density length correlation function as a function of the 'bins' for dominant active force (red) and dominant networking force (blue) after 200000 time steps. 50 bins represents half of the circumference of the ring. Parameters are: $N = 80, \lambda = 1, \gamma = 0.9, n_0 = 10, \ell = 0.2, L = 1.0$. 101

6.6 Snapshot of the chains configuration at initial condition $t = 0$ and at $t = 10000$ for the parameters: $f = 0.1, \epsilon = 2, \gamma = 1, k_BT = 1, \lambda = 1, N = 100$. We see that the clump of chains is more significant with the increase of the networking force strength. 102
6.7 Snapshot of the chains configuration at initial condition $(t = 0)$ and at $t = 10000$ for the parameters: $f = 0.1, \epsilon = 5, \gamma = 1, k_BT = 1, N = 100$. We can see that the chains starts clumping as predicted by the theory. 102
6.8 Correlation function for fixed active force and different value of the networking force strength. Parameters are: $f = 0.9, \gamma = 0.9, \lambda = 1, k_BT = 1, N = 100, Nbins = 50$. We observe a new peak that rises with the increase of the active force. That peak shift to higher value of the length (bin). 103
6.9 Average polarisation current density as a function of the networking force ϵn_0 for different values of the active force. As the networking force increases, the current goes down sharply until there is almost no current flowing in the ring. The parameters used are: $N = 80$ chains, $L = 1.0$, $l = 0.2$, $k_B\,T = 1.0$, $\gamma = 1.0$ and 200000 time steps. We observe a small shift of the critical value of the networking force strength toward a large value of ϵ. 103
6.10 Number of bins unoccupied by the chains in the ring as a function of the networking force. The parameters used are: $N = 80$ chains, $L = 1.0$, $l = 0.2$, $k_B\,T = 1.0$, $\gamma = 1.0$ and 200000 time steps. 104

Part I

Introduction and background

Chapter 1

Introduction and motivations

Polymeric network systems represent intriguing structures that are abundant in nature as well as in man-made materials. This type of material provides mechanical basics for many processes, for example: in tyre industry for reinforcement of the resistivity of the tyre, in rubber like material to study the elastic properties and even in living organisms to understand the self organisation of the filaments within the cells. The network is defined as being a macromolecule formed by the assemblage of many polymer chains. The chains are linked by the use of a "cross-linker" (connectors). The biological network is constituted of filaments and motor proteins that serve as cross-linker. Those network are complex and give the shape of the cell and its mechanical stability. Due to the motion of certain type of cross-linkers, the network behaves on one hand as an highly deformable solid in a microscopic length scale and on the other hand, like a liquid in a microscopic length scale. These characteristics qualify it to be a fascinating material that scientists strive to understand.

Polymer networks in general have the ability to be deformed due to a weak external (or internal) force regardless of the type of the cross-linkers used to form the network. The structure and properties of the network are determined by the characteristics of both polymer chains and cross-linkers. The role of the connectors is to help creating physical bond between polymer chains. The cross-linkage procedure depends on the type and intrinsic features of the connectors. Nature has provided many types of physical bonds in macromolecular materials. We distinguish: the *permanent*[1], the *reversible-movable*[2] (called reversible in chapter 3) and the *active-movable*[3](called active in chapter 4) cross-linkers. The reversible or temporary cross-linker is in generally both

[1]A bond is said permanent when it freezes as soon it is attached to the chain. It is generally called covalent bond

[2]A bond is said reversible when it can detach and reattach. A reversible bond is movable if it changes position or moves along the chains.

[3]The active-movable type of cross-link is the cross-link that generates a force while moving.

reversible and movable example is the non-processive motor protein: myosin II. An active cross-linker is not necessarily a reversible cross-linker (example of processive motor protein: a single processive motor can move continuously along its track for several microns without being detached depnding on the time scale. Kinesins, most dyneins and certain types of myosin protein). Each chain can be several micrometers long and is made of many subunits called monomers. The chains can be semi-flexible, flexible or rigid depending on its stiffness [1]. The elastic properties of the network are defined by how soft each single polymer is and the type of cross-linker used. Biological systems are best examples to illustrate a polymer network with reversible types of cross-linker. One particular example and well known network that has been widely explored by many scientists is the cytoskeleton. This type of network can be internally driven out of equilibrium by the motion of the motor protein (reversible) cross-linker that uses polar chains as path way. The physics of biological systems is a growing field in science which is trying to find its way between physics and biology. There is no doubt that Physics plays a key role in the understanding of many events at microscopic length scale. The cell is a microscopic (Typically 10-100 mm in diameter for eukaryotic[4] cells and 0.2-2 mm in diameter for prokaryotic[5] cells) and thermal environment. It is not easy for theoretical physicists to describe with accuracy the properties of an organelle within the cell because of the size. Nevertheless, many techniques have been developed to understand such microscopic systems.

The concept of a field takes an important place in many well known physics terminologies. The examples of well known fields that one uses in a regular basis are: Electric field, gravity field, electrostatic field, electromagnetic field, etc... Using the field theory in the context of polymer representation can be challenging, not to mention if it is planned to be used for a polymer mixture like a network structure. The use of field theory approach to describe a polymer network that contains both permanent and reversible cross-link is elaborated in this dissertation in chapter 3. The field theory has been originally developed for a permanent polymer network formation by Edwards(1988) and later extended for an active polymer network by Fantoni and Müller-Nedebock (2011) to an active system [2, 3]. The field-theory was shown to be useful in the context of converting polymer degrees of freedom to collective degrees of freedom, that themselves have been shown to be particularly useful in polymer network theories. The field theory will automatically assure the cross linking constraints. Here, we work on the scenario where the reversible cross-linker moves along the chain. Results show that the field theory is also applicable for reversible polymer network. The density fluctuation calculation reveals that

[4]The eukaryotic cells are known by the presence of the membrane-bound nucleus. Example are plant cells, human cells, and some fungi.

[5]Prokaryotic cells example is bacteria. They are known by their lack of the membrane-bound nucleus.

the cross-linkers as well as the chains density fluctuate around their mean field values which is the saddle point solution. Including the polarity of the polymers, we prove that there is two possible network configurations that occur in a primitive one dimensional system: the network with all the (+) ends of the chains pointing in the same directions ("parallel network") and the network where the chains have opposite direction to each other ("anti-parallel network"). The investigations have revealed that adding the reversible type of cross-linker inside a permanent network tends to make the network softer.

The polar polymer network model is later identified to a minimal model of the biological network called the "contractile ring". This organelle is well known to be the one responsible for the physical division of the cell. Its operation mode remains a mystery, but knowing the assemblage and the dynamics of filaments within it will give a insight on its behaviour. We address this network from a dynamical point of view. The field theory shows evidence of being adaptable to usage in a so-called Martin, Siggia, Rose (1972) [4] formalism for the dynamics of the filaments and the cross-linkers. Here we focus on collective dynamics of the chains within the ring. In the dynamical formalism, we learn less about the elastic coefficients of this complex material, but we should be able to model structural informations that could be gleaned from suitable experiments. This is done using the Random Phase Approximation (RPA) [5–9]. This latter approximation may also add insights from a simple motility assays as recently calculated by Banerjee, Marchetti and Müller-Nedebock (2011), where detachment and reattachment formed important ingredients in describing the filament dynamics [10]. The mechanical stability of the ring is investigated looking at the density-density correlation function. We observe that the force generated by the motor myosin II seems to stabilise the ring. The force generated in order to keep the chains linked (the networking force) causes the contraction behaviour of the ring and breaks the structural integrity of the ring. We implement a simple one dimensional Langevin dynamics simulation to add more depth to the elaborated theory and analytical investigation. The two investigation results show that the sustained polarisation current flowing through the ring goes from a current regime to an almost no current regime with the increase of the networking force. This suggests a phase change inside the ring occurring when the chains go from an homogeneous distributed state ("unstable" ring) to a completely heterogeneous or separated state ("stable" ring which is maintained by the myosin II activity). The work done in chapters 5 and 6 will be submitted for publication and is in its final preparation.

Motivations

When biological filaments, such as F-actin or microtubules are combined with active cross-links, that come in the form of dimers of motors or motor clus-

ters (such as kinesins and dyneins for microtubules, and myosins for actin) the systems show contractile behaviour. This means the volume of the filaments network decreases when the activity of the motors is switched on. At the same time, one expects the other elastic properties of the network to differ significantly from those of permanently cross-linked filaments networks made of similar filaments but without the moving molecular machines.

The present work has been motivated by the need to bring an insight on the problem of connectivity during network formation and the need to understand the contractile behaviour of the actomyosin network (which is a minimal model of the contractile ring). The polymer network has captured our interest because of the complexity that increases when the network contains both the reversible-movable or active-movable and the permanent cross-linkers. We are interested on extending the theory of Edwards [2] and include movable cross-linkers. Understanding how this type of network is formed may helps understand the features of biological network.

Outline

The dissertation is outlined as follow:

Chapter 1: This chapter is a general introduction of the whole dissertation.

Chapter 2: This chapter is a general introduction of all the concepts that one need to be acquainted with in order to be prepared the reader not familiar with some concepts when enter deeply into this dissertation. It contents a short overview of the kind of network one will deal with later on. It highlights all type of polymer chains and the minimal constituents of the contractile ring. It also gives a brief introduction of the method elaborated by Edwards to develop the permanent polymers network formation using field theory formulation.

Chapter 3: This chapter is the main first part of the project. It elaborates the network formation method using field theory. The network elaborated contains reversible-movable and permanent cross-links. It presents the response of network due to an external deformation using the replica method.

Chapter 4: In this chapter, we suppose that the network have already been formed. We present a primitive one dimensional network made of polar chains and the two reversible and permanent cross-linker. We view the reversible cross-linker as a bipolar myosin II motor protein that move along the cross-linked chains. We introduce the concept of "sliding ring" and investigate the behaviour of the network in the two distinct example

of network conformation formed with a randomly one dimensional polar chains.

Chapter 5: We investigate the collective chains dynamics behaviour changing in the minimal linear contractile ring model. We present the MSR and the RPA formalism using the collective variables and calculate the density-density fluctuation of the system. We focus on understanding the role of each force involved in the mechanism of the chains' dynamics.

Chapter 6: This chapter presents the finite periodic contractile ring model. We investigate the cause of the contractile behaviour of the ring by look at the two forces evoked in the previous chapter. This is done by using the collective variables dynamics formalism elaborated in the chapter 5. We also implement a simple Langevin Dynamics Simulation(LDS) to add depth to the analytical ring behaviour investigation.

Chapter 7: This chapter is a general conclusion of the dissertation. It summarises the results, and gives the perspective for a possible future investigation on the similar problem.

Appendix: This part presents details of the calculations made in the dissertation.

Chapter 2

General background

2.1 Introduction

The present chapter is an introduction to concepts that will be used later in this dissertation. The chapter is made for the readers to familiarize themselves with some basics concepts used for this dissertation. In section 2.2, we present a general review in polymer theory starting from a single and moving to many chains system. The section 2.3 presents the idea of Edwards on permanent polymer network representation using the field theory borrowed from quantum field theory [2]. We explain the cross-linkage problem in a polymer mixture. In section 2.4, we introduce in brief one example of a natural network that will be the object of interest of the two last chapters. The properties and the composition of this later type of network are highlighted. We limit ourselves to the simplified version of this network using the actomyosin system to mimic its structural behaviour.

2.2 Basic concepts of polymer theory

2.2.1 Single polymer chain: Ideal chain model

A polymer chain is a macromolecule composed of a large number of small (not always identical) units called "monomers". All monomers are connected to each other using the connectors or cross-linkers permanently in synthetic polymers, but there are those being polymers that can grow. Each connecting joint allow rotation in space so that the chain can take many conformations [11, 12]. The most widely used chain behaves like an ideal random chain. Those chains are also known by their highly modulate structure. For instance, depending on their characterisations (i.e. elasticity, bending modulus, bulk properties, local stiffness). One can distinguish several type of polymer chains [11–14] . Each type of chain provides a good theoretical representation and a good approximation in a solvent. The difference between the chains types

is embedded in the constant called *"the flexural rigidity"* and noted κ. This constant is analogue to a spring constant and is related to the *"persistence length"* noted l_p by the relation (Hooke's law for spring) $l_p = \frac{\kappa}{k_B T}$ ($k_B = 1.38064852 \times 10^{-23}$ m^2 kg s^{-2} K^{-1} is the Boltzmann constant, and T the temperature). The persistence length is the correlation length scale defined by the relation: $\langle \vec{t}(s) \cdot \vec{t}(s+T) \rangle = e^{-T/l_p}$ with $\vec{t}(s) = \frac{\partial \vec{R}(s)}{\partial s}$ a tangent vector of the chain with the length constraint $|\vec{t}(s)| = 1$ for s, $\vec{R}(L_0 - L)$ is the end-to-end vector of the chain. We describe below ideal chain. It is basically described by the *random walk*. Our consideration here neglects the *excluded volume*[12]. The ideal chain is simply a polymer assumed to be a random walk like chain. It is very reliable due to the fact that it eases the mathematical calculation and simplify the difficulties that polymer study can raise.

2.2.1.1 Flexible polymer chain

The flexible chain also called, is characterised by its many degree of freedom. Consider the Fig. 2.1 of a chain composed of N number of subunits of length b each ($\vec{b}_i = \vec{R}_i - \vec{R}_{i-1}$) called the "effective bond length" or "bond vector" [14]. The two ends of the chain fluctuate without touching each other. The mean end-to-end displacement of the chain is equal to zero because all the bond vectors are sum over all the monomers and canceled each other due to the isotropy property of the system. Therefore, we have: $\langle \vec{R} \rangle = \sum_{i=1}^{N} \langle \vec{b}_i \rangle = \vec{0}$ with the mean square:

$$\begin{aligned} \langle R^2 \rangle &= \sum_{i=1}^{N} \sum_{j=1}^{N} \langle \vec{b}_i \cdot \vec{b}_j \rangle \\ &= \sum_{i=1}^{N} \langle \vec{b}_i^{\,2} \rangle + \sum_{i,j=1; i \neq j}^{N} \langle \vec{b}_i \cdot \vec{b}_j \rangle. \end{aligned} \tag{2.1}$$

For $i \neq j$, $\langle \vec{b}_i . \vec{b}_j \rangle = 0$, therefore,

$$\langle R^2 \rangle = \sum_{i=1}^{N} \langle \vec{b}_i^{\,2} \rangle = Nb^2 = Lb. \tag{2.2}$$

With $L = Nb$ the contour length of the chain. We deduce that $R \sim \sqrt{\langle R^2 \rangle} = N^{1/2} b$, $R \ll L$. This expression shows that the freely jointed chain has a non linear conformation. It can therefore form an entangled coil or other complicated structure depending on the surrounding solvent and other parameters like temperature or cross-linkers where $R \sim N^{1/2}$ scaling will not necessarily apply. This type of chain has a trajectory equivalent to a Brownian particle trajectory. The single chain is characterised by the persistence length l_p

($L >> l_p$), the flexural rigidity κ and the continuous contour parameter (arc length) of the chains ($0 < s < L$). As example of flexible chain we can cite: rubber like chain, one strand of DNA, etc... The Edwards Hamiltonian of this type of chain is given by the following expression:

$$H[\vec{R}(s)] = \frac{3}{2\,\ell}\int_0^L \mathrm{d}s\,\left|\vec{t}(s)\right|^2 = \frac{3}{2\,\ell}\int_0^L \mathrm{d}s\left|\frac{\partial\overrightarrow{R}(s)}{\partial s}\right|^2 . \tag{2.3}$$

ℓ is called the "Kuhn length" and it is known to be the distance between two monomer in the polymer chain. The Edwards Hamiltonian (equation (2.3)) is used in equation (2.6) to calculate the partition function. Considering that the

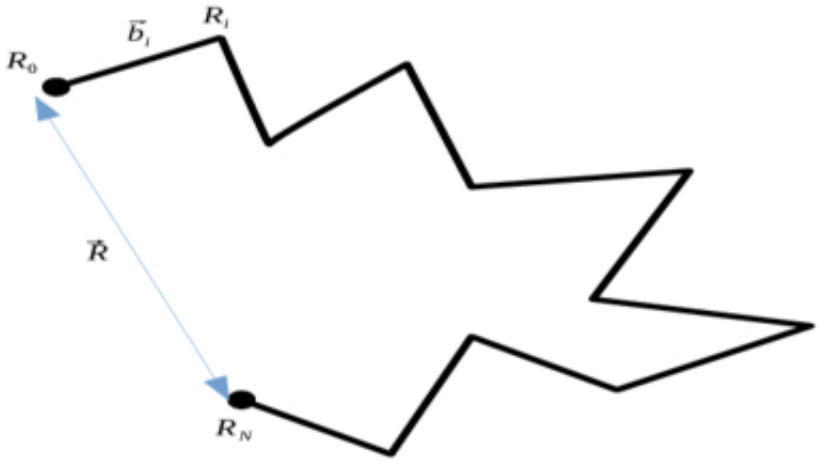

Figure 2.1: *Self avoiding chain*

chain have a Gaussian distribution. In this case, the chain is called "Gaussian chain" and the central limit theorem gives the chain probability distribution for the end-to-end distance of the chain. The probability is written as followed: $P(\overrightarrow{R}(s)) = \aleph \exp\left[-\frac{3}{2L^2}\sum_{i=1}^{N}(b_i)^2\right]$, $\aleph$ is the normalisation factor.

2.2.1.2 Semi-flexible polymers chain

Also called "Worm-like chain" or "Kratky Porod chain model", the semi-flexible polymer is less flexible than the flexible chain. It is stiff and can only bend weakly due to thermal fluctuation [15] . Its contour length is far more smaller than the persistence length ($L \leq l_p$). If L is too small, the chain reaches the rod limit. The expression of its effective Edwards Hamiltonian is given by

$$H[\overrightarrow{R}(s)] = \frac{\kappa}{2}\int_0^L \mathrm{d}s\left|\frac{\partial\overrightarrow{t}(s)}{\partial s}\right|^2 = \frac{\kappa}{2}\int_0^L \mathrm{d}s\left|\frac{\partial^2\overrightarrow{R}(s)}{\partial s^2}\right|^2 . \tag{2.4}$$

The equation 2.4 is used in the partition function together with the constraint $\delta(|\vec{t}(s)|-1), \forall s$. This model of chain is a special case of the flexible chain with a very small bond angle [11].

2.2.1.3 Other types of chains

- **Rouse chain/ Bead-spring chain** This model of chain is different from the flexible chain only by the fact that in between each bead (monomer) there is a supposed spring with a finite equilibrium length. It is popular for its application in computational simulations.
- **Freely jointed(rotating) chain:** This chain is the flexible chain with the monomer unit length all equal. It has no fixed angle between each monomer. It is generally useful to study the general properties of any type of chain.
- **Real chain:** This chain is a *self-avoiding walk* chain. It allows the excluded volume principle.

2.2.1.4 Path integral: Representation for the polymeric chain

Also called *functional integral*, the path integration is generally an integral that runs over all the possible degree of freedom that are associated with the variable over which the integration is made. This distinguishes itself from the integration that runs over all the micro-states of the system in statistical mechanics. In the specific case of polymeric chain, the path integral simply means the integration over all the possible trajectories of the chain. In other words, integration over all the possible trajectories that must be taken in order to move from one end to the other end of the chain [16–18]. This concept was introduced first by Nobert Wiener (1921-1930) and Marc Kac as a form of propagator to solve the diffusion problem. It was latter developed by Richard Feynman(1948) [19] as solution of the Schrödinger equation in statistical physics. He proposed to add up the statistical weight of the trajectories of each chain. The path integral shows its utility when studying the statistical fluctuations of the polymer chains which have line like structure. A single non-rigid polymer chain has the property to fluctuate around a specific configuration. The chain, is well defined by the distance between its two ends (the end-to-end distance R). The two ends of a single chain are labelled with R_0 and $R_L \equiv R_N$ (N represents the number of monomers in the polymer chain). The corresponding contour parameter of the chain at the ends are: $s = 0$ and $s = L \equiv N$, s being the arc length along the chain. In brief, the path integration for polymer as its name revealed is the integration over all the paths taken to go from one end to the other end of the chain [16, 18]. The

mathematical representation is given by:

$$\aleph \sum_{\text{All paths R(s)}} \equiv \int_{\mathbb{R}} [\mathrm{d}\, R(s)] \equiv \int_{\mathbb{R}} DR(s). \tag{2.5}$$

With $\aleph$ being the normalisation constant. The partition function of the desired Hamiltonian $H(R(s))$ is given by:

$$Z \quad = \aleph \int_{\mathbb{R}} DR(s) \exp\left(-\beta H(R(s))\right). \tag{2.6}$$

2.2.2 Many polymer chain system

In the previous section, we have presented the properties of a single chain. We used the random walk as basic model and it will be used for the coming chapters of this dissertation. For a single chain system, the only interaction the chain experiences is with itself whereas in a mixture of many chains, each chain can experience a contact with itself and also with the other chains. If the system becomes dense, the self interaction can be neglected [14, 20–22]. This section presents many chains system properties that will be developed for the later work. The question one can be tempted to ask is: what kind of difficulties one can experience from such systems? We can enumerate the screening effect, excluded volume problem at macroscopic level (i.e. for the whole system as one), the connectivity issue and many more. This latter is the most interesting when thinking about a network. Consequently, it will be the centre of our attention in chapter 4. From many body theory, one can borrow approximation like mean field approximation to simplify the system, and makes it more easy to study without losing any important information on the system.

2.2.2.1 Self consistent field theory (SCFT)

The SCF method is a method borrowed from many-body systems and also used in polymer science when dealing with a dense polymer mixture. Having a mixture of N number of polymer chains, sometimes we would like to have informations about the dynamics of the whole system. This task is never easy since the system is too dense. In order to ease the problem, polymer physicists use the mean field approximation borrowed from the quantum field theory and therefore use it for their benefit [14, 18, 21, 23]. The ideas behind the SCFT technique is to reduce a system of many polymer chains to a simple system of a single polymer chain. This single chain now moves inside an external potential field $V(r)$ which is the remaining $(N-1)$ polymer chains that have been smeared out. This is done after having randomly chosen one chain between the N chains of the system (see Fig. 2.2). The external potential $V(r)$ is often called the "self consistent field" or "mean field potential". This approximation neglects the correlation between the labelled chain and the remaining

chains. Once the approximation is performed, one is able to track the one chain that has been labelled and deduce the whole system behaviour. This is a very powerful technique for calculating polymer mixture phase separation and also inter-facial structure like polymer. This method is also widely used in experiments, precisely in fluorescence microscopy.

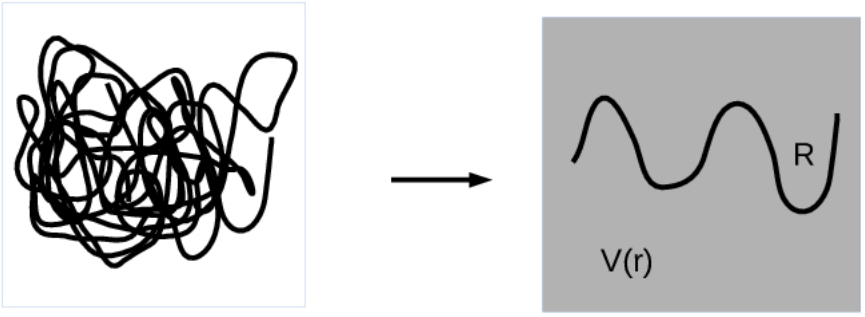

Figure 2.2: *Self-consistence method: The many chains system is simplified to a single chain inside an external field created by the other chains.*

2.3 Network formed by polymer chains: Edwards formulation

Deam and Edwards(1976, 1988) have presented a new field theoretical model to handle polymer chain network formation [2, 22]. The theory is all based on the cross-link process at random points [2, 13, 14, 22]. Edwards exploits the Wiener integral to describe a Gaussian molecule (polymer network). Assuming that one has a system constituted of a fixed number (N_c) of cross-linkers having fixed functionality [1], and a fixed number N of polymers (chains). Edwards defined each cross-link by a set of chains $\{i, j\}$ associated with a set of position $X = \{s_i, s_j\}$ where s is the contour length. Mathematically, the delta function is used to enforce the cross-linkage as $\delta(X(s_i) - X(s_j))$. This means that there is a cross-link between the positions s_i of the i^{th} chain and the position s_j of the j^{th}. It imposes a specific topology of the network). The probability of having a specific configuration of the network after the formation is given by:

$$P^{(0)}[X] = \frac{\exp\left(-\mathcal{H}^{(0)}/T^{(0)}\right) \times \prod_{i,j} \delta(X(s_i) - X(s_j))}{Z^{(0)}[X]}. \tag{2.7}$$

[1] the functionality here refers to the number of possible available seat where the cross-linkage can take place or simply the number of chains that one cross-linker can link in order to form a network.

With the normalisation condition: $\int [dX]\, P^{(0)}[X] = 1$ and the partition function $Z^{(0)}[X]$. This initial partition function is the complete statistical mechanics of the description of the network at the initial stage i.e. right after the cross-linkage. The partition function here also includes the network linear response to a small perturbation and is given by the following expression:

$$Z^{(0)}[X] = \int [\mathrm{d}X]\, \exp\left(-\mathcal{H}^{(0)}/T^{(0)}\right) \prod_{i,j} \delta(X(s_i) - X(s_j)). \tag{2.8}$$

2.3.1 Edwards field theory formulation

2.3.1.1 Equilibrium network

To make predictions about some physical observables of polymer mixture like system, it is certainly not interesting to account for all the monomers belonging to each individual polymer. The better and best way is to focus on the behaviour of the polymeric chain as one object. For an equilibrium or permanently crosslinked polymer chains network, the average behaviour of the network does not change over time. The system does not need any additional energy to maintain itself in a constant state. The statistical physics of such system is straight forward. In the field-theoretical context, each chain is represented with its path integral formulation. The partition function of the many chain system is therefore given in a form of a multiple path integral, one path for each individual chain. It turns out that the field-theory description for polymeric chains system brings many advantages. In order to perform the transformation from the particle-based into the field-based theory, an elegant method was developed by S. Edwards (1988) [2]. Edwards illustrates using field theory representation a permanent polymer chain network formation. He has shown how to use the field theory to construct such network using the generating functional. It is not easy to deal with the connectivity problem that raises the networking formation. The challenge is to be able to specified which chain is link to which one and at which part of the chain's arc length. For example, a network prepared repeatedly with the same sample (i.e. same number of connectors and same number of chains) have high chance to have complete different conformation at each time. A field theoretical treatment that has been introduced by Edwards and his co-workers (1970, 1976, 1988) resolves some issues related to the problem of enforcing the cross-link between chains in a mathematical formulation [2, 24, 25]. The method used is based on the idea of Gaussian functional integral expression for a complex field variable

ϕ.

$$\aleph \int [\mathrm{d}\phi]\,[\mathrm{d}\phi^*] \prod_{i=1}^{N} \phi(x_i) \prod_{\mathrm{j}=1}^{N} \phi^*(x_\mathrm{j}) e^{-\int_x \phi^*(x)\,\phi(x)} = \sum_{\text{all pairs}} \delta(x_{i,1} - x_{j,1})\,\delta(x_{i,2} - x_{j,2}) ... \delta(x_{i,N} - x_{j,N}) \tag{2.9}$$

This expression is cast into the partition function and contributes to pairwise linked the chains in all possible way. This is generally called *Wick's theorem* (see section 3.2.0.1). It it used to perform the cross-linkage between the chains and the cross-linker agents and therefore construct a network. The simple way to transfer the formalism from particles to field description is to replace the former Kronecker delta function by the Dirac delta function because the chains is a continuous object [13, 22]. It is convenient to use a pair of fields (ϕ, ϕ^*) both complex and one being the complex conjugate of the other one. That means, the two fields can be written as $\phi = \phi_1 + i\phi_2$ and $\phi^* = \phi_1 - i\phi_2$. The equations (3.11) and (3.12) show that the cross-link cannot be made between two identical fields. Using the example of the same system described on the previous section, Edwards has used the field ϕ to label the position on the chain where cross-links can take place (supposed to be at the end of each chain so, the functionality of each chain is 2). The conjugate field is placed on the cross-linkers. The partition function representing all the possible way to form a network with a mixture of N chains and N_c permanent cross-linkers with functionality f each is given by equation (2.10):

$$Z = \aleph \int_{\mathbb{R}} [d\phi][d\phi^*] \left[\int_{r_0}\int_{r_L} \phi(r_0) G(r_0 - r_L, L)\phi(r_L)\right]^N \left[\int_r \phi^{*f}(r)\right]^{N_c} e^{\left(-\int_r \phi(r)\phi^*(r)\right)} \tag{2.10}$$

where the expression $\left[\int_{r_0}\int_{r_L} \phi(r_0) G(r_0 - r_L, L)\phi(r_L)\right]^N$ counts all the chains and goes from one end to the other end of each chain of total length L. $G(r_0 - r_L, L)$ is a Green function which has a Gaussian distribution like expression. $\left[\int_r \phi^{*f}(r)\right]^{N_c}$ counts all the cross-linkers and the exponential term simply allows the cross-linkage between the chains and the cross-linkers. An example is illustrated in section 3.3.3.1.

2.3.1.2 Non-equilibrium network

A non-equilibrium polymer network is a network of polymer that has movable cross-link. There is no surprise to know that the formalism for dynamical networks poses significant challenges to both experimentalists and theorists. The study of such network is the purpose of the present dissertation. There is is therefore no need to elaborate more here.

2.3.1.3 Type of disorder inside the system

In this section, we look at the behaviour of the network if we introduce disorder into the system. First, what do we mean by disorder? Thinking of a real material, the disorder could be vacancy in the crystal, impurity etc.. In the case of many polymers system, the disorder could be due for example to the disorder in the position of the polymers (or cross-linkers position) inside the network. It is important to distinguish the type of possible cross-links in various aspects. This will guide us on how to write the model. There is an important distinction worth to point out at the very beginning. This has to do with whether or not the degree of freedom of the system changes over the relevant time scale or not. We distinguish the "quenched disorder" and the "annealed disorder". In the quenched disorder, the configuration of disordered degree of freedom is frozen in the system. That means, it does not changes over the relevant time scale of the system. For the annealed disorder, the degree of freedom changes over the time scale of the system. This could includes an external dynamics due to the dynamics of the annealed disorder. The quenched disorder simply means a new parameter in the Hamiltonian whereas the annealed disorder could fall apart to many subclasses of disorder (that we are not going to develop here). The two type of disorder demand different way of dealing with them. A conceptually simple annealed case is where we suppose that the degree of freedom is at equilibrium. That means, it will be introduced in the Hamiltonian as a new degree of freedom of the system. That means, the system will be treated as if it has few more degree of freedom and the partition function averaged over all the degree of freedom of the system. For the quenched disorder, it will be wrong to average the partition function. We rather need to think about physical quantities like the free energy for each individual sample and then, average this quantity as opposed to averaging the partition function.

2.3.1.4 The replica method

The replica method is an indirect way to deal with the logarithm appearing in the quenched average. The aim of this method is to compute the average value of the free energy of a many body disordered system easily [2, 22, 26, 27]. The free energy in statistical physics is known to be the central issue for any equilibrium problems. For a case of a system made of many objects like the one presented above, the free energy is written as: $F(\beta, N) = -k_B T \ln(Z(\beta, N))$ where $Z(\beta, N)$ is the canonical partition function of the system and $\beta = 1/k_B T$ (k_B is the Boltzmann constant and T the temperature of the system). The degree of freedom here could be the way the chains are connected or else. In thermodynamic limit, i.e. for large number of chains ($N \to \infty$), there is a random cross-linkage issue to circumvent. This randomness influences the free energy calculation in the sense that, it is not easy to perform an average over

the disorder on the system. The cross-link being permanent, it means, that we will have to perform a so called "quenched average" while averaging over all the disorder of the system. The logarithm appearing on the free energy does not make things easier. So, the need of this replica method is unavoidable. Averaging the free energy over the disorder on the system gives:

$$-\beta F(\beta, N) = \lim_{N\to\infty} \frac{1}{N} \langle \log(Z(\beta, N)) \rangle_{\mathrm{d}}. \tag{2.11}$$

with $\langle ... \rangle_{\mathrm{d}}$ representing the average over the disorder. The calculation of the free energy is resumed to the calculation of the average $\langle \log(Z(\beta, N)) \rangle_d$. Calculate this average is not an easy task to perform because the average is over the logarithm of the partition function. However, knowing that the average is on the logarithm not the partition function itself, one can approximate this average using the following formula:

$$\log Z = \lim_{n\to 0} \frac{Z^n - 1}{n}, \quad n \in \mathbb{N}. \tag{2.12}$$

The equation (2.12) is also called the "replica trick". The trick behind this is to reduce the logarithm of the partition function into the average of the product of all the partition function of the replicas of the system. n represents the number of replicas of the initial system with the same set of elements (same initial condition). $Z^n = \prod_{\alpha=1}^{n} Z_\alpha$ with α the replica number ($\alpha \in [1, ..., n]$). The relation (equation (2.11)) is now given by:

$$-\beta F(\beta, N) = \lim_{n\to 0} \left(\lim_{N\to\infty} \frac{1}{nN} \left(\langle Z^n \rangle_d - 1 \right) \right), \tag{2.13}$$

with

$$Z^n = 1 + n \log Z + ... \tag{2.14}$$

The method has been used a lot and is controversial and difficult to interpret.

2.3.2 Elastic properties of the network

Let us consider the 3D network with spacial directions (e_x, e_y, e_z). We label all the chains with the same vector position in each direction $r = (r_x, r_y, r_z)$ (Fig. 3.6). where r_x, r_y, r_z mean the chain label vector along the direction e_x, e_y, and e_z. If the network is stretched affinely in one direction, the length of the network in that direction is multiply by a factor $\lambda > 1$ (λ is the deformation factor). The size of the network therefore in the two other directions is modified by a factor of $\overline{\lambda} < 1$. If we consider that the network is incompressible (i.e. the volume is conserved when the force is applied), then the simple relation we can have between those two factors, is $\lambda(\overline{\lambda})^2 = 1$. The free energy for a

single non flexible and non-interacting polymer chain with the contribution of the deformation factor is given by :

$$F_{\text{chain}} = \frac{3}{2} k_B T(\lambda^2 + \frac{2}{\lambda}). \tag{2.15}$$

For N polymers chains, the free energy is $F_N = NF_{\text{chain}}$. We introduce the deformation tensor Λ which is a 3×3 matrix [22, 28] given by:

$$\begin{pmatrix} \overline{\lambda} & 0 & 0 \\ 0 & \overline{\lambda} & 0 \\ 0 & 0 & \lambda \end{pmatrix} = \begin{pmatrix} \lambda^{-1/2} & 0 & 0 \\ 0 & \lambda^{-1/2} & 0 \\ 0 & 0 & \lambda \end{pmatrix} \qquad \lambda > 1. \tag{2.16}$$

Hence, the volume of the network changes from V before the deformation to $\tilde{V} = \Lambda V$ after the deformation. The statistical weight of a particular copy of the network (one particular replica of the network) is $Z = e^{-\beta F}$ with F the free energy of this particular replica of the network. Following Deam and Edwards spirit (1976, 1988), the network configuration can be specified and imposed at the fabrication by imposing the position of the cross-linkers [2, 22]. In that way, the network configuration could be conserved during the deformation (this is more elaborated in section 3.5).

2.4 Example of biopolymer network: The Contractile ring

2.4.1 What is the contractile ring and its role in the living cell cycle?

Majority of living organisms like humans cells experience physical division during their life cycle. This process is called the "mitosis". During the mitosis, when all the chromosomes and the genetic code of the cell are equally separated, a ring made of several filaments and motor proteins is formed at the middle of the cell [29–32]. The building process of this ring remains a mystery. After the organelle is formed, it exerts a tensile force when the filaments move. The reduction of the size of the organelle leads to the formation of a cleavage furrow [33–36] therefore, the complete physical separation of the cell in two daughter cells ("*cytokenesis*"). The four basic steps of the mitosis are pictorially shown in the Fig. 2.3.

- During the prophase, the nucleus of the mother cell condenses and the organelle called mitotic spindle (formed by micro tubule and kinesin motor protein) is formed. This organelle helps the choromosome to move during the mitosis process.
- At the metaphase stage, all the chromosomes get ready for the division. They all align themself at the middle of the cell.

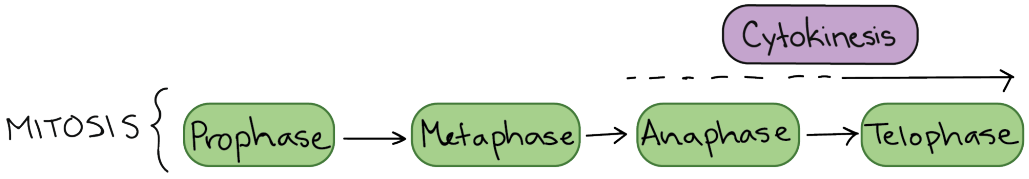

Figure 2.3: *The four main steps of the mitosis. The cytokinesis which is the final stage of the physical division of the cell overlaps with the anaphase and telophase. The cytokinesis may start at either anaphase or telophase, depending on the cell, and it finishes shortly after the telophase process.*

- At the anaphase, which is the first step of the cytokinesis [2], the chromosomes separate into two identical chromosomes carrying the same genes. Those chromosomes migrate each toward the two poles of the cell.
- At the telophase, the cell is already almost completely separated. The mitotic spindle that was condensed before are decondensed and breaks down into two blocks. An organelle called the actomyosin contractile ring is formed at the middle of the cell creating a cleavage furrow on the cell membrane. The actin myosin network constituent of the ring exerts then enough pressure to complete the division of the cell [31, 37–40].

The widely accepted minimal constituent of the contractile ring are the active filaments and the myosin II motor proteins [29, 30, 39, 41–43]. The filaments form a bundle network cross-linked by the myosin II protein. The organelle self organises and generates enough force to constrict the cell until its final separation. The mechanism behind this contraction behaviour is still to be explored. Nowadays, the contractile behaviour of the ring is known to be the major tenet of the cell division process. The intriguing question is "How does the contraction occur and what it the cause of the contraction?".

Suggestions in order to understand the contractile behaviour of the ring have been elaborated by some authors all with different and interesting models for the ring. The most commonly used is the minimal model of actomyosin network to represent the contractile ring(i.e. a random network of actin filament and myosin II). Literature suggests that all the filaments are aligned in antiparallel manner and that the motion of the myosin II is responsible for the contraction [35, 44]. Others claim that the polymerisation and depolymerisation of the chains are responsible for the contractile behaviour of the ring [31, 45]. Another idea suggests that the ring does not need the activity of the myosin II in order to produce tensile stress [42] and they argue that the bundle actin filaments contracts when the motor myosin II reaches the ends of the

[2] cytokinesis is the physical separation of the cell into two daughter cells

chains and stops [35]. To have a more clear idea on what is really happening, one need to know first what the ring is made of.

2.4.2 The actin-filaments

The actin filament generally short named "F-actin" is a microfilament found in the cytoskeletal of the cell. It has a polymeric structure and made of many subunits called globular actin (G-actin) [1]. This chain is about $10^4\,nm$ of length and its persistence length is about $10^3\,nm$. Each of those subunits has a mass of 50 KDa [3] and a size of a few nano-meter. The F-actin is formed by the polymerisation of the G-actin. Both G-actin and F-actin are polar therefore, we can distinguish the two ends of the F-actin: the + or barbed end and the − or pointed end. The polymerisation mostly occurs at the + end of the chain and the depolymerisation at the − end [1]. Going from the G-actin to the F-actin, the system need to be fuelled by an energy from a chemical process called "hydrolysis". The hydrolysis is the chemical process that transforms the molecule Adenosine Triphosphate(ATP) into the Adenosine Diphosphate (ADP). This chemical reaction is able to release an energy in the order of magnitude roughly equal to $\Delta\mu = 25kT = 8.10^{-10}J$ [1]. Since the reaction is reversible, we have both polymerisation and depolymerisation at both ends of the F-actin.

$$\underbrace{ATP + H_2O}_{\text{Stored energy}} \quad \rightleftharpoons \quad \underbrace{ADP + P_i + \Delta\mu}_{\text{Used energy}} \tag{2.17}$$

2.4.3 The molecular motors: Myosin II

The motor protein myosin II is a protein found into all eukariotic cells. It is best known for its contribution of the contractile behaviour in muscle cells. It is responsible for the motion of the F-actin as it uses this filament as path way. Moving toward the + end of the chain, it has the ability to transform the chemical energy into mechanical energy and uses it to move along the chain [1, 46–48]. Almost like man made machine, this protein uses the energy stored by the chemical reaction(hydrolysis) shown in equation (2.17) to generate motion. This motor is known as non-processive[4]. That is why it is suitable for reversible cross-linker description. The activity of the motor proteins is fuelled by the ATP [1, 10, 46].

In addition to actin and myosin protein, the ring comprises other proteins. The other polymers components found in the ring are the intermediate filaments and the microtubules. This latter serve as tracks way for two class of

[3] $1KDa$(Kilo Dalton) $= 1.66 * 10^{-24}g$, is a mass unite used by biochemists. It represents the mass of one hydrogen atom.

[4] non-Porcessive means that the motor protein attaches and detaches while moving along the chain

motor proteins: kinesins and dynein. Each of those motors move by different mechanisms. Other types of myosin motor move toward the − end of the filament.

2.4.4 Sliding-filaments theory

The *Sliding filament theory* is an hypothesis first elaborated by Hugh Huxley and his research team [1, 10, 37, 47, 49]. The theory explains well the contraction mechanism in muscle. It is based on filaments sliding passing each other driven by the myosin II motor proteins. The appropriate subunit in which this theory is applicable is called sarcomere[5]. It explains well how the motor pulls the filaments and make them slide in respect to each other. This theory is also sometimes called the *cross-bridge theory*. It states that the acting filament and the motor protein myosin II are connected together in such a way that they form a network. The cross bridge cycle [6] steps of the motor myosin II are:

1 **Working stroke:** The motor head bind to the head of the enzyme causing the myosin to be detached from the filament.

2 **Unbinding:** The change the conformation: The APT turn into to $ADP + P_i$, (hydrolyse) releasing energy to it change the myosin II conformation become its hight.

3 **Recovery stroke:** The phosphate group is released.

4 **Binding:** The ADP is released and the myosin II goes back to its original position but one step further.

2.5 Conclusion

This chapter is an introductory chapter. It recapitulates important concepts one might need to know in order to understand the present work. We have started by the description of the basics on polymer theory. We have presented different type of single polymeric chain. We have explained the concept of many chains using the example of the Gaussian chain. We have also presented in brief a concept of the polymer network elaborated by Edwards. We have presented how Edwards used the field theory to represent the permanent polymer network in a general views. We later presented a biological network called the contractile ring. That ring is formed during the cell division and helps to

[5]Sarcomer is a network of linear aligned filaments cross-link by myosin II. It is found inside the muscle tissue and is the base of muscle contraction). The theory has been elaborated in order to well understand muscle contraction. The network is basically formed by myosin II and actin filaments that are ordering aligned to each other.

[6]The cross bridge cycle is the whole process for one motor head to move from position on the chains to its next position

the complete physical separation of the cell in two daughter cells. We present in brief the constituent of the minimal model (that will be used in chapter 6 to investigate the contractile ring) of the ring and elaborate about the feature of each constituents.

Part II

Polymer network formation using field theory

Chapter 3

Polymer network with movable and permanent cross-link

3.1 Introduction

Materials made of randomly cross-linked polymers such as gels, elastomer, rubbers, cytoskeleton networks etc... are ubiquitous in nature and have been largely explored by scientists in many ways [21, 28, 50–52]. Between 1920 and 1960, S. Edwards, De Gennes, and Flory had developed successful methods to use in the field of polymer physics [2, 22]. We can cite for example: The scaling law such as for excluded volume, the renormalisation group theory for self-avoiding walk, the field theory method for polymer network. This latter technique (see section 2.3) has been borrowed from the quantum field physics and now applied in polymer physics [2, 3, 13, 14, 53]. The field theory applied for polymer network constitutes a new field of research that builds a bridge between statistical mechanics for polymer science, soft condensed matter science, quantum mechanics and other branches of statistical physics. This innovation has opened doors for an insight into many important problems in polymer science including excluded volume effect, and even the interesting problem of polymer cross-linkage.

The selected point of our interest in the present chapter is the problem of connectivity between polymer chains. The connectivity problem remains an interesting question mainly when the geometry of the system is restricted. It is not easy to blend polymer chains to form a network even in a case of identical polymer chains. We may consider adding a third party of the mixture named “cross-linker” or simply “connector”. This entity usually helps to ease the process and, depending on its properties (i.e. its functionality[1] and how it operates) it may create a permanent or temporary bond between two or more polymer chains.

[1] The functionality of the cross-link is the number of chains that this later can cross-links.

The aim of this chapter is to develop a good model of polymer network using the field theory concept first elaborated by Edwards (1988) [2] for the permanent network. We propose to include temporary cross-linkers in addition to the normal permanent cross-linkers. For that, we will use two distinct type of cross-linkers: the *permanent* cross-links will be seated at the extreme ends of the chains, and the *reversible* cross-linkers which will seat at a random position along the chains as end-links. The terminology "reversible" will be used in this chapter to mention the fact that the cross-link is non-processive (i.e. attach and detach) and movable (i.e. not static).

The field theory has already proven itself to be worth using to represent permanent polymer network. For a new reader in Edwards' field theory techniques, we will for the purpose of having an understandable model, split the network into two and then after combine to form one. The way we plan to split it is as follows: we first present a network made of chains and only reversible cross-linkers. Secondly, we present the full network made of reversible and permanent cross links. Along the way of the network formation understanding, one will have to deal with " quenched " and " annealed " average since the two types of cross-linkers have completely different properties and behaviours. The deformation study of the network shows that adding the reversible cross-linker in a permanent network contributes of making the network become softer. This holds if we suppose that there is always enough reversible cross-linker inside the network so that there is no chance that the reversible cross-linker be completely detached from the chains.

3.2 Cross-linkage of Gaussian chains

The cross-link is simply defined as a bond that links two or more chains together. If many polymeric chains are all cross-linked, the chains therefore form one macromolecule called "network". The cross-linkage process is best understood when illustrated with an example. We start with a minimal model of two chains so that we clear things from the very beginning. Let us label the chains, chain(1) and chain(2) as seen in the Fig. 3.1. The cross-linking agents are used to establish the connection between the two chains [50, 54–56]. Those chains are parametrised by r and R as the position in space. The available cross-link position in space on each chain is labelled with x and X respectively for the chain(1) and the chain(2). s and S being the arc length for the two chains $0 < s\,,\, S < L$.

In order to include a cross-linkage process inside any theory, one needs to think about good mathematical tools. The connection between two chains will be established if and only if the two chains meet the same position in space.

Pictorially, we must constrain the chain(1) to be connected with the chain(2) at the same point in space (see Fig. 3.1). By Cross-linking the two chains at the

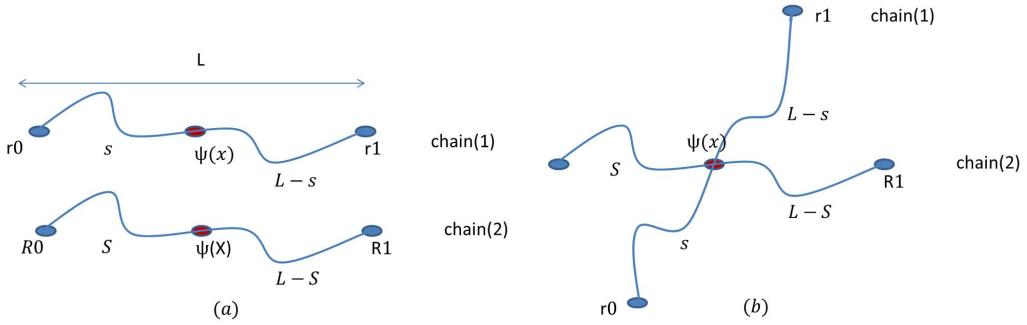

Figure 3.1: *(a):The figure presents two strands of polymer chains. On the chain (1), the labels r_0 and r_1 stand for the starting end of the chain and the finishing end of the chain. x is the spatial position along the chain where the reversible cross-linker can be anchored. The total length of the chain(1) is L as well as for the chain(2). s and $L-s$ represent the distances from r_0 to the position x and from the position x to the final end of the polymer chain r_1 respectively. The same reasoning is made with the chain(2). ψ is the field placed at x and X on chain(1) and (2), respectively. (b): the cross-link of the two chains imposes the same position in space so that $\psi(r(s)) = \psi(R(S)) = \psi(x)$*

position x and X of either chain, we constrain the two chains to meet at one exact spatial positions so that $r(s) = R(S)$. The mathematical representation of such constraint is given by the use of the Dirac delta functional $\delta(r(s)-R(S))$ (see section 3.2.0.1 for more elaboration). This latter function reveals which monomer on which chain is linked to which monomer on the other chain. The delta functional is imposed into the partition function of the network and we have the following expression:

$$Z = \int [\mathrm{d}\, r(s)]\, [\mathrm{d}\, R(S)]\, G[R(S)]\, \delta(r(s) - R(S)). \tag{3.1}$$

Where $G[R(S)]$ is the probability distribution of the chain. The chain being Gaussian, the Wiener measure is:

$$G[R(S)] = \aleph \exp\left(-\frac{3}{2\,l}\int_0^L \left(\frac{\partial R(S)}{\partial S}\right)^2 \mathrm{d}S\right). \tag{3.2}$$

$\aleph = \left(\frac{3}{2\,\pi\,l\,S}\right)^{3/2}$ is the normalisation constant and l is the the Kuhn length. Having a look at the Fig. 3.1, the Green's function of the system of the two chains cross-linked can be divided and given by the composition property of the green's function called the Chapman-Kolmogorov equation [11]. This equation

represents the average over all the possible spatial positions of the junction point $x = X$. The actual Green function is given by:

$$G(\vec{r}, s) = \aleph \int [\mathrm{d}\vec{r}(\tau)]\, e^{-\int_0^s d\tau \left(\frac{\partial \vec{r}}{\partial \tau}\right)^2} \delta(\vec{r}(0) - \vec{r}(s) - \vec{r}) \tag{3.3}$$

Starting from the end of one chain and ending at one end of the other chain, one can write:

$$\int_{\mathbb{R}} \mathrm{d}^3 x\, G(r_0 - x, s)\, G(x - r_1, L - s) = G(r_0 - r_1, L), \tag{3.4}$$

$$\int_{\mathbb{R}} \mathrm{d}^3 X\, G(R_0 - X, S)\, G(X - R_1, L - S) = G(R_0 - R_1, L). \tag{3.5}$$

We will be using those two equations in all our calculations. $G(r_0 - x, s)$ represents the probability distribution to go from one end (r_0) of the chain(1) and end at the position x knowing that, the distance between those two points is s; $G(x - r_1, L - s)$ is the probability of going from x to the other end (r_1) of the chain(1) with a distance $L - s$. $G(r_0 - r_1, L)$ is the probability of going from one end (r_0) of the chain(1) to the other end (r_1) with a distance L between the two ends. The same interpretation holds for Green's functions of the chain(2). The statistical weight of whole the system of the two chain linked at the position x is then:

$$\begin{aligned} Z = \int \mathrm{d}^3 x\, G(r_0 - x, s)\, G(x - r_1, L - s) \\ \times G(R_0 - x, S)\, G(x - R_1, L - S) \end{aligned} \tag{3.6}$$

With $G(r_0 - x, s) = \left(\frac{3}{2\,\pi\, s\, l}\right)^{3/2} \exp\left(-\frac{3}{2ls}(r_0 - x)^2\right)$ and $\int G(r_0 - x, s) d^3 r_0 = 1$. Similar formula is applied for the other probabilities. Including the field placed at the middle of the chains (Fig. 3.1), one can write the partition function as:

$$\begin{aligned} Z[\psi] = \int \mathrm{d}^3 x\, G(r_0 - x, s)\, \psi(x)\, G(x - r_1, L - s) \\ \times G(R_0 - X, S)\, \psi(X)\, G(X - R_1, L - S)\, \delta(r(s) - R(S)). \end{aligned} \tag{3.7}$$

3.2.0.1 Wick's theorem

The problem of polymer linkage was clearly treated by Edwards, Freed (1970) and other [2, 3, 24, 25, 51]. We recall below some basic averages using Gaussian distribution as statistical weight. The following formulae are generally used in field theory. We Consider the field ϕ at each point r, the Gaussian basic identity:

$$\frac{\int \phi^2 e^{\frac{-1}{2} a^{-1} \phi^2} [\mathrm{d}\,\phi]}{\int e^{\frac{-1}{2} a^{-1} \phi^2} [\mathrm{d}\,\phi]} = a. \tag{3.8}$$

The more generalised formulae are given by a similar expression:

$$\frac{\int \phi_\alpha \phi_\beta e^{\frac{-1}{2}\sum_\alpha \phi_\alpha^2 a_\alpha^{-1}} \mathrm{d}\,\phi}{\int e^{\frac{-1}{2}\sum_\alpha a_\alpha^{-1}\phi_\alpha^2} \mathrm{d}\,\phi} = \delta_{\alpha\beta} a_\beta. \tag{3.9}$$

If we consider now that we have a $n \times n$ matrix a and its inverse a^{-1}, we rewrite the Gaussian formulae above and write it as follow:

$$\frac{\int \phi_\alpha \phi_\beta e^{\frac{-1}{2}\sum_i \sum_j \phi_i (a_{ij}^{-1}) \phi_j} \mathrm{d}\,\phi}{\int e^{\frac{-1}{2}\sum_i \sum_j \phi_i (a_{ij}^{-1}) \phi_j} \mathrm{d}\,\phi} = a_{\alpha\beta}, \tag{3.10}$$

It is often useful to use the complex conjugate of the field. This complex conjugate ϕ^* is a complementary field of the initial field ϕ.

$$\begin{aligned} \langle \phi(r)\phi^*(r')\rangle &= \frac{\int \phi(r)\,\phi^*(r')\, e^{-1/2\int(\phi_1^2(r)+\phi_2^2(r))\,\mathrm{d}^3 r}[\mathrm{d}\,\phi_1]\,[\mathrm{d}\,\phi_2]}{\int e^{-1/2\int(\phi_1^2(r)+\phi_2^2(r))\,\mathrm{d}^3 r}[\mathrm{d}\,\phi_1]\,[\mathrm{d}\,\phi_2]} \\ &= \delta(r-r'). \end{aligned} \tag{3.11}$$

$$\begin{aligned} \langle \phi(r)\phi(r')\rangle &= \frac{\int \phi(r)\,\phi(r')\, e^{-1/2\int(\phi_1^2(r)+\phi_2^2(r))\,d^3 r}\,[\mathrm{d}\,\phi_1]\,[\mathrm{d}\,\phi_2]}{\int e^{-1/2\int(\phi_1^2(r)+\phi_2^2(r))d^3 r}\,[\mathrm{d}\,\phi_1]\,[\mathrm{d}\,\phi_2]} \\ &= 0. \end{aligned} \tag{3.12}$$

with $\phi = \phi_1 + i\phi_2$, $\phi^* = \phi_1 - i\phi_2$. The notation $\int_{\mathbb{R}}[\mathrm{d}\phi]$ stands for the functional integration over the field ϕ. The equation (3.11) is called the Wick's theorem, and its more generalized form is written as followed

$$\begin{aligned} \langle \phi(r_1)\ldots\phi(r_n)\,\phi^*(r_1')\ldots\phi^*(r_m')\rangle &= \aleph \int [\mathrm{d}\,\phi_1]..\,[\mathrm{d}\,\phi_n]\,[\mathrm{d}\,\phi_1^*]..\,.[\mathrm{d}\,\phi_m^*]\,\phi(r_1)\ldots\phi(r_n) \\ &\quad \times \phi^*(r_1')\,\phi^*(r_2')\ldots\phi^*(r_m')\, e^{-\int \phi(r)\,\phi^*(r)\,\mathrm{d}^3 r} \\ &= \begin{cases} 0 & \text{for} \quad n \neq m \\ \displaystyle\sum_{\text{all pairs of } r_i \text{ and } r_j'} \prod_{i,j=1} \delta(r_i - r_j') & \text{for} \quad n = m. \end{cases} \end{aligned} \tag{3.13}$$

With $\aleph^{-1} = \int e^{-\int \phi(r)\phi^*(r)\,d^3 r}[\mathrm{d}\,\phi_1]\ldots[\mathrm{d}\,\phi_n]\,[\mathrm{d}\,\phi_1^*]\ldots[\mathrm{d}\,\phi_m^*]$. The Dirac delta function is used to enforce the linkage at the positions r_n and r_m'. According to the theorem, the cross-link occur only between a field and its complex i.e. between $\phi(r_L)$ and $\phi^*(R_L)$ for example. It does not occur between a pair of $\phi(r_L)$ or a pair of $\phi^*(r_L)$. In other words, the cross-link is established only between two complementary fields. Consequently, the field is placed on the chain and its complex on the cross-linker in order to establish the cross-link between the chains using the cross-linkers.

3.3 Model description

The field theory representation of a permanent polymer network was elaborated by Edwards (1988) [2] and later developed by Fantoni and Müller-Nedebock (2011) [3] for an reversible system with different type of linking. We extend the model by including the reversible cross-linkers inside the permanent polymer network. We consider a mixture of a fixed number N of polymeric chains each with the same contour length L. We include a fixed number N_a of reversible cross-linkers, also called " reversible-movable or simply movable cross-linker " due to its mobility inside the network formed. The reversible-movable cross-linker has a fixed functionality[2] equal to 2. The same mixture contents N_p number of permanent (or "passive") cross-linkers each with functionality p. Each chain is considered having identical properties and taken as ideal (Gaussian) chain for simplicity purpose. We would like to count all the possible network configurations that can be extracted from that particular mixture keeping in our mind that all the network are randomly formed. In order to do that, we propose to split the work in two and after combine them to have a reversible and permanent cross-link in the same network. This will not affect the final representation or the physics behind this is for us a way to clear things from the beginning so that no one get lost. We present first a simple network of two chains and the reversible cross-link We will notice that for the present model, we have chosen to have the reversible cross-link laying somewhere along the chain, and the permanent cross-link at the very end of the chain. At the end of the present formulation, we will make sure that we still treat the two type of cross-links differently in terms of replicas (annealed average for movable cross-link and quenched average for permanent cross-link).

3.3.1 Reversible network

A reversible network is a network made of chains and reversible cross-linkers. As stated above, the reversible cross-linker has a functionality 2 therefore, it can cross-link two chains. Using the field theory formulation, we can place the field ψ at a random position along the chain and its complex field ψ^* at the end of each reversible cross-linker (see Fig. 3.2). The reversible cross-link can

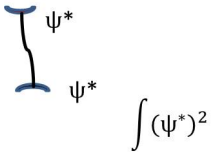

Figure 3.2: *Reversible cross-linker made of two available seats.*

[2]the functionality is the number of chains that the cross-linker can connect.

change place while moving and has therefore a non-processive properties like the myosin II motor protein . When we add a bias directional along the arc of the chains, we can model a motor protein albeit in quasi-equilibrium setting (see chapter 4). The partition function of the network represented in Fig. 3.1 is given by the following expression:

$$\begin{aligned} Z_{rev} = & \int_0^L \mathrm{d}\, s \int_0^L \mathrm{d}\, S \int [\mathrm{d}\, \psi(x)] \int [\mathrm{d}\, \psi^*(x)] \\ & \int \mathrm{d}^{\,3}\, x\, G(r_0 - x, s)\, \psi(x)\, G(x - r_1, L - s) \\ & \int \mathrm{d}^{\,3}\, X\, G(R_0 - X, S)\, \psi(X)\, G(X - R_1, L - S) \\ & \times \left[\int \mathrm{d}^3\, x\, \psi^{*2}(x) \right] e^{-\int \mathrm{d}^3\, x\, \psi(x)\, \psi^*(x)}. \end{aligned} \tag{3.14}$$

The expression $\left[\int \mathrm{d}^3\, x\, \psi^{*2}(x)\right]$ (one cross-linker) counts the cross-links. Here, $e^{-\int \mathrm{d}^3\, x\, \psi(x)\, \psi^*(x)}$ represents the cross-linkage constraint between the two chains and the cross-linker agent. If one wants to count all the possible positions taken by the reversible cross-linker inside the same topology network, one needs to consider the cross-linker position as a degree of freedom. Since the cross-linkers move along the chains, the average over all the possible position occupied by it is called the *"annealed disorder"* and treated as a normal degree of freedom in the partition function (see section 2.3.1.3). The cross-linker position replicates itself as well as the fields and the distance from the ends of the chains to the cross-link position (This is because the reversible cross-link changes position constantly while moving). Let n be the number of replicas, the statistical weight for all the n^{th} replicas is given by:

$$\begin{aligned} Z^n_{rev} = & \{ \prod_{\alpha=1}^{n} \int_0^L \mathrm{d}\, s_\alpha \int_0^L \mathrm{d}\, S_\alpha \int [\mathrm{d}\, \psi_\alpha(x_\alpha)] \int [\mathrm{d}\, \psi^*_\alpha(x_\alpha)] \\ & \int \mathrm{d}^3\, x_\alpha\, G(r_0 - r(x_\alpha), s_\alpha) \psi_\alpha(x_\alpha) G(x_\alpha - r_1, L - s_\alpha) \\ & \int \mathrm{d}^3\, X_\alpha\, G(R_0 - X_\alpha, S_\alpha)\, \psi_\alpha(X_\alpha)\, G(X_\alpha - R_1, L - S_\alpha) \\ & \times \left[\int \mathrm{d}^3\, x_\alpha\, \psi^{*2}_\alpha(x_\alpha) \right] \} \, e^{-\sum_{\alpha=1}^{n} \int \mathrm{d}^3\, x_\alpha\, \psi_\alpha(x_\alpha)\, \psi^*_\alpha(x_\alpha)}. \end{aligned} \tag{3.15}$$

For a more dense system with N chains and N_a movable cross-linker agents, the statistical weight of the system including all the replicas, is given by:

$$\begin{aligned} Z_{rev}^{n} = & \prod_{\alpha=1}^{n} \int_0^L \mathrm{d}\, s_\alpha \int_0^L \mathrm{d}\, S_\alpha \int [\mathrm{d}\, \psi_\alpha(x_\alpha) \int [\mathrm{d}\, \psi_\alpha^*(x_\alpha)] \\ & \times \left[\int \mathrm{d}^3\, x_\alpha\, G(r_0 - x_\alpha, s_\alpha)\, \psi_\alpha(x_\alpha)\, G(x_\alpha - r_1, L - s_\alpha) \right]^{N/2} \\ & \times \left[\int \mathrm{d}^3\, X_\alpha\, G(R_0 - X_\alpha, S_\alpha)\, \psi_\alpha(X_\alpha)\, G(X_\alpha - R_1, L - S_\alpha) \right]^{N/2} \\ & \times \left[\int \mathrm{d}^3\, x_\alpha\, \psi_\alpha^{*2}(x_\alpha) \right]^{N_a} e^{-\sum_{\alpha=1}^{n} \int \mathrm{d}^3\, x_\alpha\, \psi_\alpha(x_\alpha)\, \psi_\alpha^*(x_\alpha)}. \end{aligned} \tag{3.16}$$

This expression supposes that we have equal $N/2N_a$ number of each components of chains that cross-link.

3.3.2 Permanent part of the network

The permanent network is a network formed with chains and permanent cross-linkers. A cross-linker is called permanent when as soon it connects the chains, it freezes. For the present model, we suppose that this particular cross-linker links the chains only at their very ends. The functionality of the permanent cross-linker is p. We chose for $p > 2$ to avoid a situation where one can have a very long chain instead of a network like structure. To differentiate from the reversible cross-link, we label the permanent cross-linker with different field ϕ^*. The end of the chains are then label with the corresponding field ϕ. The wick's theorem ensures the connectivity between the chains and the cross-linkers (see Fig. 3.3). A variable is called quenched if and only if it completely freezes inside

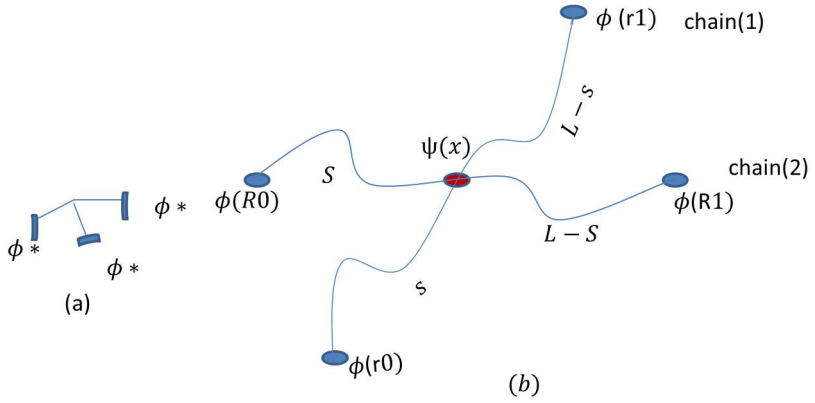

Figure 3.3: *(a): the passive cross-linker agent with functionality 3; (b): cross-link of chains (1) and (2) by the permanent (at the ends) and the reversible cross-linker along the chains.*

the system after the network is formed. This type of cross-link does not allow individual chains to be totally relaxed. In this case, the time scale associated with the randomness of the cross-linkage is too long so that the variable is view as frozen even when the chains fluctuates [2, 11, 22, 24, 27, 57, 58]. Taking into account all the n replicas of the network, the fields are now:

$$\phi(r_0^{(\alpha)}) \rightarrow \phi(r_0^{(1)}, ..., r_0^{(n)}), \tag{3.17}$$
$$\phi(r_1^{(\alpha)}) \rightarrow \phi(r_1^{(1)}, ..., r_1^{(n)}). \tag{3.18}$$

The label $\alpha = 1, ..., n$ counts all the replicas possible of the system, n being the number of replicas [2, 22]. The partition function for only a permanent network formed by N chains and N_p permanent cross-linkers with functionality p is given by the following expression:

$$\begin{aligned} Z_{per}^n = & \int [\mathrm{d}\,\phi(r^{(\alpha)})]\,[\mathrm{d}\,\phi^*(r^{(\alpha)})] \\ & \times \left[\int \mathrm{d}^3\, r_0^{(\alpha)}\, \mathrm{d}^3\, r_1^{(\alpha)}\, \phi(r_0^{(\alpha)}) \prod_{\alpha=1}^{n} G(r_0^{(\alpha)} - r_1^{(\alpha)}, L)\, \phi(r_1^{(\alpha)})\right]^N \\ & \times \left(\int \phi^{*p}(r^{(\alpha)})\right)^{N_p} e^{-\prod_{\alpha}^{n} \int_{r^{(\alpha)}} \phi(r^{(\alpha)})\, \phi^*(r^{(\alpha)})}. \end{aligned} \tag{3.19}$$

Here we have ignored the reversible cross-link (see Fig. 3.3).

3.3.3 Reversible cross-link into permanent network

Illustrated by the Fig. 3.4, the present network model contains both reversible and permanent cross-links. Including the two type of cross-linkers in the same network can be a challenging problem. Nevertheless, since we have already presented the network that contains the two cross-linkers each separately, we now combine to have the complete network. The equations (3.16) and (3.19) together give:

$$\begin{aligned} Z^n = & \aleph \int [\mathrm{d}\,\psi_\alpha(x_\alpha)]\,[\mathrm{d}\,\psi_\alpha^*(x_\alpha)]\,[\mathrm{d}\,\phi(r^{(\alpha)})]\,[\mathrm{d}\,\phi^*(r^{\alpha})] \\ & \times \left[\prod_{\alpha=1}^{n} \int \mathrm{d}\, r_0^{(\alpha)}\, \mathrm{d}\, r_1^{(\alpha)} \int_0^L \mathrm{d}\, s_\alpha\, \mathrm{d}\, x_\alpha\, \phi(r_0^{(\alpha)}) \prod_{\alpha=1}^{n} G_\alpha \times (1 + \psi_\alpha(x_\alpha)\, e^{-\beta\,\eta})\, G'_\alpha \times \phi(r_1^{(\alpha)})\right]^N \\ & \times \left[\int \mathrm{d}^3\, r^{(\alpha)}\, \phi^{*p}(r^{(\alpha)})\right]^{N_p} \left[\int \mathrm{d}^3\, x_\alpha\, \psi_\alpha^{*2}(x_\alpha)\right]^{N_a} \\ & \times e^{-\sum_{\alpha=1}^{n} \int \mathrm{d}^3\, x_\alpha\, \psi_\alpha(x_\alpha)\, \psi_\alpha^*(x_\alpha)}\; e^{-\prod_{\alpha}^{n} \int \mathrm{d}^3\, r^{(\alpha)}\, \phi(r^{(\alpha)})\, \phi^*(r^{(\alpha)})}. \end{aligned} \tag{3.20}$$

Where $e^{-\beta\eta} = z$ is the fugacity or the Boltzmann factor which insures the "*on / off*" ("attachment/ detachment") behaviour of the reversible cross-link,

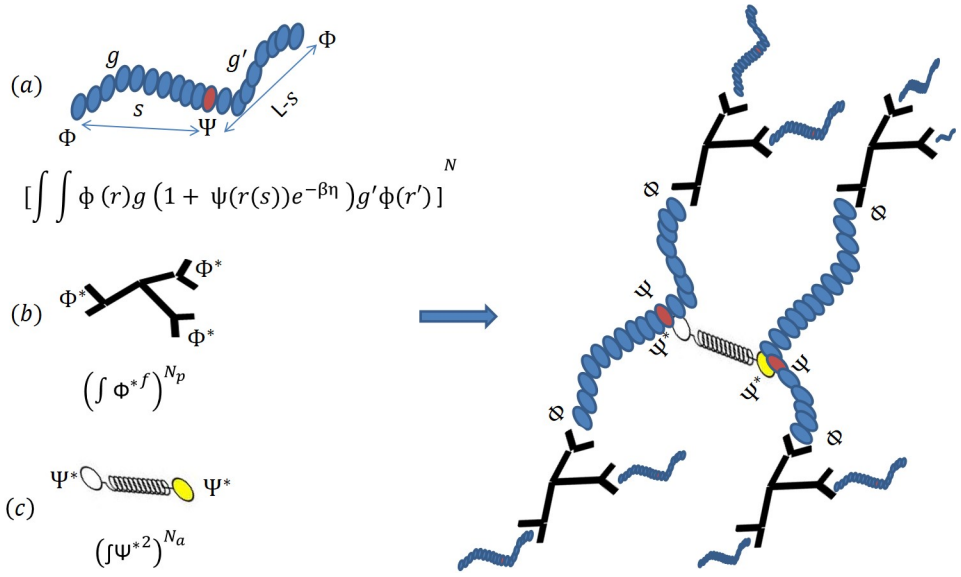

Figure 3.4: *$g = G(r - r(s), s)$ and $g' = G(r(s) - r', L - s)$ are used as the shorthand notation for the Green's functions, $r = r_0 = r(s_0)$ and $r' = r_L = r(s_L)$.s is the arc length of the chain, N is the number of polymer chains. Network Formation: (a)Polymeric chain. (b) Permanent cross-linker and (c) Reversible cross-linker assumed to be represented by a spring attached at each motor head. The combination of all those three components gives a network where the reversible and permanent cross-linker are seated along and at the ends of the chains respectively.*

η is the chemical potential and $\beta = 1/k_B T$. If the reversible cross-link is removed, then, $\psi_\alpha(x_\alpha)$ is turned off i.e. $\psi_\alpha(x_\alpha) = 0$ and we have only a permanent network (section 3.3.2). For simplification of the coming calculus, we suppose that the reversible cross-link seats at the middle of the chains, i.e.: $s_\alpha = L - s_\alpha = L/2$ and also $S_\alpha = L - S_\alpha = L/2$. The equation (3.20) shows a difference in the way the cross-link replicas are count (See inside the exponential of equation (3.20)). The fixed cross-links are handle as a *product* over all the replicas inside the exponential whereas the reversible (movable) cross-link appear as a *sum* over the replicas indices inside the exponential [24, 25, 51]. In order to ease the calculation, we exponentiate the whole expression using the integration formula:

$$X^N = \frac{N!}{2\pi i} \oint_c e^{\mu X - (N+1)\log\mu}\, \mathrm{d}\mu. \tag{3.21}$$

For the following calculation, we suppose that the whole polymer network has a contour length L. Applying equation (3.21) into equation (3.20), and supposing that N, N_a and $N_p \gg 1$ such that $N_{,a,p} + 1 \simeq N_{,a,p}$ (where $N_{,a,p}$ equivalent to N, N_a and N_b, respectively). The constants $N_{,a,p}$ and 8π in front of the equation will be considered inside the normalization constant. μ, μ_a and μ_p represent the chemical potentials for the chain, the reversible and permanent cross-linkers respectively. Those variables will treated as constant

upon the saddle point approximation. Consequently, they will be neglected in the calculation for simplification since they do not influence the physical meaning of the result. The partition function finally yield:

$$Z^n = \aleph \oint_c \mathrm{d}\,\mu\,\mathrm{d}\,\mu_a\,\mathrm{d}\,\mu_p \int \prod_{\alpha=1}^{n} [\mathrm{d}\,\psi_\alpha]\,[\mathrm{d}\,\psi_\alpha^*]\,[\mathrm{d}\,\phi]\,[\mathrm{d}\,\phi^*]\,e^{-\chi(\mu,\mu_a,\mu_p,\psi,\psi^*,\phi,\phi^*)}. \quad (3.22)$$

where the functional $-\chi$ plays the role of the expression $-\beta\,H[\psi,\psi^*,\phi,\phi^*]$ which is the effective functional Hamiltonian with $\beta = 1/k_BT$. $G_\alpha = G(r_0^{(\alpha)} - x_\alpha, L/2)$, $G'_\alpha = G(x_\alpha - r_1^{(\alpha)}, L/2)$ and

$$\begin{aligned} -\chi = \mu \int_{r_0^{(\alpha)}, r_1^{(\alpha)}} \int_{x_\alpha} \prod_{\alpha=1}^{n} \phi(r_0^{(\alpha)})\,G_\alpha(1+\psi_\alpha\,e^{-\beta\eta})\,G'_\alpha\,\phi(r_1^{(\alpha)}) \\ - \int_{r^{(\alpha)}} \phi\phi^* - \sum_{\alpha=1}^{n} \int_{x_\alpha} \psi_\alpha\psi_\alpha^* + \mu_a \sum_{\alpha=1}^{n} \int_{x_\alpha} \psi_\alpha^{*2}(x_\alpha) + \mu_p \int_{r^{(\alpha)}} \phi^{*p}(r^{(\alpha)}) \quad (3.23) \\ - N\log\mu - N_a\log\mu_a - N_p\log\mu_p. \end{aligned}$$

The contribution $(-N\,\log\mu - N_a\,\log\mu_a - N_p\,\log\mu_p)$ is neglected in the saddle point approximation for future calculations because it does not influence the physical meaning of the result.

3.3.3.1 Example

For the sake of clarity on the formalism elaborated above, we here consider an example of polymers network with permanent and reversible cross-link. We suppose $N_p = 4$ permanent cross-linkers with functionality $p = 3$, $N_a = 3$ reversible cross-linkers with functionality $a = 2$ and $N = 6$ chains. For that precise mixture, we count three of network topology that can be formed (see Fig. 3.5) with that mixture. Including all the possible replicas of the system, we count all the possible networks configuration formed with that same mixture. The partition function using the properties of the Gaussian chains is given by equation 3.24.

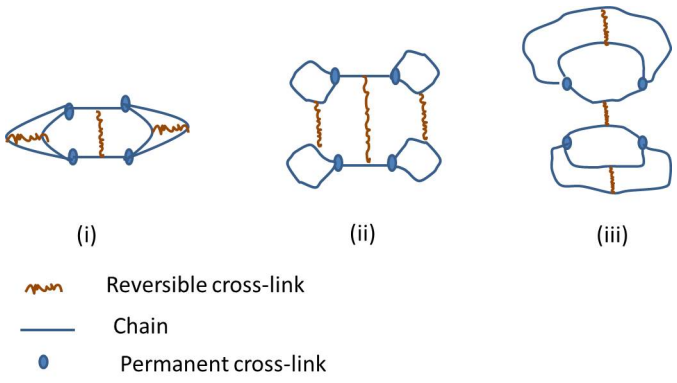

Figure 3.5: *Example of network form with 4, 3 and 6 permanent, reversible cross-linkers and chains respectively.*

$$
\begin{aligned}
Z_{\text{example}} = & \iiint \phi(r_1)\, g(r_1, r(x_1))\, \psi(r(x_1))\, g(r(x_1), r_1')\, \phi(r_1') \mathrm{d}^3 r_1 \mathrm{d}^3 r_1'\, [\mathrm{d}r(x_1)] \\
& \int .. \phi(r_2)\, g_2\, \psi(r(x_2))\, g_2'\, \phi(r_2') \int .. \phi(r_3)\, g_3\, \psi(r(x_3))\, g_3'\, \phi(r_3') \int .. \phi(r_4) \\
& g_4 \psi(r(x_4))\, g_4'\, \phi(r_4') \int .. \phi(r_5)\, g_5\, \psi(r(x_5))\, g_5'\, \phi(r_5') \int .. \phi(r_6)\, g_6\, \psi(r(x_6)) \\
& g_6'\, \phi(r_6') \int \psi^{*2}(r(x_a))\, [\mathrm{d}(r(x_a))] \int \psi^{*2}(r(x_b)) \int \psi^{*2}(r(x_c)) \int \phi^{*3}(r_i) \\
& \mathrm{d}^3 r_i \int \phi^{*3}(r_{\mathrm{j}}) \int \phi^{*3}(r_k) \int \phi^{*3}(r_{\mathrm{l}}) \\
= & \int \ldots \int \prod_{\epsilon,\gamma=1}^{6} g_\epsilon\, g_\gamma' \, [\delta(r_1 - r_i)\, \delta(r_1' - r_{\mathrm{l}})\, \delta(r_2 - r_i)\, \delta(r_2' - r_{\mathrm{l}})\, \delta(r_3 - r_i) \\
& \delta(r_3' - r_{\mathrm{j}})\, \delta(r_4 - r_{\mathrm{l}})\, \delta(r_4' - r_{\mathrm{k}})\, \delta(r_5 - r_{\mathrm{j}})\, \delta(r_5' - r_{\mathrm{k}})\, \delta(r_6 - r_{\mathrm{j}})\, \delta(r_6' - r_{\mathrm{k}}) \quad (3.24) \\
& \delta(r(x_1) - r(x_2))\, \delta(r(x_3) - r(x_4))\, \delta(r(x_5) - r(x_6))]\, \mathrm{d}^3\, \mathrm{all}[\mathrm{d}]\mathrm{all} \\
& + \text{all other way to construct the network with topology (i)} \\
& + \int \ldots \int \prod_{\epsilon,\gamma=1}^{6} g_\epsilon\, g_\gamma' [\delta(r_{1,\mathrm{j}})\, \delta(r_{1,\mathrm{j}}')\, \delta(r_{2,i})\, \delta(r_{2,i}')\, \delta(r_{3,\mathrm{k}})\, \delta(r_{3,\mathrm{k}}')\, \delta(r_{4,\mathrm{l}})\, \delta(r_{4,l}') \\
& \delta(r_{5,i})\, \delta(r_{5,\mathrm{k}}')\, \delta(r_{6,\mathrm{j}})\, \delta(r_{6,\mathrm{l}}')\, \delta(r(x_{1,2}))\, \delta(r(x_{3,4}))\, \delta(r(x_{5,6}))] \mathrm{d}^3\, \mathrm{all}[\mathrm{d}]\, \mathrm{all} \\
& + \text{all other way to construct the network with topology (ii)} \\
& + \int \ldots \int \prod_{\epsilon,\gamma=1}^{6} g_\epsilon\, g_\gamma' [\delta(r_{1,i})\, \delta(r_{1,\mathrm{j}}')\, \delta(r_{2,i})\, \delta(r_{2,i}')\, \delta(r_{3,i})\, \delta(r_{3,\mathrm{j}}')\, \delta(r_{4,\mathrm{l}})\, \delta(r_{4,\mathrm{k}}') \\
& \delta(r_{5,\mathrm{l}})\, \delta(r_{5,\mathrm{k}}')\, \delta(r_{6,\mathrm{l}})\, \delta(r_{6,\mathrm{k}}')\, \delta(r(x_{1,2}))\, \delta(r(x_{3,4}))\, \delta(r(x_{5,6}))]\, \mathrm{d}^3\, \mathrm{all}[\mathrm{d}]\, \mathrm{all} \\
& + \text{all other way to construct the network with topology (iii).}
\end{aligned}
$$

where the indices (i, j, k, l) indicating the permanent cross-links; (a, b, c) the three reversible cross-links and $(1, 2, 3, 4, 5, 6)$ the polymers chains indices. r and r' represent the two ends of the chains. g is the Green's function shorthand notation. The delta functional imposes the cross-linkage at a specific position depending on the network configuration.

3.4 Saddle point approximation

Equation (3.22) shows that the field theoretical formulation of the Hamiltonian of the system that is highly non-Gaussian. In such conditions, the saddle point approximation becomes necessary. This approximation neglects defects (like loop formation) in the network [2, 22]. We perform the saddle point approximation (SPA) in order to have a Gaussian form of the expression (equation (3.23)) and then, ease all the integrations over the field variables. We first solve the set of saddle point equations in order to find the critical points also called the saddle point solutions noted $(\overline{\psi}, \overline{\psi^*})$ and $(\overline{\phi}, \overline{\phi^*})$. The set of saddle point equations is given at equation (3.25). Including all the replicas of the system, we count a set of $2n$ equations from the derivation over the reversible cross-link ψ and ψ^* (this is due to the annealed disorder). We also count $(n+1)$ equations from the derivative over the permanent cross-link ϕ and ϕ^*. Proceeding with the functional derivative over each variables, we end up with the following set of non-usual equations for any α^{th} replica. We assume that all the replicas are identical.

$$\begin{cases} \dfrac{\delta(-\chi)}{\delta\,\psi_\alpha}|_{(\overline{\psi},\overline{\psi^*}),(\overline{\phi},\overline{\phi^*})} = 0, & \text{(e1)} \\ \dfrac{\delta(-\chi)}{\delta\psi^*_\alpha}\,|_{(\overline{\psi},\overline{\psi^*}),(\overline{\phi},\overline{\phi^*})} = 0, & \text{(e2)} \\ \dfrac{\delta(-\chi)}{\delta\,\phi}|_{(\overline{\psi},\overline{\psi^*}),(\overline{\phi},\overline{\phi^*})} = 0, & \text{(e3)} \\ \dfrac{\delta(-\chi)}{\delta\,\phi^*}\,|_{(\overline{\psi},\overline{\psi^*}),(\overline{\phi},\overline{\phi^*})} = 0. & \text{(e4)} \end{cases} \tag{3.25}$$

After having performed the functional derivative, we have:

$$\begin{cases} \mu \int_{r_0^{(\alpha)},r_1^{(\alpha)}} \overline{\phi}(r_0^\alpha) \prod_{\alpha=1}^{n} [G(r_0^\alpha - r_1^\alpha, L)\, e^{-\beta\,\eta}]\, \overline{\phi}'(r_1^\alpha) - \sum_{\alpha=1}^{n} \overline{\psi}^*_\alpha(y_\alpha) = 0, & \text{(e1)} \\ -\sum_{\alpha=1}^{n} \overline{\psi_\alpha}(y_\alpha) + 2\mu_a \sum_{\alpha=1}^{n} \overline{\psi}^*_\alpha(y_\alpha) = 0, \quad \forall\alpha & \text{(e2)} \\ -\overline{\phi}^*(R^\alpha) + 2\,\mu \int_{x_\alpha,r_0^{(\alpha)}} \overline{\phi}(r_0^{(\alpha)}) \prod_{i=1}^{n} \left[G(r_0^\alpha - R^\alpha, L)(1 + \overline{\psi}_\alpha(y_\alpha)\, e^{-\beta\,\eta})\right] = 0, & \text{(e3)} \\ -\overline{\phi}(R^\alpha) + \mu_p\, p\, \overline{\phi}^{*(p-1)}(R^\alpha) = 0. & \text{(e4)} \end{cases} \tag{3.26}$$

Although it has been a long debate about the replica symmetry, for the purpose of simplicity, and because we know that it works very well, we will here assume that all the replicas are symmetric (replicas symmetry ansatz) [22, 59, 60], we can write the Green's function as: $G_\alpha = G(r_o^{(\alpha)} - x_\alpha), G'_\alpha = G(x_\alpha - r_1^{(\alpha)})$ and the field $\overline{\psi}_\alpha = \overline{\psi}_\alpha(x_\alpha), \overline{\phi} = \overline{\phi}(r_0^{(\alpha)}), \overline{\phi}' = \overline{\phi}(r_1^{(\alpha)})$. We solve equation (3.26) by using simple substitution until we get only one equation with only one variable $(\overline{\psi}^*)$. We then perform the integration and by taking the Fourier transform of both parts of the equation, we identify the coefficients. The variable $\overline{\phi}^*$ is calculated using the similar combination made for the variable $(\overline{\psi}^*)$. We use the equation (3.5) to ease the calculations. We propose to calculate the saddle point solution for one replica and generalise later for all the replicas.

3.4.1 Saddle point solution for all reversible cross-links: $n = 1$

The set of saddle point equations is solved using the Gaussian assumption on the Green's function and the fields: The Fields are assumed to have a Gaussian distribution like structure. We can therefore write the expression: $\overline{\phi}^*(r) = A\, e^{-a\, r^2}$, $\overline{\psi}^*(x) = B\, e^{-b\, x^2}$ ie, $(\alpha = 1)$ and the Green's function $G\, G' = G(r_o - x, L/2)G(x - r_1, L/2) = G(r_0 - r_1, L) = \aleph \exp(-\frac{3}{2\, l\, L}\,(r_0 - r_1)^2)$. We assume that the is always enough reversible cross-linker in the system i.e. $(\psi_\alpha\, e^{-\beta\eta} \gg 1)$. Detailed steps of the calculation are developed in Appendix A.1. We use substitution between the equations until we have one equation with only one unknown. We replace the fields and the Green's function by their Gaussian expression and then solve for the constants a, b, A and B.

$$\overline{\psi}(x) = 2\,\mu_a\, B\, \exp\left[-b\, x^2\right] \quad , \quad \overline{\psi}^*(x) = B \exp\left[-b\right], \tag{3.27}$$

$$\overline{\phi}(r) = \mu_p\, p\, A^{(p-1)} \exp\left[-a\, r^2\right] \quad , \quad \overline{\phi}^*(r) = A^{(p-1)}\, \exp\left[-a\, r^2\right]. \tag{3.28}$$

with the constants for

$$a = \frac{-3(p-1)}{lL(p-2)}, \quad b = \frac{-6(p-1)}{lL(p-2)}, \tag{3.29}$$

$$A = \frac{2^{2/3} 3^{1/3} e^{(-2\beta\eta)(e^{5\beta\eta} l^2 L^2)^{2/3}}}{\pi^2((-lL)^{7/2}\sqrt{lL})^{2/3}} \quad \text{for } N = 1, p = 3, \tag{3.30}$$

$$B = \frac{e^{-3\beta\eta}\sqrt{lL}(e^{5\beta\eta} l^2 L^2)^{2/3}((-lL)^{7/2}\sqrt{lL})^{4/3}\sqrt{\pi}}{2^{1/3} 3^{1/6} l^7 L^7}. \tag{3.31}$$

Including all the replicas of the system, we have:

$$\begin{aligned} \overline{\psi_\alpha}(x_\alpha) &= \prod_{\alpha=1}^{n} 2\,\mu_a\, B\, \exp\left[-\frac{6\,(p-1)}{l\,L\,(p-2)}\, x_\alpha^2\right] \\ &= (2\,\mu_a\, B)^n \exp\left[-\frac{6(p-1)}{lL(p-2)} \sum_{\alpha=1}^{n} x_\alpha^2\right], \end{aligned} \tag{3.32}$$

$$\begin{aligned}\overline{\psi^*_\alpha}(x_\alpha) &= \prod_{\alpha=1}^{n} B \exp\left[-\frac{6\,(p-1)}{l\,L\,(p-2)}x_\alpha^2\right] \\ &= B^n \exp\left[-\frac{6(p-1)}{lL(p-2)}\sum_{\alpha=1}^{n} x_\alpha^2\right],\end{aligned} \tag{3.33}$$

$$\begin{aligned}\overline{\phi}(r^{(1)}, r^{(2)}, ..., r^{(n)}) &= \mu_p\, pA^{(p-1)} \exp\left[-\frac{6\,(p-1)}{l\,L\,(p-2)}\,(r^{(1)}, r^{(2)}, ..., r^{(n)})^2\right] \\ &= \mu_p\, pA^{(p-1)} \exp\left[-\frac{6\,(p-1)}{l\,L\,(p-2)}\prod_{\alpha=1}^{n}(r^{(\alpha)})^2\right],\end{aligned} \tag{3.34}$$

$$\begin{aligned}\overline{\phi^*}(r^{(1)}, r^{(2)}, ..., r^{(n)}) &= A^{(p-1)} \exp\left[-\frac{6(p-1)}{l\,L\,(p-2)}\,(r^{(1)}, r^{(2)}, ..., r^{(n)})^2\right] \\ &= A^{(p-1)} \exp\left[-\frac{6(p-1)}{l\,L\,(p-2)}\prod_{\alpha=1}^{n}(r^{(\alpha)})^2\right].\end{aligned} \tag{3.35}$$

Where $(r^{(1)}, ..., r^{(n)}) = r^{(\alpha)} \neq \sum_{\alpha=1}^{n} r^{(\alpha)}$. The fixed cross-links are handle as a *product* over all the replicas inside the exponential whereas the reversible (movable) cross-link appear as a *sum* over the replicas indices inside the exponential [24, 25, 51].

3.4.2 Average density

In the assumption of a dense system, we can always think of viewing the two cross-links as collective variables. The calculation of the average density of each cross-linker will give an idea on an average behaviour of all. In fact, for a large cross-link density, the fluctuation is expected to be small as opposed to a diluted system where the density is low. The latter assumption suggests that due to the distance between each link, the fluctuation will be mostly given by individual cross-link formation. The present model assumes large density and therefore introduce small fluctuation as presented by T. Vilgis (2000) [14]. We compute here the average density of the two cross-link type. This is done using simple statistical formula for average taking the partition function as statistical weight. An second alternative of calculation using the generating functional method is presented in Appendix A.2.

In the Appendix A.2, we derive that $\langle\rho(x)\rangle = \langle\psi^{*2}(x)\rangle$. We expand the functional Hamiltonian around the saddle point solution up to the second order in the fluctuation [3]. We are allowed to write field as follows: $(\psi^*(x) = \overline{\psi}^* + \Delta\psi^*)$

according to the mean field approximation scheme.

$$\begin{aligned}\langle\psi^{*2}(x)\rangle &= \frac{\int [\mathrm{d}\,\phi]\,[\mathrm{d}\,\phi^*]\,[\mathrm{d}\,\psi]\,[\mathrm{d}\,\psi^*]\,[\mathrm{d}\,\psi^*(x)]\,e^{-\chi\,[\phi,\phi^*,\psi,\psi^*]}}{\int [\mathrm{d}\,\phi]\,[\mathrm{d}\,\phi^*]\,[\mathrm{d}\,\psi]\,[\mathrm{d}\,\psi^*]\,e^{-\chi\,[\phi,\phi^*,\psi,\psi^*]}} \\ &= \frac{\int [\mathrm{d}\phi]\,[\mathrm{d}\,\phi^*]\,[\mathrm{d}\,\psi]\,[\mathrm{d}\,\psi^*](\overline{\psi}^* + \Delta\psi^*)^2 e^{-\chi\,[\phi,\phi^*,\psi,\psi^*]}}{\int [\mathrm{d}\,\phi]\,[\mathrm{d}\,\phi^*]\,[\mathrm{d}\,\psi]\,[\mathrm{d}\,\psi^*]\,e^{-\chi\,[\phi,\phi^*,\psi,\psi^*]}}.\end{aligned} \tag{3.36}$$

We Taylor expand the functional $\chi[\psi,\psi^*,\phi,\phi^*]$ around the saddle point solution up to the second order.

$$\begin{aligned}\chi(\phi,\phi^*,\psi,\psi^*) &= \chi^{(0)}(\phi,\phi^*,\psi,\psi^*)|_{(\overline{\psi},\overline{\psi^*});\overline{\phi},\overline{\phi^*})} \\ &+ \underbrace{\chi^{(1)}(\phi,\phi^*,\psi,\psi^*)|_{(\overline{\psi},\overline{\psi^*});(\overline{\phi},\overline{\phi^*})}}_{=0}\Big(\Delta\phi,\Delta\psi,\Delta\phi^*,\Delta\psi^*\Big) \\ &+ \chi^{(2)}(\phi,\phi^*,\psi,\psi^*)|_{(\overline{\psi},\overline{\psi^*});(\overline{\phi},\overline{\phi^*})}\Big((\Delta\phi)^2,(\Delta\psi)^2,(\Delta\phi^*)^2, \\ &(\Delta\psi^*)^2\Big) + \text{higher orders in} \quad \Delta\phi \\ &\simeq \chi_{sp} - \frac{1}{2}(\Delta\phi,\Delta\phi^*,\Delta\psi,\Delta\psi^*)H_{\text{ess}}\begin{pmatrix}\Delta\phi\\ \Delta\phi^*\\ \Delta\psi\\ \Delta\psi^*\end{pmatrix},\end{aligned} \tag{3.37}$$

where $\chi^{(i)}$ stands for the derivative of χ to the i^{th} order $(i = 0,1,2,...)$. H_{ess} stand for a 4×4 Hessian matrix and have the following expression:

$$H_{\text{ess}} = \begin{bmatrix} \frac{\delta^2\chi}{\delta\phi\delta\phi} & \frac{\delta^2\chi}{\delta\phi\delta\phi^*} & \frac{\delta^2\chi}{\delta\phi\delta\psi} & \frac{\delta^2\chi}{\delta\phi\delta\psi^*} \\ \frac{\delta^2\chi}{\delta\phi^*\delta\phi} & \frac{\delta^2\chi}{\delta\phi^*\delta\phi^*} & \frac{\delta^2\chi}{\delta\phi^*\delta\psi} & \frac{\delta^2\chi}{\delta\phi^*\delta\psi^*} \\ \frac{\delta^2\chi}{\delta\psi\delta\phi} & \frac{\delta^2\chi}{\delta\psi\delta\phi^*} & \frac{\delta^2\chi}{\delta\psi\delta\psi} & \frac{\delta^2\chi}{\delta\psi\delta\psi^*} \\ \frac{\delta^2\chi}{\delta\psi^*\delta\phi} & \frac{\delta^2\chi}{\delta\psi^*\delta\phi^*} & \frac{\delta^2\chi}{\delta\psi^*\delta\psi} & \frac{\delta^2\chi}{\delta\psi^*\delta\psi^*} \end{bmatrix}_{(\overline{\phi},\overline{\phi}^*,\overline{\psi},\overline{\psi}^*)}. \tag{3.38}$$

Using the equation (3.37) and adding the fluctuation term $\Delta\psi^* = \psi^* - \overline{\psi}^*$ into

equation (3.36), we obtain:

$$\begin{aligned}\langle\psi^{*2}(x)\rangle &= \frac{\left[\begin{array}{c} e^{-\chi_{sp}}\int [\mathrm{d}\,\Delta\phi]\,[\mathrm{d}\,\Delta\phi^*]\,[\mathrm{d}\,\Delta\psi]\,[\mathrm{d}\,\Delta\psi^*] \\ \left(\overline{\psi}^{*2}+2\overline{\psi}^{*}\Delta\psi^{*}+(\Delta\psi^{*})^{2}\right)e^{-\frac{1}{2}(\Delta\phi,\ldots)H_{ess}\left(\begin{array}{c}\Delta\phi\\ \cdots\end{array}\right)}\end{array}\right]}{e^{-\chi_{sp}}\int [\mathrm{d}\,\Delta\phi]\,[\mathrm{d}\,\Delta\phi^*]\,[\mathrm{d}\,\Delta\psi]\,[\mathrm{d}\,\Delta\psi^*]\,e^{-\frac{1}{2}(\Delta\phi,\ldots)H_{ess}\left(\begin{array}{c}\Delta\phi\\ \cdots\end{array}\right)}}, \\ &= \overline{\psi}^{*2}+2\,\overline{\psi}^{*}\,\langle\Delta\psi^{*}\rangle+\langle(\Delta\psi^{*})^{2}\rangle. \end{aligned} \tag{3.39}$$

With $(\Delta\,\phi,\ldots)=(\Delta\,\phi,\Delta\,\phi^*,\Delta\,\psi,\Delta\,\psi^*)$. After performing the Gaussian integration, we obtain:$\langle\Delta\,\psi^*\rangle=0$ and $\langle(\Delta\,\psi^*)^2\rangle=H_{ess}^{-1}$ finally:

$$\langle\rho(x)\rangle=\langle\psi^{*2}(x)\rangle=\underbrace{\overline{\psi}^{*2}}_{\text{dominant term}}+\underbrace{H_{\text{ess}}^{-1}}_{\text{fluctuation term}}\simeq\overline{\psi}^{*2}. \tag{3.40}$$

This method and the method presented in Appendix A.2 Both give the same results. The result (equation (3.40)), has two terms: The dominant term and a fluctuation term. The dominant term of the expression is the saddle point solution of the field attached to the cross-linker powered by the functionality of the cross-linker. In a similar way, we also by the same method of calculation found the average density associated with the permanent cross-link: $\langle\rho(r)\rangle=\langle\phi^{*p}(r)\rangle\simeq\overline{\phi}^{*p}(r)$+fluctuation term. We can conclude that the average density of each cross-link shows a Gaussian profile describing the distribution of each cross-link inside the network. For a sufficiently high density, we expect the contribution for the fluctuation to become negligible. This will imply that there is a small fluctuation around the distribution of each cross-link inside the network on average. This results are expected because we have built the present model using Gaussian chains. A real non-equilibrium polymer network is dominated by Brownian motion in a thermal environment. Consequently, the fluctuation appearing into the density average could explained as provided from thermal motion.

3.5 Field theory approach for network deformation

We investigate here the elastic properties of a polymeric network made of movable and permanent cross-linkers as presented above. The elastic properties are investigated by studying the network deformation due to an external force. The challenge that one faces is to elaborate a good understandable model that describes the deformation behaviour of a network that has movable cross-links.

The replica theory elaborated by Edwards et al. has revealed itself to be a good method to deal with network replicas formed during the deformation [2, 22, 24]. We account for all the replicas of a randomly chosen network topology of the network among all the isomers. Let us call the chosen network configuration m. For the sake of simplicity, we suppose an isovolumetric[3] This type of network is advantageous compared to the "contractile network" [4]. This latter type of network is more appropriate for active networks but require to include more parameters such as the excluded volume and the Osmotic pressure due to the instability of the network. We chose to regard the present network as an isovolumetric network for sake of simplicity. We assume that

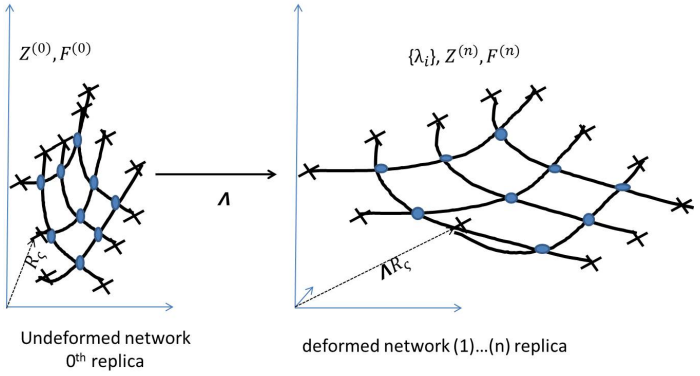

Figure 3.6: *Simple affine deformation of a network with topology m. We distinguish the o^{th} (undeformed) and the other n (deformed) replicas. The permanent (in black cross) and the reversible (blues dots) cross-linkers. $R_\varsigma = r$ is the spacial position of the permanent cross-link number ς.*

the permanent cross-links are homogeneously spread out in space and serves as skeleton to the network. We have control over the fixed cross-link, that means, by shifting each of them by a factor of $\lambda = \sum_{i=1}^{3} \lambda_i$, we will be able to investigate the whole network response to that shift. The network fluctuates freely while the fixed points fluctuates after deformation in average. The Fig. 3.6 illustrates the affine deformation of a network with topology m. The 0^{th} replica is the network before the deformation (i.e. the configuration of the network just after the formation) [2]. The other n^{th} replicas are all the network after the deformation. All the $(n+1)$ replica have the same topology since the network has been suppose isovolumetric. The spacial vector describing the position of each the permanent cross-link is r. For the zeroth replica, we have $r^{(0)}$ and

[3] Isovolumetric means that the network deform the identically in all the faces. Here, all the diagonals of the deformed tensor equation (2.16) are not identical. $\lambda_x \neq \lambda_y = \lambda_z$

[4] In the "contractile network" all the diagonal elements of the deformation matrix are identical ($\lambda_x = \lambda_y = \lambda_z = \lambda$).

for any of the n deformed replica, $r^{(\alpha>1)}$ with $\alpha \in 1, ..., n$. Assuming an affine deformation of the end-links, the following relation holds.

$$r^{(\alpha>0)} = \lambda r^{(0)}. \tag{3.41}$$

In the present assumption, we suppose not double replication on the reversible cross-link. We assume that this latter is attached to an elastic background network (made of permanent network that affinely deformed). We can therefore assume identical reversible cross-link in each replica i.e. $\sum_{\alpha=0}^{n} \psi_\alpha(x_\alpha) = (n+1)\psi(x)$. In the spirit of Edwards, all the possible configurations of the $(n+1)$ replicated network are calculated by taking the average of the partition function of all the deformed network over all the disorder into the network. There are two type of disorder into the system: 1) The disorder due to the way of choosing one configuration network from many network formed with the same mixture. 2) The disorder over the random self assembly in a particular network configuration chosen. We use the similar replica formalism used by Edwards [2].

$$\begin{aligned} Z_m^{(0)} = & \int [\mathrm{d}\phi, \phi^*, \psi, \psi^*] \left[\int \phi^{*p}\right]^{N_p} \left[\int \psi^{*2}\right]^{N_a} e^{-\int \phi\phi^* - \int \psi\psi^*} \\ & \times \left[\iint_{r_0^{(0)}, r_1^{(0)}} \phi(r_0^{(0)}) [G(r_0^{(0)} - r_1^{(0)}, L) \int_x (1 + \psi(x)z)]\, \phi(r_1^{(0)})\right]^N . \end{aligned} \tag{3.42}$$

Here z is the fugacity for the reversible cross-linker. The partition function for the n^{th} deformed replica network is:

$$\begin{aligned} Z_m^{(n)} = & \int [\mathrm{d}\phi, \phi^*, \psi, \psi^*] \left[\int \phi^{*p}\right]^{N_p} \left[\int \psi^{*2}\right]^{N_a} e^{-\int \phi\phi^* - \int \psi\psi^*} \\ & \times \left[\iint_{r_0^{(\alpha)}, r_1^{(\alpha)}} \phi(r_0^{(\alpha)}) \prod_{\alpha=1}^{n} [G(r_0^{(\alpha)} - r_1^{(\alpha)}, L) \int_{x_\alpha} (1 + \psi_\alpha(x_\alpha)z)]\, \phi(r_1^{(\alpha)})\right]^N . \end{aligned} \tag{3.43}$$

The partition function for all the $(n+1)$ replicas is given by:

$$\begin{aligned} \left[Z_m^{(n+1)}(\lambda)\right]_d &= \aleph \int Z_m^{(0)} Z_m^{(n)} \\ &= \aleph \int [\mathrm{d}\phi, \phi^*, \psi, \psi^*] \exp\left[-\chi_T^{(n+1)}(\lambda)\right], \end{aligned} \tag{3.44}$$

with

$$
\begin{aligned}
-\chi_T^{(n+1)}(\lambda) = \mu \iint\limits_{r_0^{(\alpha)}, r_1^{(\alpha)}} \phi^*(r_0^{(\alpha)}) \prod_{\alpha=0}^{n} \Big[\int\limits_{x_\alpha} G(r_0^{(\alpha)} - x_\alpha, \frac{L}{2}) \, (1 + \psi_\alpha(x_\alpha)\, z) \\
\times G(x_\alpha - r_1^{(\alpha)}, \frac{L}{2}) \Big] - \int\limits_{r^{(\alpha)}} \phi\phi^* - \sum_{\alpha=0}^{n} \int\limits_{x_\alpha} \psi_\alpha(x_\alpha) \\
+ \mu_a \sum_{\alpha=0}^{n} \int\limits_{x_\alpha} \psi_\alpha^{*2}(x_\alpha) + \mu_p \int\limits_{r^{(\alpha)}} \phi^{*p}(r^{(\alpha)}) \\
- (N \log \mu + N_a \log \mu_a + N_{\mathrm{p}} \log \mu_{\mathrm{p}}).
\end{aligned}
\tag{3.45}
$$

The functional $-\chi_T^{(n+1)}(\lambda)$ contains all the $(n+1)$ replicas of the network and $r^{(\alpha)} = (r^{(0)}, r^{(1)}, ..., r^{(n)})$. The symbol $[..]_{\mathrm{d}}$ means the average over all the disorder of the system. The saddle point equations are given by the set of following equations:

$$
\begin{cases}
(n+1)\overline{\psi}^*(y) = z^n \, \mu \iint_{r_0^{(\alpha)}, r_1^{(\alpha)}} \overline{\phi}(r_0^{(\alpha)}) \prod_{\alpha=0}^{n} \Big[G(r_0^{(\alpha)} - r_1^{(\alpha)}, L) \Big] \overline{\phi}(r_1^{(\alpha)}), & \text{(e1')} \\
\overline{\psi}(x) = 2\mu_a \overline{\psi}^*(x), & \text{(e2')} \\
\overline{\phi}^*(R^\alpha) = \int_{r_0^{(\alpha)}} \overline{\phi}(r_0^{(\alpha)}) \prod_{\alpha=0}^{n} \Big[G(r_0^{(\alpha)} - R^{(\alpha)}, L) \int_{x_\alpha} (1 + \overline{\psi}_\alpha(x_\alpha) z) \Big], & \text{(e3')} \\
\overline{\phi}(R^\alpha) = p\mu_p \overline{\phi}^{*(p-1)}(R^\alpha). & \text{(e4')}
\end{cases}
\tag{3.46}
$$

The equations (3.46) are solved by introducing the equation (3.41). This allows us to split the permanent cross-links as follow:

$$
\begin{aligned}
\phi(r^{(\alpha)}) &= \phi(r^{(0)}, r^{(1)}, ..., r^{(n)}), \\
&= \phi(r^{(0)}, \underbrace{\lambda r^{(0)}, ..., \lambda r^{(0)}}_{\text{n replicas}}), \\
&= \phi(r^{(0)}) \underbrace{\delta(r^{(1)} - \lambda r^{(0)}) ... \delta(r^{(n)} - \lambda r^{(0)})}_{\text{n replicas}}.
\end{aligned}
\tag{3.47}
$$

The equation (3.47) into the equation (3.46) allows the following transforma-

tion:

$$\begin{aligned}
&\iint_{r_0^{(\alpha)},r_1^{(\alpha)}} \overline{\phi}(r_0^{(\alpha)}) \prod_{\alpha=0}^{n} [G(r_0^{(\alpha)} - r_1^{(\alpha)}, L)] \overline{\phi}(r_1^{(\alpha)}) \\
&= \iint_{r_0^{(0)},r_1^{(0)}} \overline{\phi}(r_0^{(0)}) G(r_0^{(0)} - r_1^{(0)}, L) \overline{\phi}(r_1^{(0)}) \\
&\times \prod_{\alpha=1}^{n} \left[\delta(r_0^{(\alpha)} - \lambda r_0^{(0)}) G(r_0^{(\alpha)} - r_1^{(\alpha)}, L) \delta(r_1^{(\alpha)} - \lambda r_1^{(0)}) \right] \\
&= \iint_{r_0^{(0)},r_1^{(0)}} \overline{\phi}(r_0^{(0)}) G(r_0^{(0)} - r_1^{(0)}, L) \overline{\phi}(r_1^{(0)}) \prod_{\alpha=1}^{n} \left[G(r_0^{(\alpha)} - r_1^{(\alpha)}, L) \right] \overline{\phi}(r_1^{(0)}).
\end{aligned} \tag{3.48}$$

We suppose that the fields and the Greens's functions are Gaussian. Therefore, we can write their expressions using Gaussian exponential $\overline{\phi}(r) = Ae^{-ar^2}$; $\overline{\psi}(x) = Be^{-br^2}$; $\prod_{\alpha=0}^{n} G(r^{(\alpha)}, L) = (\frac{3}{2lL})^{3(n+1)/2} e^{-\frac{3}{2lL}(1+n\lambda^2)r^{(\alpha)2}}$. We assume that there is enough reversible cross-linker in the network and we have $1 \ll z \int_x \overline{\psi}(x)$ so, $\int_x (1 + z\,\overline{\psi}(x)) \simeq z \int_x \overline{\psi}(x)$. This assumption can be made here because, equation (3.59) shows that it is proportional to the number of cross-links. After having introduced those approximations into the equation (3.46), we solve the set of equations by a simple substitution and we find the constants:

$$a = \frac{8(6 + Ln + 12n\lambda^2)}{L}, \tag{3.49}$$

$$b = \frac{2a + 3(1 + n\lambda^2)}{L}, \tag{3.50}$$

$$\begin{aligned}
A = \Bigg[& 2^{-3-2n} 3^{-11/2-9n/2} z^{-4(n+1)(1/L)^{3(-1-3n)/2}} L(n+1)^2 \pi^{-2-n} (1/b)^{-n} \\
& \left(\frac{3^{3(n+1)/2} z^{n+1} (1/L)^{3(n+1)/2} \sqrt{b}}{(n+1)\sqrt{2b}} \right)^{-2n} (512l^2n^2 + 48Ln(131 + 259n\lambda^2) \\
& + 9(2145 + 8482n\lambda^2 + 8385n^2\lambda^4)) \Bigg]^{1/(5+4n)},
\end{aligned} \tag{3.51}$$

$$B = \frac{3^{(n+1)}/2 z^{n+1} (1/L)^{3(n+1)/2} \sqrt{b} A^2}{(n+1)\sqrt{2b}}. \tag{3.52}$$

Details of the calculations is presented in Appendix A.3. We have supposed for simplification in the calculations that the functionality of permanent cross-linkers is $p = 3$ and that the constants $\mu, \mu_a, \mu_p, l = 1$. The equation (3.44) can be written as follow:

$$\left[Z_m^{(n+1)}(\lambda) \right]_d = \aleph \int [\mathrm{d}\underline{O}] \exp[-\chi_{sp}(\lambda)] \exp[-\frac{1}{2} \underline{O}\, \underline{\underline{H}}\, \underline{O}^T], \tag{3.53}$$

$-\chi_{sp}(\lambda)$ is the functionality that depends on the saddle points solutions. $\underline{\underline{H}}$ is the Hessian matrix of the functionality $-\chi_T^{(n+1)}(\lambda)$ in the saddle point approximation. $\underline{O} = (\phi, \phi^*, \psi, \psi^*)$ is a super vector of field and $\underline{O}^T$ is its transpose. After integration over the super vector field, we have:

$$\left[Z_m^{(n+1)}(\Lambda)\right]_d \simeq \exp[-\chi_{sp}(\lambda)]. \tag{3.54}$$

Solving the equation (3.45) for the saddle point solutions, we have:

$$-\chi_{sp}(\lambda) = A^2\left(\frac{3}{2L}\right)^{3(n+1)/2}\left(\frac{\pi}{2\,a+\frac{3(n+1)}{2L}}\right)^{1/2} B^{n+1}(\pi/b)^{(n+1)/2} + A\sqrt{\frac{6\pi}{a}} - (n+1)\frac{B^2}{2}\sqrt{\frac{2\pi}{b}} + (n+1)\frac{B^2}{4}\sqrt{\frac{2\pi}{b}} - 3A^3\sqrt{\frac{3\pi}{a}}. \tag{3.55}$$

We replace equations (3.46) in equation (3.55). The free energy of the deformed network with topology m is calculated as:

$$\begin{aligned}[F_m(\lambda)]_d = \overline{F}_m(\lambda) &= -k_B T[\log[Z_m^{(n+1)}(\lambda)]]_d \\ &= -k_B T\int_d P_m \log[Z_m^{(n+1)}(\lambda)]_d.\end{aligned} \tag{3.56}$$

With $P_m = \frac{Z_m^{(0)}}{\overline{Z}^{(0)}}$ being the probability of choosing the topology m between all the possible network configurations formed by the same mixture. $Z_m^{(0)}$ and $\overline{Z}^{(0)}$ are respectively the partition functions of the network with topology m just after the fabrication and for all the possible network formed just after the fabrication with the same mixture of polymeric chains and crosslinkers. $[..]_d$ means the average over all the disorder possible. The calculation of the free energy is simplified using a simple mathematical trick called the replica trick (see section 2.3.1.4) and based on the following expression: $A^n = 1 + n\log(A) + \mathrm{O}(n^2)$. The logarithm of the partition function is now written as: $[\log[Z_m^{(n+1)}(\lambda)]]_d = \lim_{n\to 0}\frac{[Z_m^{(n+1)}(\lambda)]_d - 1}{n}$. We Taylor expand the partition function up to the first order in n and calculate the free energy. We obtain:

$$\overline{F}_m(\lambda) = \frac{c' N k_{\mathrm{B}} T\lambda^2}{R_g} - \frac{a'(z^{1/5} + b' R_g)}{z^{6/5}\, R_g^{3/4}} N k_{\mathrm{B}} T\lambda^2. \tag{3.57}$$

The force needed to deform the network by a factor of λ is simply the force per unit area of the undeformed network that is to be stretched. This force is given by the gradient of the free energy. After calculation done, we have the

following expression:

$$f_m(\lambda) = \frac{\partial \overline{F}_m(\lambda)}{\partial \lambda} = \left[\frac{c'}{R_g} - \frac{a'\,(z^{1/5} + b'\,R_g)}{z^{6/5}\,R_g^{3/4}}\right] N k_{\mathrm{B}} T\,\lambda,$$

$$= \left[\frac{0.4032218}{R_g} - \frac{0.057006\,z^{8/5}\rho^2(r)}{R_g^{5/4}}\right] N k_{\mathrm{B}}\,T\,\lambda. \qquad (3.58)$$

$c' = \dfrac{46411 \times 11^{3/10}}{6 \times 2600 \times 2^{9/10} \times \pi^{1/10}} = 0.403218$, $a' = 0.08650, b' = 6.5808489$, N is the normalisation constant which can be ignored and $R_g^2 = l\,L/6$ is the radius of gyration of the network. The expression of the force presents two interesting terms: The first term is the force of the deformed permanent network. Its has the same structure as the force found by Edward et al. [2, 22]. The second term, represents the contribution of the force that the reversible cross-linkers add to the force. The minus sign suggests that if we add the reversible cross-linkers to the permanent network, the network become soft. This with the assumption that there is enough reversible cross-linkers in the chain. In the grand canonical ensemble, the average number density of the reversible cross-linkers is given by:

$$\langle N_{rev}\rangle = z\frac{\partial}{\partial z}\log[Z_m^{(n+1)}(\lambda)]_d = (n+1)\int_{r_1^{(\alpha)}} \overline{\phi}^*(r_1^{(\alpha)}). \qquad (3.59)$$

The local density[5] $\rho(r)$ is identified from (equation (3.59)) as $\rho(r) = (n+1)\,\overline{\phi}^*(r)$ ($n = 0$ in the the replica trick). We then use the equation (e4') in the set of (equation 3.46) to introduce the local density into the force expression (equation (3.58)). While identifying the corresponding equation in the saddle point equations, force is calculated by working backward and then have its expression in term of the local density of the reversible cross-linker.

3.6 Conclusion

In this chapter, we have presented a continuous description of a polymeric network containing both permanent and reversible cross-links. The motion of the reversible cross-linker can be identified to the non-processive myosin II motor protein found inside the cytoskeleton. The system is treated as a near equilibrium system. The generating functional borrowed from equilibrium statistical physics is therefore used. This is done by including a Dirac delta functional inside the partition function of the system. All the possible network

[5]The integration of the local density over all space gives the number of particles by definition: $\int \rho(r)dV = N$.

formed using the same mixture is therefore counted through the partition function. The behaviour of the two type of cross-linker allows us to count them differently. The permanent cross-link is treated with quenched average while the reversible cross-link is treated with annealed average. The saddle point approximation is used to ease the integration over the degree of freedom of the network. The calculation of the average density reveals that the chains fluctuate around a mean value which is the saddle point solution. This results is also true for any type of cross-linkers involved in the network. We learn that the use of the field theory gives a better and global understanding of the system. The benefits of the technique used here is that the calculation are less complicated than if we were to use the delta function instead of the exponential expression. The field theory has proven itself to be useful in the context of converting polymer degree of freedom to collective degree of freedom (density variable), that have themselves been shown to be particularly useful in polymer network theory. We investigated the elasticity properties of the randomly cross-linked polymer network containing both permanent and reversible cross-links. The stretching force calculated shows that, introducing the reversible cross-linker into the permanent network makes the network become softer.

Chapter 4

Slipping link in a permanent network of polar chains

4.1 Introduction

We present here two alternatives network topologies formed with polar polymer chains and both permanent and active-movable cross-linkers. Here, we think of the cross-linker as being made of two motor heads connected by a spring (i.e. motor clusters) that slides along the chains. Each motor head moves along the chains toward the (+) end of the chain to which it is attached while the permanent cross-linker lie at the very ends of the chain. The local cross-linking and the polarity of the filaments raise two possible and distinguishable polymer network configurations depending on the chains' orientations relative to one another. The behaviour of each network is defined by the active-movable (or active) cross-linker and by the orientation of the polar filament with respect to its cross-linked filament. The ends of the chains are firmly anchored with the permanent cross-link and serve as backbone for the whole network. The active properties of the network are determined by looking at the active cross-linker movement along the filaments. We demonstrate that, depending on the orientation of the filaments with respect to one another, we have distinct type of network elasticity problem with each type of network exhibiting a particular behaviour.

The present chapter investigates the characteristics of the two possible networks configuration that arise by including the polarity of the polymer chains. We found that the polarity alignment is essential to predict the active-movable cross-linker behaviour. For an extreme one-dimension network of two chains, the active cross-linker is either a slipping ring or just slides along the chains. In the latter case, the spring provides a non trivial coupling between the polymer chains. In both cases, the network presents a "X" kind of shape. We calculate the average density of each type of cross-linker and show that the density fluc-

tuates each around the saddle point solution of the cross-linker. Those saddle point solutions happen to be the mean value of the cross-linker.

4.2 Model description

The present model illustrates two alternative behaviours of the active-movable cross-link inside the network formed with polar filaments. For the purpose of simplicity, we limit ourself here to the an extreme situation of one dimensional version of polar chains network as a small example illustrating the possible behaviour of the network due to a biasing acting force. The three dimensional network of polar chains is complicated to implement because, the polymers are randomly oriented in the network. We assimilate the active cross-link to the myosin II protein. This latter cross-link moves (never detached itself from the chain i.e. no reversibility behaviour here) preferentially toward the (+) ends of the chains. The active cross-linker is therefore viewed as a "slipping link".

The idea of "*slip-link*" network has been elaborated by Ball and Edwards (1980) and Vilgis (1988) where the polymer network is supposed to be confined in a tube [24, 55]. In the present model, instead of making the chains slide (case we explore iin Chapters 5 and 6), we fix their ends using the permanent cross-link as explained in Chapter 3. The polarity of the chains introduces a biasing force generated by the motion of the slipping cross-link. We investigate the network behaviour due to the motion of this latter cross-link. We suppose that the moving linker stops when it reaches the very ends of the chains. We look here at the primitive model formed by two polymers and a pair of motor protein head attached by a spring. Our aim of interest is on understanding what happens to the polymer network when the active cross-linker placed at a random position along the chains moves. The permanent cross-linkers lie at the ends of the chains with functionality four. The behaviour of the network can be predicted without doing any calculation only by looking at the direction of the biasing force on the network. For the one dimensional model, we distinguish two situations: when the two chains have the same direction (i.e. their + ends are oriented in the same direction) from one another, we say that the network is "*parallel*" (Fig. 4.1) as opposite to the "*anti-parallel*" (Fig. 4.2) network when the chains have opposite directions. The cross-link between two chains is mathematically represented by the Dirac delta function $\delta(X_a - x_b)$. This enforces the connection between the two chains at position X_a and x_b.

4.3 Reversible cross-link as slipping ring

In this network configuration, the + ends of the two chains have the same direction. The model is illustrated on the Fig. 4.1. The preferential direction of the active linker imposes the direction of the moving link. In the case where the two chains are parallel, *Slipping ring* (Fig. 4.1) moves on the same direction. The slip link is therefore view as a "moving ring". Ball et al. (1980) [24] in their model have treated similar sliplink network of model where moving non polar chains were confined inside a tube. When the active cross-link moves, the position along the arc lengths also varies as well as the cross-linker position itself. That allows us to perform the integration over these two degrees of freedom in the partition function. The propagator of the network is given by:

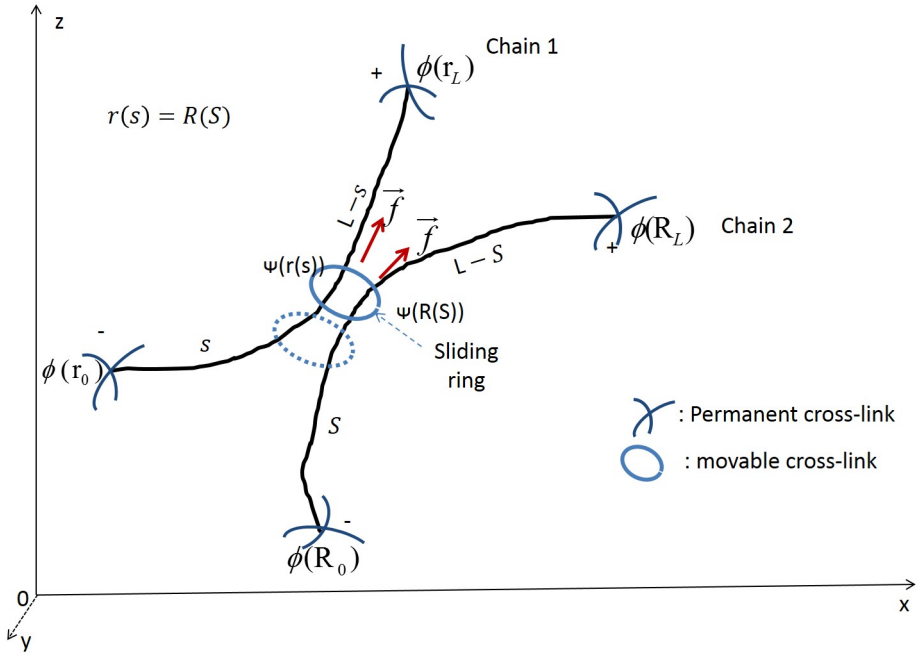

Figure 4.1: *Ring-model of network: The fields ϕ and ψ represent the passive and active cross-linkers. This latter linker is free to move toward the (+) end of the chains. $r(s)$ and $R(S)$ are, respectively, the label of the chain (1) and the chain (2). $r_0 = r(s = 0)$, $r_L = r(s = L)$,$R_0 = R(S = 0)$,$R_L = R(S = L)$. $x = r(s)$ and $X = R(S)$ are the spacial positions of the motor head along the chain(1) and chain(2) with the arc lengths s and S respectively.*

$$G = G(r_0 - r(s); s)\, G(r(s) - r_L; L - s) \\ G(R_L - r(s); L - s)\, G(r(s) - R_0; s). \tag{4.1}$$

The partition function is given by the following expression:

$$
\begin{aligned}
Z = \int [\mathrm{d}\psi]\,[\mathrm{d}\psi^*]\,[\mathrm{d}\phi]\,[\mathrm{d}\phi^*] \Bigg[\int \mathrm{d}s\,\mathrm{d}r_0\,\mathrm{d}r_L\,\mathrm{d}x\,\phi(r_0)\,G(r_0 - x; s) \\
\times e^{-\beta f \Delta x}\,\psi(x)\,G(x - r_L; L - s)\,\phi(r_L) \Bigg] \Bigg[\int \mathrm{d}S\mathrm{d}X\,\mathrm{d}R_0\,\mathrm{d}R_L\,\phi(R_0) \\
\times G(x - R_0; S)\,e^{-\beta f \Delta x}\,\psi(x)\,G(R_L - x; L - S)\,\phi(R_L) \Bigg] \\
\times \left[\int_r \phi^{*4} \right]^4 \left[\int_x \psi^{*2} \right] e^{-\int \phi\phi^* - \int \psi\psi^*} \times \underbrace{\text{rest of network } [\phi^*]}_{(i)}.
\end{aligned}
\tag{4.2}
$$

Where $e^{-\beta f \Delta x} = e^{-\beta \omega}$ is the Boltzmann weight for the force f. $\omega = \pm f\,\Delta x$ and being the work performed by the movable linker ($\pm$ for the polarity of the polymers). Δx is the displacement of the reverse cross-linker associated to the motion of the linker via the force f. This force f is a conservative biasing force therefore, not a real active force. It has been introduced in the model to mimic the effect of the active force in an equilibrium setting [61]. The (i) in equation (4.2) represents the rest of network linked by ϕ. Because we would like to limit ourselves to a very simple case of only two chains, we will not include that part in the calculation to come since it will make calculation harder by adding more parameters.

As stated above, the motion of the active cross-link is guided by the direction of the (+) ends of the cross-linked polymer chains. In this case, the contractile behaviour of the network chain is not quite represented. This is due to the motion of the slipping link toward the (+) direction in both chains. That means, the elasticity properties of the spring that connects the two motor head is negligible. We chose to look at only one replica of the network. When the active linker moves, it exerts a force and when reaches the permanent links at the ends of the chains, it stops. For a suppose system of N chains in one dimensional system, the chains are all nicely aligned so that they form a bundle network like structure [52]. If the length of each chain is long enough, we may expect to have a polymer bundle kind of structure otherwise a probably "X" polymer network like structure. Of course those latter behaviour predictions are only assumptions, there have not been any mathematical prove to confirmed. We assume that the two chains have the same properties and can be labelled with the same label. Instead of having many integrations over x, X, s, S, R and r for all the chains, we will reduce it to few integrations and render the system

least complicated to solve. The equation (4.2) can be simplified as:

$$\begin{aligned} Z &= \int [\mathrm{d}\psi]\,[\mathrm{d}\psi^*]\,[\mathrm{d}\phi]\,[\mathrm{d}\phi^*]\,\left[\int_r \phi^*\right]^4 \left[\int_x \psi^{*2}\right] e^{-\int \phi\,\phi^* - \int \psi\,\psi^*} \\ &\times \left[\int_{r_0,r_L,x} \phi(r_0)\,G(r_0-r_L;L)\,e^{-\beta\,f\,\Delta x}\,\psi(x)\,\phi(r_L)\right]^2, \\ &= \aleph \int [\mathrm{d}\,\psi]\,[\mathrm{d}\,\psi^*]\,[\mathrm{d}\,\phi]\,[\mathrm{d}\,\phi^*]\,\exp\left(-\chi'[\psi,\psi^*,\phi,\phi^*]\right). \end{aligned} \tag{4.3}$$

With

$$\begin{aligned} -\chi'[\psi,\psi^*,\phi,\phi^*] &= \mu_p \int_r \phi^{*4} + \mu_a \int_x \psi^{*2} - \int_r \phi\,\phi^* - \int_x \psi\,\psi^* \\ &\quad \mu \int_{r_0,r_L,x} \phi(r_0)\,G(r_0-r_L;L)\,e^{-\beta\,f\,\Delta x}\,\psi(x)\,\phi(r_L) \\ &\quad - 2\log\mu - 4\log\mu_p - \log\mu_a. \\ &\simeq \mu_p \int_r \phi^{*4} + \mu_a \int_x \psi^{*2} - \int_r \phi\,\phi^* - \int_x \psi\,\psi^* \\ &\quad - \mu \int_{r_0,r_L,x} \phi(r_0)\,G(r_0-r_L;L)\,e^{-\beta\,f\,\Delta x}\,\psi(x)\,\phi(r_L). \end{aligned} \tag{4.4}$$

The term $(-2\log\mu - 4\log\mu_p - \log\mu_a)$ is neglected in the saddle point approximation. The saddle point equation are:

$$\frac{\delta(-\chi')}{\delta\psi}|_{sp} = 0;\ \frac{\delta(-\chi')}{\delta\psi^*}|_{sp} = 0;\ \frac{\delta(-\chi')}{\delta\phi}|_{sp} = 0;\ \frac{\delta(-\chi')}{\delta\phi^*}|_{sp} = 0. \tag{4.5}$$

we obtain the following set of equations:

$$\begin{cases} \mu\,e^{-\beta f\Delta x} \int_{r_0,r_L} \overline{\phi}(r_0)G(r_0-r_L,L)\overline{\phi}(r_L) - \overline{\psi}^*(x) = 0, & \text{(e1)} \\ 2\mu_a\overline{\psi}^*(x) - \overline{\psi}(x) = 0, & \text{(e2)} \\ 2\mu\,e^{-\beta f\Delta x} \int_{r_L,x} \overline{\phi}(r_L)\,G(r_0-r_L,L)\,\overline{\psi}(x) - \overline{\phi}^*(r) = 0, & \text{(e3)} \\ 4\,\mu_p\overline{\phi}^{*3}(r) - \overline{\phi}(r) = 0. & \text{(e4)} \end{cases} \tag{4.6}$$

We solve the set of equation (4.6) using the following Gaussian assumption: $G(r_0-r_L,L) = \frac{3}{2L}e^{\frac{-3}{2L}(r_0-r_L)^2}$, $\overline{\psi}^*(x) = Be^{-bx^2}$ and $\overline{\phi}(r) = Ae^{-ar^2}$. This is done by substitution: we replace equation (e1) into equation (e2) then, the result goes into equation (e3) with equation (e4), we have one equation we only one

unknown $\overline{\phi}$ given by:

$$\begin{aligned}\overline{\phi}^{1/3}(r) = 4\,\mu_p\mu^2(e^{-\beta f\Delta x})^2(4\mu_p)^{1/3}\int_{r_L}\overline{\phi}(r_L)\,G(r_0-r_L,L)\\ \times\int_{r_0,r_L}\overline{\phi}(r_0)\,G(r_0-r_L,L)\overline{\phi}(r_L).\end{aligned} \tag{4.7}$$

We replace now the field and the Green's function by their values respective and by identification, solve for the constant a and A. The constants b and B are solved using the equation (e1). We have the constants expressions:

$$a = \frac{3}{4L},\quad b = \frac{9}{4L}, \tag{4.8}$$

$$A = \frac{L^{3/8}\left(24L^2+1\right)^{3/16}}{2^{5/8}(3\pi)^{3/8}\mu^{3/4}(e^{3\beta f\Delta x/4})\mu_a^{3/8}\sqrt[8]{\mu_p}}, \tag{4.9}$$

$$B = \frac{\sqrt{2}L\mu_a e^{\beta\Delta \mathrm{x} f}}{3\pi\sqrt{\frac{1}{b}}\mu\sqrt{\frac{L}{\frac{3}{2}\left(\sqrt{24L^2+1}-1\right)-3}}}. \tag{4.10}$$

The saddle point solutions in equation (4.4) allows to calculate the free energy as:

$$\overline{\phi}(r) = Ae^{-\frac{3r^2}{4L}} \quad ; \quad \overline{\phi}^*(r) = \left(\frac{A}{4\mu_p}\right)^{1/3}e^{-\frac{3r^2}{4L}}, \tag{4.11}$$

$$\overline{\psi}^*(x) = Be^{-\frac{9}{4L}x^2} \quad ; \quad \overline{\psi}(x) = 2\mu_a Be^{-\frac{9}{4L}x^2}. \tag{4.12}$$

The free energy is calculated assuming $-\chi'_{sp} > 0$ and supposing the constants: $L = 1$ and μ, μ_p, μ_a chosen to be unity for numerical approximation. Of course this is not always the case even for a network of two strands. Those value are taken one only in the purpose of illustration of the model. The free energy of the system is given by:

$$\begin{aligned}F &= -k_{\mathrm{B}}T\log[Z]\\ &\simeq -k_{\mathrm{B}}T(-\chi'_{sp})\\ &= -k_{\mathrm{B}}T(a'e^{-\frac{3\beta\Delta \mathrm{x} f}{2}} + b'e^{-2\beta\Delta \mathrm{x} f} + c'e^{-3\beta\Delta \mathrm{x} f}).\end{aligned} \tag{4.13}$$

with the constants $a' = 0.369617$, $b' = 0.1052$ and $c' = 0.0699017$. We show in this case that F changes with the force generated by the motor head indicating a rather complicated coupling so it is difficult to give a proper explanation of this expression.

4.4 Reversible link as motor heads attached by a spring

In this network configuration, the polymer chains are all arranged in in an anti-parallel manner. We keep in our mind that the active-movable cross-

linker used here moves toward a preferential (+ end) direction of the filament. That means, a bias force is generated by the motion of the active cross-linker. Considering a network formed by two polymers chains, The four ends of the chains are fixed by permanent cross-links. The active cross-link drives the chains that it uses as path way, oppositely to its direction of motion. For

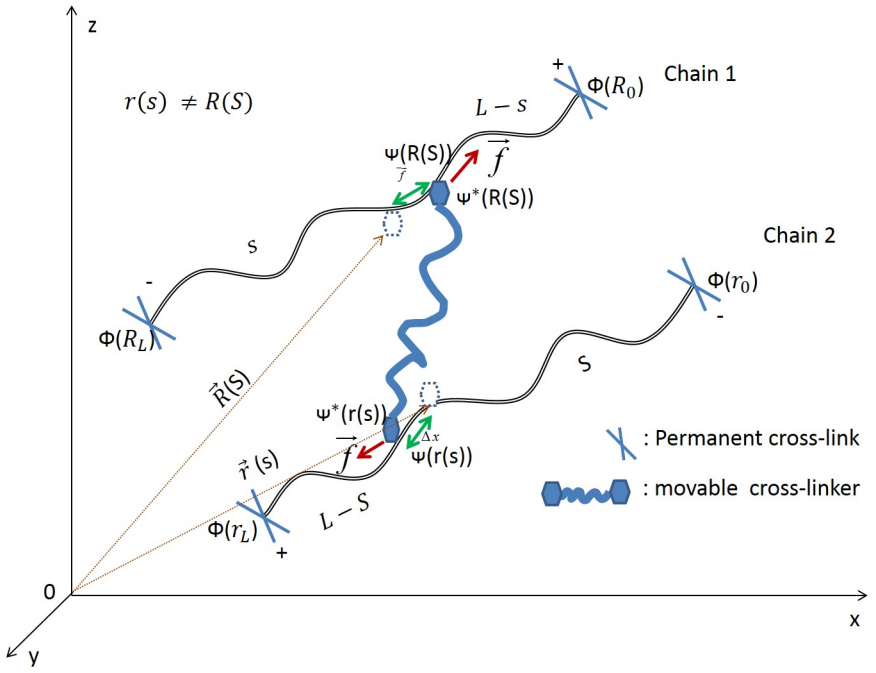

Figure 4.2: *The field ϕ and ψ are for passive and active cross-linkers. $r(s)$ and $R(S)$ are respectively the positions labelled on the chain (1) and (2). $x = r(s)$ and $X = R(s)$ are the spacial positions of the motor head along the chains with s and S the arc length of each chain. The motor heads are not in the same position along the chain ie $(r(s) \neq R(S))$. $(+)$ and $(-)$ indicate the polarity orientation of the polymer chain.*

the sake of simplicity in the notation, we work with the shorthand notation: $r(s) \equiv x$ and $R(S) \equiv X$. The contribution of each chain is given by:

$$\begin{aligned} \text{chain 1}: & \int \mathrm{d}x\, \phi(r_0)\, G(r_0 - x; s)\, e^{-\beta f \Delta x} \psi(x)\, G(x - r_L; L - s)\, \phi(r_L), \\ \text{chain 2}: & \int \mathrm{d}\, X\, \phi(R_0)\, G(R_0 - X; S)\, e^{-\beta f \Delta X}\, \psi(X)\, G(X - R_L; L - S)\, \phi(R_L). \end{aligned} \tag{4.14}$$

For simplicity, we suppose that each motor head moves with identical displacement, therefore, we can write $\Delta x = \Delta X$ and the work given by $\omega = -f\,\Delta x = f\,\Delta X$. We have used the following simplification: $r_0 = r(s_0)$; $r_L = r(s_L)$; $R_0 = R(S_0)$ and $R_L = R(S_L)$. The spring that connects the two motor heads is also deformed during the motor motion. The elastic contribution of the

spring is them taking into account and the elastic potential energy stored in the spring is given by: $E = \frac{k}{2}(x - X)^2$. The contribution of the permanent cross-links do not change from the model described at section 3.3.2. The positions of the moving cross-linker and distances from the that linker to the ends of the chains are all degrees of freedom. The statistical weight is then of the system is:

$$\begin{aligned} Z = & \int [\mathrm{d}\,\psi]\,[\mathrm{d}\,\psi^*]\,[\mathrm{d}\,\phi]\,[\mathrm{d}\,\phi^*]\,e^{-\int_r \phi\,\phi^* - \int_x \psi\,\psi^*} \\ & \times \left[\int_{r_0}\int_{r_L}\int_x\int_s \phi(r_0)\,G(r_0 - x; s)\,e^{-\beta\,f\,\Delta x}\,\psi(x)\,G(x - r_L; L - s)\,\phi(r_L)\right] \\ & \times \left[\int_{R_0}\int_{R_L}\int_X\int_S \phi(R_0)\,G(R_0 - X; S)\,e^{-\beta\,f\,\Delta X}\,\psi(X)\,G(X - R_L; L - S)\,\phi(R_L)\right] \\ & \times \left[\int_r \phi^{*4}\right]^4 \left[\int_{X,x} \psi^*(x)\,e^{-\beta\,E}\psi^*(X)\right], \end{aligned} \tag{4.15}$$

The present network configuration has interesting contractile properties, therefore, we are going to use the present network configuration for the future calculations.

$$\begin{aligned} Z &= \aleph \int [\mathrm{d}\,\psi(x)]\,[\mathrm{d}\,\psi^*(x)]\,[\mathrm{d}\,\phi]\,[\mathrm{d}\,\phi^*]\,e^{-\int_r \phi\,\phi^* - \int_x \psi(x)\,\psi^*(x)} \\ &\times \left[\int_{r_0,r_L,x} \phi(r_0)\,G(r_0 - r_L; L)\,e^{-\beta\,f\Delta x}\,\psi(x)\,\phi(r_L)\right] \\ &\times \left[\int_{R_0,R_L,X} \phi(R_0)\,G(R_0 - R_L; L)\,e^{-\beta\,f\,\Delta X}\,\psi(X)\,\phi(R_L)\right] \\ &\times \left[\int_r \phi^{*4}\,\mathrm{d}r\right]^4 \left[\int_{x,X} \psi^*(x)\,e^{-\beta\,\frac{k}{2}\,(x-X)^2}\,\psi^*(X)\right], \\ &= \aleph \int [\mathrm{d}\,\psi]\,[\mathrm{d}\,\psi^*]\,[\mathrm{d}\,\phi]\,[\mathrm{d}\,\phi^*]\,\exp\left(-\chi''[\psi, \psi^*, \phi, \phi^*]\right). \end{aligned} \tag{4.16}$$

With

$$\begin{aligned} -\chi'' = & \mu\left[\int_{r_0,r_L,x} \phi(r_0)\,G(r_0 - r_1; L)\,e^{-\beta\,f\Delta x}\,\psi(x)\,\phi(r_L)\right] - \log\mu \\ & + \mu'\left[\int_{R_0,R_L,X} \phi(R_0)\,G(R_0 - R_L; L)\,e^{-\beta f\,\Delta X}\,\psi(X)\,\phi(R_L)\right] - \log\mu' \\ & + \mu_p \int_r \phi^{*4} + \mu_a \int_{x,X} \psi^*(x)\,e^{-\beta\,\frac{k}{2}\,(x-X)^2}\,\psi^*(X) - 4\,\log\mu_p - \log\mu_a \\ & - \int_r \phi\,\phi^* - \int_x \psi(x)\,\psi^*(x). \end{aligned} \tag{4.17}$$

The steepest descent equations are given by the set of equations:

$$\frac{\delta(-\chi'')}{\delta\psi(y)}|_{sp} = 0;\ \frac{\delta(-\chi'')}{\delta\psi^*(y)}|_{sp} = 0;\ \frac{\delta(-\chi'')}{\delta\phi}|_{sp} = 0;\ \frac{\delta(-\chi'')}{\delta\phi^*}|_{sp} = 0. \tag{4.18}$$

We neglect the constant $(-\log\mu - \log\mu' - 4\log\mu_p - \log\mu_a)$ in the saddle point approximation. If we suppose that the two chains are identical, the equation (4.19) is simplify as:

$$\begin{aligned} -\chi'' = 2\mu &\left[\int_{r_0,r_L,x} \phi(r_0)\, G(r_0 - r_1; L)\, e^{-\beta f \Delta x}\, \psi(x)\, \phi(r_L)\right] \\ &+ \mu_p \int_r \phi^{*4} + \mu_a \int_{x,X} \psi^*(x)\, e^{-\beta \frac{k}{2}(x-X)^2}\, \psi^*(X) \\ &- \int_r \phi\, \phi^* - \int_x \psi(x)\, \psi^*(x). \end{aligned} \tag{4.19}$$

We use the shorthand notion $G = G(r_0 - r_L; L)$.

$$\begin{cases} 2\mu \int_{r_0,r_L} \overline{\phi}(r_0) G e^{-\beta f \Delta x} \overline{\phi}(r_L) - \overline{\psi}^*(y) = 0, & \text{(e1)} \\ 2\mu_a \int_x \overline{\psi}^*(x) e^{-\beta \frac{k}{2}(x-X)^2} - \overline{\psi}(x) = 0, & \text{(e2)} \\ 2\mu \int_{y,r_0} \overline{\phi}(r_0) G e^{-\beta f \Delta x} \overline{\psi}(y) - \overline{\phi}^* = 0, & \text{(e3)} \\ 4\,\mu_p \overline{\phi}^{*3} - \overline{\phi} = 0. & \text{(e4)} \end{cases} \tag{4.20}$$

As the chains are supposed Gaussian, the following expressions hold: $G = Ne^{\frac{-3}{2L}(r_0 - r_L)^2}$, $\overline{\psi}^*(x) = Be^{-bx^2}$ and $\overline{\phi}(r) = Ae^{-ar^2}$. The delta function Gaussian expression are expressed as:

$$\delta(x) = \lim_{\epsilon \to 0} \frac{1}{\epsilon\sqrt{\pi}} \exp\left(\frac{-x^2}{\epsilon^2}\right), \tag{4.21}$$

we have the transformation:

$$\delta(x - X) = \sqrt{\frac{\beta k}{2\pi}} \exp\left(\frac{-\beta k}{2}(x - X)^2\right) \tag{4.22}$$

We introduce equation (4.22) into the saddle point equation (equation (e2)). We combine the four equations (4.20) and obtain a linear equation in $\overline{\phi}$. Afterwards, we identify the constants A and a, b and B. The saddle point solutions are given by:

$$\overline{\phi}(r) = Ae^{-\frac{9r^2}{4L}} \quad ; \quad \overline{\phi}^*(r) = \left(\frac{A}{4}\right)^{1/3} e^{-\frac{9r^2}{4L}}, \tag{4.23}$$

$$\overline{\psi}^*(x) = Be^{-\frac{3}{8L}x^2} \quad ; \quad \overline{\psi}(x) = 2B\sqrt{\frac{2\pi}{k}} e^{-\frac{3}{8L}x^2}. \tag{4.24}$$

With the constants given by the expressions: $a = \frac{9}{4L}$; $b = \frac{3}{8L}$,

$$A = \frac{k^{3/8}L^{3/4}}{2\ 6^{3/8}\pi^{3/4}\left(\frac{L}{6L+1}\right)^{3/16}e^{-\frac{3}{4}f\Delta x}}, \tag{4.25}$$

$$B = \frac{\left(\frac{k^{3/8}L^{3/4}}{\left(\frac{L}{6L+1}\right)^{3/16}e^{-\frac{3}{4}f\Delta x}}\right)^{2/3}}{2\ 3^{3/4}\sqrt{2\pi}\sqrt[4]{\frac{1}{k}}}, \tag{4.26}$$

for the parameters ($\mu = \mu_a = \mu_p = 1, \beta = 1$ for simplification purpose). The free energy is derived from the partition function. After having calculated the saddle point solutions, we put their expressions back into the equation (4.19) and then replace it into the equation (4.16) (see equations (3.53) and (3.54). After having performed the integration over the fields, we have:

$$Z \simeq \exp\left(-\chi''_{sp}\right). \tag{4.27}$$

The functional χ''_{sp} is the functional χ'' at the saddle point solutions. The free energy is calculated using $L = 1$ and we have:

$$\begin{aligned} F &= -k_{\mathrm{B}}T\log[Z] \\ &\simeq -k_{\mathrm{B}}T(-\chi''_{sp}), \\ &= -k_{\mathrm{B}}T\left(0.1355\,k\sqrt{\frac{3-4k}{(18-24k)k}} + \frac{0.0854063}{\left(\frac{1}{k}\right)^{3/4}}\right)e^{-f\Delta x} \\ &- 0.000348723\,k_{\mathrm{B}}T\,k^{3/2}\,e^{3f\Delta x} + 0.197522\,k_{\mathrm{B}}T\,\sqrt{k}\,e^{f\Delta x} \end{aligned} \tag{4.28}$$

We show in this case that F changes with the force generated by the motor head indicating a rather complicated coupling so it is difficult to give a proper explanation of this expression. The full averaging over the position of the cross-linker takes place when we include the deformation of the network. The spring constant in the expression indicate that the spring is not negligible in the present model.

4.4.1 Average density

We calculate the average density of the cross-linkers using the generating formula as performed in section 3.4.2.

- The average density profile for the permanent cross-linker is given by:

$$\langle\rho(r)\rangle = \frac{1}{z_h}\frac{\delta z_h}{\delta h(r)}|_{h=1}. \tag{4.29}$$

With the generating functional expressed as follow:

$$Z_h = \int [\mathrm{d}\,\psi]\,[\mathrm{d}\,\psi^*]\,[\mathrm{d}\,\phi]\,[\mathrm{d}\,\phi^*]\,\exp\Big\{\mu\int \phi(r_0)\,G_1\,e^{-\beta\,f\,s}\,G_1'\,\phi(r_L) + \mu'\int \phi(R_0)\,G_2\,e^{-\beta\,f\,S}\,G_2'\,\phi(R_L) + \mu_p\int \phi^{*4}(r)\,h(r) + \mu_a\int_{x,X}\psi^*\,e^{-\beta\,E}\,\psi^* - \int \phi\,\phi^* - \int \psi\,\psi^* + \ldots\Big\}. \tag{4.30}$$

Performing the functional derivative over h, we end up with the following expression: $\langle\rho(r)\rangle = \langle\mu_p\,\phi^{*4}(r)\rangle \simeq \langle\phi^{*4}(r)\rangle$. Applying the statistical mechanical average formula, we have:

$$\begin{aligned}\langle\rho(r)\rangle &= \langle\phi^{*4}(r)\rangle \\ &= \overline{\phi}^{*4}(r) + 4\overline{\phi}^{*4}(r)\langle\Delta\phi^*\rangle + \overline{\phi}^{*2}(\langle\Delta\phi^*\rangle)^2 \\ &= \overline{\phi}^{*4}(r) + \text{fluctuation term.}\end{aligned} \tag{4.31}$$

The power four on the field ϕ represents the functionality of the permanent cross-linker.

- Similarly, for the average density profile of the active cross-linker, we use the formula:

$$\langle\rho(x)\rangle = \frac{1}{z_J}\frac{\delta z_J}{\delta J(x)}|_{J=0}. \tag{4.32}$$

with the generating functional expression given by:

$$Z_h = \int [\mathrm{d}\,\psi]\,[\mathrm{d}\,\psi^*]\,[\mathrm{d}\,\phi]\,[\mathrm{d}\,\phi^*]\,\exp\Big\{\mu\int \phi(r_0)\,G_1\,e^{-\beta\,f\,\Delta x}\,G_1'\,\phi(r_L) + \mu'\int \phi(R_0)\,G_2\,e^{-\beta\,f\,\Delta X}G_2'\,\phi(R_L) + \mu_p\int \phi^{*4}(r) + \mu_a\int_{x,X}\psi^*\,e^{-\beta\,E}\psi^*h(x) - \int \phi\,\phi^* - \int \psi\,\psi^* + \ldots\Big\}. \tag{4.33}$$

With the shorthand notations $G_1 = G(r_0 - x, s)$, $G_1' = G(x - r_L, L - s)$, $G_2 = G(R_0 - X, S)$, and $G_2' = G(X - R_L, L - S)$. The calculation gives:

$$\begin{aligned}\langle\rho(x)\rangle &= \langle\int_X \psi^*(x)\,e^{-\beta\,E}\,\psi^*(X)\rangle \\ &= \int_X \overline{\psi}^*(x)\,e^{-\frac{\beta\,k}{2}(x-X)^2}\,\overline{\psi}^*(X) + \text{Fluctuating term.}\end{aligned} \tag{4.34}$$

The average density results from the two types of cross-linkers show that both cross-linker average densities contain a dominant term and a fluctuating term.

The network with linkers like slipping motor heads presented above shows interesting and can be identified to the sarcomeric unit in muscle fibre or even to a simple version of contractile ring found at the later stage of the cell division (see chapter (5)). The contractile ring is modelled as a specific example of active network in the chapter 5.

4.5 Conclusion

We have presented in this chapter two specific one-dimensional network configuration of polar polymers with active-movable (active) and permanent cross-links. Emphasis went on the active cross-linker that mimics the non- reversible motor protein head and generates an active biasing force while moving. The polarity of the polymer allows us to think of two possible configuration of polymer relative to each other for at least a the minimal model of two chains. The active-movable cross-link imposes the orientation of the two cross-linked chains. For the two configurations found are made of four permanent cross-links with functionality four and placed at the very ends of the chains. The behaviour of each the network configuration depends on the chains primary distribution into the network formed. When the chains are parallel, the moving cross-linker is viewed as a moving ring called "slipping-ring". The moving ring slides and stops at the ends on the chains. The spring that connects the two motor heads is neglected and simply slides to one end of the chains. For the case where the chains are anti-parallel, the two moving cross-link heads move in opposite directions, both following the (+) ends of the chains. The spring provides a non trivial coupling between the polymer chains. The elasticity of the network is more pronounced because the moving cross-link pulls and pushes the chains. The ends of the chains are kept fixed. The average density reveals that each cross-linker fluctuates around a mean density which is the saddle point solution powered by the functionality of the respective cross-linker. In the case of anti-parallel chains, the average density includes the position of the linker along the chain. We saw that in the two network configurations, for the primitive one dimensional network, the network has always an "X" like shaped. For a three dimensional network, the chains' configuration in the network is not clear because no investigation has been done in the present dissertation on this regards.

Part III

Natural active network: Example of the contractile ring

Chapter 5

Collective dynamics of the filaments inside an actomyosin network

5.1 Introduction

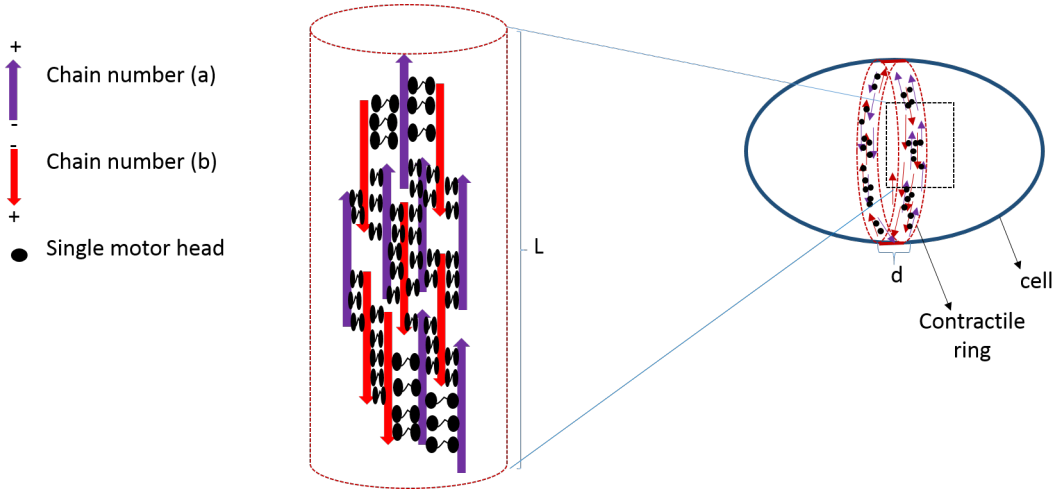

Figure 5.1: *Contractile ring as a linear periodic system. d is the width of the ring, $L = 2\pi R$ (R is the radius of the ring) is the total length of the ring, it is simply the contour area length of the ring if we suppose that the linear ring model is the ring that have been opened.*

This chapter presents an introduction of the formalism that will be used in chapter 6 to investigate a natural network (the contractile ring). Here, we unfold the ring (Fig. 5.1) and present a simple one-dimensional model for a linear F-actin bundle network of length L. We look at the dynamics of the filaments within the network. The motors internally drive the system away

from equilibrium. Consequently, the normal equilibrium statistical physics tools cannot be applied. The mathematical tools to be used here are well known and widely used in polymer physics. We make use of the functional integral formalism elaborated by Martin, Siggia, Rose (1973) to investigate the statistical dynamics of a classical system [4]. This is done by casting the dynamical equations of the system inside the generating functional through the delta functional. Doing that, we introduce a response field that does not commute with the random variable. The stability of the system is investigated using the assumption of a dense polymer system. We use the collective variables and the dynamical Random Phase Approximation (RPA) following the scheme of Fredrickson et al. [5]. This formalism elaborated for a minimal model nevertheless allows us to capture the basic collective behaviour of the chains within the network and predicts the condition under which the chains in the network stay homogeneous or not. We also investigate numerically the role of the interacting forces on the dynamic behaviour of the chains ensemble.

5.2 Linear model describing the contractile ring

We present an effective one-dimensional geometry of a linear periodic filament bundle network. All the chains are distributed along the same axis. The network consists of N polar and rigid filaments. Each chain can only be oriented toward one direction, either to the left (the $(+$ end) of the rod is pointing in the $(-x)$ direction of the (ox) axis) or to the right (the $(+$ end) of the rod is pointing in the $(+x)$ direction of the (ox) axis)). The entire bundle length is labelled with L. In the case of a non external forces acting on the pair of cross-linked filaments, the total momentum of the system (filament pair) is conserved. In that circumstance, the centre of mass of the whole system does not move while the filaments are moving. It implies that the cross-linked filaments move in the same or opposite direction depending on the orientation of filament in respect to one another. Therefore, we look at two possible scenarios of networks: When the cross-linked filaments have the same orientation (we call this system "parallel bundle network") and when they have opposite orientation ("anti-parallel bundle network"). Experiments have shown that a one dimensional linear filament bundle network cross-linked by myosin II [62]. That network can only *contract* or *elongate* as a simple response of the activity of the motor inside the network. The contraction or elongation processes on the system are sorted out by looking at the orientation of the cross-linked filaments at their initial stage (i.e. just after the cross-linkage) [41].

We define the numbers N^+ and N^- of chains pointing to the right and to the left, respectively. Each chain $a \in [1, ..., N^{\pm}]$ is labelled with the position of its centre of mass x_a and its orientation σ_a, i.e., with the set of variables $\{x_a, \sigma_a\}$ for the a^{th} filament. For simplicity, all the chains are considered rigid

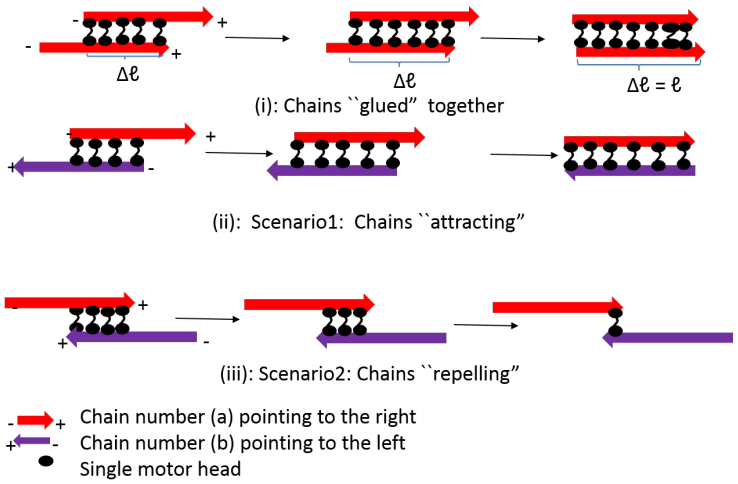

Figure 5.2: *The motor head moves toward the (+) end of the chain making the chain slide moving toward the (−) end direction of the chain. (i): Parallel filaments Bundle network. (ii): Anti-parallel with their (−) ends close to each other. The chains move closer to one another, the overlap distance between them increases and more motor is recruited to fit the empty space between the chains and then lead to the contraction behaviour. (iii): Anti-parallel with their (+) ends close to each other. The chains repel each other leading the expansion the system.*

and have the same length l. That allows us to exclude any possible rotation of the chains along the (oy) or (oz) axis. The variables σ_a defined the orientation of the chains a which takes value $\sigma_a = \pm 1$. The chain number a can cross-link any other chain number b as long as the two chains overlap. The degree of overlap depends on the distance between two overlapping chains and is given by the relation: $\Delta\ell = (\ell - |x_a - x_b|)\,\Theta(\ell - |x_a - x_b|)$, $(\Delta\ell \in [-\ell, \ell])$. Literature [34, 35, 42, 62] indicates that the contraction of such system depends on two major conditions: 1) The orientation of the cross-linked filaments relative to each other inside the system or, in other words, the initial condition (just before the motor is activated). 2) How overlapping filaments ends are aligned with one another inside the system. The myosin II motor head walks toward (+) end of the chain. The filaments are all randomly aligned inside the network. We therefore distinguish three different scenarios to represent the behaviour of the rods bundle network like active system:

5.2.1 Case of two parallel chains: $\sigma_a\sigma_b > 0$

Here, the chains are parallel (the barbed (+) end of all the overlapping chains points toward the same direction) and overlap (Fig. 5.2). When the motors start moving, we notice that both chains move in the same direction. They tend to stay "*glued*" together during this whole dynamics. In this scenario, the active force is almost constant and can be neglected without changing the global behaviour of the system.

5.2.2 Case of two antiparallel chains: $\sigma_a\sigma_b < 0$

For the case of chains pointing in opposite directions, each chain has two alternative movements: either moving to the right or to the left with equal probability. The choice of the movement of each filament strongly depends on its $+/-$ ends orientation relative to the chain with which it overlaps.

(i) **Scenario1**: "*Attracting chains*"

If the $(-)$ end of the two chains are close to each other, the two chains move close to each other driven by the pairwise force between the chains. This occur until the system reaches its maximum overlapping distance ($\Delta\ell_{max} = \ell$) (see Fig. 5.2). Once the maximal overlapping distance is reached, the two connected chains stop attracting each other. At that stage the chains start passing each other and the overlapping distance decreases until the chains no longer overlap (Fig. 5.2).

(ii) **Scenario2**: "*Repelling chains*"

If the motor heads start walking close to the $(+)$ ends of the chains, it is more likely to see those latter move further apart from each other (Fig. 5.2).

For a particular scenario of anti-parallel chains, the proximity of the ends of the chains determines if the chains will *repel* (i.e. system will *expand*) or *attract* (i.e. system will *contract*). During each of those processes, the density of the motor cluster (n_0) engaged varies because the number of motor heads depends on how large is the overlapping distance between the connected chains. In other words, the larger the overlap distance between the chains, the bigger is the number of motor heads involved in the cross-link and the lower will be the cross-linking energy. The average density of motors clusters is represented in the (Fig. 5.3). This suggests that if we have to define a number M of

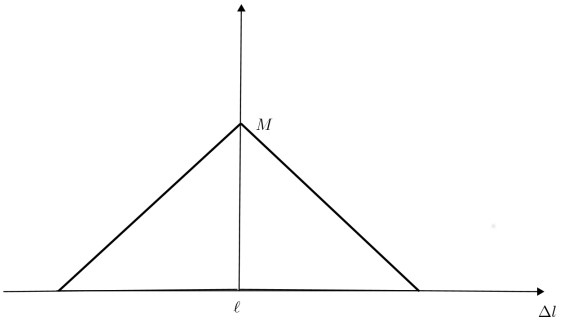

Figure 5.3: *Prediction of the average density of the motor head in antiparallel chains system.*

motor heads in a motor cluster that cross-link the filaments, M will be linearly proportional to the overlapping distance ($M \propto |\Delta\ell|$). At this point, we can

also predict that the network is energetically favourable to take more motor head if there is still available space. This happens if the motors are recruited to the overlap space between the chains and proportional to the overlapping distance. In reality, this might not be the case in real system, but we use this simple idealisation here. The question one should ask is : " what causes the contractile behaviour of the ring? ". We think that the key to answer this question is to understand the forces and their role play in the ring.

5.2.3 Mathematical representation of the model

The forces exerted on each chain inside the ring have been investigated. Each pair of chains is cross-linked by a pair of motor cluster sitting where the two randomly oriented chains overlap. The network is formed when all the chains newly involved in it overlap at least with one other chain segment that is already involved in the network. The condition to have the chains a and b cross-linked is: $|(x_a - \sigma_a \frac{\ell}{2}) - (x_b - \sigma_b \frac{\ell}{2})| < \ell$ or $|(x_a - \sigma_a \frac{\ell}{2}) - (x_b - \sigma_b \frac{\ell}{2})| > \ell$ for the chains a and b to be pull or push, respectively. We suppose that all the motor heads in the motor cluster seating on the same chain are all oriented in the same direction. At low Reynolds number, the velocity $\vec{v}_a$ of the filament number a, is proportional to the force $\vec{f}_a$ applied on the filament by one motor head connected to it. The motor clusters occupy the overlapping region with an uniform density n_0. Since the motor is always walking toward the + end of the chains, the sign of the force will depend on the orientation of the chain. The present model is similar to the one shown in the previous chapter (section 4.2). We can therefore enumerate all the forces acting on the actin-bundle network.

(i) **The active force:**

Inside the bundle chains network, the motor cluster made of many motor myosin II is able to move and cause the simple active force in a presence of ATP[1]. This motion is guide by the alignment of the chains with one another. The Fig. 5.2 depicts the preferentially move of the chains under the ATP. We suppose that each motor head on the cluster have the same orientation along the same chain. During its motion, each motor head generates a force with a strength f in order to pull or push the filament on which it is attached to (see cross-bridge cycle description at section 2.4.4). This force is a repulsive force (by definition) and defined

[1] ATP is the Adenosine triphosphate. It serves to transport the chemical energy within the cells.

for the chain number a by the explicit following expression:

$$\begin{aligned} F_{\text{act}} &= f\, n_0\, \sigma_a \sum_{b;\, b\neq a}^{N} \Delta\ell\, \delta_{a,b} \\ &= f\, n_0\, \sigma_a \sum_{b;\, b\neq a}^{N} (\ell - |x_a - x_b|)\, \Theta(\ell - |x_a - x_b|)\, \delta_{a,b}. \end{aligned} \tag{5.1}$$

Where ($\Delta\ell = (\ell - |x_a - x_b|)\, \Theta(\ell - |x_a - x_b|)$) is the overlapping distance between the cross-linked chains a and b; N is the total number of chains in the system supposing that the system has equal number of chains pointing to the left and pointing to the right $N^+ = N^-$; n_0 is the density of motor head inside the motor cluster. σ_a is the orientation of the chain a; $\delta_{a,b}$ is the Kronecker delta function that enforces the connection between the chains a and b. Its role is to emphasize that the cross-linkage is between the chain a and the chain b. The Heaviside theta function $\Theta(\ell - |x_a - x_b|)$ when the chains interact (i.e. any $a \neq b$ chain can cross-link as long as they overlap). The parameter $f\, n_0$ is an adjustable parameter.

$$\Theta(\ell - |x_a - x_b|) = \begin{cases} 0 & \text{if} \quad \ell < |x_a - x_b|, \\ 1 & \text{if} \quad \ell \geq |x_a - x_b|. \end{cases}$$

In the case of parallel cross-linked chains, the motor proteins moves toward the same direction (+ end of each chains). That is why in our model for parallel cross-linked chains the force generated by the motor protein is neglected. If the cross-linked chains are "anti-parallel", the active force will move toward opposite direction and causes the chains sliding movement. The sign of the active force will therefore depend on the orientation of the first chain a, and its expressions for the two situations are given by:

$$F_{\text{act}} = F_{\text{act}}^{\pm\pm} + F_{\text{act}}^{\pm\mp} = \begin{cases} F_{\text{act}}^{\pm\pm} & = \text{constant} \backsimeq 0, \\ + & \\ F_{\text{act}}^{\pm\mp} & = \pm f\, n_0 \sum_{b;\, b\neq a}^{N} (\ell - |x_a^{\pm} - x_b^{\mp}|)\, \Theta(\ell - |x_a^{\pm} - x_b^{\mp}|). \end{cases} \tag{5.2}$$

The force $F_{\text{act}}^{\pm\pm}$ means the active force generated by the chains a and b pointing respectively to the (right/left) and (right/ left). $F_{\text{act}}^{\pm\mp}$ is the active force between the $(+/-)$ oriented chain a and the $(-/+)$ oriented chain b. The sign of this force is defined in such a way that if we switch chains around, the active force should maintain the same sign while the chains swap their directions.

(ii) **The networking force:** Also named "overlapping force" is defined as an attractive force by its nature. When the motor clusters link two overlapping chains, they create an energy advantage to stay linked versus an entropic disadvantage (due to the surrounding) causing unlinking of the chains. This force is therefore derived from the networking energy stored by the system during the network formation. If we suppose that we have two chains that overlap in the system, as the chains move closer to one another, the overlapping distance between them increases and more motor is recruited to fit the empty space between the chains (see scenario1 Fig. 5.2). This force does not induce any dynamics of the system but it acts similar to an attractive force well known (example: gravitational force). This force tends to maintain the chains linked together. It is stronger than the active force and therefore its role is to maintain the homogeneity inside the system. This force is derived from the energy created when the chains overlap. The networking energy between the chains a and b is defined as:

$$\begin{aligned} E_{\text{net}}(x_a - x_b) &= \kappa\,(\ell - |x_a - x_b|)\,\Theta(\ell - |x_a - x_b|), \\ &= \epsilon n_0\,(\ell - |x_a - x_b|)\,\Theta(\ell - |x_a - x_b|). \end{aligned} \tag{5.3}$$

The networking force is then the negative gradient of the energy and has the following expression:

$$\begin{aligned} F_{\text{net}} &= -\nabla_{x_a} E_{\text{net}}\,, \\ &= -\kappa\,\Theta(\ell - |x_a - x_b|)\,\text{sign}(x_a - x_b), \\ &+ \kappa\,(\ell - |x_a - x_b|)\,\delta(\ell - |x_a - x_b|)\text{sign}(x_a - x_b). \end{aligned} \tag{5.4}$$

The second term of the networking force vanishes because the delta function is only relevant when $(\ell - |x_a - x_b|) = 0$ and is multiplied by 0. This second term on the force goes away and we left with the expression of the networking force on the chain a as:

$$F_{\text{net}} = -\epsilon\, n_0 \sum_{b;b\neq a}^{N} \Theta(\ell - |x_a - x_b|)\,\text{sign}(x_a - x_b). \tag{5.5}$$

$\kappa = \epsilon\, n_0$ is an adjustable parameter that represents the strength of the networking force. ϵ is the internal energy that each motor head generates in order to stay connected to the chain. $\text{sign}(x_a - x_b)$ means that the force can be negative or positive depending on the orientation of the cross-linked chains. $\text{sign}(x_a - x_b) = +1$ for $(x_a > x_b)$ and -1 for $(x_a < x_b)$. This force is therefore always an attractive force no mater the chains configuration. The sign of the force should change leading to the system behaviour changing. If we keep the same orientation of the cross-linked chains, by changing the sign of the networking force, this later goes from

attractive to repulsive or vice-versa. This is why we can say that this force is a reversible force. Depending on the orientation of the chains, we have:

$$F_{\text{net}} = F_{\text{net}}^{\pm\pm} + F_{\text{net}}^{\pm\mp} = \begin{cases} F_{\text{net}}^{\pm\pm} & = -\epsilon\, n_0 \sum\limits_{b;b\neq a}^{N} \Theta(\ell - |x_a^{\pm} - x_b^{\mp}|), \\ + & \\ F_{\text{net}}^{\pm\mp} & = -\epsilon\, n_0 \sum\limits_{b;b\neq a}^{N} \Theta(\ell - |x_a^{\pm} - x_b^{\mp}|). \end{cases} \tag{5.6}$$

The sign of the networking force is crucial in order to determine what kind of movement the chains experience inside the system. When $\epsilon > 0$, there is a possibility of decrease the number of contacts (number of cross-linker or motor head inside the motor cluster). That results to lowering the contribution of the motor cluster between the connected chains. However, it also diminishes the entropy of the system and therefore increases the free energy. In such situations, the cross-linked chains will repel and result in an "ordered phase" of the system in which all the chains clump and form two clouds of chains. If $\epsilon < 0$, the entropy of the system is dominant. The system stays homogeneous. The system therefore exhibits an isotropic phase with the two species of chains that interact with one another. In this case, we have a "disordered phase". We keep in mind that this force is an equilibrium force. It causes the system to collapse so that we do not have an extended steady state of the system. This force is constant and says that there is a constant amount of energy per unit length that the cross-linked chains can gain or lose.

5.2.3.1 Langevin equations

The filaments are very small about $(5-10\,\text{nm})$ in diameter [1]. The Reynolds number is very small, therefore, the inertial effect which is captured by the term $(m\frac{d\vec{v}}{dt})$ is safely disregarded while writing the Langevin equations. For a network of two chains a and b between the N^+ and N^- chains, respectively. Each chain in the system is tracked using their centre of mass x_a^+ and x_b^- for rods pointing toward the right and the left directions, respectively. The dynamical equations for the motion of each chain inside the system is given by the following set of equations:

$$\begin{cases} L_a^+(t) : -\gamma\, \partial_t x_a^+ + f_a^+(t) + F_{int}^+ = 0. \\ L_b^-(t) : -\gamma\, \partial_t x_b^- + f_b^-(t) + F_{int}^- = 0. \end{cases} \tag{5.7}$$

The subscript $+/-$ means the dynamics of the right/left pointing rod. $f_{a/b}^{+/-}(t)$ is the stochastic force. This force has a zero mean $\langle f_{a/b}^{+/-}(t)\rangle = 0$ and its correlation given by the fluctuation dissipation theorem $\langle f_{a/b}^{+/-}(t) f_{a/b}^{+/-}(t')\rangle =$

$\lambda\,\delta(t-t')$. λ is the strength of the thermal noise force and is related to the drag coefficient with $\lambda = \frac{2\gamma}{\beta}$, ($\beta = 1/k_BT$, k_B is the Boltzmann constant and T is the temperature of the system). It has a Gaussian distribution given by the following probability:

$$P[f^{+/-}_{a/b(t)}] = \aleph e^{-\frac{1}{2\lambda}\int |f^{+/-}_{a/b}(t)|^2}. \tag{5.8}$$

The interacting force $F^{+/-}_{int}$ is composed of forces including the contributions from the interactions between parallel, anti-parallel in the mixture of two types of filaments orientation. Its explicit expression is given by:

$$F^{\sigma_a/\sigma_b}_{int} \;=\; F^{\sigma_a\sigma_a/\sigma_b\sigma_b}_{int} \;+\; F^{\sigma_a\sigma_b/\sigma_b\sigma_a}_{int}, \tag{5.9}$$

and explicitly decomposed as follow:

$$\begin{aligned} F^{+}_{int} &= F^{++}_{int} + F^{+-}_{int} \\ &= F^{++}_{\text{net}} + F^{+-}_{\text{act}} + F^{+-}_{\text{net}}, \qquad (5.10) \\ F^{-}_{int} &= F^{--}_{int} + F^{-+}_{int} \\ &= F^{--}_{\text{net}} + F^{-+}_{\text{act}} + F^{-+}_{\text{net}}. \qquad (5.11) \end{aligned}$$

The appropriate signs for the forces are all given as follow:

$$F^{++}_{\text{net}} < 0 \quad ; \quad F^{--}_{\text{net}} < 0, \tag{5.12}$$
$$F^{++}_{\text{act}} \sim 0 \quad ; \quad F^{--}_{\text{act}} \sim 0, \tag{5.13}$$
$$F^{+-}_{\text{net}} < 0 \quad ; \quad F^{-+}_{\text{net}} < 0, \tag{5.14}$$
$$F^{+-}_{\text{act}} > 0 \quad ; \quad F^{-+}_{\text{act}} < 0. \tag{5.15}$$

5.3 The formalism

We here discuss the behaviour of the system described above and suppose it to be a dense chains solution. We express each type of chain in term of polymer density variable via the so called random phase approximation (RPA). We use the collective properties of each type of chain and deduce the density-density correlation function. The system is dynamic, meaning that the normal statistical physics treatment cannot be applied here. A technique called Martin, Siggia, Rose (MSR) formalism elaborated by Martin, Siggia and Rose (1973) is used here [4, 63].

5.3.1 Martin-Siggia-Rose (MSR) formalism

The starting point of the formalism is to cast the Langevin equations (equations (5.7)) into the generating functional using the Dirac delta functional.

The delta functional is used to convert the Langevin equations into the functional form using it inside the exponential function form. This transformation is called the Hubbard Stratonovich transformation (HST) and it is done by introducing a new variable in the generating functional: the response field is a variable associated to each dynamical variable. Two clear reviews of this method have been presented by Jensen, Martin, Siggia and Rose [4, 63]. The method has revealed itself to be a good mathematical tool to calculate the statistical properties of a classical dynamical system. Its contribution is to introduce inside the generating functional the response density field variable which is the complex conjugate of the variable. By respecting the time ordering constraint presented by Jensen [63], this new variable is also called the auxiliary field and its average with the field and himself gives zero ($\langle x(t)\hat{x}(t')...\rangle = 0$ and $\langle \hat{x}(t)\hat{x}(t')...\rangle = 0$) under the condition that $t > t'$. These conditions insure the causal nature of the response function. The generating functional can then be written as:

$$Z \quad = \langle \int \prod_{a=1}^{N^+} \prod_{b=1}^{N^-} [\mathrm{d}x_a^+(t)]\,[\mathrm{d}x_b^-(t)]\,\delta[L_a^+]\,\delta[L_b^-]\,J_{x^{\sigma_a}}\,J_{x^{\sigma_b}}\rangle_{\{f^{\sigma_a},f^{\sigma_b}\}}. \tag{5.16}$$

The delta functional is rewritten in its exponential form using the following HST formula:

$$\delta(L^{\sigma_a}) = \int_{\mathbb{R}} [\mathrm{d}x^{\sigma_a}]\,\exp\left[i\int_t \hat{x}^{\sigma_a} L^{\sigma_a}\right]. \tag{5.17}$$

(Just to recall the notations $\sigma_{a/b} = \pm 1$ or right/left oriented rod). The Jacobian of the transformation J can be chosen as unity under the circumstances where specific causality rules are applied to all averages computed in this system, as shown in Jensen [63]. $\hat{x}^{\sigma_a}$ is the auxiliary field associated to the variable x^{σ_a}. This auxiliary field is used to generate the response function [5, 14, 64]. After averaging over the Gaussian nature of the stochastic force, we have:

$$\begin{aligned}&\int_t [\mathrm{d}\,x^{\sigma_a}]\,[\mathrm{d}\,\hat{x}^{\sigma_a}]\,[\mathrm{d}\,f^{\sigma_a}]\,\exp\left\{-\frac{1}{2\lambda}\int_t (f^{\sigma_a})^2 \;+\; i\int_t \widehat{x}^{\sigma_a}(t)\,f^{\sigma_a}(t)\right\}\\ &= \sqrt{2\,\pi\,\lambda}\int_t [\mathrm{d}\,x^{\sigma_a}][\mathrm{d}\,\hat{x}^{\sigma_a}]\,\exp\left\{-\frac{\lambda}{2}\int_t (\hat{x}^{\sigma_a})^2(t)\right\}.\end{aligned} \tag{5.18}$$

The generating functional then gives:

$$\begin{aligned}Z = \frac{1}{\aleph}\int_{-\infty}^{+\infty} \prod_{a=1}^{N^+}\prod_{b=1}^{N^-} [\mathrm{d}\,x_a^+(t)]\,[\mathrm{d}\,\hat{x}_a^+(t)]\,[\mathrm{d}\,x_b^-(t)][\mathrm{d}\,\hat{x}_b^-(t)]\\ \times\exp\left[-\tfrac{\lambda}{2}\sum_{a=1}^{N^+}\int_t(\hat{x}_a^+)^2 \;-\; i\gamma\sum_{a=1}^{N^+}\int_t \hat{x}_a^+\,\dot{x}_a^+ \;+\; i\sum_{a=1}^{N^+}\int_t \hat{x}_a^+\,F_{int}^+\right]\\ \times\exp\left[-\tfrac{\lambda}{2}\sum_{b=1}^{N^-}\int_t(\hat{x}_b^-)^2 - \;i\gamma\sum_{b=1}^{N^-}\int_t \hat{x}_b^-\,\dot{x}_b^- \;+\; i\sum_{b=1}^{N^-}\int_t \hat{x}_b^-\,F_{int}^-\right].\end{aligned} \tag{5.19}$$

For the purpose of making the equations easily readable with less indices, we will for the rest of the calculations use the shorthand notation a and b to indicate the rods pointing to the right and left both without the sign (+ and -) respectively. That means, we use the change: $x_a^+ \to x_a$, $x_b^- \to X_b$. In order to deduce the correlation and the responses function of the chains in the network, we introduce a source field term inside the generating functional. That source term is coupled with the variable in which one is interested. It is therefore coupled with the hatted variable in such a way that the functional derivative gives the expression we had before plus an additional term that couple the source term and the variable. We call $h(t)$ and $\hat{h}(t)$ the source fields associated with any variable $x(t)$ and to its associate auxiliary field $\hat{x}(t)$, respectively. We introduce the source term associated with chains pointing right as an example:

$$\begin{aligned} Z[h(t),\hat{h}(t)] = \frac{1}{\aleph} \int_{-\infty}^{+\infty} \prod_{a=1}^{N^+} \prod_{b=1}^{N^-} [\mathrm{d}\, x_a(t)]\,[\mathrm{d}\,\hat{x}_a(t)]\,[\mathrm{d}\, X_b(t)]\,[\mathrm{d}\,\hat{X}_b(t)] \\ \times \exp\left[-\frac{\lambda}{2} \sum_{a=1}^{N^+} \int_t (\hat{x}_a)^2 \;-\; i\gamma \sum_{a=1}^{N^+} \int_t \hat{x}_a\, \dot{x}_a \;+\; i \sum_{a=1}^{N^+} \int_t \hat{x}_a\, F_{int}^+ \right] \\ \times \exp\left[-\frac{\lambda}{2} \sum_{b=1}^{N^-} \int_t (\hat{X}_b)^2 \;-\; i\gamma \sum_{b=1}^{N^-} \int_t \hat{X}_b\, \dot{X}_b \;+\; i \sum_{b=1}^{N^-} \int_t \hat{X}_b\, F_{int}^- \right] \\ \times \exp\left[i \int_t \sum_{a=1}^{N^+} \left(x_a\, h \;+\; \hat{x}_a\, \hat{h} \right) \right]. \end{aligned} \tag{5.20}$$

We see from equation (5.20) that the functional derivate over the source field gives the expression we had before (5.19). This technique is called the generating functional approach. The correlation function of the position of the system of chains is deduced by taking the functional derivation in respect to the source term $h(t)$. The chains pair correlation function will contain informations on the screening effect of the chains inside the system. It is given by the expression:

$$\langle x_a(t)\, x_a(t') \rangle \;=\; \frac{1}{Z[0,0]} \left[-\frac{\delta^2 Z[h\,,\widehat{h}]}{\delta h(t)\;\delta h(t')} \right]_{|_{h\,,\,\widehat{h}=0}} . \tag{5.21}$$

The + pointing chains response function is given by:

$$\langle x_a(t)\, \widehat{x}_a(t') \rangle \;=\; \frac{1}{Z[0,0]} \left[-\frac{\delta^2 Z[h\,,\widehat{h}]}{\delta h(t)\;\delta \widehat{h}(t')} \right]_{|_{h\,,\,\widehat{h}=0}} . \tag{5.22}$$

The generating functional can be reduced to its simplest expression and be written as:

$$Z \;=\; \frac{1}{\aleph'} \int_{\mathbb{R}} \prod_{a=1}^{N^+} \prod_{b=1}^{N^-} [\mathrm{d}\, x_a(t)]\,[\mathrm{d}\,\hat{x}_a(t)]\,[\mathrm{d}\, X_b(t)]\,[\mathrm{d}\,\hat{X}_b(t)]\, e^{\mathcal{L}}. \tag{5.23}$$

With the shorthand notation $\mathcal{L} = i \int L$ being the effective Lagrangian. This Lagrangian can be split into the interacting and the non-interacting Lagrangian ($\mathcal{L} = \mathcal{L}_{int} + \mathcal{L}_0$).

$$\mathcal{L}_0 = -\frac{\lambda}{2}\sum_{a=1}^{N^+}\int_t (\hat{x}_a)^2 - i\gamma\sum_{a=1}^{N^+}\int_t \hat{x}_a\,\dot{x}_a - \frac{\lambda}{2}\sum_{b=1}^{N^-}\int_t (\hat{X}_b)^2 - i\gamma\sum_{b=1}^{N^-}\int_t \hat{X}_b\,\dot{X}_b, \tag{5.24}$$

$$\mathcal{L}_{int} = i\sum_{a,b=1}^{N}\int_t \hat{x}_a\,F^{+}_{int} + i\sum_{a,b=1}^{N}\int_t \hat{X}_b\,F^{-}_{int}. \tag{5.25}$$

5.3.2 Introduction of collectives variables

It is convenient for such large system to use a collective variables which are the density variables (cf. [5, 64]). We chose to use the collective variables because we would like to render independent the dynamics of many chains [7, 8, 65]. The density variable is given by: $\rho(x) = \sum_{a=1}^{N}\delta(x - x_a)$ for any chain characterised by its position in space labelled with x. This collective variables is best expressed in Fourier space. We use the Fourier transformation formula: ($f(k) = \frac{1}{\sqrt{2\,\pi}}\int_x e^{i\,k\,x} f(x)$; $f(x) = \sqrt{2\,\pi}\int_k e^{-i\,k\,x} f(k)$). The collective variables and their corresponding auxiliary field variables in Fourier space are written as:

$$\rho^{+}(k,t) = \sum_{a=1}^{N^+} e^{-i\,k\,x_a(t)} \quad ; \quad \varphi^{+}(k\,,\,t) = \sum_{a=1}^{N^+}\hat{x}_a\,e^{-i\,k\,x_a(t)}, \tag{5.26}$$

$$\rho^{-}(k\,,\,t) = \sum_{b=1}^{N^-} e^{-i\,k\,X_b(t)} \quad ; \quad \varphi^{-}(k\,,\,t) = \sum_{b=1}^{N^-}\hat{X}_b\,e^{-i\,k\,X_b(t)}. \tag{5.27}$$

The variable φ is the conjugate field density of the density variable ρ. For the full model of the ring, the appropriate density variables should be expressed in Fourier series because the ring is a periodic system. For the present linear ring model, we use the Fourier transform to express the density variables. The interacting Lagrangian after having introduced the collective variables gives:

$$\mathcal{L}_{int} = \frac{i}{2}\int_t\int_k \Big[\varphi_a(k,t)\,F^{++}_{int}(k)\,\rho_a(k',t') + \varphi_b(k,t)\,F^{--}_{int}(k)\,\rho_b(k',t') \\ \varphi_a(k,t)\,F^{+-}_{int}(k)\,\rho_b(k',t') + \varphi_b(k,t)\,F^{-+}_{int}(k)\,\rho_a(k',t')\Big]. \tag{5.28}$$

The explicit steps of the calculation can be seen in Appendix B.1 The shorthand notation used for the rest of the calculation is: $\rho_a \equiv \rho^{+}$ and $\varphi_a \equiv \varphi^{+}$,

$\rho_b \equiv \rho^-$ and $\varphi_b \equiv \varphi^-$. we include the possibility to have interaction that might be due to the response density field φ. The interacting part of the Lagrangian function can be written $\mathcal{L}_{int}$ as using the following argument:

$$\varphi(k,t)\rho(k',t') = \frac{1}{2}\left[\varphi(k,t)\rho(k',t') + \rho(k,t)\varphi(k',t')\right], \tag{5.29}$$

and we have:

$$\begin{aligned}\mathcal{L}_{int} = \frac{i}{2}\int_t\int_k \Big[&\varphi_a(k,t)\,F^{++}_{int}(k)\,\rho_a(k',t') + \rho_a(k,t)\,F^{++}_{int}(k')\,\varphi_a(k',t') \\ &+ \varphi_b(k,t)\,F^{--}_{int}(k)\,\rho_b(k',t') + \rho_b(k,t)\,F^{--}_{int}(k')\,\varphi_b(k',t') \\ &+ \varphi_a(k,t)F^{+-}_{int}(k)\rho_b(k',t') + \rho_b(k,t)F^{+-}_{int}(k')\varphi_a(k',t') \\ &+ \varphi_b(k,t)\,F^{-+}_{int}(k)\,\rho_a(k',t') + \rho_a(k,t)\,F^{-+}_{int}(k')\,\varphi_b(k',t')\Big].\end{aligned} \tag{5.30}$$

With $k' = -k$ and $t' = -t$. We define two density super vectors:

$$\underline{\rho}(k,t) \;= (\rho_a(k,t)\,,\,\varphi_a(k,t)\,,\,\rho_b(k,t)\,,\,\varphi_b(k,t))\,. \tag{5.31}$$

The interacting Lagrangian after having performed the Fourier transform over the time gives:

$$\mathcal{L}_{int} = \frac{i}{2}\int_\omega\int_k \left[\underline{\rho}(k,\omega)\,\underline{\underline{F}}_{int}(k)\,\underline{\rho}^T(k',\omega')\right]. \tag{5.32}$$

Were $\underline{\rho}^T$ is the transpose of the supper vector $\underline{\rho}$. $\underline{\underline{F}}_{int}(k)$ is a 4×4 matrix having the following expression:

$$\underline{\underline{F}}_{int}(k) = \begin{pmatrix} 0 & F^{++}_{int}(k) & 0 & F^{+-}_{int}(k) \\ F^{++}_{int}(k) & 0 & F^{+-}_{int}(k) & 0 \\ 0 & F^{-+}_{int}(k) & 0 & F^{--}_{int}(k) \\ F^{-+}_{int}(k) & 0 & F^{--}_{int}(k) & 0 \end{pmatrix}. \tag{5.33}$$

with:

$$F^{\pm\pm}_{int}(k) = -\frac{2i\sqrt{\frac{2}{\pi}}\,n_0\,\epsilon\sin^2\left(\frac{kl}{2}\right)}{k}, \tag{5.34}$$

$$F^{\pm\mp}_{int}(k) = \pm\frac{2\sqrt{\frac{2}{\pi}}\,n_0(f\,+\,ik\,\epsilon)\sin^2\left(\frac{kl}{2}\right)}{k^2}. \tag{5.35}$$

To express the generating functional in term of the collective variables. We introduce an unity expression equation (5.36) inside the equation (5.23) and

obtains the equation (5.37).

$$1 = \int_{\mathbb{R}} [\mathrm{d}\,\rho_a]\,[\mathrm{d}\,\rho_b]\,[\mathrm{d}\,\varphi_a]\,[\mathrm{d}\,\varphi_b]\,\delta[\rho_a(k,t) - \sum_{a=1}^{N^+} e^{-ik\,x_a(t)}]\,\delta[\rho_b(k,t) - \sum_{b=1}^{N^-} e^{-ik\,X_b(t)}]$$
$$\delta[\varphi_a(k,t) - \sum_{a=1}^{N^+} \hat{x}_a\, e^{-ik\,x_a(t)}]\delta[\varphi_b(k,t) - \sum_{b=1}^{N^-} \hat{X}_b\, e^{-ik\,X_b(t)}]. \tag{5.36}$$

$$Z = \frac{1}{\aleph'} \int_{\mathbb{R}} \prod_{a=1}^{N^+} \prod_{b=1}^{N^-} [\mathrm{d}\,x_a(t)]\,[\mathrm{d}\,\hat{x}_a(t)]\,[\mathrm{d}\,X_b(t)]\,[\mathrm{d}\,\hat{X}_b(t)]\rho_a]\,[\mathrm{d}\,\rho_b][\mathrm{d}\,\varphi_a]\,[\mathrm{d}\,\varphi_b]$$
$$\exp\left(i\,\mathcal{L}\right)\delta[\rho_a(k,t) - \sum_{a=1}^{N^+} e^{-i\ k\,x_a(t)}]\,\delta[\rho_b(k,t) - \sum_{b=1}^{N^-} e^{-ik\,X_b(t)}]$$
$$\delta[\varphi_a(k,t) - \sum_{a=1}^{N^+} \hat{x}_a\, e^{-ik\,x_a(t)}]\,\delta[\varphi_b(k,t) - \sum_{b=1}^{N^-} \hat{X}_b\, e^{-ik\,X_b(t)}]. \tag{5.37}$$

We now use the exponential expression of the delta functional. Doing that, we introduce the auxiliary fields variable associated with each collective variables. All the Jacobian of the transformations are unity. The whole expression is developed and we have the equation (5.38):

$$Z = \frac{1}{\aleph'} \int_{\mathbb{R}} \prod_{a=1}^{N^+} \prod_{b=1}^{N^-} [\mathrm{d}\,x_a(t)]\,[\mathrm{d}\,\hat{x}_a(t)]\,[\mathrm{d}\,X_b(t)]\,[\mathrm{d}\,\hat{X}_b(t)]$$
$$[\mathrm{d}\,\rho_a]\,[\mathrm{d}\,\rho_b]\,[\mathrm{d}\,\varphi_a]\,[\mathrm{d}\,\varphi_b]\,e^{\mathcal{L}}. \tag{5.38}$$

With the shorthand notation $\mathcal{L} = \mathcal{L}_{int} + \mathcal{L}_3 + \mathcal{L}_q$ where

$$\mathcal{L}_q = -i \int_{k,t} \left(\hat{\rho}_a \rho_a + \hat{\rho}_b \rho_b + \hat{\varphi}_a \varphi_a + \hat{\varphi}_b \varphi_b\right). \tag{5.39}$$

is the quadratic Lagrangian. The new non-interacting Lagrangian is:

$$\mathcal{L}_3 = -\,i \int_{k,t} \left(\sum_{a=1}^{N^+} \hat{\rho}_a\, e^{-ik\,x_a(t)} + \sum_{a=1}^{N^+} \hat{\varphi}_a\, \hat{x}_a\, e^{-ik\,x_a(t)} \right.$$
$$\left. + \sum_{b=1}^{N^-} \hat{\rho}_b\, e^{-ik\,X_b(t)} + \sum_{b=1}^{N^-} \hat{\varphi}_b\, \hat{X}_b\, e^{-ik\,X_b(t)} \right). \tag{5.40}$$

The exponential inside the equation (5.38) gives now:

$$\exp\left[\mathcal{L}\right] = \exp\{\mathcal{L}_{int} + \mathcal{L}_q\} \times \exp\{\mathcal{L}_3 + \mathcal{L}_0\}. \tag{5.41}$$

The quadratic part of the effective Lagrangian will vanish while giving an identity matrix. The non interacting part of the Lagrangian is treated using

the Gaussian approximation known as Random Phase Approximation (RPA) (see section 5.3.3). The non interacting part of the Lagrangian is approximated as:

$$\exp[\mathcal{L}_3 + \mathcal{L}_0] \simeq \exp[\frac{1}{2}\langle \mathcal{L}_3^2 \rangle_0]. \tag{5.42}$$

Where $\langle (...) \rangle_0 = \int_{\mathbb{R}} [\mathrm{d}\, x_a]\, [\mathrm{d}\, \hat{x}_a]\, [\mathrm{d}\, X_b]\, [\mathrm{d}\, \hat{X}_b]\, (...)\, \exp[\mathcal{L}_0]$ represents the average of (...) with $e^{\mathcal{L}_0}$ as statistical weight.

5.3.3 Random phase approximation(RPA)

We study here the collective behaviour of the chains in order to understand the stability of the system. We would like to include the correlation effects between polymers chains and therefore, the structure factor must be calculated. This is done under the RPA. We assume that the system is dense enough and that each species of chain is homogeneously distributed. We therefore describe the chain mixture within the loop expansion of field theory. Other works have implemented this approximation for dynamical dense charged polymer mixture [5, 8, 64]. It has been shown to be particularly convenient for the investigation of collective dynamics using a field variable like density variable. The method presented here follows the scheme of Fredrickson et al. (1990) [5]. It is useful to notice that the approximation is done on the non-interacting part of the Lagrangian, and the interacting part will be dealt with later. By describing the collective dynamics of a dense system of polymers, we can say without doubt that the dynamics version of the RPA turns out to be equivalent to the Gaussian approximation. The Fredrickson's method used here provides access to quantities like collective correlation functions and response functions. We later investigate where the RPA of the homogeneous system fails as one indicator of possible phase transition. This is done by looking at the correlation function obtained under the RPA. The expression $\mathcal{L}_3^2$ is expanded as shown in equation (5.42) and the average of each terms are taken over $\mathcal{L}_0$ (non-interacting part). (more details of the calculations is presented in the Appendix B.2.1). The 4×4 matrix $\underline{\underline{S}}_0$ called *non-interacting matrix* is deduced. The symmetry of this matrix respect the relation $(S_{ij}(k,t) = S_{ij}(k',t'))$ with $k' = -k, t' = -t$. The explicit elements of this matrix are workout in the Appendix B.2.1. We introduce the Fourier transform on time $(t \to \omega)$ and use the shorthand notation $\int_\omega = \frac{1}{\sqrt{2\pi}} \int_\omega$ and have the expression:

$$\begin{aligned}\exp(-\mathcal{L}_3 - \mathcal{L}_0) &= -\frac{1}{2} \int_\omega \int_k \underline{\hat{\rho}}(k,\omega) \begin{pmatrix} S_{11} & S_{12} & 0 & 0 \\ S_{21} & 0 & 0 & 0 \\ 0 & 0 & S_{33} & S_{34} \\ 0 & 0 & S_{43} & 0 \end{pmatrix} \underline{\hat{\rho}}^T(k',\omega') \\ &= -\frac{1}{2} \iint_{k,\omega} \underline{\hat{\rho}}(k,\omega) \underline{\underline{S}}_0(k,\omega) \underline{\hat{\rho}}^T(k',\omega'). \end{aligned} \tag{5.43}$$

The elements of this non-interacting matrix are for the diagonals and the off-diagonal elements, the dynamics collective correlation function and the response function, respectively. After having performed the change of variables inside the generating functional, this latter functional is rewritten in terms of the collective variables and one can deduce the density-density correlation functions by taking the $(1,1)$ element of the correlation matrix $\left(i\underline{\underline{F}}_{int} + \underline{\underline{S}}_0^{-1}\right)^{-1}$.

$$Z = Z_{\text{MF}} \int_{\mathbb{R}} [\mathrm{d}\underline{\Delta\rho}]\, e^{-1/2 \iint_{k,\omega} \Delta\rho(k,\omega)\left(i\underline{\underline{F}}_{int} + \underline{\underline{S}}_0^{-1}\right)\Delta\rho^T(k',\omega')}. \tag{5.44}$$

The approximation permits us to make use of the mean field assumption where the density field fluctuates around a density background which is the mean field density $\rho_{\text{MF}} = \frac{N}{L}$. The density field therefore splits into the mean field density and the fluctuation density $\rho = \rho_{\text{MF}} + \Delta\rho$. L is the total length of the system, and N the total number of chains in the mixture. Introducing the mean field argument into the generating functional, we obtain equation (5.44) where Z_{MF} is the mean field generating functional which is a constant and can be included in the normalisation constant and be neglected for the rest of the calculation. The generating functional expression can be written as seen in the equation (5.45) where the fluctuation term is implicitly written under the density variable.

$$\begin{aligned} Z &= \frac{1}{\aleph'} \int_{\mathbb{R}} [\mathrm{d}\,\underline{\rho}]\,[\mathrm{d}\,\underline{\hat{\rho}}]\, \exp\left[\mathcal{L}\right] \\ &= \frac{1}{\aleph'} \int_{\mathbb{R}} [\mathrm{d}\,\underline{\rho}]\,[\mathrm{d}\,\underline{\hat{\rho}}] \exp\Bigg[-\frac{1}{2}\iint_{k,\omega} \underline{\hat{\rho}}(k,\omega)\underline{\underline{S}}_0(k,\omega)\underline{\hat{\rho}}^T(k',\omega') \\ &- \frac{i}{2}\iint_{k,\omega} \underline{\rho}(k,\omega)\,\underline{\underline{F}}_{int}(k)\,\underline{\rho}^T(k',\omega') \\ &+ i\iint_{k,\omega} \underline{\rho}(k,\omega)\,\underline{\underline{Q}}(k,\omega)\,\underline{\rho}^T(k',\omega')\Bigg]. \end{aligned} \tag{5.45}$$

where $\underline{\underline{Q}}(k,\omega)$ is a 4×4 matrix call the quadratic matrix and gives an identity matrix which is neglected for the rest of our calculation. Upon integrating out the hatted field $\hat{\rho}$, the results for the generating functional is finally given by equation (5.46):

$$Z = \frac{1}{\aleph'} \int_{\mathbb{R}} [\mathrm{d}\,\underline{\rho}] \exp\left[-\frac{1}{2}\iint_{k,\omega} \underline{\rho}(k,\omega)\,\left(i\underline{\underline{F}}_{int}(k) + \underline{\underline{S}}_0^{-1}(k,\omega)\right)\underline{\rho}^T(k',\omega')\right]. \tag{5.46}$$

We use the generating functional approach by introducing a source field cou-

pled to the super-vector field $\underline{\rho}(k,\omega)$ and get:

$$\begin{aligned} Z[\underline{h}(k,\omega)] &= \frac{1}{\aleph'}\int_{\mathbb{R}}[\mathrm{d}\,\underline{\rho}]\,\exp\Bigg[-\frac{1}{2}\iint_{k,\omega}\underline{\rho}(k,\omega)\,\left(i\underline{\underline{F}}_{int}(k)+\underline{\underline{S}}_0^{-1}(k,\omega)\right)\\ &\quad \underline{\rho}^T(k',\omega')+\iint_{k,\omega}\underline{\rho}(k,\omega)\,\underline{h}(k',\omega')\Bigg]\\ &= \frac{1}{\aleph'}\int_{\mathbb{R}}[\mathrm{d}\,\underline{\rho}]\,\exp\left[-\frac{1}{2}\iint_{k,\omega}\underline{h}(k,\omega)\,\left(i\underline{\underline{F}}_{int}(k)+\underline{\underline{S}}_0^{-1}(k,\omega)\right)\,\underline{h}^T(k',\omega')\right]. \end{aligned} \tag{5.47}$$

The correlation functions can be deduced by performing the functional derivative over the source field vector term $\underline{h}$.

$$\begin{aligned} \langle\rho(k,\omega)\,\rho(k',\omega')\rangle &= \frac{1}{Z[0]}\left[\frac{\delta^2 Z}{\delta\underline{h}(k,\omega)\,\delta\underline{h}(k',\omega')}\right]_{\underline{h}(0)=0}\\ &= \delta(k+k')\,\delta(\omega+\omega')\,A^{-1}(k,\omega)\\ &\equiv A^{-1}(k,\omega). \end{aligned} \tag{5.48}$$

Where $G(k,\omega)=A^{-1}(k,\omega)=\left(i\underline{\underline{F}}_{int}(k)+\underline{\underline{S}}_0^{-1}(k,\omega)\right)^{-1}$ is the dynamical correlation matrix of the system. The density-density correlation function is the diagonal of this correlation matrix and the response function the off diagonal of the matrix. Details of the calculation of the non interaction matrix is presented in Appendix B.2.1. We have developed the approximation without the drift velocity. For the present generic formalism presentation, we ignore the drift velocity in the Langevin equation. Nevertheless, for the periodic ring model described in the next chapter (chapter 6), this velocity is important and will be investigated. In the linear ring, this velocity does not play important role at long time limit because, after a long time, the chains move apart from one another in the system. This is as opposed to the chains that continuously overtake one another in the periodic ring model. This latter model has a sustain current flowing through it so the importance of the investigation of the drift velocity for the periodic ring (see section 6.5). We therefore expect the physics for the periodic model to be different from the one presented here.

5.4 The RPA results

5.4.1 Density-density correlation function

From the RPA calculation, we have been able to determine the density-density correlation function which is the $(1,1)$ element of the correlation matrix. Probing this function will provide us informations on how and under which conditions the filaments change their behaviour inside the network [65]. The explicit

expression for the correlation function is given by equation (5.49). This equation represents an initial discussion on the correlation function. A deeper analysis of the dynamics correlation function for the finite ring model is more pertinent and should be covered in the next chapter (chapter 6).

$$\begin{aligned} G_{11}(k,\omega) = \{&2\sqrt{2}\,\pi^{3/2}\,\gamma^2\,k^4\,\lambda\,\left(64\,\eta^4\,\lambda^2\,n_0^2\left(f^2\,+2\,k^2\,\epsilon^2\right)-16\,\pi\,\eta^2\lambda^2\,k^4\,n_0\,\epsilon\right.\\ &\left.+\pi^2k^2\left(4\gamma^4\omega^2+\lambda^2k^4\right)\right)\}/\{4096\,f^4\,\eta^8\,n_0^4\,+\,2048\,\pi\,f^2\,\eta^6\,k^4n_0^3\epsilon\\ &-128\,\pi^2\,\eta^4\,k^2\,n_0^2\,\left(f^2\,\left(k^4-4\,\omega^2\right)-2\,k^2\,\epsilon^2\,\left(k^4+4\,\omega^2\right)\right)\\ &+\pi^4\,k^4\,\left(k^4+4\,\omega^2\right)^2-32\,\pi^3\,\eta^2\,k^6\,n_0\,\epsilon\,\left(k^4+4\,\omega^2\right)\}. \end{aligned} \tag{5.49}$$

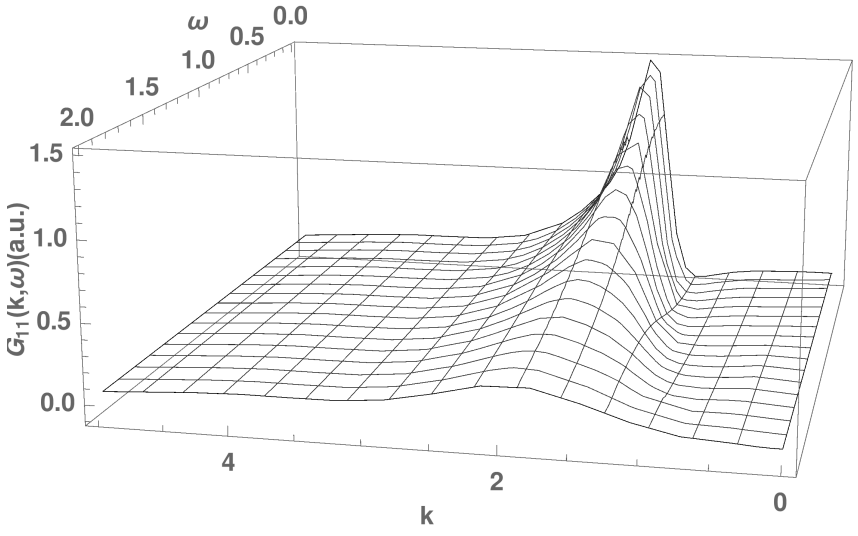

Figure 5.4: *Density-density correlation function plotted for the parameters values:* $\lambda = 1, l = 2.5, n_0 = 10, \gamma = 0.9, f = 0.1, \epsilon = 0.1$. *The graph shows that the peak shrinks toward the small* ω *direction.*

With $\eta = \sin(k\,l/2)$. The Fig. 5.4 displays a sharp peak at small frequency value. The peak observed suggests a dominant length scale in the system. It therefore reveals an interesting dynamic phenomenon of the filaments within the network. The higher value of the peak is observed for the value of the frequency is less or equal to 0.5 ($\omega \leq 0.5$) and for low value of the wave vector k. The Fig. 5.4 tells us that the linear ring network features are best seen at long time limit where the system reaches an almost steady state. We plot the correlation function for many values of the frequency this is shown at Fig. 5.5. This figure shows that the peak is maximal at low frequency. This means that, looking at the system too early will not provide accurate informations on the filaments' behaviour in the network. For the rest of the analysis, we

will work at large time and space limit (i.e. small ω and k). We probe the correlation function with different values of the length of the single filament ℓ. We notice that around the value ($\ell = 2.5$), the peak of the correlation function is at its higher value. The system thus starts to display some behaviour changing. We use the value $\ell = 2.5$ and probe the correlation function for the frequency value $\omega = 0.5$ for the rest of the analysis. The values at which one expects the filaments to overlap for an homogeneous system are found to be: $n_0 \geq 10, \ell \geq 2.5$. We use the parameters: $\lambda = 1, \gamma = 0.9$ and are

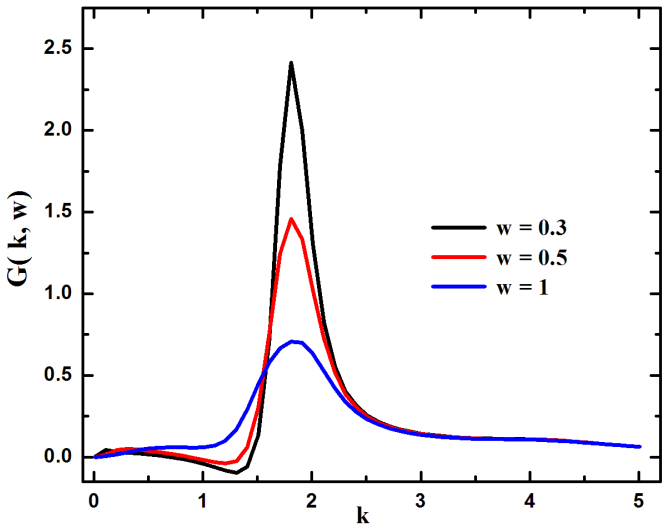

Figure 5.5: *Correlation function plotted for the parameters values:* $\lambda = 1, l = 2.5, n_0 = 10, \gamma = 0.9, f = 0.1, \epsilon = 0.1$ *and for different values of the frequency* $\omega = 0.1, 0.5, 1$ *from top to bottom respectively. The maximal peak is observed at smaller frequency value.*

interested on understanding the network behaviour changing caused by the interacting forces (active and networking forces). The Fig. 5.6 presents the correlation function of the mixture of randomly distributed chains for different values of the active force while the networking force is kept constant. Taking the networking force strength small and negative (attractive $\epsilon < 0$) (see section 5.2.3) for the sign convention of the networking force). In this case, the system remains an homogeneous mixture of the two species of chains randomly distributed in a bundle network resulting to a "disordered phase" of the system. On the other hand, taking the networking force positive (repulsive $\epsilon > 0$), that means there is a possibility that between two cross-linked chains, the number of cross-linkers decrease caused by the fact that the chains will move apart from one another. That will results to diminish the contribution

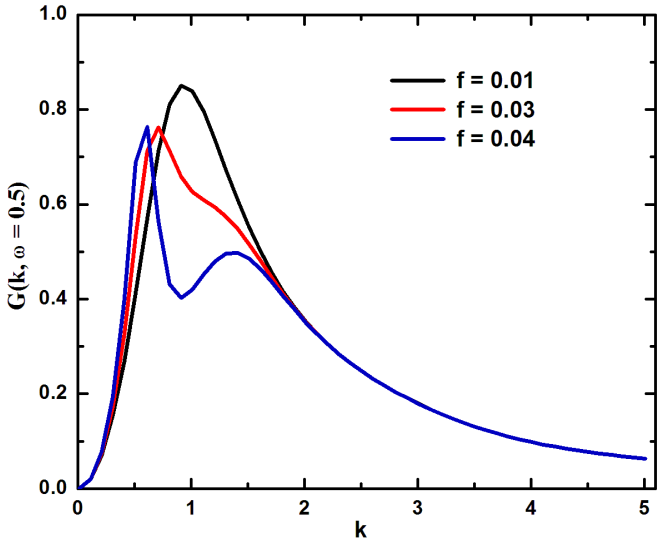

Figure 5.6: *Dependence of the density-density correlation function for* $\omega = 0.5$*, the attractive force(*$\epsilon = -0.01$*) and* $l = 2.5, \lambda = 1, \gamma = 0.9, n_0 = 10$ *and for different value of the active force* $f = 0.01, 0.03, 0.04$ *as indicated on the figure.*

of the motor head between the connected chains until the chains no longer overlap. In this case, the entropy of the system diminishes and therefore the free energy will increase. The chains in the system will repel themselves and clump to form clouds of chains. This leads to an "ordered phase" of the system.

The Fig. 5.6 presents a raising peak with the increase of the active force value (with $\epsilon < 0$). That new peak is less pronounced than the first higher maxima and shift to higher value of k. Around the value $f = 0.045$, the correlation function starts to diverge announcing the instability of the system and therefore, the phase separation. The Fig. 5.7 and 5.8 present the influence of the networking force on the system for a small value of the active force $f = 0.01$. The Fig. 5.7 shows the attractive behaviour of the chains inside the system due to the attractive feature of the networking force ($\epsilon < 0$). After a long time, the system become homogeneous and therefore unstable and this is the disordered phase state of the system. The Fig. 5.8 presents the repulsive feature of the networking force is observed when ($\epsilon > 0$). Those two latter graphs show that the sign of the networking force changes the behaviour of the system as predicted by the model description. In other words, since the active force is always attractive, changing the sign of the networking force has revealed the reversibility behaviour of the networking force. The reversibility in the present context means that, if one swaps the order or the orientation of the connected chains, The chains still attract one another due to the networking

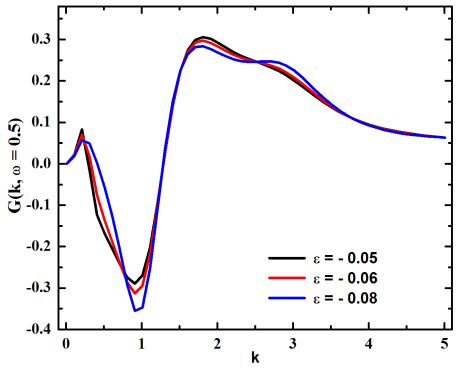

Figure 5.7: *Plot of the correlation function dependence of the attractive networking force* $\epsilon = -0.05, -0.06, -0.08$ *with the other parameters* $f = 0.01, \omega = 0.5, l = 2.5, \lambda = 1, \gamma = 0.9, n_0 = 10$.

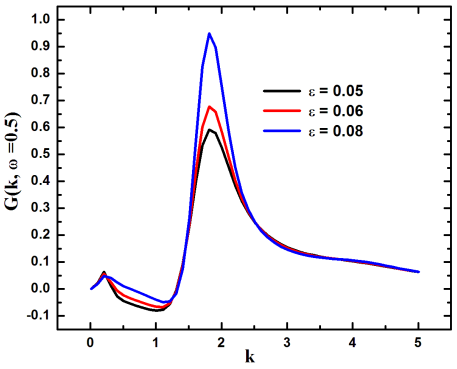

Figure 5.8: *Plot of the correlation function dependence of the networking force* $\epsilon = 0.05, 0.06, 0.08$ *when the sign of the networking force is swapped (from negative to positive value). The parameters are:* $f = 0.01, \omega = 0.5, l = 2.5, \lambda = 1, \gamma = 0.9, n_0 = 10$.

force and therefore leads to the contraction of the network. The effect of the networking force here could be identified at the effect of the networking contribution while the active force effect could be equated to the active contribution.

We probe the correlation function (equation 5.49). The numerator is always positive and varies very little. We analyse the denominator of the function (equation (5.50)). We plot an approximate phase diagram at a critical value of the wave vector calculating by switching off the active force in the numerator of the correlation function. We obtain $k_{\rm cr} \simeq 0.1$ with the parameters $\ell = 2.5$, $n_0 = 10$, $\gamma = 1$, $\lambda = 1$, $\omega = 0.5$. The approximate Phase diagram plot shown in Fig. 5.9 presents the two regions where the system is unstable and where it is stable. We look at the critical networking force strength in depth in the contractile ring system in the next chapter in details (section 6.6).

$$\begin{aligned} d = {} & f^4(4096\eta^8 n_0^4) + f^2(-128\pi\eta^4 k^2 n_0^2 \left(\pi k^4 - 16\eta^2 k^2 n_0 \epsilon - 4\pi\omega^2\right)) \\ & + (\pi^2 k^4 \left(k^4 + 4\omega^2\right) \left(\pi^2 k^4 - 32\pi\eta^2 k^2 n_0 \epsilon + 256\eta^4 n_0^2 \epsilon^2 + 4\pi^2\omega^2\right)). \end{aligned} \tag{5.50}$$

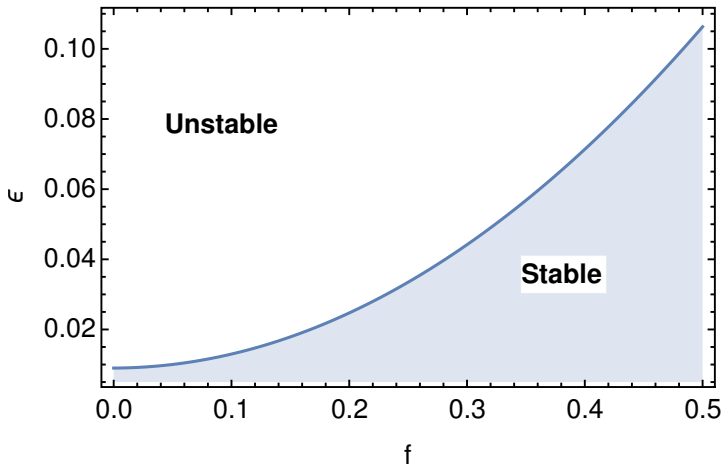

Figure 5.9: *Plot of the density-density correlation function equation (5.4) at different value of ϵ and f. The parameters are: $k = 0.1$, $\ell = 2.5$, $n_0 = 10$, $\gamma = 1$, $\lambda = 1$, $\omega = 0.5$. The critical values of ϵ and f must not be zero for the correlation function to keep its physical meaning.*

5.5 Conclusion

We have presented in this chapter a minimal one dimensional linear actomyosin bundle network model that mimics the contractile ring. The theory elaborated allowed us to capture the basic main behaviour of a randomly oriented chains bundle network. We presented a collective dynamical behaviour of the chains inside the network. This collective study of the system have been implemented using the MSR formalism. By assuming that we have a dense system of chains allows us to study its properties using the RPA method. The density-density correlation function deduced from the RPA have been probed and the stability of the system investigated. Results show that the two chains species co-exist and their behaviours are defined by their initial orientation from to one another. We conclude that in a case of randomly oriented chains in a bundle network, two type of behaviours can be observed: The "contractile" and the "expansion" behaviour of the network. The two behaviours are determined by the action of the motor protein myosin II. A more concrete system is studied in chapter 6.

We have shown here that, the concentration of the chain inside the network causes an increase in the peak of the density-density correlation function at small frequency and low wave vector depending on the forces strength f and ϵ. These peaks are understood to emerge from the chains behaviour in the network. The investigation of the parameters shows the evidence of the dependence of the single chain length (that has been pointed out in chapter 5 for the example of bundle network). We therefore think that the self consistence treatment of the problem could provide a better picture of the chains dynam-

ics. This is in respect to the Gaussian chain approximation that have been implemented with the collective (non-interactive) chains distribution. The RPA fails where there is a clear indicator that the conformation of the chains within the system are no longer Gaussian. The Phase diagram plot presented in Fig. 5.9 shows the region where the RPA breaks down.

Chapter 6

The contractile ring model

6.1 Introduction

According to the cell theory, each cell derives from a preexisting cell [35, 37]. Many tissue in living organism must repair often such as: white blood cells, skin cells etc... During cell division process, the mother cell splits in two identical daughter cells. The process by which the cell experiences a physical division is called "mitosis". Steps of this process have been detailed in section 2.4.1. At the last stage of the mitosis, an organelle is formed at the cortex of the cell. The widely used and approved to be the most likely plausible theory developed to explain the cell division is the theory of "the contractile ring". This theory was first introduced by Marsland and Landau (1954) [30] and agreed by most scientists as being the basic mechanism of the cell division process. The theory predicts that the cell is pinched off by the contractile ring which is formed on the cell cortex at the later stage of the division process. The organelle contains various proteins and the number of its proteins makes

Figure 6.1: *The contractile ring. The green dots represent the motor myosin II. The blue and red arrows represent the actin filaments that are clockwise and anti-clockwise oriented respectively.*

it a complex and interesting material. The ring contains one of the proteins frequently found in muscle cell and known to be responsible for the muscle contraction. This protein is called the myosin II motor protein. The ring contains many other interesting proteins, but for the sake of simplicity, we limit ourselves to a minimal ring model constituted of actin filaments and the myosin II. However, this minimal description of the ring gives nevertheless a good general understanding of the dynamical behaviour of the filaments within the ring.

We elaborate in this chapter a full model representing the periodic contractile ring as oppose to the limited linear ring model presented in chapter 5. As pictorially represented in Fig. 6.1, the chains are randomly distributed and due to their polarity, can move clockwise or anti-clockwise depending on their barbed (+) end orientation. The formalism elaborated for the simple linear ring (see section 5.3) model is used here for the periodic ring model. The periodicity of the ring permits us to rescale the forces by introducing the periodicity constrain. In the present chapter, we investigate the filaments networking formation using the myosin II as cross-linker and the stability study of the ring. Together with the analytical investigation of the model, we implement a simple Langevin Dynamics Simulation. The role played by each force in the behaviour of the chains within the ring is highlighted. Conclusion drawn form the two investigations lead to say that the force generated by the myosin II motor protein seems to dominate the mechanical stability of the ring while the force generated to keep the filaments connected is responsible for the contractile behaviour of the ring.

6.2 The periodic ring model

We investigate the dynamical behaviour of the supposed rigid filaments within the ring. The linear ring model assumptions still holds here. That means, an equal number of chains moving to the left and to the right that interact with one another and generate the active and networking forces.
The circumference of the ring is $L = 2\pi R$ with R being the radius of the ring. The maximum value (just after the ring formation) of R is $R = D_{\text{cell}}/2$ with D_{cell} representing the diameter of the cell before being pinched. The two interacting forces (networking and active) described in the section 5.2.3 have the same characteristics for the periodic ring model. Nevertheless, their expression are slightly modified to include the periodic boundary conditions. The forces between the chains number i and the chain number j, are given by:

$$F^R_{\text{act}}(x_i - x_j) = F_{\text{act}}(x_i - x_j) + F_{\text{act}}(x_i - x_j + L) + F_{\text{act}}(x_i - x_j - L), \quad (6.1)$$

$$F^R_{net}(x_i - x_j) = F_{net}(x_i - x_j) + F_{\text{net}}(x_i - x_j + L) + F_{\text{net}}(x_i - x_j - L). \quad (6.2)$$

By adding and subtracting the total circumference of the ring (L) to the original distance between the two interacting chains , we are calculating the minimal

distance between every two filaments that overlap. The length L is added or subtracted to the distance if negative ($(x_i - x_j) < 0$) or positive ($(x_i - x_j) > 0$)), respectively. This technique is mostly used in simulations when one has a periodic system. It ensures that the chains remain inside the confined region (ring circumference) so that there number of chains is conserved for the whole simulation. The two forces' new expressions are valid if the condition $\frac{L}{2} > l$ always holds. The forces are defined for this periodic system as a repetition of themselves. we can therefore define $F^R_{act}(x)$ and $F^R_{net}(x)$ as repetitions of the two functions in the interval $[-L, L]$. The Fourier series of a function $f(x)$ is given by the formula: $f(x) = \sum_{m=-\infty}^{+\infty} c_m \exp(ikx)$ with the Fourier coefficients computed by $c_m = (1/L)\int_0^L \mathrm{d}x f(x)\exp(-ikx)$. The Kronecker δ is written in terms of an inverse Fourier coefficient: $\delta_{m,m'} = \frac{1}{L}\int_0^L \mathrm{d}x\, e^{2\pi i(m-m')x/L}$. The Fourier coefficient of a (periodic) Dirac delta function are given by $c_m = \frac{1}{L}\int_0^L \mathrm{d}x\, \delta(x - x')e^{-2\pi imx/L} = \frac{1}{L}e^{-2\pi imx'/L}$. We construct the periodic Dirac delta function through the following construction that must also replace the appropriate expression above:

$$\delta_L(x) = \sum_{-\infty}^{\infty} \delta(x - mL) = \frac{1}{L}\sum_{m=-\infty}^{\infty} e^{\frac{2i\pi mx}{L}} = \frac{1}{L}\sum_{k\neq 0} e^{i\pi kx}. \tag{6.3}$$

The calculation of the Fourier coefficients of the two forces give:

$$F^{R,m}_{\text{net}} = -\frac{2in_0\epsilon}{\pi m}\sin^2\left(\frac{m\pi l}{L}\right), \quad \text{or} \quad F^{R,k}_{\text{net}} = -\frac{4in_0\epsilon}{Lk}\sin^2\left(\frac{kl}{2}\right), \tag{6.4}$$

and

$$F^{R,m}_{\text{act}} = \begin{cases} \dfrac{fl^2n_0}{L} & \text{if} \quad m = 0, \\ \dfrac{fLn_0}{\pi^2m^2}\sin^2\left(\frac{m\pi l}{L}\right) & \text{if} \quad m \neq 0, \end{cases} \tag{6.5}$$

or

$$F^{R,k}_{\text{act}} = \begin{cases} \dfrac{fl^2n_0}{L} & \text{if} \quad k = 0, \\ \dfrac{4fn_0}{Lk^2}\sin^2\left(\frac{kl}{2}\right) & \text{if} \quad k \neq 0. \end{cases} \tag{6.6}$$

with $k = \frac{2\pi m}{L} = \frac{m}{R}$. The $2N$ Langevin equations describing the dynamics of the chains within the ring are given in equation (6.7). In this equation, we have included the drift velocity v_0 within the ring. The system forms a background

of homogeneously distributed chains. The drift velocity is therefore important for fluctuations around the background density.

$$\gamma\left(\dot{x}_i^{\pm}(t)+v_0\right)=f_i^{\pm}(t)+\sum_{j=1,j\neq i}F^R_{\text{net}}(x_i^{\pm}(t)-x_{\text{j}}^{\pm}(t)) + \sum_{j=1}\left[F^R_{\text{net}}(x_i^{\pm}(t)-x_{\text{j}}^{\mp}(t))\pm F^R_{\text{act}}(x_i^{\pm}(t)-x_{\text{j}}^{\mp}(t))\right]. \tag{6.7}$$

6.3 Correlation function

The correlation function matrix for the finite periodic ring system is calculated using the RPA method presented for the linear ring on chapter 5. We will not repeat the formalism in this chapter since the method is the same. Details of the calculation can be found in Appendix B.2.2. The correlation matrix for $k\neq 0$ is calculated and given by $G^R(k,\omega)=B^{-1}(k,\omega)=(i\underline{\underline{F}}^R_{int}(k)+(\underline{\underline{S}}^R_0)^{-1}(k,\omega))^{-1}$. The matrix $G^R(k,\omega)$ is given by the equation (B.92). With:

$$\underline{\underline{F}}^R_{int}=\begin{pmatrix} 0 & F^{R,k}_{\text{net}} & 0 & F^{R,k}_{\text{net}}-F^{R,k}_{\text{act}} \\ F^{R,k}_{\text{net}} & 0 & F^{R,k}_{\text{net}}-F^{R,k}_{\text{act}} & 0 \\ 0 & F^{R,k}_{\text{net}}+F^{R,k}_{\text{act}} & 0 & F^{R,k}_{\text{net}} \\ F^{R,k}_{\text{net}}+F^{R,k}_{\text{act}} & 0 & F^{R,k}_{\text{net}} & 0 \end{pmatrix}, \tag{6.8}$$

and the non interacting matrix,

$$\underline{\underline{S}}^R_0=\begin{pmatrix} S^{R,v_0}_{11}(k,\omega) & S^{R,v_0}_{12}(k,\omega) & 0 & 0 \\ S^{R,v_0}_{21}(k,\omega) & 0 & 0 & 0 \\ 0 & 0 & S^{R,v_0}_{33}(k,\omega) & S^{R,v_0}_{34}(k,\omega) \\ 0 & 0 & S^{R,v_0}_{43}(k,\omega) & 0 \end{pmatrix}. \tag{6.9}$$

With the components:

$$S^{R,v_0}_{11}(k,\omega)=\frac{2\sqrt{\frac{2}{\pi}}\gamma^3k^2N}{\pi\lambda^2L^2\left(k^4+\frac{4\gamma^4(\omega-kv_0)^2}{\lambda^2}\right)}. \tag{6.10}$$

$$S^{R,v_0}_{12}(k,\omega)=\frac{-\sqrt{\frac{2}{\pi}}\,\gamma\,k\,N}{2\,\pi\,\lambda\,L^2\left(k^2+\frac{2\,i\,\gamma^2(\omega-k\,v_0)}{\lambda}\right)}. \tag{6.11}$$

$$S_{21}^{R,v_0}(k,\omega) = \frac{\sqrt{\frac{2}{\pi}}\gamma k N}{2\pi\lambda L^2\left(k^2 - \frac{2i\gamma^2(\omega - kv_0)}{\lambda}\right)}. \tag{6.12}$$

The other elements of the matrix are: $S_{33}^{R,v_0}(k,\omega) = S_{11}^{R,v_0}(k,\omega)$; $S_{34}^{R,v_0}(k,\omega) = S_{12}^{R,v_0}(k,\omega)$ and $S_{43}^{R,v_0}(k,\omega) = S_{21}^{R,v_0}(k,\omega)$ by symmetry. The correlation matrix is:

$$G^R(k,\omega) = \begin{pmatrix} G_{11}^R(k,\omega) & G_{12}^R(k,\omega) & G_{13}^R(k,\omega) & G_{14}^R(k,\omega) \\ G_{21^R}(k,\omega) & G_{22}^R(k,\omega) & G_{23}^R(k,\omega) & G_{24}^R(k,\omega) \\ G_{31}^R(k,\omega) & G_{32}^R(k,\omega) & G_{33}^R(k,\omega) & G_{34}^R(k,\omega) \\ G_{41}^R(k,\omega) & G_{42}^R(k,\omega) & G_{43}^R(k,\omega) & G_{44}^R(k,\omega). \end{pmatrix}, \tag{6.13}$$

6.4 Ring contraction

We investigate the tensile stress produced by the ring during its contraction. In order to do so, we calculate the total energy stored in the system due to the cross-linking process. The active forces cancel themselves out because they are equal and oppositely directed for the chains pointing left and right. This force therefore does not contribute to the tensile force. The model elaborated shows that it is energetically advantageous to form a network cross-linking that tends to lower the energy. The more the filaments overlap with one another, the lower the overlap energy become. This means that it does not cost energy to the system to bind the chains together but rather, energy is released when chains bind and it costs energy to untie the cross-linked chains. We calculate here the dynamical total average of the cross-linking (networking) energy and are interested to know how this energy varies with the ring diameter. The

expression of the average networking energy is given by:

$$\begin{aligned}
\langle E^R_{\text{net}} \rangle &= \frac{1}{2} \int_\omega \sum_{k\neq 0} \langle \rho \, V^R_{\text{net}}(k) \, \rho \rangle \\
&= \frac{1}{2} \int_\omega \sum_{k\neq 0} \langle \rho_{\text{k}=0} \, V^R_{\text{net}}(k) \, \rho_{\text{-k}=0} \rangle + \frac{1}{2} \int_\omega \sum_{k\neq 0} \langle \rho_{\text{k}\neq 0} \, V^R_{\text{net}}(k) \, \rho_{\text{-k}\neq 0} \rangle \\
&= \frac{1}{2} \int_\omega \sum_{k\neq 0} \langle \rho_0 \, V^R_{\text{net}}(k) \, \rho_0 \rangle + \frac{1}{2} \int_\omega \sum_{k\neq 0} \langle \Delta\rho \, V^R_{\text{net}}(k) \, \Delta\rho \rangle \\
&= \langle E^R_{\text{net}} \rangle_{\text{MF}} + \frac{1}{2} \int_\omega \sum_{k\neq 0} V^R_{\text{net}}(k) \langle \Delta\rho \, \Delta\rho \rangle \\
&= \langle E^R_{\text{net}} \rangle_{\text{MF}} + \frac{1}{2} \int_\omega \sum_{k\neq 0} V^R_{\text{net}}(k) \, G^R_{11}(k,\omega). \qquad (6.14)
\end{aligned}$$

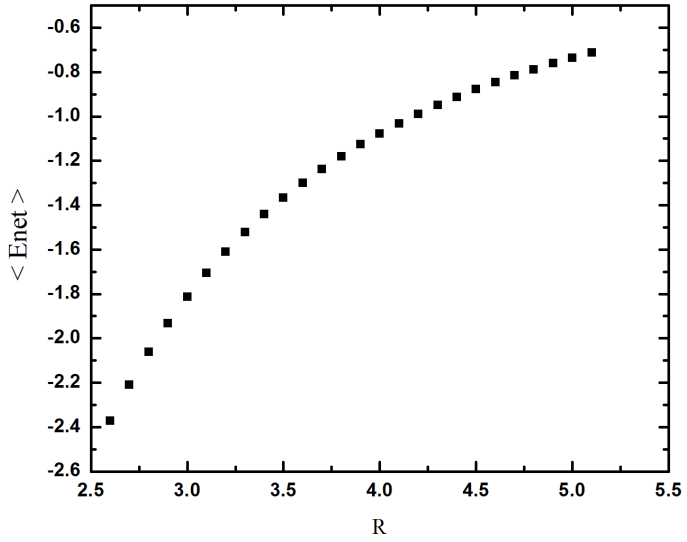

Figure 6.2: *Total networking energy plotted against the radius of the ring with the parameters:* $\lambda = \gamma = 1, n_0 = 10, f = 0, \epsilon = 1, N = 10, \omega = 0.5$. *The plot shows that the energy increases with the radius of the ring. This means that the contraction of the ring is indeed due to the networking force.*

Where $\rho_0 = \rho_{\text{MF}}$, the networking interacting potential is:

$$V^R_{\text{net}}(k) = \frac{4\, n_0\, \epsilon \sin^2\left(\frac{kl}{2}\right)}{L} = \frac{2\, n_0\, \epsilon \sin^2\left(\frac{kl}{2}\right)}{\pi R} \qquad (6.15)$$

The contractile force is deduced by taking the negative gradient of the total networking potential in respect to the radius of the ring in Fourier space,

this gives: $F^R_{\text{net}}(k) = ik\,V^R_{\text{net}}(k)$. The plot on Fig. 6.2 shows that the energy increases with the radius of the ring. That suggests that the ring contracts. Theoretically, when the radius of the ring increases, the system has to perform more work in order to maintain the interaction between the chains The only force responsible for this contraction is the networking force. The active force for a close periodic system seems to only play the role of making the chains overtake each other but it never leads to the contraction for the case of periodic system.

6.5 Effective single chain dynamics: Investigation of the drift velocity

The dynamics of the chains inside the ring is studied here using a Self-consistent field theory(SCFT). Also called the Hartree fock method, the SCFT is one of the central starting point of many methods that describe many polymers system in an accurate manner [23, 65]. The idea is to use the mean field approximation in order to reduce the dynamics of a many polymers chains system to the dynamics of a single chains moving inside an external vector field (see section 2.2.2.1) created by the other chains that have been smeared out. The created vector field accounts for the interactions between the segment of the labelled chain and the other chains segments. It also depends on the species of the chains (i.e. the orientation of the chains to which the segments belong). The solution of the non-linear equations behaves as if each polymer chain is subjected to a mean field created by all the rest of the chains. We choose one arbitrary chain and track its dynamics. Here, the full MSR includes the action of all possible interaction between the chains. Treating the system collectively, we isolate the dynamics equation for the labelled chain as well as for the rest of the chains. We use the RPA and that leads to have all the terms that include the labelled chain variable ($x_\ell(t)$ and its conjugate field $\hat{x}_\ell(t)$) written as the product of pairs of the fields. The latter field is coupled to the self-consistent average of the remaining fields (due to the remaining chains). The details of the calculations are developed in the Appendix B.3. Our focus is to find the drift velocity on the ring. This task will be achieved by a simple identification of the terms inside the new effective Langevin equation after having performed all the calculations.

The Langevin equations here include the dynamics equation for the labelled chain and the dynamical equations for all the others chains with all possible interactions inside the system. Since the present system contains two different type of chains (defined by their orientations within the ring), we defined N^+ and N^- the number of left and right moving chains respectively. We randomly choose to label one chain between the chains moving right. The Langevin equa-

tions are given by the set of dynamical equations for the labelled + oriented chain, for the (N^+-1) remaining clockwise oriented chains and the N^- equations for the anti-clockwise oriented chains. The dynamical equations are then given by:

For the labelled chain:

$$L_\ell^+ : 0 = -\gamma\,\dot{x}^+(t) + f^+(t) + \sum_{\alpha=1}^{N^+-1} F_{int}^R(x_\ell^+ - x_\alpha^+) + \sum_{\beta=1}^{N^-} F_{int}^R(x_\ell^+ - x_\beta^-). \quad (6.16)$$

For the (N^+-1) remaining + pointing chains:

$$\begin{aligned} L^+ : 0 = \sum_{\alpha=1}^{N^+-1} \Bigg[& -\gamma\,\dot{x}_\alpha^+(t) + f_\alpha^+(t) + \sum_{\alpha'\neq\alpha}^{N^+-1} F_{int}^R(x_\alpha^+ - x_{\alpha'}^+) \\ & + \sum_{\beta=1}^{N^-} F_{int}^R(x_\alpha^+ - x_\beta^-) + F_{int}^R(x_\alpha^+ - x_\ell^+) \Bigg]. \end{aligned} \quad (6.17)$$

For the (N^-) remaining − pointing chains:

$$\begin{aligned} L^- : 0 = \sum_{\beta=1}^{N^-} \Bigg[& -\gamma\,\dot{x}_\beta^-(t) + f_\beta^-(t) + \sum_{\beta'\neq\beta}^{N^-} F_{int}^R(x_\beta^- - x_{\beta'}^-) \\ & + \sum_{\alpha=1}^{N^+} F_{int}^R(x_\beta^- - x_\alpha^+) + F_{int}^R(x_\beta^- - x_\ell^+) \Bigg]. \end{aligned} \quad (6.18)$$

The subscript ℓ means the labelled chains. The shorthand notations $\sum_{\alpha'\neq\alpha}^{N^+-1} F_{int}^R(x_\alpha^+ - x_{\alpha'}^+)$ and $\sum_{\beta\neq\beta'}^{N^-} F_{int}^R(x_\beta^- - x_{\beta'}^-)$ represent the interacting forces that the chains +/− oriented exerts on the two +/− oriented chains respectively. $\sum_{\alpha=1}^{N^+-1} F_{int}^R(x_\ell^+ - x_\alpha^+)$ and $\sum_{\beta=1}^{N^-} F_{int}^R(x_\ell^+ - x_\beta^-)$ are the interacting force that the labelled chain exerts on the (+) and (-) oriented chains respectively. $\sum_{\beta,\alpha=1}^{N^-,(N^+-1)} F_{int}^R(x_\alpha^+ - x_\beta^-)$ and $\sum_{\beta,\alpha=1}^{N^-,(N^+-1)} F_{int}^R(x_\beta^- - x_\alpha^+)$ represent the interacting forces between the + and the − oriented chains and of the − and the + oriented chains respectively. The Langevin equations cast into the generating functional give:

$$Z = \frac{1}{\aleph} \int_{\mathbb{R}} \left(\prod_{\alpha=1}^{N^+-1} [\mathrm{d}\,x_\alpha^+]\,[\mathrm{d}\,\hat{x}_\alpha^+] \right) \left(\prod_{\beta=1}^{N^-} [\mathrm{d}\,x_\beta^-]\,[\mathrm{d}\,\hat{x}_\beta^-] \right) [\mathrm{d}\,x_\ell^+]\,[\mathrm{d}\,\hat{x}_\ell^+]\, e^{\mathcal{L}'}, \quad (6.19)$$

with $\mathcal{L}' = \mathcal{L}'_{int} + \mathcal{L}'_0 + \mathcal{L}'_\ell$ and

$$\begin{aligned}\mathcal{L}'_\ell = &-\frac{\lambda}{2}\int_t (\hat{x}^+_\ell)^2 - i\gamma\int_t \hat{x}^+_\ell\,\dot{x}^+_\ell + i\int_t \hat{x}^+_\ell \sum_{\alpha}^{N^+-1} F^R_{int}(x^+_\ell - x^+_\alpha)\\ &+ i\int_t \hat{x}^+_\ell \sum_{\beta=1}^{N^-} F^R_{int}(x^+_\ell - x^-_\beta),\end{aligned} \tag{6.20}$$

$$\begin{aligned}\mathcal{L}'_{int} = &\, i\sum_{\alpha\neq\alpha'}\int_t \hat{x}^+_\alpha\, F^R_{int}(x^+_\alpha - x^+_{\alpha'}) + i\sum_{\alpha=1}^{N^+-1}\int_t \hat{x}^+_\alpha\, F^R_{int}(x^+_\alpha - x^+_\ell)\\ &+ i\sum_{\alpha,\beta}\hat{x}^+_\alpha\, F^R_{int}(x^+_\alpha - x^-_\beta) + i\sum_{\beta\neq\beta'}\int_t \hat{x}^-_\beta\, F^R_{int}(x^-_\beta - x^-_{\beta'})\\ &+ i\sum_{\beta=1}^{N^-}\int_t \hat{x}^-_\beta\, F^R_{int}(x^-_\beta - x^+_\ell) + i\sum_{\alpha,\beta}\hat{x}^-_\beta\, F^R_{int}(x^-_\beta - x^+_\alpha),\end{aligned} \tag{6.21}$$

$$\begin{aligned}\mathcal{L}'_0 = &-\frac{\lambda}{2}\sum_{\alpha=1}^{N^+-1}\int_t (\hat{x}^+_\alpha)^2 - i\gamma\sum_{\alpha=1}^{N^+-1}\int_t \hat{x}^+_\alpha\,\dot{x}^+_\alpha - \frac{\lambda}{2}\sum_{\beta=1}^{N^-}\int_t (\hat{x}^-_\beta)^2\\ &- i\gamma\sum_{\beta=1}^{N^-}\int_t \hat{x}^-_\beta\,\dot{x}^-_\beta.\end{aligned} \tag{6.22}$$

we introduce the collective variables:

$$\rho^+(x^+) = \sum_{\alpha}^{N^+-1}\delta(x^+ - x^+_\alpha(t)) \quad ; \quad \rho^-(x^-) = \sum_{\beta}^{N^-}\delta(x^- - x^-_\beta(t)) \tag{6.23}$$

and their response field:

$$\varphi^+(x^+) = \sum_{\alpha}^{N^+-1}\hat{x}^+_\alpha\,\delta(x^+ - x^+_\alpha(t)) \quad ; \quad \varphi^-(x^-) = \sum_{\beta}^{N^-}\hat{x}^-_\beta\,\delta(x^- - x^-_\beta(t)). \tag{6.24}$$

To complete the present approximation in a careful manner, we emphasize that the actual density is split in the mean density $\overline{\rho}_0 = \rho_0 = \frac{N}{L}$ (N is the total number of chains in the system) and the density fluctuation ($\Delta\rho$). This background and the fluctuations are included into the RPA. For the linear ring model, the fluctuation around the background density (which is the density where the wave number vanishes $k = 0$) have not been explicitly included into the RPA calculation. Here, the density is split in two: The background density

($\rho_{k=0} = \rho_0 = \frac{N}{L}$) and the fluctuation around the background ($\rho_{k\neq 0} = \Delta\rho$). The RPA here is performed by integrating over the $k \neq 0$ part (see Appendix B.3). We write the collective variable inside the RPA with the collective fluctuation density $\underline{\Delta\rho}$ vector. The expression containing the interaction between the labelled chain and the other chains are kept the same except the interacting forces that goes into the correlation matrix. The density $\underline{\rho}(x,t) = \underline{\rho}_0 + \underline{\Delta\rho}(x,t)$ In Fourier space, we have: $\underline{\rho}(k,\omega) = \underline{\rho}_0 + \underline{\Delta\rho}(k,\omega)$, with $\underline{\rho}_0 = \frac{N}{L}(1,1,1,1)$. The density fluctuation for each chain species is now written as:

$$\begin{aligned}
\Delta\rho^+(k,t) &= \rho^+(k,t) - \rho_0^+, \\
\Delta\rho^-(k,t) &= \rho^-(k,t) - \rho_0^-, \\
\Delta\varphi^+(k,t) &= \varphi^+(k,t), \\
\Delta\varphi^-(k,t) &= \varphi^-(k,t),
\end{aligned} \tag{6.25}$$

The Jacobian of the transformation is one. We perform a change of variables when introducing the expression in the generating functional equation (B.98), we have:

$$\begin{aligned}
Z = \frac{1}{\aleph} \int_{\mathbb{R}} &[\mathrm{d}x_L^+][\mathrm{d}\hat{x}_L^+]\,[\mathrm{d}\,\Delta\rho^+]\,[\mathrm{d}\,\Delta\rho^-]\,[\mathrm{d}\,\Delta\varphi^+]\,[\mathrm{d}\,\Delta\varphi^-] \\
&\int_{\mathbb{R}} [\mathrm{d}\,\widehat{\Delta}\rho^+]\,[\mathrm{d}\,\widehat{\Delta}\rho^-]\,[\mathrm{d}\,\widehat{\Delta}\varphi^+]\,[\mathrm{d}\,\widehat{\Delta}\varphi^-] \\
&\exp\Big[\mathcal{L}'_\ell + \mathcal{L}'_0 + \mathcal{L}'_{int} + \mathcal{L}''_q + \mathcal{L}''_3\Big].
\end{aligned} \tag{6.26}$$

Performing the RPA over all the chains except the labelled chain we have:

$$\begin{aligned}
Z = \frac{1}{\aleph} \int_{\mathbb{R}} &[\mathrm{d}\,x_\ell^+]\,[\mathrm{d}\,\hat{x}_\ell^+]\,[\mathrm{d}\,\underline{\Delta\rho}]\,\exp\left[-\frac{\lambda}{2}\int_t (\hat{x}_\ell^+)^2 - \,\mathrm{i}\,\gamma\int_t \hat{x}_\ell^+\,x_\ell^+\right] \\
&\exp\left[i\iint_{k,\omega} \underline{f}(k)\,\underline{\Delta\rho}(k,\omega) + i\int_t \underline{f}(x_\ell^+)\,\underline{\rho}_0^T\right] \\
&\underbrace{\exp\left(-\frac{1}{2}\iint_{k,\omega} \underline{\Delta\rho}(k,\omega)\,\left(i\underline{\underline{F}}^R_{int} + (\underline{\underline{S}}^R_0)^{-1}\right)\underline{\Delta\rho}^T(k',\omega')\right)}_{\text{RPA}},
\end{aligned} \tag{6.27}$$

$k' = -k$ and $\omega' = -\omega$. The density fluctuation super vectors and its conjugate are defined by:

$$\underline{\Delta\rho}((k,\omega)) = \left(\Delta\rho^-(k,\omega),\,\Delta\varphi^-(k,\omega),\,\Delta\rho^-(k,\omega),\,\Delta\varphi^+(k,\omega)\right), \tag{6.28}$$

$$\underline{\widehat{\Delta}\rho}((k,\omega)) = \left(\widehat{\Delta}\rho^-(k,\omega),\,\widehat{\Delta}\varphi^-(k,\omega),\,\widehat{\Delta}\rho^-(k,\omega),\,\widehat{\Delta}\varphi^+(k,\omega)\right), \tag{6.29}$$

and

$$\underline{f}(x_\ell^+) = \left(\hat{x}_\ell^+ F_{int}^R(x_\ell^+ - x^-), F_{int}^R(x^- - x_\ell^+), \hat{x}_\ell^+ F_{int}^R(x_\ell^+ - x^+), F_{int}^R(x^+ - x_\ell^+)\right). \tag{6.30}$$

and the symmetry relation relation $F_{int}^R(x^- - x_\ell^+) = -F_{int}^R(x_\ell^+ - x^-)$ holds. We perform the Gaussian integration over the density fluctuation $\Delta\rho$ and have:

$$Z = \frac{1}{\aleph'} \int_{\mathbb{R}} [\mathrm{d}\, x_\ell^+]\, [\mathrm{d}\, \hat{x}_\ell^+] \exp\left(\frac{1}{2} \iint_{k,\omega} \underline{f}(k) \left(i\underline{\underline{F}}_{int}^R + (\underline{\underline{S}}_0^R)^{-1}\right)^{-1} \underline{f}^T(k')\right)$$
$$\exp\left[-\frac{\lambda}{2} \int_t (\hat{x}_\ell^+)^2 \; - \; i\gamma \int_t \hat{x}_\ell^+ \, \dot{x}_\ell^+ \; + \; i \int_t \underline{f}(x_\ell^+)\, \underline{\rho}_0^T\right]. \tag{6.31}$$

with $\frac{1}{\aleph'} = \sqrt{\frac{2\pi}{det[\left(i\underline{\underline{F}}_{int}^R + (\underline{\underline{S}}_0^R)^{-1}\right)]}}$ is a constant. Where $\underline{f}(k)$ is the super-vector Fourier transform of $\underline{f}(x_\ell^+)$. We expand the expression

$$\left(-\frac{1}{2} \int_{k,\omega} \underline{f}(k) \left(i\underline{\underline{F}}_{int}^R + (\underline{\underline{S}}_0^R)^{-1}\right)^{-1} \underline{f}^T(k')\right) \tag{6.32}$$

in the equation (6.31) and Taylor expand it up to the second order in λ for the $(\hat{x}_\ell^+)^2$ coefficient and up to the first order in λ for the $\hat{x}_\ell^+$ coefficient. we can therefore rewrite the generating functional as:

$$Z = \frac{1}{\aleph'} \int_{\mathbb{R}} [\mathrm{d}\, x_\ell^+]\, [\mathrm{d}\, \hat{x}_\ell^+] \exp\left[-\frac{\lambda}{2} \int_t (\hat{x}_\ell^+)^2 \; - \; i\gamma \int_t \hat{x}_\ell^+ \, \dot{x}_\ell^+\right]$$
$$\exp\left(-\frac{\lambda}{2} \iint_{k,t} (\hat{x}_\ell^+)^2(t)\, a(k) \; - \; i\gamma \iint_{k,t} \hat{x}_\ell^+(t)\, b(k)\right. \tag{6.33}$$
$$\left. -i\gamma \int_t \hat{x}_\ell^+(t)\, c(t) \; + \; i \int_t d(t)\right).$$

The expression (equation (6.34))

$$\exp\left[-\frac{\lambda}{2} \iint_{k,t} \hat{x}_\ell^{+2}(t) a(k) - i\gamma \int_t \hat{x}_\ell^+(t) \left(\int_k b(k) + c(t)\right) + i \int_t \mathrm{d}(t)\right], \tag{6.34}$$

inside the exponential in the equation (6.33) represents the effective Langevin equation. This equation describes the dynamics of the labelled chain and its interaction with the rest of the chains. The understanding of the coefficients of this equation leads to understand the dynamics of the whole system. The velocity imposed by the random motion of the system of chains can be deduced. From the equation (6.34), by doing the MSR formalism backward to identify

the coefficients of the new dynamical equation. We identify the following terms: the effective stochastic force ($f_{\text{eff}}(k) = \int_k a(k)$) associated with the hatted square field coefficient in Fourier space. The effective drag force coupled with the hatted field $F_{\text{eff,d}} = \left(\int_k b(k) + c(t)\right)$. The drift velocity can therefore be deduced by:

$$\begin{aligned} F_{\text{eff,d}} &= \underbrace{\int_k b(k)}_{=0} + c(t) \\ &= \gamma_{\text{eff}}\, v_{\text{drift}}\,. \end{aligned}$$

The effective friction coefficient is the friction coefficient for the new effective Langevin equation that gives the dynamics of the labelled chains and the rest of the chains in the system. It is related to the friction coefficient for the labelled chain by the expression: $\gamma_{\text{eff}} = \gamma + \Delta\gamma$ where $\Delta\gamma$ is the friction coefficient fluctuation which can be neglected. The calculation of the Fourier series for $k = 0$ of the coefficients c leads to the expression.

$$v_{\text{drift}} = v_0 = \frac{f\, l^2\, n_0\, \rho_0}{\gamma}. \tag{6.35}$$

The average drift velocity of the chains inside the ring is a linear expression of the active force. The expression means the drift of the whole system depends on the orientation of the labelled chain. We could write the drift velocity as $v_0 = \sigma_\ell\, v_0$, with $\sigma_\ell = \pm 1$ the orientation of the labelled chain. The expression suggests that if we switch off the active force, the system of chains will have no preferential direction and it will drift toward the direction imposed by the labelled chain. The drift velocity result is not an unexpected one. In fact one could have guessed it without having to do such heavy calculation.

6.6 Polarisation current density

The chains are polars and move to the right or left. The dynamics of the chains due to the active force create a current flowing through the total ring. We can defined a polarisation current density that flows in the ring. We divide the ring in small equal area (called 'bins' in simulations). We measure the current density through each small area and sum over the total circumference of the ring to have the total current flowing through the entire ring. The total current density measured in each small section is defined by :

$$j(x,t) = j^+(x,t) - j^-(x,t), \tag{6.36}$$

with $j^\pm(x,t) = \sum_{i=1}^{N} \sigma_i\, \dot{x}_i^\pm\, \delta(x - x_i^\pm(t))$. For the whole ring, the total current density is the sum over all the current density flowing in each small section.

This is given by:

$$J(x,t) = \frac{1}{L}\int_0^L j(x,t). \tag{6.37}$$

The average current density can be calculated from the RPA. This is done here for one species by investigating the average response field $\langle\hat{\rho}(x,t)\rangle$. We later generalise to the system of two species of chains. The generating functional approach is used to calculate the average. We add to the generating functional a linear source field term $h_i(t)$ and its hatted field $\hat{h}_i(t)$ both coupled to the position and their conjugate fields respectively. The generating functional including the source fields is defined as:

$$\begin{aligned} Z[h_i(t),\hat{h}_i(t)] = \int_{\mathbf{R}} J_i \prod_i^N [dx_i,\hat{x}_i]\, \exp\Bigg[-\frac{\lambda}{2}\sum_{i=1}^N\int_t \hat{x}_i^2 + \sum_{i=1}^N\int_t h_i(t)x_i(t) \\ i\sum_{i=1}^N\int_t \hat{x}_i(t)\left(-\gamma(\dot{x}_i - v_0) + \sum_{\mathrm{j}=1}^N F_{int}^{R,tot}(x_i,x_{\mathrm{j}}) - i\hat{h}_i(t)\right)\Bigg]. \end{aligned} \tag{6.38}$$

$J_i = 1$ is the Jacobian of the transformation. The average response field $\langle\hat{\rho}(x,t)\rangle$ is calculated using the following formula:

$$\langle\hat{\rho}(x,t)\rangle = \frac{1}{Z[0,0]}\int_k e^{ikx}\left[\sum_{i=1}^N \frac{\partial Z}{\partial\hat{h}_i(t')}\right]_{(\hat{h}_i=0, h_i=-ik\delta(t-t'))}. \tag{6.39}$$

We perform the functional integral and derivative over the hatted fields $\hat{x}$ and $\hat{h}$ successively. we use the relation $\sum_{i=1}^N \int_k e^{ik(x-x_i(t'))} = \sum_{i=1}^N \delta(x-x_i(t')) = \rho$ and after simplification, we have:

$$\begin{aligned} \langle\hat{\rho}(x,t)\rangle &= \frac{i\gamma}{\lambda}\left\langle\sum_{a=1}^N \dot{x}_i\delta(x-x_{\mathrm{a}})\right\rangle - \frac{i\gamma}{\lambda}v_0\left\langle\sum_{a=1}^N\delta(x-x_{\mathrm{a}})\right\rangle \\ &\quad - \frac{i}{\lambda}\left\langle\sum_{a=1}^N F_{int}^{R,tot}\delta(x-x_{\mathrm{a}})\right\rangle \\ &= \frac{i\gamma}{\lambda}\langle j^{\pm}\rangle \pm \frac{i\gamma}{\lambda}v_0\rho_0 - \frac{i}{\lambda}\left\langle\sum_{a=1}^N F_{int}^{R,tot}\delta(x-x_{\mathrm{a}}^{\pm})\right\rangle. \end{aligned} \tag{6.40}$$

The filaments within the ring are all supposed to be homogeneously distributed. That means, the average response field is zero $\langle\hat{\rho}\rangle = 0$. The average polarisation current density for each chain species in each small section of the ring, is given by the contribution due to the drift and the total force coupled with the correlation functions (equation (6.41)).

$$\langle j^{\pm}(x,t)\rangle = \pm v_0\rho_0 + \frac{1}{\gamma}\left\langle \sum_{i=1}^{N} F_{int}^{R,tot}\delta(x - x_i^{\pm})\right\rangle . \tag{6.41}$$

with the arguments

$$\rho^{\pm}(x,t)F(x) = \int_0^L \mathrm{d}x'\rho^{\pm}(x,t)F(x-x')\left(\rho^{+}(x',t') + \rho^{-}(x',t')\right), \tag{6.42}$$

we have:

$$\begin{aligned}
\sum_{i=1}^{N} F_{int}^{R,tot}\delta(x - x_i^{\pm}) &= (F_{net}^{R,+} + F_{act}^{R,+})\rho^{+}(x,t) - (F_{net}^{R,-} - F_{act}^{R,-})\rho^{-}(x,t) \\
&= \int_0^L \mathrm{d}x'\,\rho^{+}(x,t)(F_{net}^{R,+} + F_{act}^{R,+})\left(\rho^{+}(x',t') + \rho^{-}(x',t')\right) \\
&- \rho^{-}(x,t)\left(F_{net}^{R,-} - F_{act}^{R,-}\right)\left(\rho^{+}(x',t') + \rho^{-}(x',t')\right) \\
&= \int_0^L \mathrm{d}x'\,\rho^{+}(x,t)F_{act}^{R,+}(x-x')\rho^{-}(x',t') \\
&+ \rho^{-}(x,t)F_{act}^{R}(x-x')\rho^{+}(x',t') \\
&= 2\int_0^L \mathrm{d}x'\,\rho^{+}(x,t)F_{act}^{R,+}(x-x')\rho^{-}(x',t').
\end{aligned} \tag{6.43}$$

Consequently, the current density gives:

$$\langle j(x,t)\rangle = 2v_0\rho_0 + \frac{2}{\gamma}\left\langle \int_0^L \mathrm{d}x'\rho^{+}(x,t)\,F_{act}^{R}\,\rho^{-}(x',t')\right\rangle . \tag{6.44}$$

For symmetry reasons, the networking force sums up to zero. The average polarisation current density is associated with the sustained flow in the ring and is computed as follows:

$$\overline{J}_0 = \frac{1}{L}\int_0^L dxJ(x,0) = \frac{2fl^2n_0\rho_0^2}{\gamma} + \frac{2}{\gamma}\int_{\omega}\sum_{k\neq 0} F_{act}^{R,k}\,\langle\rho^{+}(k,\omega)\rho^{-}(k',\omega')\rangle_{\mathrm{RPA}}. \tag{6.45}$$

The additional term to the drift of the active force in the (equation (6.45)) depends on the cross-correlation function. This latter function is identified to be the $(1,3)$ or $(3,1)$ element of the dynamics correlation matrix in the RPA ($G_{13}^{R} = G_{31}^{R} = \langle\rho^{+}(k,\omega)\rho^{-}(k',\omega')\rangle$). The expression is heavy to handle analytically. We therefore, investigate the total polarisation current density with numerical methods. The numerical analysis of the function G_{13}^{R} shows

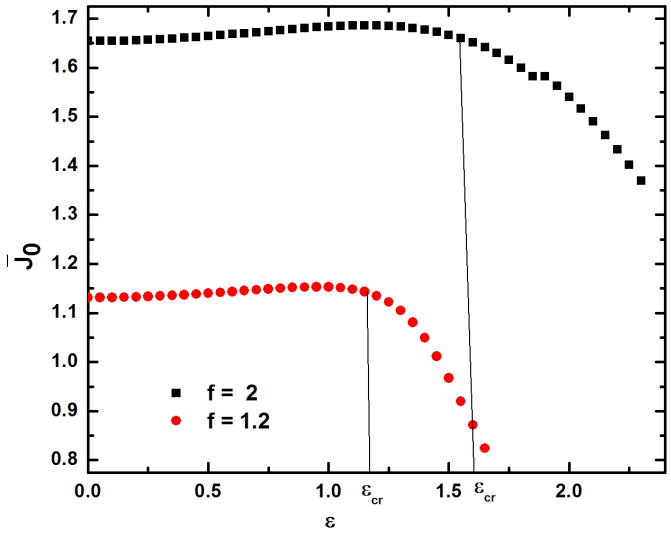

Figure 6.3: *Analytic polarisation current density. Parameters are:* $f = 1, N = 20, L = 1, l = 0.2, \lambda = 1, \gamma = 1$. *We observe a decrease of the current through the ring with the increase of the networking force. The critical value of the networking force is given in equation (6.46).* ϵ_{cr} *on the plot indicates where the plot starts changing phase.*

that, the numerator never changes sign and remains positive. The denominator d (equation (6.48)) behaves differently so we calculate the critical value of the networking force at almost at steady state ($\omega = 0$) and by neglecting the active force ($f = 0$). The critical value of the networking force strength (ϵ) (equation (6.46)) is:

$$\epsilon_{\rm cr}(f=0) = \frac{\pi^{3/2}\, k^2\, \lambda\, L}{2\sqrt{2}\,\gamma\,\eta^2\, n_0\, N} = \frac{\pi^{3/2}\,\lambda\, L^3}{2\sqrt{2}\,\gamma\, l^2\, n_0\, N} \tag{6.46}$$

with $\eta = \sin(\frac{kl}{2}) \simeq \frac{kl}{2}$. Solving the denominator for the critical networking force for any values of f at $\omega = 0$ gives

$$\epsilon_{\rm cr}(f) = \frac{\sqrt{2}\,(2\,\gamma^2\, f^2\, n_0^2\, N^2\, (2\,\pi^3\, k^4 \ell^4\, - \eta^4\,) + \pi^3\,\lambda^2\, k^6\, L^4\,)}{4\,\pi^{3/2}\,\gamma\, k^6\,\lambda\, l^2 L\, n_0\, N} \tag{6.47}$$

The numerator of the equation (6.47) has an additive term in f^2. That means, f makes the critical value of the networking force more severe ($\epsilon_{cr}(f \neq 0) > \epsilon_{cr}(f = 0)$) so the shift of the critical networking force observed in the Fig. 6.3. The Fig. 6.3 shows a continuity and a sharp decline at the critical networking force values ϵ_{cr} for different values of f. These critical points represent where the system starts changing phase. Our theory is made to work only until the ring has a gap (RPA relies on the fact that the system is homogeneous only).

At ϵ_{cr} the chains separate and the theory no longer works. Consequently, Our theory cannot be apply further than ϵ_{cr}. The RPA predicts nevertheless where the homogeneous background fails. This method is a mean field kind of approximation but known to be very reliable to study the stability of homogeneous systems. Comparing this result with what is to come in the numerical simulation (Fig. 6.9), we see that the polarisation current has a down turn at the critical networking force values and there is a shift of the ϵ_{cr} with the increase of the active force.

$$\begin{aligned}\mathrm{d} = & f^4\left[4\gamma^4 n_0^4 N^4\left(2\pi^3 k^4\ell^4-\eta^4\right)^2\right]\\ & + f^2\left[4\pi^{3/2}\gamma^2 k^4\lambda L n_0^2 N^2\left(2\pi^3 k^4\ell^4-\eta^4\right)\left(\pi^{3/2}k^2\lambda L-2\sqrt{2}\gamma\eta^2 n_0 N\epsilon\right)\right]\\ & + \pi^3 k^8\lambda^2 L^2\left(\pi^3\lambda^2 k^4 L^2-4\sqrt{2}\pi^{3/2}\gamma\eta^2\lambda k^2 L n_0 N\epsilon+8\gamma^2\eta^4 n_0^2 N^2\epsilon^2\right). \quad (6.48)\end{aligned}$$

6.7 Numerical simulation

We implement a simple one-dimensional Langevin dynamics simulation (LDS) to investigate the filaments behaviour inside a periodic ring system [66, 67]. At initial, all the chains lie within a one-dimensional periodic box of circumference $L = 2\pi R$ with their centre of mass having random positions each between $[0, L]$. The LDS consists of solving numerically the dynamical equations expressed equation (6.7). As the simulation proceeds, each chain moves and therefore changes position. We can track each filament and see each chain trajectory (Fig. 6.4). The simulation steps are as follows:

1. **Initialisation**: We set the initial condition by given random centre of mass positions to each chain of same length. All the chains lie between 0 and L.

2. **Calculate the forces**: The stochastic force is defined by generating a normal distributed number using the box-müller algorithm. The pairwise interacting forces between two overlapping chains are calculated using the definition of each force as defined in the equations (6.2) and (6.1). We implement the force on each chain by taking the total interaction with the chain for which we would like to know the force, and the rest of the chains in the ring. We do that by calculating the distance between two overlapping chains. Let us define $r_{ij} = x_i - x_\mathrm{j}$ as the distance between the chains i and j, with $x_{i/j}$ the spatial centre of mass position of the chain number i/j. The condition $j \neq i$ prevents counting the interaction between the same chains many times. The finite periodic ring supposes that the forces be implemented using the minimal distance between each pair of chains. The double counting of the pairwise forces between chains is prevents using the argument of the conservative force so, we use the Newtown's third law $f_{i,j} = -f_{j,i}$ to calculate the force.

The total force acting on a single chain is given by the summation of all the pairwise forces between that chain and the rest of the chains in the system (equation (6.49)).

$$f_i^{\text{total}} = \sum_{j \neq i}^{N-1} f_{i,j} \tag{6.49}$$

Where $f_{\text{i,j}}$ is the force that the chain number i exerts on the chain number j. An alternative method to calculate the force is to simply generate images of all the chains found outside of the box (to the left and/or to the right of the box). We thereafter add or subtract the total length of the box to the distance between the centre of mass of two overlapping chains. The periodicity of the ring makes the two ends of the simulating box identical.

3. **Time integration**: We update each chain position using the Langevin equation (equation (6.7)). Each chain moves and interacts with the other chains after each time step ($dt = 0.00001$ here) as the result for a diffusion process. The spatial position of each single chain is updated over the time using the Verlet algorithm [66–70]. We assume that all the chains conserve their initial orientation during their motion.

4. **Periodic boundary conditions**: We impose the periodic boundary condition to the system. This is done by creating an image of each chain as $x' = x \pm L$ (x' and x being respectively the spacial chain's image position and chain's position, respectively. Each image is the exact copy of the real chain and has the same orientation as for the real chain from which it has been copied. The image of a chain replaces the chain if this latter goes beyond the box boundary. In such situation, its copy is placed appropriately at the opposite side of the box where the chain is close by. The values of the new forces are therefore calculated using the position of the image which has taken the place of the chain in the simulating box.

   We plot an example of the trajectories of a sample of seven chains over the time (Fig. 6.4). The plot exhibits the push/pull behaviour that the chains experience as a result of their interaction with one another as predicted by the theory.

5. **Macroscopic quantities**: After having prepared the sample (initialisation) and solved the equation of motion, we proceed with the implementation of some macroscopic quantities on the system. Those quantities are implemented after a long time step when the system has been almost equilibrated. The steady state is reached when the properties of the system no longer change with the time. The mistake that can occur during the measurement are almost the same that one can encounter in

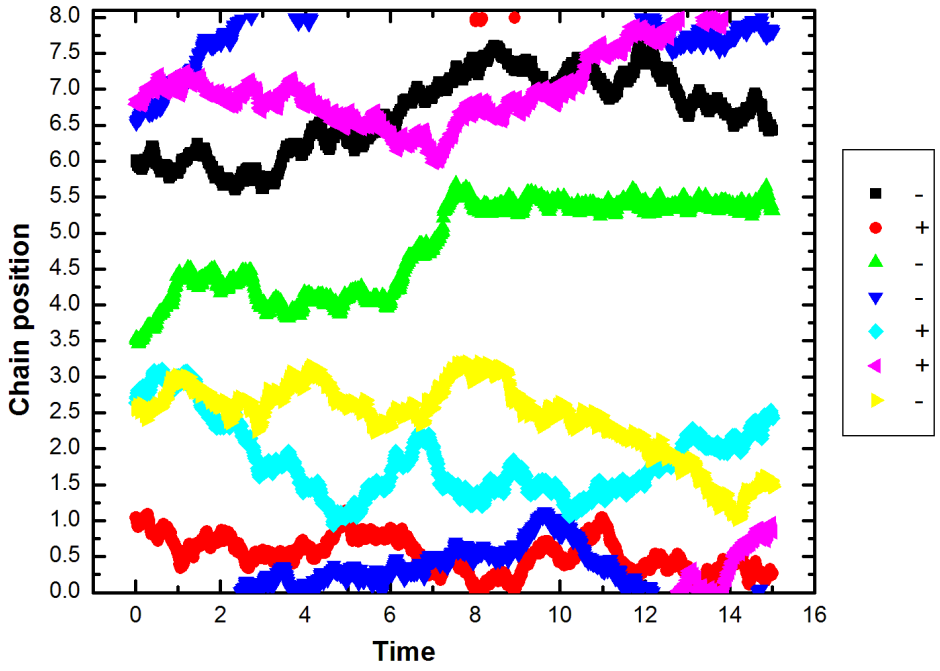

Figure 6.4: *Trajectories of a sample of seven chains confined in a ring of circumference L. Parameters are: $N = 7, f = 0.1, \epsilon = 0.1, \lambda = 1, \gamma = 0.9, n_0 = 10, \ell = 0.2, L = 1.0$ The signs $+$ and $-$ in the legend represent the orientation of each chain.*

real experiments, i.e., the sample may not be well prepared or the measurement too short. Those mistakes can lead to a system that undergoes irreversible changes during the simulation. The quantities are measured in terms of the position and/or momenta of the chain in the ring. The observables measured here are: The average length density, the average polarisation current density, the density-density correlation function.

6.7.0.1 Correlation function

The structure of the chains within the ring is characterised by their distribution function $\langle \rho(r)\rho(r') \rangle$. This function for the present model is the length density-density correlation function. It provides good insight in the understanding of the general organisation of the chains within the ring with different values of the forces. We implement the length density function in each bin and plot the total length density-density correlation function over the bins. The (Fig. 6.5) presents the plot of the pair correlation function over fifty 'bins'. For the networking force lager than the active force (curve in blue), there is almost no current flowing in the ring after a long time steps (200000). The number of

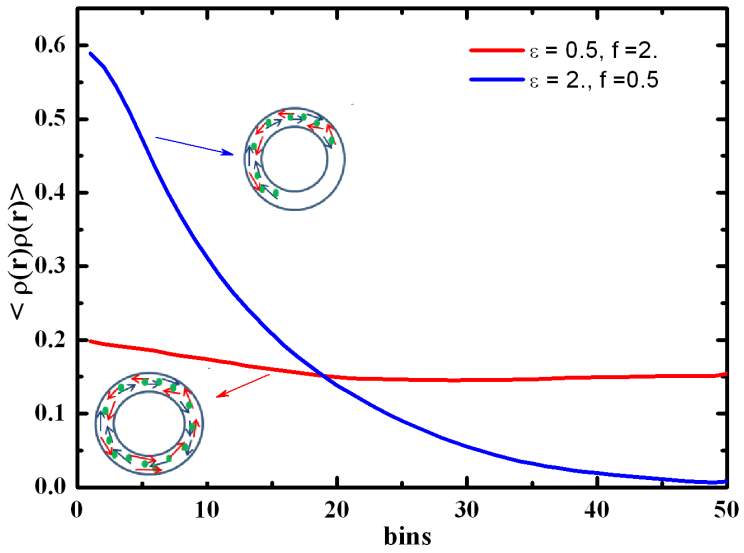

Figure 6.5: *Density-density length correlation function as a function of the 'bins' for dominant active force (red) and dominant networking force (blue) after 200000 time steps. 50 bins represents half of the circumference of the ring. Parameters are:* $N = 80, \lambda = 1, \gamma = 0.9, n_0 = 10, \ell = 0.2, L = 1.0$.

empty bins increases with hight networking force. Those observations suggest that the ring loses its structural integrity and the current stops flowing through the ring. The red curve presents a case where the active force dominates the networking force. Consequently, the ring conserves its homogeneity and the current still flows through the ring without interruption in any sort. The correlation function gives an almost flat curve. The observations so far suggest a change of phase of the system causes by the networking force. This phase change seems to occurs at short distance (bin). The correlation function turns from an almost flat to a strong peak with the increase of the networking force.

6.7.1 Chains density profile

We take snapshots of the configuration of the chains inside the ring for the active force $f = 0.1$ and the networking force strength $\epsilon = 2$ and $\epsilon = 5$ (Fig. 6.6 and the Fig. 6.7). This is observed in the correlation function plot (Fig. 6.8) with the increase of the peak that shifts to larger length. This new arising peak suggests a new length scale that gives informations on the configuration of the chains within the ring as observed on the snapshots figures (Fig. 6.7 and Fig. 6.6).

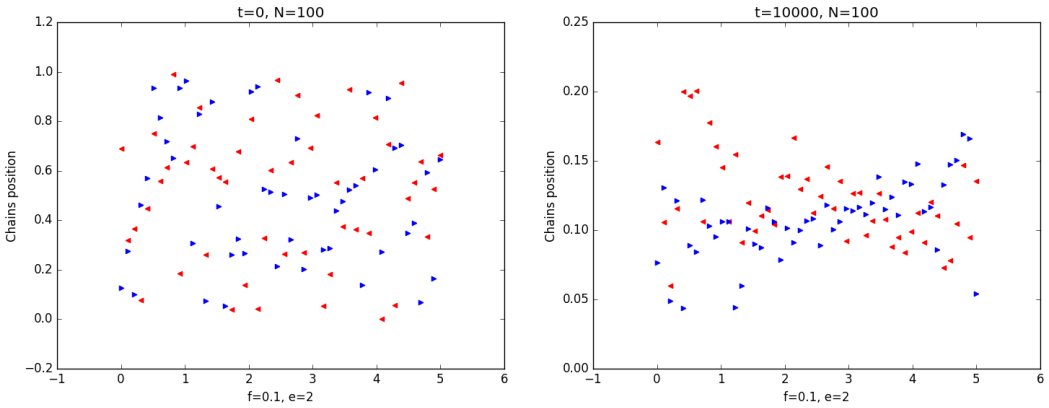

Figure 6.6: *Snapshot of the chains configuration at initial condition* $t = 0$ *and at* $t = 10000$ *for the parameters:* $f = 0.1, \epsilon = 2, \gamma = 1, k_BT = 1, \lambda = 1, N = 100$. *We see that the clump of chains is more significant with the increase of the networking force strength.*

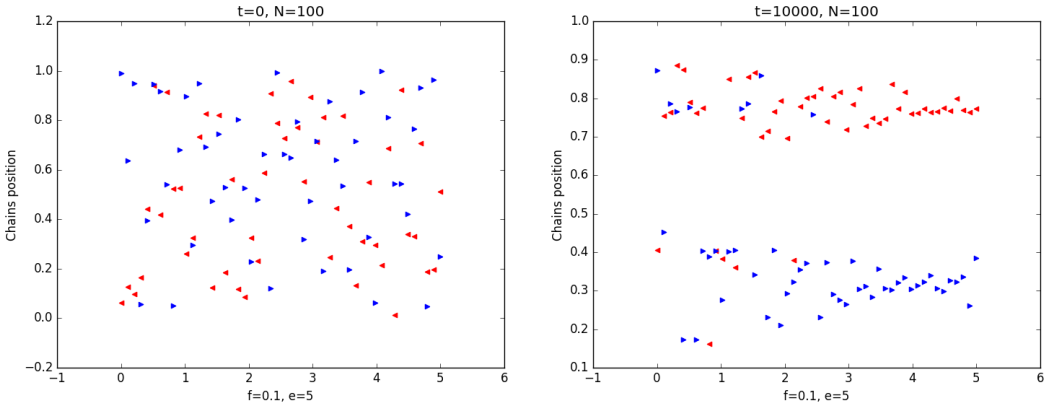

Figure 6.7: *Snapshot of the chains configuration at initial condition* $(t = 0)$ *and at* $t = 10000$ *for the parameters:* $f = 0.1, \epsilon = 5, \gamma = 1, k_BT = 1, N = 100$. *We can see that the chains starts clumping as predicted by the theory.*

6.7.1.1 Phase transition within the ring

We investigate the phase transition on the ring. The order parameter of the system is the polarisation current density. We study the change of the current with the forces. Investigations has shown that the active force does not cause a major phase change. The average polarisation current density with the change of the networking force is plotted in Fig. 6.9 with a constant active force. The plot shows that for fixed value of the active force fn_0, the long time average of the current density goes through a transition and reached an almost non-conducting regime. This transition occurs at higher networking force with a large active force. This results has been observed in the correlation function (Fig. 6.5). The investigation of the structural integrity of the ring presented in

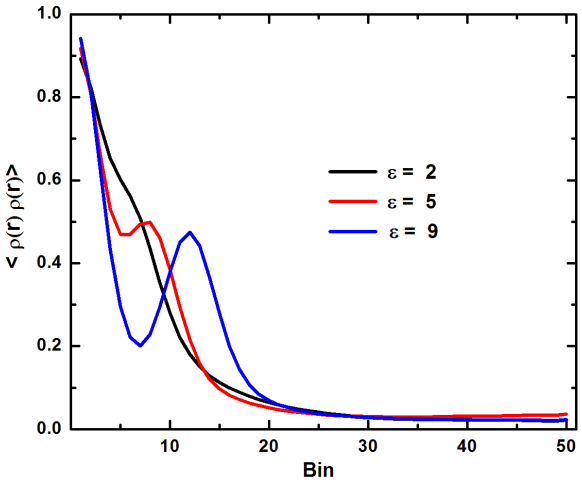

Figure 6.8: *Correlation function for fixed active force and different value of the networking force strength. Parameters are:* $f = 0.9, \gamma = 0.9, \lambda = 1, k_B T = 1, N = 100, Nbins = 50$. *We observe a new peak that rises with the increase of the active force. That peak shift to higher value of the length (bin).*

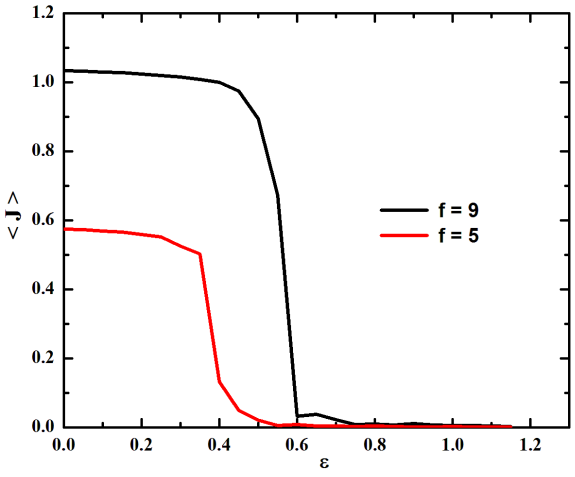

Figure 6.9: *Average polarisation current density as a function of the networking force* ϵn_0 *for different values of the active force. As the networking force increases, the current goes down sharply until there is almost no current flowing in the ring. The parameters used are:* $N = 80$ *chains,* $L = 1.0$, $l = 0.2$, $k_B T = 1.0$, $\gamma = 1.0$ *and* 200000 *time steps. We observe a small shift of the critical value of the networking force strength toward a large value of* ϵ.

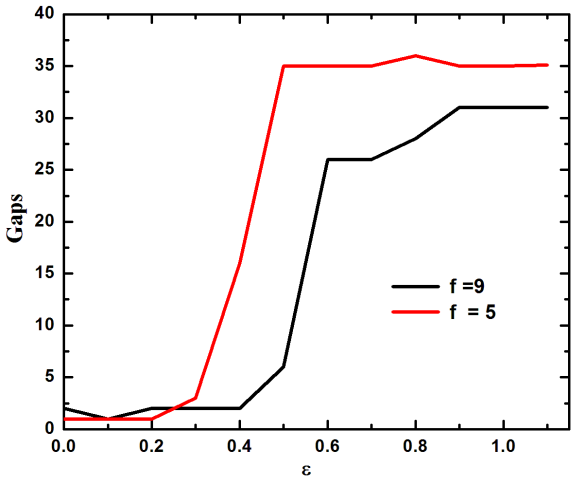

Figure 6.10: *Number of bins unoccupied by the chains in the ring as a function of the networking force. The parameters used are:* $N = 80$ *chains,* $L = 1.0$, $l = 0.2$, $k_B T = 1.0$, $\gamma = 1.0$ *and* 200000 *time steps.*

(Fig. 6.10) confirms the transition from current flowing to a no current flowing regime. We observe a strong gap arising in the segment density close to these corresponding points. The total 'gaps' in the system is a clear indicator of if the structural integrity of the ring is maintained or not.

6.8 Conclusion

In the present chapter, we looked at the effect of the motors protein myosin II assuming a very simple continuum model: "the contractile ring model". We focused our investigations on the collective chains behaviour within the ring and the role that each force plays on the chains' dynamics. As already stated, the motor protein myosin II gives the dynamics to the chains within the ring. It also simultaneously causes the chains to pull and push each other leading to a constant overtake of the chains inside the periodic ring. Similar investigation has been done by Kruse et al [35] for a non periodic contractile ring model. The authors have shown that the contraction of the acto-myosin occurs when the motor protein stops at the end of the chains. The question we addressed here was to know which force originate the contractile behaviour of the ring and also in which circumstances the structural integrity of the ring is improved. To answer those questions, we have investigated the tensile force generated inside the ring during the contraction. Results have shown that the energy generated by the network to maintain the chains connected is the one responsible for the contractile behaviour of the ring. The active force only causes the chains to overtake each other. These observations specifically hold in the case of a finite periodic ring. This suggests that even in case of low ATP, the ring still contracts. The constant overtaking of the chains within the ring leads to a constant current flowing and a maintenance of the mechanical structure (the stability) of the ring. Along with the analytical investigation, we numerically probed the ring system using a simple one-dimensional Langevin Dynamics Simulation (LDS). Results showed that the analytical predicted behaviour of the filaments inside the ring is valid. The system phase separate and therefore lose its mechanical structure with the increase of the networking force (Fig. 6.5, Fig. 6.9) . Once again, we saw that, the active force is not the one causing the contraction of the ring. Nevertheless, this force is needed in the system because it gives the dynamics to the chains through the ATP.

Part IV

Summary and outlook

Chapter 7

Summary and outlook

The physics of a randomly linked polymers with reversible and permanent cross-linkers is challenging. Understanding the network formation process leads to a better insight in the basic behaviour of the network, e.g. for a network made of polar chains, the orientation of the chains to one another just after the formation is crucial in the understanding on how the network behaves. The reversible-movable and active-movable cross-linkers can generate forces at the microscopic scale. The interplay of the forces gives rise to so called the contractility. Physical tools and concepts such as field theoretical approach for polymer networks, collective dynamics, instability and self organisation can help to understand such network structure and behaviour changes.

The first part of this dissertation presents a field theoretical technique to construct a network that has both reversible-movable (reversible) plus permanent cross-links, and active-movable (active) plus permanent cross-links. This is done following the scheme of Edwards (1988) formulated for a permanent polymer network [2]. We adapted the technique by including the reversible-movable cross-linker inside the permanent network. We showed that the field theory elaborated for permanent network also holds for reversible types of cross-links. This has been well elaborated in (chapter 3). The field theory treatment of the polymer network has provided a good solution to resolve some issues that were encountered in polymer network formation e.g. the role of cross-link between polymers. Treating the system using statistical physics have required to consider the disorder (i.e. the random arrangement) of the polymer chains inside the network. The two distinguishable types of cross-linkers are treated differently while averaging over all the replicas of the network. Because one is fixed and the other one movable, the average over all the degree of freedom of the network is either a "quenched average" or an "annealed average", respectively. The quenched part of the average is handled using the mathematical transformation called the replica trick. We wrote the partition function of the system that includes all the replica of the network. It was shown that the field theory implemented for the network of permanently cross-linked polymers is certainly

also applicable to reversible cross-linked polymers. The average densities of the linkers show that each polymer chain inside the network fluctuates around a mean value which is the saddle point solution of the chain at the cross-linking position. This is similar to all cross-links. The investigation of the response of the network due to a small deformation revealed that by adding the reversible cross-linker inside a permanent network, it becomes softer. This holds at the condition that there are enough reversible cross-linkers.

In chapter 4, we showed how the polarity of the polymer impacts on the network behaviour. We looked at an extreme example of an one-dimensional network of randomly oriented polar chains. Two possible networks made of two polar polymers are explored. The polarity of the chains together with the active cross-linker that moves in the preferential direction generate a force. This latter force is modelled as a bias on the movable cross-linker position in a quasi-equilibrium setting (represents by the introduction of the Boltzmann weight). The active-movable cross-linker is then represented with two motor heads attached by a spring. The cross-linker is viewed as a slipping-ring in the case of the polymer chains having the same polarity orientation. The spring that connects the two motor heads is neglected and simply slides to the ends of the chains. In the anti-parallel case, the spring is included and provides a non trivial coupling between the polymer chains. This network is used to mimic the actomyosin network where the motor myosin II is the cross-linker moving toward the (+) end of the actin filament.

In the second part of the dissertation we looked at the contractile behaviour in the contractile ring. We focused our attention on the role of the active force versus the role of the networking force. The formalism elaborated highlights the collective dynamics and properties of the chains behaviour within the ring. We have investigated the correlation function of the system using the dynamical Random Phase Approximation (RPA) by following the scheme of Fredrickson and Helfand (1990) [5]. Along with the Langevin dynamics simulation, We have shown that the active force pushes the filaments past each other, but motor attachment (networking force) is also an attractive force. This strongly depends on the chains' polarity orientation relative to one another. The increase of the active force enhances the stability of a homogeneous phase. The active force therefore does not contribute in the contractile behaviour of the ring but rather makes the chains constantly overtake one another. On the other hand, the force generated by the myosin II in order to maintain the chains connected (networking force $\epsilon < 0$) tends to attract the chains and therefore leads to the contractile behaviour of the ring. We know that the system needs ATP in order to push or pull the filaments in a preferential direction [1]. The investigation of the phase change in the ring system has shown that the system goes from a polarisation current flowing regime (hight active force value) to an almost no current flowing in the ring at long time scale with the

increase of the networking force ($\epsilon > 0$). The ring loses its structural integrity when the networking force dominates the active force and when the other way around, maintains its mechanical stability.

Outlook

The network of polymer filaments has attracted the attention of many polymers physicists for years now. Many important insights have been gained so far, but there is still many fundamental challenging questions that one needs to answer. We can say with confidence that more work on the matter still lies ahead.

In the present dissertation, we looked at the effect of the motors assuming a very simple continuum model. We made some predictions that could be tested in a real contractile ring in a more microscopic length scale. This means, including motor proteins and their dynamics rather than using the approach showed in the present dissertation.

The investigation of the network formation and the cell's physical division could be a great insight in the understanding of self-organisation at the cellular level. The physics study of the mechanisms hiding behind the contractile behaviour or any other biological phenomena is an exciting journey and constitutes more than a theoretical point of interest. One can perform an experimental investigation to confirm the results founds.

Appendices

Appendix A

Details for calculations in chapters 3 and 4

The functional derivative formula is given by:

$$\frac{\delta F[\psi(r)]}{\delta\psi(r')} = \lim_{\epsilon\to 0} \frac{F[\psi(r)+\epsilon\delta(r-r')] - F[\psi(r)]}{\epsilon}. \tag{A.1}$$

If we have a function for example: $F[\psi(x)] = A\int_x \psi(x)$, the functional derivative of this function is given by:

$$\frac{\delta F[\psi(x)]}{\delta\psi(x')} = A\int_x \delta(x-x'). \tag{A.2}$$

A.1 Solve the saddle point (SPA) equations calculation

Details of the calculation of the saddle point approximation in section 3.4.1 is presented here. We solve for the saddle point solution of the Hamiltonian $-\chi$ and then, Taylor expand the equation (3.23) up to the second order in the saddle point solutions and later, perform the integration. The saddle point solutions are calculated by solving the set of saddle point equations (equation (A.3)) with one replica ($\alpha = 1$).

$$\begin{cases} \dfrac{\delta(-\chi)}{\delta\,\psi_\alpha}|_{(\overline{\psi},\overline{\psi^*}),(\overline{\phi},\overline{\phi^*})} = 0, & \text{(e1)} \\ \dfrac{\delta(-\chi)}{\delta\psi_i^*}|_{(\overline{\psi},\overline{\psi^*}),(\overline{\phi},\overline{\phi^*})} = 0, & \text{(e2)} \\ \dfrac{\delta(-\chi)}{\delta\,\phi}|_{(\overline{\psi},\overline{\psi^*}),(\overline{\phi},\overline{\phi^*})} = 0, & \text{(e3)} \\ \dfrac{\delta(-\chi)}{\delta\,\phi^*}|_{(\overline{\psi},\overline{\psi^*}),(\overline{\phi},\overline{\phi^*})} = 0. & \text{(e4)} \end{cases} \tag{A.3}$$

with

$$
\begin{aligned}
-\chi = \mu \int_{r_0^{(\alpha)}, r_1^{(\alpha)}} \int_{x_\alpha} \prod_{\alpha=1}^{n} \phi(r_0^{(\alpha)})\, G_\alpha (1 + \psi_\alpha\, e^{-\beta\eta})\, G'_\alpha\, \phi(r_1^{(\alpha)}) \\
- \int_{r^{(\alpha)}} \phi\phi^* - \sum_{\alpha=1}^{n} \int_{x_\alpha} \psi_\alpha \psi_\alpha^* + \mu_a \sum_{\alpha=1}^{n} \int_{x_\alpha} \psi_\alpha^{*2}(x_\alpha) + \mu_p \int_{r^{(\alpha)}} \phi^{*p}(r^{(\alpha)}) \quad \text{(A.4)} \\
- N \log \mu - N_a \log \mu_a - N_p \log \mu_p.
\end{aligned}
$$

The expression $(-N \log \mu - N_a \log \mu_a - N_p \log \mu_p)$ is neglected for future calculations because it does not influence the physical meaning of the results. The saddle point equations is given by:

$$
\begin{cases}
\mu \int_{r_0, r_1} \overline{\phi}(r_0)\, G(r_0 - r_1, L)\, e^{-\beta\,\eta}]\, \overline{\phi}'(r_1) - \overline{\psi}^*(y) = 0, & \text{(e1)} \\
-\overline{\psi}(y) + 2\mu_a\, \overline{\psi}^*(y) = 0, & \text{(e2)} \\
-\overline{\phi}^*(R) + 2\,\mu \int_{x, r_0} \overline{\phi}(r_0)\, G(r_0 - R, L)(1 + \overline{\psi}\, e^{-\beta\,\eta}) = 0, & \text{(e3)} \\
-\overline{\phi}(R) + \mu_p\, p\, \overline{\phi}^{*(p-1)}(R) = 0. & \text{(e4)}
\end{cases}
\quad \text{(A.5)}
$$

We combine equations (e3), (e4), (e1) and (e2), and have

$$
\begin{aligned}
\overline{\psi}(y) &= 2\mu\mu_a e^{-\beta\eta} \int_{r_1} G(r_1, L) p^2 \mu_p^2 \left[2\mu \int r_0 \overline{\phi}(r_0) G(r_0 - R, L) \int_x (1 + \psi(x) e^{-\beta\eta}) \right]^{2(p-1)} \\
&= 8\mu_a \mu \mu_p^2 e^{-\beta\eta} \int_{r_1} \left[\int_{r_0} \overline{\phi}(r_0) G(r_0 - R, L) \int_x (1 + \psi(x) e^{-\beta\eta}) \right]^{2(p-1)} G(r_1, L) \\
&= 8\mu_a \mu \mu_p^2 p^2 e^{-\beta\eta} \left[\overline{\phi}(R) G(R, L) \int_x (1 + \overline{\psi}(x) e^{-\beta\eta}) \right]^{2(p-1)} \int_{r_1} G(r_1, L)
\end{aligned}
\quad \text{(A.6)}
$$

We assume Gaussian distribution, and can write $\phi(r) = Ae^{-ar^2}$, $\psi(x) = Be^{-bx^2}$ and $G(r, L) = (\frac{3}{2lL})^{3/2} e^{3r^2/2lL}$. Using the Gaussian approximation and supposing that there is always enough reversible cross-linker in the network ($e^{-\beta\eta} \gg 1$), the equation (A.6) gives:

$$
Be^{-by^2} = \frac{8\pi}{b} B^2 A^2 (\frac{3}{2lL})^3 p^2 \mu_a \mu \mu_p \sqrt{\frac{\pi l L}{3}} e^{-3\beta\eta} (\sqrt{\pi/b})^{p-1} e^{-2(a+3/lL)(p-1)R^2}. \quad \text{(A.7)}
$$

We Fourier transform the two side of the equation A.7 and by identification, we find the constants b and B.

$$b = 2(p-1)\left(a + \frac{3}{lL}\right), \tag{A.8}$$

$$B = \frac{\sqrt{\frac{2}{3}} l^3 L^3 \pi^{-p-\frac{1}{2}} \left(\frac{1}{b}\right)^{-p} e^{3\beta\eta} \sqrt{(p-1)\left(a+\frac{3}{lL}\right)}}{9A^2\sqrt{b}\mu p^2 \mu_a \sqrt{lL}\mu_p}. \tag{A.9}$$

The equation (e3) and (e4) combined give:

$$Ae^{-aR^2} = 2^{p-1} p\pi^{\frac{p-1}{2}} \mu_p \left(\sqrt{\frac{1}{b}} B\mu e^{-\beta\eta}\right)^{p-1} \left(\frac{3}{2}\right)^{p-1} \left(\frac{Ae^{-aR^2-\frac{3R^2}{lL}}}{lL}\right)^{p-1}. \tag{A.10}$$

By identification, we have

$$a = -\frac{3(p-1)}{lL(p-2)}, \tag{A.11}$$

$$A = \left(\frac{p\pi^{\frac{p}{2}-\frac{1}{2}} \mu_p e^{\beta\eta} 2^{-\frac{3p}{2lL}+\frac{3}{2lL}+p-1} 3^{\frac{3p}{2lL}-\frac{3}{2lL}} \left(\frac{1}{lL}\right)^{\frac{3p}{2lL}-\frac{3}{2lL}} \left(\sqrt{\frac{1}{b}} B\mu e^{-\beta\eta}\right)^p}{\sqrt{\frac{1}{b}} B\mu}\right)^{\frac{1}{2-p}}. \tag{A.12}$$

For simplification, we take the $p = 3$, $\mu = \mu_a = \mu_p = 1$.

A.2 Calculate the density fluctuation using the generating functional method

The density fluctuation of a cross-linker can be derived from the generating functional. The method is to linearly coupled a source fields term $h(x)$ to the reversible field variable within the Hamiltonian inside the generating functional expression (equation (3.22)) [57]. We obtain the following expression with the source term included:

$$\begin{aligned} Z_{[h(x)]} = \oint_c \mathrm{d}\,\mu\,\mathrm{d}\,\mu_a\,\mathrm{d}\,\mu_p \int_{-\infty}^{+\infty} [\mathrm{d}\,\psi]\,[\mathrm{d}\,\psi^*]\,[\mathrm{d}\,\phi]\,[\mathrm{d}\,\phi^*]\,\exp\Bigg(\mu \int_{r_0,r_1}\int_x \phi \\ G(1+\psi\, e^{-\beta\,\eta})\, G'\,\phi' - \int_r \phi\,\phi^* - \int_x \psi\,\psi^* + \mu_a \int_x \psi^{*2}(x)\, h(x) + \mu_p \\ \int_r \phi^{*p}(r) - N\,\log\mu - N_a\,\log\mu_a - N_p\,\log\mu_p\Bigg) \\ = \int_{-\infty}^{+\infty} [\mathrm{d}\,\psi][\mathrm{d}\,\psi^*]\,[\mathrm{d}\,\phi]\,[\mathrm{d}\,\phi^*]\,e^{-\chi[\phi,\phi^*,\psi,\psi^*,h]}. \end{aligned} \tag{A.13}$$

The density of the reversible cross-link is obtained by doing the summation over all the positions of the motors head along the polymeric chain: $\rho(x) = \sum_{i=1}^{N_a} \rho(x_i) = \sum_{i=1}^{N_a} \delta(x - x_i)$. $\langle ... \rangle$ denotes the statistical average. Using the generating functional approach, the density fluctuation average is given by:

$$
\begin{aligned}
\langle \rho(x) \rangle &= \langle \sum_{i=1}^{N_a} \delta(x - x_i) \rangle \\
&= \frac{1}{Z_{h(x)=1}} \frac{\delta\, Z_{h(x)}}{\delta\, h(x')} \,|_{h(x)=1} \\
&= \frac{1}{Z_{h(x)=1}} \frac{\delta}{\delta\, h(x')} \left(\oint_c \mathrm{d}\,\mu \mathrm{d}\,\mu_a\, \mathrm{d}\,\mu_p \int_{-\infty}^{+\infty} [\mathrm{d}\,\psi]\,[\mathrm{d}\,\psi^*]\,[\mathrm{d}\,\phi]\,[\mathrm{d}\,\phi^*]\,\mu_a \right. \\
&\quad \psi^{*2}(x')\, \exp\Bigg[\mu \int_{r_0,r_1} \int_x \phi\, G(1 + \psi\, e^{-\beta\,\eta}) G' \phi' - \int_r \phi\, \phi^* - \int_x \psi\, \psi^* \\
&\quad + \mu_a \int_x \psi^{*2}(x)\, h(x) + \mu_p \int_r \phi^{*p}(r) - N\, \log \mu - N_a\, \log \mu_a \\
&\quad \left. - N_p\, \log \mu_p \Bigg] \right)_{h(x)=1} \\
&= \langle \psi^{*2}(x) \rangle .
\end{aligned}
\tag{A.14}
$$

With the result from equation (A.14) the density fluctuation of the reversible cross-link is given by the fluctuation of the cross-link itself powered by the functionality of the cross-linker. We are therefore be interested on calculated $\langle \psi^{*2}(x) \rangle$. The expansion of the generating functional up to the first order is given by:

$$
\begin{aligned}
Z_h &\simeq \exp[-\chi[\overline{\phi}, \overline{\phi}^*, \overline{\psi}, \overline{\psi}^*, h]], \\
\log Z_h &= -\chi[\overline{\phi}, \overline{\phi}^*, \overline{\psi}, \overline{\psi}^*, h] = -\chi_{sp,h}, \\
\langle \psi^{*2}(x) \rangle &= \frac{\delta \log Z_h}{\delta\, h} |_{h=1} \\
&= \frac{\delta}{\delta\, h} (-\chi_{sp,h}) |_{h=1}, \\
&= \mu \int_{r_0,r_1} \int_x \overline{\phi}\, G(1 + \psi\, e^{-\beta\,\eta}) G' \overline{\phi}' - \int_r \overline{\phi}\, \overline{\phi}^* - \int_x \overline{\psi \psi}^* \\
&\quad + \mu_a\, \overline{\psi}^{*2} + \mu_p \int_r \overline{\phi}^{*p}(r) \\
&= \underbrace{\overline{\psi}^{*2}(x)}_{\text{dominant term}} + \text{fluctuation term} .
\end{aligned}
\tag{A.15}
$$

The dominant term is the classical expression and the fluctuation the quantum term. The fluctuation term has the following expression:

$$\frac{1}{\mu_a}\left(\mu\int_{r_0,r_1}\int_x \overline{\phi}G(1+\psi e^{-\beta\eta})G'\overline{\phi}' - \int_r \overline{\phi\phi}^* - \int_x \overline{\psi\psi}^* + \mu_p\int_r \overline{\phi}^{*p}(r)\right). \quad \text{(A.16)}$$

Similar calculation is done for the permanent cross-link. The results show that it fluctuates around its saddle point solution.

A.3 Details of calculation on the Network deformation

The partition function for all the (n+1) replicas is given by:

$$\begin{aligned}\left[Z_m^{(n+1)}(\lambda)\right]_d &= \aleph\int Z_m^{(0)}Z_m^{(n)} \\ &= \aleph\int[\mathrm{d}\phi,\phi^*,\psi,\psi^*]\exp\left[-\chi_T^{(n+1)}(\lambda)\right], \end{aligned} \quad \text{(A.17)}$$

with

$$\begin{aligned}-\chi_T^{(n+1)}(\lambda) = \mu\iint\limits_{r_0^{(\alpha)},r_1^{(\alpha)}}\phi^*(r_0^{(\alpha)})\prod_{\alpha=0}^{n}\Big[\int_{x_\alpha}G(r_0^{(\alpha)}-x_\alpha,\frac{L}{2})\,(1+\psi_\alpha(x_\alpha)\,f) \\ G(x_\alpha-r_1^{(\alpha)},\frac{L}{2})\Big] - \int\limits_{r^{(\alpha)}}\phi\phi^* - \sum_{\alpha=0}^{n}\int_{x_\alpha}\psi_\alpha(x_\alpha) + \mu_a\sum_{\alpha=0}^{n}\int_{x_\alpha}\psi_\alpha^{*2}(x_\alpha) \\ + \mu_p\int\limits_{r^{(\alpha)}}\phi^{*p}(r^{(\alpha)}) - (N\log\mu + N_a\log\mu_a + N_{\mathrm{p}}\log\mu_{\mathrm{p}}).\end{aligned} \quad \text{(A.18)}$$

The functional $-\chi_T^{(n+1)}(\lambda)$ contains all the $(n+1)$ replicas of the network and $r^{(\alpha)} = (r^{(0)}, r^{(1)}, ..., r^{(n)})$. We suppose that all the reversible fields are replicated the same way in all replica (i.e $\sum_{\alpha=0}^{n}\psi_\alpha(x_\alpha) = (n+1)\psi(x)$). We use the simplification $z = e^{-\beta\eta}$ and have the saddle point equations given by the set of following equations:

$$\begin{cases}\dfrac{\delta(-\chi_T^{(n+1)}(\lambda))}{\delta\,\psi_\alpha(y_\alpha)}|_{(\overline{\psi},\overline{\psi^*}),(\overline{\phi},\overline{\phi^*})} = 0, & \text{(e1')}\\ \dfrac{\delta(-\chi_T^{(n+1)}(\lambda))}{\delta\psi_\alpha^*(y_\alpha)}|_{(\overline{\psi},\overline{\psi^*}),(\overline{\phi},\overline{\phi^*})} = 0, & \text{(e2')}\\ \dfrac{\delta(-\chi_T^{(n+1)}(\lambda))}{\delta\,\phi(R^\alpha)}|_{(\overline{\psi},\overline{\psi^*}),(\overline{\phi},\overline{\phi^*})} = 0, & \text{(e3')}\\ \dfrac{\delta(-\chi_T^{(n+1)}(\lambda))}{\delta\,\phi^*(R^\alpha)}|_{(\overline{\psi},\overline{\psi^*}),(\overline{\phi},\overline{\phi^*})} = 0. & \text{(e4')}\end{cases} \quad \text{(A.19)}$$

$$\begin{cases} (n+1)\overline{\psi}^{*}(y) = \mu \iint_{r_0^{(\alpha)}, r_1^{(\alpha)}} \overline{\phi}(r_0^{(\alpha)}) \prod_{\alpha=0}^{n} \left[zG(r_0^{(\alpha)} - r_1^{(\alpha)}, L) \right] \overline{\phi}(r_1^{(\alpha)}), & \text{(e1')} \\ \overline{\psi}(x) = 2\mu_a \overline{\psi}^{*}(x), & \text{(e2')} \\ \overline{\phi}^{*}(R^{\alpha}) = \int_{r_0^{(\alpha)}} \overline{\phi}(r_0^{(\alpha)}) \prod_{\alpha=0}^{n} \left[G(r_0^{(\alpha)} - R^{(\alpha)}, L) \int_{x_\alpha} (1 + \overline{\psi}_\alpha(x_\alpha) z) \right], & \text{(e3')} \\ \overline{\phi}(R^{\alpha}) = p\mu_p \overline{\phi}^{*(p-1)}(R^{\alpha}). & \text{(e4')} \end{cases} \tag{A.20}$$

We assume affine deformation: $r^{(\alpha>0)} = \lambda r^{(0)}$ and the permanent cross-linker is written as follows:

$$\begin{aligned} \phi(r^{(\alpha)}) &= \phi(r^{(0)}, r^{(1)}, ..., r^{(n)}), \\ &= \phi(r^{(0)}, \underbrace{\lambda r^{(0)}, ..., \lambda r^{(0)}}_{\text{n replicas}}), \\ &= \phi(r^{(0)}) \underbrace{\delta(r^{(1)} - \lambda r^{(0)}) ... \delta(r^{(n)} - \lambda r^{(0)})}_{\text{n replicas}}. \end{aligned} \tag{A.21}$$

The equation (A.20) is simplify and rewritten as:

$$\begin{cases} (n+1)\overline{\psi}^{*}(y) = \mu z^{(n+1)} \int_{r_1^{(\alpha)}} \overline{\phi}^{2}(r_1^{(0)}) G(r_1^{(0)}, L) \left[G(\lambda(r_0^{(0)} - r_1^{(0)})) \right]^n, & \text{(e1')} \\ \overline{\psi}(y) = 2\mu_a \overline{\psi}^{*}(y), & \text{(e2')} \\ \overline{\phi}^{*}(R^{\alpha}) = \mu \int_{r_0^{(\alpha)}} \overline{\phi}(r_0^{(0)}) G(r_0^{(0)} - R^{(0)}, L) \left[G(\lambda r_0^{(0)} - R^{(0)}, L) \right]^n & \\ \quad \times [\int_{x_\alpha} (1 + \overline{\psi}_\alpha(x_\alpha) z)]^{(n+1)}, & \text{(e3')} \\ \overline{\phi}(R^{(\alpha)}) = p\mu_p \overline{\phi}^{*(p-1)}(R^{(\alpha)}). & \text{(e4')} \end{cases} \tag{A.22}$$

With $R^{(\alpha>0)} = \lambda R^{(0)}$. We introduce the Gaussian assumption: $\overline{\phi}(r) = Ae^{-ar^2}$, $\overline{\psi}^{*}(x) = Be^{-bx^2}$ and the Green's function $G(r, L) = (\frac{3}{2lL})^{3/2} e^{\frac{-3r^2}{lL}}$. The equation $(e1')$ gives:

$$B(n+1)e^{-by^2} = A^2\mu \left(\frac{3}{2}\right)^{\frac{3(n+1)}{2}} z^{n+1} \left(\frac{1}{lL}\right)^{\frac{3(n+1)}{2}} e^{-(2a + \frac{3\left(\lambda^2 n+1\right)}{2lL})(r_0^{(0)})^2}. \tag{A.23}$$

We Fourier transform both side of the equation and identify the constants:

$$b = 2a + \frac{3\left(\lambda^2 n + 1\right)}{2lL}, \tag{A.24}$$

$$B = \frac{A^2\sqrt{b}\mu 2^{-\frac{3n}{2}-\frac{3}{2}} 3^{\frac{3n}{2}+\frac{3}{2}} z^{n+1} \left(\frac{1}{lL}\right)^{\frac{3n}{2}+\frac{1}{2}}}{lL(n+1)\sqrt{\frac{4alL+3\lambda^2 n+3}{lL}}} \tag{A.25}$$

The equation (e3') and (e4') combined are solve supposing that there is enough reversible cross-linker in the network ($1 \ll z\int_x \overline{\psi}(x)$) so, $\int_x(1 + z\,\overline{\psi}(x)) \simeq z\int_x \overline{\psi}(x)$. We combine the equations and obtain one equation with one unknown ϕ. We thereafter identify the constant and have:

$$a = \frac{4(p-1)\left(lLn + 12\lambda^2 n + 6\right)}{lL\left(4p^2 - 16p + 13\right)}, \tag{A.26}$$

$$\begin{aligned} A = \Bigg[& 2^{-3-2n} 3^{-11/2-9n/2} z^{-4(n+1)(1/L)^{3(-1-3n)/2}} L(n+1)^2 \pi^{-2-n} (1/b)^{-n} \\ & \left(\frac{3^{3(n+1)/2} z^{n+1} (1/L)^{3(n+1)/2} \sqrt{b}}{(n+1)\sqrt{2b}} \right)^{-2n} (512 l^2 n^2 + 48 Ln(131 + 259 n\lambda^2) \\ & + 9(2145 + 8482 n\lambda^2 + 8385 n^2 \lambda^4)) \Bigg]^{1/(5+4n)}. \end{aligned} \tag{A.27}$$

$$\begin{aligned} \left[Z_m^{(n+1)}(\lambda) \right]_d &= \aleph \int_{\mathbb{R}} [\mathrm{d}\phi, \phi^*, \psi, \psi^*] \exp\left[-\chi_T^{(n+1)}(\lambda) \right], \\ &= \aleph \int_{\mathbb{R}} [\mathrm{d}\underline{O}] \exp[-\chi_{sp}(\lambda)] \exp[-\frac{1}{2} \underline{O}\, \underline{\underline{H}}\, \underline{O}^T], \\ &= \aleph \sqrt{\frac{(2\pi)^3}{det(\underline{\underline{H}})}} \exp[-\chi_{sp}(\lambda)], \\ &\simeq \exp[-\chi_{sp}(\lambda)]. \end{aligned} \tag{A.28}$$

$$\begin{aligned} -\chi_{sp}(\lambda) = A^2 \left(\frac{3}{2L} \right)^{3(n+1)/2} & \left(\frac{\pi}{2a + \frac{3(n+1)}{2L}} \right)^{1/2} B^{n+1} (\pi/b)^{(n+1)/2} + A\sqrt{\frac{6\pi}{a}} \\ & - (n+1)\frac{B^2}{2}\sqrt{\frac{2\pi}{b}} + (n+1)\frac{B^2}{4}\sqrt{\frac{2\pi}{b}} - 3A^3\sqrt{\frac{3\pi}{a}}. \end{aligned} \tag{A.29}$$

The constants are replaced into the equation (A.29) and calculate the free energy and the tensile stress.

A.3.1 Calculate the number of reversible cross-linkers

While solving the saddle point equations, we have assumed that there is a large fraction of reversible cross-linker in the system. The average number of

reversible cross-linker is given for a grand canonical ensemble by the formula:

$$\begin{aligned}\langle N_{\text{rev}}\rangle &= z\frac{\partial}{\partial z}\log[Z_m^{(n+1)}(\lambda)],\\ &= z\frac{\partial}{\partial z}\left[-\chi_{sp}(\lambda)\right],\\ &= (n+1)\mu\int_{r_0^{(\alpha)}}\int_{r_1^{(\alpha)}}\overline{\phi}(r_0^{(\alpha)})\left[\prod_{\alpha=0}^{n}G(r_0^{(\alpha)}-r_1^{(\alpha)},L)\int_x(1+\overline{\psi}(x)z)\right].\end{aligned}$$

Using the (e3'), we identify the term in the equation (A.30) and have:

$$(n+1)\int_{r_1^{(\alpha)}}\overline{\phi}(r_1^{(\alpha)}) = \langle N_{\text{rev}}\rangle\,. \tag{A.30}$$

We identity the local density of reversible cross-linkers as $\rho(r) = (n+1)\,\overline{\phi}(r_1^{(\alpha)})$.

Appendix B

Details calculation on chapters 5 and 6

B.1 Introduction of collective variables

We define the microscopic monomer density as $\rho(x) = \sum_{a=1}^{N} \delta(x - x_a(t))$ for any chain number a. The collective variables are best expressed in Fourier space. We use then the Fourier transformation formula: ($f(k) = \frac{1}{\sqrt{2\pi}} \int_x e^{ikx} f(x)$; $f(x) = \sqrt{2\pi} \int_k e^{-ikx} f(k)$). We write the Fourier expansion of the change density as:

$$\rho(\vec{x}) = \frac{1}{V} \sum_{k=1}^{N} \rho_{\vec{k}} e^{i\vec{k}.\vec{x}} \tag{B.1}$$

$$\begin{aligned} \rho_{\vec{k}} &= \iiint \mathrm{d}^3\vec{x}\rho(\vec{x})e^{-i\vec{k}.\vec{x}} \\ &= \sum_{i=1}^{N} \iiint \mathrm{d}^3\vec{x}\delta(\vec{x} - \vec{x}_i)e^{-i\vec{k}.\vec{x}_i}. \end{aligned} \tag{B.2}$$

Therefore, $\rho_{\vec{k}} = \sum_{i=1}^{N} e^{-i\vec{k}.\vec{x}_i}$ is the density Fourier component when $\vec{k} \neq 0$. It also represents the density fluctuation over the average density. For $\vec{k} = 0$, the density is simply the total number of chains in the network divided by the total length of the system $\rho_{\vec{k}=0} = \rho_0 = \frac{N}{L}$. This latter density is often called the mean field density under the mean field approximation and in some cases can be neglected. $\rho_{\vec{k}}$ is dimensionless.

We introduce the collective variables inside the interacting Lagrangian.

$$\begin{aligned}\mathcal{L}_{int} &= i\sum_{a,b=1}^{N}\int_t \hat{x}_a F^{+}_{int} + i\sum_{a,b=1}^{N}\int_t \hat{X}_b F^{-}_{int} \\ &= i\sum_{a\neq a'}^{N^+}\int_t \hat{x}_a F^{++}_{int} + i\sum_{a,b}^{N}\int_t \hat{x}_a F^{+-}_{int} \\ & i\sum_{b\neq b'}^{N^-}\int_t \hat{X}_b F^{--}_{int} + i\sum_{a,b}^{N}\int_t \hat{X}_b F^{-+}_{int}.\end{aligned} \tag{B.3}$$

Those interacting forces can be explicitly expresses as follow:

$$F^{++}_{int} = F_{int}(x_a - x_{a'}), \tag{B.4}$$
$$F^{--}_{int} = F_{int}(X_b - X_{b'}), \tag{B.5}$$
$$F^{+-}_{int} = F_{int}(x_a - X_b), \tag{B.6}$$
$$F^{-+}_{int} = F_{int}(X_b - x_a). \tag{B.7}$$

Those forces mean the interaction between two + pointing rods, two − pointing rods, one rod pointing to the + direction with the other pointing to the − direction and one rod pointing to the − direction with the other pointing to the + direction respectively.
We now introduce the collective variable into $\mathcal{L}_{int}$. We introduce an identity expression which is the delta function expression $\int_x \delta(x - x_a) = 1$ so we have:

$$\begin{aligned} i\sum_{a\neq a'}^{N^+}\int_t \hat{x}_a F^{++}_{int} &= i\sum_{a\neq a'}^{N^+}\int_t \hat{x}_a F_{int}(x_a - x_{a'}) \\ &= i\sum_{a\neq a'}^{N^+}\int_t\int_{x,x'} \hat{x}_a \delta(x - x_a(t)) F_{int}(x - x')\delta(x' - x_{a'}(t)) \\ &= i\int_t\int_{x,x'}\left(\sum_{a=1}^{N^+}\hat{x}_a\delta(x - x_a(t))\right) F_{int}(x - x')\left(\sum_{a'=1}^{N^+}\delta(x' - x_{a'}(t))\right).\end{aligned} \tag{B.8}$$

and

$$\begin{aligned} i\sum_{a,b}^{N}\int_t \hat{x}_a F^{+-}_{int} &= i\sum_{a,b}^{N}\int_t \hat{x}_a F_{int}(x_a - X_b) \\ &= i\int_t\int_{x,X}\left(\sum_{a=1}^{N^+}\hat{x}_a\delta(x - x_a(t))\right) F_{int}(x - X)\left(\sum_{b=1}^{N^-}\delta(X - X_b(t))\right).\end{aligned} \tag{B.9}$$

In Furier space, we have the following density expression:

$$\delta(x - x_a(t)) = \int_k \exp\left[ik(x - x_a(t))\right] \tag{B.10}$$

$$\hat{x}_a(t)\delta(x - x_a(t)) = \int_k \hat{x}_a(t) \exp\left[ik(x - x_a(t))\right]. \tag{B.11}$$

Those expressions are best expressed in Fourier space. With $\int_k \equiv \frac{1}{2\pi}\int_k$. We have:

$$\begin{aligned}
&i \int_t \int_{x,x'} \sum_a^{N^+} \hat{x}_a(t)\delta(x - x_a(t))F_{int}(x - x') \sum_{a'}^{N^+} \delta(x' - x_{a'}(t)) \\
&= i \int_t \int_{k,k'} \int_{x,x'} \sum_a^{N^+} \hat{x}_a(t) e^{[ik(x - x_a(t))]} F_{int}(x - x') \sum_{a'}^{N^+} e^{[ik'(x' - x_{a'}(t))]} \\
&= i \int_t \int_{k,k'} \int_{x,x'} \sum_a^{N^+} \hat{x}_a(t) e^{-ikx_a(t))} F_{int}(x - x') \sum_{a'}^{N^+} e^{-ik'x_{a'}(t)}\, e^{ikx + ik'x'} \\
&= i \int_t \int_{k,k'} \int_{x,x'} \varphi^+(k,t) F_{int}(x - x') \rho^+(k',t)\, e^{ikx + ik'x'}.
\end{aligned} \tag{B.12}$$

We can therefore deduce the expression of the collective variables written in Fourier space:

$$\varphi^+(k,t) = \sum_a^{N^+} \hat{x}_a(t) e^{-ikx_a(t))} \quad ; \quad \rho^+(k,t) = \sum_a^{N^+} e^{-ik'x_a(t)}, \tag{B.13}$$

where φ^+ is the complex conjugate of ρ^+. Two similar collective variables are also defined for the left pointing chains as φ^- and ρ^-.
We work with only the plus pointing chains and can introduce two new variables: the centre of mass variable $c = \frac{x+x'}{2}$ and the relative coordinate $r = x - x'$. From those new variables, we can deduce $x = r - x'$ and write:

$$\begin{aligned}
&i \int_t \int_{k,k'} \int_{x,x'} \varphi^+(k,t) F_{int}(x - x') \rho^+(k',t)\, e^{ikx + ik'x'} \\
&= i \int_t \int_{k,k'} \int_{r,c} \varphi^+(k,t) e^{ic(k + \frac{k'}{2})} F_{int}(r) e^{i\frac{r}{2}(k - k')} \rho^+(k',t) \\
&= i \int_t \int_{k,k'} \int_r \varphi^+(k,t) \delta(k + k') F_{int}(r) e^{i\frac{r}{2}(k - k')} \rho^+(k',t) \\
&= i \int_t \int_k \int_r \varphi^+(k,t) F_{int}(r) e^{-ikr} \rho^+(k',t) \\
&= i \int_t \int_k \varphi^+(k,t) F_{int}^{++}(k) \rho^+(k',t).
\end{aligned} \tag{B.14}$$

$F_{int}(k) = \int_r F_{int}(r)e^{-ikr}$ is the Fourier transform of $F_{int}(r)$. we use $k' = k', t' = -t$. We can therefore write the following equalities:

$$i\sum_{a\neq a'}^{N^+}\int_t \hat{x}_a(t)F_{int}^{++} = i\int_t\int_k \varphi^+(k,t)F_{int}^{++}(k)\rho^+(k',t), \tag{B.15}$$

$$i\sum_{b\neq b'}^{N^-}\int_t \hat{X}_b(t)F_{int}^{--} = i\int_t\int_k \varphi^-(k,t)F_{int}^{--}(k)\rho^-(k',t), \tag{B.16}$$

$$i\sum_{a,b}^{N}\int_t \hat{x}_a(t)F_{int}^{+-} = i\int_t\int_k \varphi^+(k,t)F_{int}^{+-}(k)\rho^-(k',t), \tag{B.17}$$

$$i\sum_{a,b}^{N}\int_t \hat{X}_b(t)F_{int}^{-+} = i\int_t\int_k \varphi^-(k,t)F_{int}^{-+}(k)\rho^+(k',t). \tag{B.18}$$

We can therefore deduce the interacting Lagrangian :

$$\begin{aligned}\mathcal{L}_{int} = \quad & i\int_t\int_k \varphi^+(k,t)F_{int}^{++}(k)\rho^+(k',t) + i\int_t\int_k \varphi^-(k,t)F_{int}^{--}(k)\rho^-(k',t) \\ & i\int_t\int_k \varphi^+(k,t)F_{int}^{+-}(k)\rho^-(k',t) + i\int_t\int_k \varphi^-(k,t)F_{int}^{-+}(k)\rho^+(k',t).\end{aligned} \tag{B.19}$$

We include the possibility to have interaction that might be due to the response star field φ. So we can therefore split the expression as using this argument:

$$\varphi(k,t)\rho(k',t) = \frac{1}{2}\left[\varphi(k,t)\rho(k',t) + \rho(k,t)\varphi(k',t)\right]. \tag{B.20}$$

We implement the change into the interacting Lagrangian and have:

$$\begin{aligned}\mathcal{L}_{int} = \frac{i}{2}\int_t\int_k \Big[& \varphi^+(k,t)F_{int}^{++}(k)\rho^+(k',t) + \rho^+(k,t)F_{int}^{++}(k')\varphi^+(k',t) \\ & + \varphi^-(k,t)F_{int}^{--}(k)\rho^-(k',t) + \rho^-(k,t)F_{int}^{--}(k')\varphi^-(k',t) \\ & + \varphi^+(k,t)F_{int}^{+-}(k)\rho^-(k',t) + \rho^-(k,t)F_{int}^{+-}(k')\varphi^+(k',t) \\ & + \rho_b^*(k,t)F_{int}^{-+}(k)\rho^+(k',t) + \rho^+(k,t)F_{int}^{-+}(k')\varphi^-(k',t)\Big].\end{aligned} \tag{B.21}$$

We define a super-vector :

$$\underline{\rho}(k,t) = \left(\rho^+(k,t), \varphi^+(k,t), \rho^-(k,t), \varphi^-(k,t)\right), \tag{B.22}$$

and

$$\underline{\rho}(k',t) = \left(\rho^+(k',t), \varphi^+(k',t), \rho^-(k',t), \varphi^-(k',t)\right). \tag{B.23}$$

We can therefore write:

$$\mathcal{L}_{int} = \frac{i}{2}\int_t\int_k\left[\underline{\rho}(k,t)\underline{\underline{F}}_{int}(k)\underline{\rho}^T(k',t')\right]. \tag{B.24}$$

Were $\underline{\rho}^T$ is the transpose of the supper vector $\underline{\rho}$. We time Fourier transform and have:

$$\mathcal{L}_{int} = \frac{i}{2}\int_\omega\int_k\left[\underline{\rho}(k,\omega)\underline{\underline{F}}_{int}(k)\underline{\rho}^T(k',\omega')\right], \tag{B.25}$$

For the finite and periodic ring, The equation (B.25) is obtained the Fourier series instead of the Fourier transform. The Fourier series of a function $f(x)$ is given by the formula: $f(x) = \sum_{m=-\infty}^{+\infty} c_m \exp(ikx)$ with the Fourier coefficients computed by $c_m = (1/L)\int_0^L \mathrm{d}x f(x)\exp(-ikx)$. The Kronecker δ iw written in term of an inverse Fourier coefficient: $\delta_{m,m'} = \frac{1}{L}\int_0^L \mathrm{d}\, e^{2\pi i(m-m')x/L}$. The Fourier coefficient of a (periodic) Dirac delta function are given by $c_m = \frac{1}{L}\int_0^L \mathrm{d}\delta(x-x')e^{-2\pi imx/L} = \frac{1}{L}e^{-2\pi imx'/L}$. We therefore construct the periodic Dirac delta function through the following construction that must also replace the appropriate expression above:

$$\delta_L(x) = \sum_{-\infty}^{\infty}\delta(x-mL) = \frac{1}{L}\sum_{m=-\infty}^{\infty}e^{2i\pi mx/L} = \frac{1}{L}\sum_{k\neq 0}e^{i\pi kx}. \tag{B.26}$$

The periodic version of the equation (B.25) in term of the Fourier transform in t and the Fourier series in x is:

$$\mathcal{L}_{int} = \frac{i}{2}\int_\omega\sum_{k\neq 0}\left[\underline{\rho}(k,\omega)\underline{\underline{F}}^R_{int}(k)\underline{\rho}^T(k',\omega')\right], \tag{B.27}$$

where $\underline{\underline{F}}_{int}(k)$ is a 4×4 matrix having the following expression:

$$\underline{\underline{F}}_{int}(k) = \begin{pmatrix} 0 & F^{++}_{int}(k) & 0 & F^{+-}_{int}(k) \\ F^{++}_{int}(k) & 0 & F^{+-}_{int}(k) & 0 \\ 0 & F^{-+}_{int}(k) & 0 & F^{--}_{int}(k) \\ F^{-+}_{int}(k) & 0 & F^{--}_{int}(k) & 0 \end{pmatrix}. \tag{B.28}$$

Now that we have defined the collective variables, we introduce them inside the generating functional using the identity formula:

$$\begin{aligned} 1 = \int_{\mathbb{R}}[d\rho^+][d\rho^-][d\varphi^+][d\varphi^-]\delta[\rho^+(k,t) - \sum_{a=1}^{N^+}e^{-ikx_a(t)}]\delta[\rho^-(k,t) - \sum_{b=1}^{N^-}e^{-ikX_b(t)}] \\ \delta[\varphi^+(k,t) - \sum_{a=1}^{N^+}\hat{x}_a e^{-ikx_a(t)}]\delta[\varphi^-(k,t) - \sum_{b=1}^{N^-}\hat{X}_b e^{-ikX_b(t)}]. \end{aligned} \tag{B.29}$$

The equation (B.29) is now introduce into the generating functional equation (5.23) and we have:

$$\begin{aligned} Z = \frac{1}{\aleph'}\int_{\mathbb{R}} \Pi_{a=1}^{N^+}\Pi_{b=1}^{N^-}[dx_a(t)][d\hat{x}_a(t)][dX_b(t)][d\hat{X}_b(t)][d\rho^+][d\rho^-][d\varphi^+][d\varphi^-] \\ \exp\left(\mathcal{L}\right)\delta[\rho^+(k,t) - \sum_{a=1}^{N^+} e^{-ikx_a(t)}]\delta[\rho^-(k,t) - \sum_{b=1}^{N^-} e^{-ikX_b(t)}] \\ \delta[\varphi^+(k,t) - \sum_{a=1}^{N^+} \hat{x}_a e^{-ikx_a(t)}]\delta[\varphi^-(k,t) - \sum_{b=1}^{N^-} \hat{X}_b e^{-ikX_b(t)}]. \end{aligned} \tag{B.30}$$

We transform the delta functional on its exponential expression by using the formula:

$$\delta[\rho - \sum_{i=1}^{N} e^{-ikx_i(t)}] = \int_{k,t}[d\rho][D\hat{\rho}]\exp\left[i\hat{\rho}\rho + i\sum_{i=1}^{N}\hat{\rho}e^{-ikx_i(t)}\right]\underbrace{J(x)}_{1}. \tag{B.31}$$

$$\begin{aligned} Z = \frac{1}{\aleph'}\int_{\mathbb{R}} \Pi_{a=1}^{N^+}\Pi_{b=1}^{N^-}[dx_a(t)][d\hat{x}_a(t)][dX_b(t)][d\hat{X}_b(t)] \\ [d\rho^+][d\rho^-][d\varphi^+][\mathrm{d}\,\varphi^-]\exp\left(\mathcal{L}+\mathcal{L}_3+\mathcal{L}_q\right). \end{aligned} \tag{B.32}$$

Where

$$\mathcal{L}_q = -i\int_{k,t}\left(\hat{\rho}^+\rho^+ + \hat{\rho}^-\rho^- + \hat{\varphi}^+\varphi^+ + \hat{\varphi}^-\varphi^-\right), \tag{B.33}$$

is the quadratic Lagrangian. The new non-interacting Lagrangian.

$$\begin{aligned} \mathcal{L}_3 = -i\int_{k,t}\Bigg(\sum_{a=1}^{N^+}\hat{\rho}^+e^{-ikx_a(t)} + \sum_{a=1}^{N^+}\hat{\varphi}^+\hat{x}_a e^{-ikx_a(t)} \\ + \sum_{b=1}^{N^-}\hat{\rho}^-e^{-ikX_b(t)} + \sum_{b=1}^{N^-}\hat{\varphi}^-\hat{X}_b e^{-ikX_b(t)}\Bigg). \end{aligned} \tag{B.34}$$

the new non-interacting Lagrangian. The exponential inside the equation (B.32) gives now:

$$\exp\left[\mathcal{L}\right] = \exp\left[\mathcal{L}_{int}+\mathcal{L}_q\right]\times\exp[\mathcal{L}_3+\mathcal{L}_0]. \tag{B.35}$$

The quadratic term will gives an identity matrix and the non interacting part is treated using the RPA. The non interacting part of the Lagrangian can be approximate as:

$$\begin{aligned} \exp[\mathcal{L}_3+\mathcal{L}_0] &= \exp[\mathcal{L}_3]\times\exp[\mathcal{L}_0] \\ &= \langle\exp[\mathcal{L}_3]\rangle_0 \\ &\backsimeq \exp[\frac{1}{2}\langle\mathcal{L}_3^2\rangle_0]. \end{aligned} \tag{B.36}$$

Where $\langle(...)\rangle_0 = \int_{\mathbb{R}}[dx_a][d\hat{x}_a][dX_b][d\hat{X}_b](...)\exp[\mathcal{L}_0]$ means the average of $(...)$ using $e^{\mathcal{L}_0}$ as statistical weight.

B.2 Random Phase Approximation(RPA)

Initially developed by Bohm and Pines (1952) "Many electrons theory" [13, 14]. This method explains best the Phase transition a many body system. In the approximation, the quadratic term of the density fluctuation is neglected. This approximation is a common scheme to determine the density-density correlation function. It gives decent description of interacting chains. As the one uses in this dissertation, we present in this section the explicit calculus for the dynamical RPA of the system. We derive the approximation using the MSR formalism [5, 7, 8]. Using this approximation, we express the chains in terms of the collectives variable. We restrict ourself to the case where the chains are homogeneously distributed inside the ring. They are therefore supposed to have a Gaussian distribution in density fluctuation. For a dense enough system, this approximation has revealed itself to be a reasonably good approximation to study the stability of a dynamical system. Performing the approximation, we investigate where the system phase separate. The system phase separate where the density density correlation function diverges. That is an indicator of phase transition inside the system. We wish to write the generating functional in term of the density variables. From the generation functional, we use the non interacting Lagrangian for $k \neq 0$ We detail here the RPA calculations for the linear ring model and for the finite periodic model.

B.2.1 RPA for linear ring

The non interacting Lagrangian gives:

$$
\begin{aligned}
\mathcal{L}_3^2 = & \left[-i \int_{k,t} \left(\sum_{a=1}^{N^+} \hat{\rho}^+ \, e^{-ik\,x_a(t)} + \sum_{a=1}^{N^+} \hat{\varphi}^+ \, \hat{x}_a e^{-ik\,x_a(t)} \right.\right. \\
& \left.\left. + \sum_{b=1}^{N^-} \hat{\rho}^- \, e^{-ik\,X_b(t)} + \sum_{b=1}^{N^-} \hat{\varphi}^- \, \hat{X}_b \, e^{-ik\,X_b(t)} \right) \right]^2 \\
= & - \int_{k,t} \int_{k',t'} \left[\hat{\rho}^+(k,t)\, \hat{\rho}^+(k',t') \left(\sum_a^{N^+} e^{-ik\,x_a(t) - ik'\,x_a(t')} \right) \right. \\
& + \hat{\rho}^-(k,t)\, \hat{\rho}^-(k',t') \left(\sum_b^{N^-} e^{-ik\,X_b(t) - ik'\,X_b(t')} \right) \\
& + \hat{\varphi}^+(k,t)\, \hat{\varphi}^+(k',t') \left(\sum_a^{N^+} \hat{x}_a(t)\, \hat{x}_a(t')\, e^{-ik\,x_a(t) - ik'\,x_a(t')} \right) \\
& + \hat{\varphi}^-(k,t)\, \hat{\varphi}^+(k',t') \left(\sum_b^{N^-} \hat{X}_b(t)\, \hat{X}_b(t')\, e^{-ik\,X_b(t) - ik'\,X_b(t')} \right) \\
& + 2\hat{\rho}^+(k,t)\, \hat{\varphi}^+(k',t') \left(\sum_a^{N^+} \hat{x}_a(t')\, e^{-ik\,x_a(t) - ik'\,x_a(t')} \right) \\
& + 2\, \hat{\rho}^-(k,t)\, \hat{\varphi}^-(k',t') \left(\sum_b^{N^-} \hat{X}_b(t')\, e^{-ik\,X_b(t) - ik'\,X_b(t')} \right) \\
& + 2\, \hat{\rho}^+(k,t)\, \hat{\rho}^-(k',t') \left(\sum_{a,b}^{N} e^{-ik\,X_b(t) - ik'\,x_a(t')} \right) \\
& + 2\, \hat{\rho}^-(k,t)\, \hat{\varphi}^+(k',t')\, \hat{x}_a(t') \left(\sum_{a,b}^{N} e^{-ik\,x_a(t) - ik'\,X_b(t')} \right) \\
& + 2\, \hat{\rho}_a(k,t)\, \hat{\varphi}^-(k',t')\, \hat{X}_b(t') \left(\sum_{a,b}^{N} e^{-ik\,X_b(t) - ik'\,x_a(t')} \right) \\
& \left. + 2\, \hat{\varphi}^+(k,t)\, \hat{\rho}^-(k',t')\, \hat{x}_a(t)\, \hat{X}_b(t') \left(\sum_{a,b}^{N} e^{-ik\,x_a(t) - ik'\,X_b(t')} \right) \right].
\end{aligned}
\tag{B.37}
$$

For the present model, there is no correlation between two oppositely oriented chains because the chains are supposed to be independents: That means, all the correlations including + and − or (a and b) gives zero in the non-interacting matrix. We can therefore simplify the expression and take the average over

$\mathcal{L}_0$:

$$\begin{aligned}\langle \mathcal{L}_3^2 \rangle_0 = -\int_{k,t}\int_{k',t'} \Big[& \hat{\rho}^+(k,t)\,\hat{\rho}^+(k',t')\,S_{11} + \hat{\rho}^-(k,t)\hat{\rho}^-(k',t')S_{33} \\ & + \hat{\varphi}^+(k,t)\,\hat{\varphi}^+(k',t')\,S_{22} + \hat{\varphi}^-(k,t)\,\hat{\varphi}^-(k',t')\,S_{44} \\ & + 2\,\hat{\rho}^+(k,t)\,\hat{\varphi}^+(k',t')\,S_{12} + 2\,\hat{\rho}^-(k,t)\,\hat{\varphi}^-(k',t')\,S_{34} \Big] \\ = -\int_{k,t}\int_{k',t'} & \underline{\hat{\rho}}(k,t) \times \underline{\underline{S}}_0 \times \underline{\hat{\rho}}^T(k',t').\end{aligned} \tag{B.38}$$

With the following expressions of the elements of the non-interacting matrix are:

$$S_{11}(k,t) = \left\langle \sum_{a=1}^{N^+} e^{-ik\,x_a(t) - ik'\,x_a(t')} \right\rangle_0, \tag{B.39}$$

$$S_{33}(k,t) = \left\langle \sum_{b}^{N^-} e^{-ik\,X_b(t) - ik'\,X_b(t')} \right\rangle_0, \tag{B.40}$$

$$S_{22}(k,t) = \left\langle \sum_{a}^{N^+} \hat{x}_a(t)\,\hat{x}_a(t')\,e^{-ik\,x_a(t) - ik'\,x_a(t')} \right\rangle_0, \tag{B.41}$$

$$S_{44}(k,t) = \left\langle \sum_{b}^{N^-} \hat{X}_b(t)\,\hat{X}_b(t')\,e^{-ik\,X_b(t) - ik'\,X_b(t')} \right\rangle_0, \tag{B.42}$$

$$S_{12}(k,t) = \left\langle \sum_{a}^{N^+} \hat{x}_a(t')\,e^{-ik\,x_a(t) - ik'\,x_a(t')} \right\rangle_0, \tag{B.43}$$

$$S_{34}(k,t) = \left\langle \sum_{b}^{N^-} \hat{X}_b(t')\,e^{-ik\,X_b(t) - ik'\,X_b(t')} \right\rangle_0. \tag{B.44}$$

$$\tag{B.45}$$

$S_{12}(k,t) = S_{21}(k',t')$ and $S_{34}(k,t) = S_{43}(k',t')$.

B.2.1.1 Matrix S elements

$$
\begin{aligned}
S_{11}(k,t) &= \left\langle \sum_{a=1}^{N^+} e^{-ik\,x_a(t)-ik'\,x_a(t')} \right\rangle_0 \\
&= \frac{1}{\aleph} \int_{\mathbb{R}} \prod_{a,b=1}^{N} [\mathrm{d}\,x_a]\,[\mathrm{d}\,\hat{x}_a]\,[\mathrm{d}\,X_b]\,[\mathrm{d}\,\hat{X}_b]\,\exp[-ik\,x_a(t)+ik\,x_a(t')] \\
&\exp\left[i\gamma \sum_{a,b=1}^{N} \int_t \left(\hat{x}_a(t)\,\partial_t x_a(t) + \hat{X}_b(t)\,\partial_t\,X_b(t) \right) \right. \\
&\left. -\frac{\lambda}{2} \sum_{a=1}^{N^+} \int_t (\hat{x}_a(t))^2 - \frac{\lambda}{2} \sum_{b=1}^{N^-} \int_t (\hat{X}_b(t))^2 \right].
\end{aligned}
\tag{B.46}
$$

We perform the integration over the hatted field $\hat{x}_a(t)$ and $\hat{X}_b(t)$ using the Hubbard Stratonovich Transformation (HST) [1] (equation B.47).

$$
\exp\left[-\frac{a}{2}\,x^2\right] = \frac{1}{\sqrt{2\pi a}} \int_{\mathbb{R}} \exp\left[-\frac{y^2}{2\,a} - ix\,y\right]. \tag{B.47}
$$

Applying that we end up with:

$$
\begin{aligned}
S_{11}(k,t) = \frac{1}{\aleph} \int_{\mathbb{R}} \prod_{a,b=1}^{N} [\mathrm{d}\,x_a]\,[\mathrm{d}\,X_b] \sum_{a,b}^{N} \exp\left[-ik\,x_a(t) \;+\; ik\,x_a(t')\right] \\
\left(\frac{1}{2\,\pi\,\lambda}\right) \exp\left[-\frac{\gamma^2}{2\,\lambda} \sum_{a}^{N^+} \int_t \dot{x}^2(t) \;-\; \frac{\gamma^2}{2\,\lambda} \sum_{b}^{N^-} \int_t \hat{X}_b^2(t) \right].
\end{aligned}
\tag{B.48}
$$

with $x_a(t) \neq x(t)$, by time-ordering [61, 63], we can remove all the simulations and the products then, have the following expression:

$$
\begin{aligned}
S_{11}(k,t) = \frac{N}{\aleph'} \int_{\mathbb{R}} [\mathrm{d}\,x]\,[\mathrm{d}\,X]\,\exp\left[-\frac{\gamma^2}{2\,\lambda} \int_t \hat{X}^2(t) \right] \\
\exp\left[-ik\,x(t) \;+\; ik\,x(t') \;-\; \frac{\gamma^2}{2\,\lambda} \int_t \dot{x}^2(t) \right].
\end{aligned}
\tag{B.49}
$$

We use the discretisation form of x and X as:

$$
\dot{x}(t) = \frac{x_{\mathrm{j}} \;-\; x_{\mathrm{j\text{-}1}}}{\epsilon} \tag{B.50}
$$

$$
\dot{x}^2(t) = \sum \epsilon \left(\frac{\Delta x_\alpha}{\epsilon} \right)^2. \tag{B.51}
$$

[1] HST is a simple Gaussian expression that lead to the coupling of another field (hatted field) to the original field.

We have:

$$S_{11}(k,t) = \frac{N}{\aleph'}\int_{\mathbb{R}}\prod_{\mathrm{j,j'}=0}^{n}[\mathrm{d}\,x_{\mathrm{j}}]\,[\mathrm{d}\,X_{\mathrm{j'}}]\,\exp\left[\frac{-\gamma^2}{2\,\lambda}\int_t\sum_{\mathrm{j'}=1}^{n}\epsilon\left(\frac{X_{\mathrm{j'}}-X_{\mathrm{j'-1}}}{\epsilon}\right)^2\right]$$
$$\exp\left[\frac{-\gamma^2}{2\,\lambda}\int_t\sum_{\mathrm{j}=1}^{n}\epsilon\left(\frac{x_{\mathrm{j}}-x_{\mathrm{j-1}}}{\epsilon}\right)^2 - i(k+k')x_0 - i\sum_{\mathrm{j}=1}^{n}(k\,x_{\mathrm{j}}+k'\,x_{\mathrm{j-1}})\right]. \tag{B.52}$$

We consider only the case where $k' = -k$ and introduce two bond vectors defined as following: $a_{\mathrm{j}} = x_{\mathrm{j}} - x_{\mathrm{j-1}}$ and $b_{\mathrm{j'}} = X_{\mathrm{j'}} - X_{\mathrm{j'-1}}$, we have:

$$S_{11}(k,t) = \frac{N}{\aleph'}\,\delta(k+k')\int_{\mathbb{R}}\prod_{\mathrm{j,j'}=0}^{n}[\mathrm{d}\,a_{\mathrm{j}}]\,[\mathrm{d}\,b_{\mathrm{j'}}]\,\exp\left[\frac{-1}{2\,\lambda}\sum_{\mathrm{j'}=1}^{n}\left(\frac{\gamma^2\,b_{\mathrm{j'}}^2}{\epsilon}\right)\right]$$
$$\exp\left[\frac{-1}{2\,\lambda}\sum_{\mathrm{j}=1}^{n}\epsilon\left(\frac{\gamma^2\,a_{\mathrm{j}}^2}{\epsilon}\right) - i\,k\sum_{\mathrm{j}=1}^{n}a_{\mathrm{j}}\right]. \tag{B.53}$$

We now perform the integration over a_j and $b_{j'}$ and we have the expression:

$$S_{11}(k,t) = \frac{N}{\aleph'}\,\delta(k+k')\left[\exp\left(\frac{-\lambda\,\epsilon\,k^2}{2\,\gamma^2}\right)\right]^n. \tag{B.54}$$

All constant from the integration are cast into the normalisation constant $\aleph'$ and can therefore be ignored for the rest of the calculus. We perform the Fourier transformation in time and get:

$$\begin{aligned} S_{11}(k,t) &= N\,\delta(k+k')\,\exp\left(\frac{-\lambda\,k^2}{2\,\gamma^2}|t-t'|\right) \\ &= N\,\delta(k+k')\,\exp\left(\frac{-\lambda\,k^2}{2\,\gamma^2}|t|\right) \\ S_{11}(k,\omega) &= \frac{2\,N\,k^2\,\sqrt{2/\pi}\,\gamma^2\,\lambda\,\delta(k+k')}{k^4\,\lambda^2+4\,\gamma^4\,\omega^2}. \end{aligned} \tag{B.55}$$

with $\epsilon = |t-t'|/n$ and we choose $t' = 0$. The second term of the non-interacting matrix is:

$$\begin{aligned} S_{12}(k,t) &= \left\langle\sum_a^{N^+}\hat{x}_a(t')\,e^{-i\,k\,x_a(t)-i\,k'\,x_a(t')}\right\rangle_0 \\ &= \frac{1}{\aleph}\int_{\mathbb{R}}\prod_{a,b=1}^{N}[\mathrm{d}\,x_a]\,[\mathrm{d}\,\hat{x}_a]\,[\mathrm{d}\,X_b]\,[\mathrm{d}\,\hat{X}_b]\sum_{a=1}^{N^+}\hat{x}_a(t')\exp\left[-ikx_a(t)+ik'x_a(t')\right]\Theta(t'-t) \\ &\exp\left[-i\,\gamma\sum_{a=1}^{N^+}\int_t\hat{x}_a(t)\,\dot{x}_a(t) - i\,\gamma\sum_{b=1}^{N^-}\int_t\hat{X}_b(t)\,\dot{X}_b(t)\right] \\ &\exp\left[-\frac{\lambda}{2}\sum_{a=1}^{N^+}\int_t\hat{x}_a^2(t) - \frac{\lambda}{2}\sum_{b=1}^{N^-}\int_t\hat{X}_b^2(t)\right]. \end{aligned} \tag{B.56}$$

We work wit the assumption $k' = -k$. In the equation (B.56), the Heaviside function $\Theta(t)$ take the values 1 or 0 of $t > 0$ or $t < 0$, respectively. This function has been introduced in the generating functional expression to conserve the time ordering during the integration [5, 61, 63]. The summation can be dropped out and replaced by the number of chains N^- and N^+. We use the generating functional approach to introduce the hatted field $\hat{x}_a$ inside the exponential. We have now:

$$\begin{aligned} S_{12}(k,t) = \frac{N^+}{\aleph} \int_{\mathbb{R}} [\mathrm{d}\, x_a]\,[\mathrm{d}\,\hat{x}_a]\,[\mathrm{d}\, X_b]\,[\mathrm{d}\,\hat{X}_b]\, \exp\left[\sum_b \int_t (-i\gamma\, X_b\,\hat{X}_b - \frac{\lambda}{2}\,\hat{X}_b^2)\right] \\ \frac{1}{i}\frac{\delta}{\delta\hat{h}(t)} \exp\left[\sum_a \int_t -i\gamma\,\hat{x}_a\,\dot{x}_a - \frac{\lambda}{2}\sum_a \int_t \hat{x}_a^2 + i\sum_a \hat{x}_a(t)\hat{h}_a(t)\right]_{\hat{h}=1} \\ \Theta(t-t')\, \exp\left(-ik\,x(t) + ik'\,x(t')\right). \end{aligned} \tag{B.57}$$

Integrating out the hatted field, we left with:

$$\begin{aligned} S_{12}(k,t) = \frac{N^+\gamma}{\aleph\,\lambda} \int_{\mathbb{R}} \prod_{a,b=1}^{N} [\mathrm{d}\, x_a]\,[\mathrm{d}\,\hat{x}_a]\,[\mathrm{d}\, X_b]\,[\mathrm{d}\,\hat{X}_b]\, \exp\left[-\frac{\gamma^2}{2\,\lambda}\sum_b \int_t \dot{X}_b^2\right]\Theta(t-t') \\ \exp\left[-ik\,x(t) - ik'\,x(t')\right] \\ \frac{\delta}{\delta\hat{h}(t)} \exp\left[\frac{1}{2\,\lambda}\sum_a \int_t (-i\gamma\,\dot{x}_a + \hat{h}_a(t))^2\right]_{\hat{h}=1}. \end{aligned} \tag{B.58}$$

We perform the functional derivative over $\hat{h}(t)$ and we left with:

$$\begin{aligned} S_{12}(k,t) = \frac{N\,\gamma^2}{\aleph\,\lambda^2} \int_{\mathbb{R}} \prod_{a,b=1}^{N} [\mathrm{d}\, x_a]\,[\mathrm{d}\, X_b]\, \exp\left[-\frac{\gamma^2}{2\,\lambda}\sum_b \int_t \dot{X}_b^2\right]\Theta(t-t') \\ \exp\left[-ik\,x(t) - ik'\,x(t')\right]\dot{x}(t)\, \exp\left[-\frac{\gamma^2}{2\,\lambda}\sum_a \int_t \dot{x}_a^2\right]. \end{aligned} \tag{B.59}$$

As done for the S_{11} calculation, we take $x_a \neq x$ cancels out with their corresponding integrals respectively. So we can now write a new normalization coefficient including all the coefficients form the integrations:

$$\begin{aligned} S_{12}(k,t) = \frac{N^+\,\gamma^2}{\aleph'\,\lambda^2} \int_{\mathbb{R}} [\mathrm{d}\, x(t)]\,[\mathrm{d}\, X(t)]\, \exp\left[-\frac{\gamma^2}{2\,\lambda}\int_t \dot{X}^2\right]\Theta(t-t') \\ \exp\left[-ik\,x(t) - ik'\,x(t')\right]\dot{x}(t)\, \exp\left[-\frac{\gamma^2}{2\,\lambda}\sum_a \int_t \dot{x}^2\right]. \end{aligned} \tag{B.60}$$

The discretisation gives:

$$
\begin{aligned}
S_{12}(k,t) = \frac{N\,\gamma^2}{\aleph'\,\lambda^2}\int_{\mathbb{R}}\prod_{i,\mathrm{j}=1}^{n}[\mathrm{d}\,a_i]\,[\mathrm{d}\,b_\mathrm{j}]\,\exp\left[-\frac{\gamma^2}{2\,\lambda\,\epsilon}\sum_{\mathrm{j}=1}^{n}b_\mathrm{j}^2\right]\Theta(t-t') \\
\sum_{\mathrm{j}=1}(\frac{i}{\epsilon})\,\exp\left[-i\,(k+k')\,x_0 - i\sum_{\mathrm{j}=1}(k\,x_i + k' x_{i-1})\right] \\
\exp\left[\frac{-\gamma^2}{2\,\lambda\,\epsilon}\sum_{j}^{n}a_\mathrm{j}^2\right] \qquad\qquad (B.61)\\
= \frac{N\,\lambda^2}{\aleph'\,\gamma^2\,\epsilon}\,\delta(k+k')\int_{\mathbb{R}}\prod_{i,\mathrm{j}=1}^{n}[\mathrm{d}\,a_i]\,[\mathrm{d}\,b_\mathrm{j}]\,\exp\left[-\frac{\gamma^2}{2\,\lambda\,\epsilon}\sum_{\mathrm{j}=1}^{n}b_\mathrm{j}^2\right]\Theta(t) \\
\sum_i a_i\,\exp\left[\frac{\gamma^2}{2\,\lambda\,\epsilon}\sum_i a_i^2 - i\,k\,a_i\right].
\end{aligned}
$$

We use the generating functional to introduce the a_i inside the exponential and we have:

$$
\begin{aligned}
S_{12}(k,t) = \frac{N\,\lambda^2}{\aleph'\,\gamma^2\,\epsilon}\,\delta(k+k')\int_{\mathbb{R}}\prod_{i,\mathrm{j}=1}^{n}[\mathrm{d}\,a_i]\,[\mathrm{d}\,b_\mathrm{j}]\,\exp\left[-\frac{\gamma^2}{2\,\lambda\,\epsilon}\sum_{\mathrm{j}=1}^{n}b_\mathrm{j}^2\right]\Theta(t-t') \\
\frac{\delta}{\delta h(t)}\left[\exp\left(\frac{\gamma^2}{2\,\lambda\,\epsilon}\sum_i a_i^2 - \sum_i(i\,k\,a_i - a_i\,h_i(t))\right)\right].
\end{aligned}
\qquad (B.62)
$$

Integrating out a_i and b_j gives:

$$
\begin{aligned}
S_{12}(k,t) = \frac{N\,\lambda^2}{\aleph'\,\gamma^2\,\epsilon}\,\delta(k+k')\,\exp\left[\frac{\lambda\,\epsilon}{2\,\lambda^2}\,(-i\,k - h(t))^2\right]^{n-1}\Theta(t-t') \\
\frac{\delta}{\delta h_i(t)}\left(\exp\left(\frac{\lambda\,\epsilon}{2\,\gamma^2}(-i\,k - h_i(t))\right)\right)_{h=0}.
\end{aligned}
\qquad (B.63)
$$

The normalisation coefficient cancels with the constant from the integrations. After the derivation, we obtain:

$$
S_{12}(k,t) = \frac{N\,\lambda^2}{\gamma^2}\,\delta(k+k')\,\frac{k}{\lambda}\,\exp\left[-\left(\frac{k^2\,\lambda}{2\,\gamma^2}\right)\,|t-t'|\right]\Theta(t-t'). \qquad (B.64)
$$

$$
S_{12}(k,\omega) = \delta(k+k')\left[\frac{-2\,k\,\sqrt{2/\pi}\,N\,\lambda}{2\,\gamma^2\,(\frac{k^2\,\lambda}{2\,\gamma^2} - i\omega)}\right]. \qquad (B.65)
$$

The causal nature of the response functions is imposed by the relation $S_{ij}(k,\omega) = S_{ji}(k,\omega')$. That means,

$$S_{21}(k,\omega) \;=\; \delta(k+k') \left[\frac{2\,k\,\sqrt{2/\pi}\,N\,\lambda}{2\,\gamma^2\,(\frac{k^2\,\lambda}{2\,\gamma^2}+i\omega)} \right]. \tag{B.66}$$

The symmetry of the non-interacting matrix is given by the relations: $S_{11}(k,\omega) = S_{33}(k,\omega)$; $S_{34}(k,\omega) = S_{12}(k,\omega)$. The rest of the averages that vanish are due to the product of the uncorrelated terms. Therefore, it leads to an independent statistical averages which gives zero. The terms like S_{44} and S_{22} which involve the product of two hatted fields also vanish due to the "time ordered" pointed out by Jensen [63]. Completing the RPA, we found that the matrix $(\underline{\underline{S}}_0^{-1} + i\underline{\underline{F}}_{int}) = \underline{\underline{A}}(k,\omega)$ Has the following expression:

$$\underline{\underline{A}} = \begin{bmatrix} 0 & A_{12} & 0 & A_{14} \\ A_{21} & A_{22} & A_{23} & 0 \\ 0 & A_{32} & 0 & A_{34} \\ A_{41} & 0 & A_{43} & A_{44} \end{bmatrix}. \tag{B.67}$$

$$A_{12} = -\frac{2i\pi\gamma^2\omega + \pi\lambda k^2 - 8\lambda n_0 \epsilon \sin^2\left(\frac{kl}{2}\right)}{2\sqrt{2\pi}k\lambda}, \tag{B.68}$$

$$A_{21} = \frac{2i\pi\gamma^2\omega - \pi\lambda k^2 + 8\lambda n_0 \epsilon \sin^2\left(\frac{kl}{2}\right)}{2\sqrt{2\pi}k\lambda}, \tag{B.69}$$

$$A_{34} = A_{12}, \tag{B.70}$$

$$A_{43} = A_{21}, \tag{B.71}$$

$$A_{14} = \frac{2\sqrt{\frac{2}{\pi}}n_0(k\epsilon + if)\sin^2\left(\frac{kl}{2}\right)}{k^2}, \tag{B.72}$$

$$A_{32} = A_{41} = -A_{14} = -A_{23}, \tag{B.73}$$

$$A_{22} = A_{44} = -\frac{\sqrt{\frac{2}{\pi}}\,\gamma^2}{2\,\lambda}. \tag{B.74}$$

B.2.2 RPA for the periodic ring model including the drift velocity

We will present the calculation for one type of chains and extend for the two types. The density variable is $\rho(x,t) = \frac{N}{L} + \Delta\rho(x,t)$ with $\Delta\rho(x,t)$ being the fluctuation density. Its translational invariance dictates that $\int_x \hat{\rho}(x,t) =$

$\int_x \Delta\rho(x,t) = 0$, so $\langle\hat{\rho}(x,t)\rangle = \langle\Delta\rho(x,t)\rangle = 0$. The upper part of the non-interacting matrix deduced from the RPA is:

$$\underline{\underline{S}}_0 = \begin{bmatrix} \underline{\underline{S}}_0^{up} & \underline{\underline{0}} \\ \underline{\underline{0}} & \underline{\underline{S}}_0^{d} \end{bmatrix}. \tag{B.75}$$

Where $\underline{\underline{0}}$ is a 2×2 zeros matrix and $\underline{\underline{S}}_0^{up} = \underline{\underline{S}}_0^{d}$ a 2×2 matrix given by:

$$\underline{\underline{S}}_0^{up} = \begin{bmatrix} \langle\Delta\rho(x,t)\Delta\rho(x',t')\rangle & \langle\Delta\rho(x,t)\,\hat{\rho}(x',t')\rangle \\ \langle\hat{\rho}(x,t)\Delta\rho(x',t')\rangle & \langle\hat{\rho}(x,t)\hat{\rho}(x',t')\rangle \end{bmatrix}. \tag{B.76}$$

where $\langle\hat{\rho}(x,t)\hat{\rho}(x',t')\rangle = 0$ according to Jensen's (1981) convention for the Jacobian [4]. The Langevin equation including the drift velocity is

$$0 = -\gamma(\dot{x}(t) - v_0) + F_{int}^{\text{tot}}(x,x') + f(t). \tag{B.77}$$

- $S_{11}^{R,v_0}(x,t) = \langle\Delta\rho(x,t)\Delta\rho(x',t')\rangle$:

$$\begin{aligned}
\langle\Delta\rho(x,t)\Delta\rho(x',t')\rangle &= \langle(\rho(x,t)-\rho_0)\rangle\langle(\rho(x',t')-\rho_0)\rangle, \\
&= \langle\sum_{j=1}^{N}(\delta(x-x_j(t))-\rho_0\rangle\langle\sum_{j'=1}^{N}(\delta(x'-x_{j'}(t))-\rho_0\rangle, \\
&= \sum_{j\neq j'}^{N}\langle\delta(x-x_j(t)\rangle\langle\delta(x'-x_{j'}(t))\rangle - \rho_0^2 \\
&+ \sum_{j=j'}^{N}\langle\delta(x-x_j(t)\delta(x'-x_j(t))\rangle, \qquad \text{(B.78)} \\
&= \frac{N(n-1)}{L^2} - \rho_0^2 + \sum_{j=1}^{N}\langle\delta(x-x_j(t))\delta(x'-x_j(t))\rangle, \\
\langle\delta(x-x_j(t))\delta(x'-x_j(t))\rangle &= \frac{1}{L^2}\sum_{k,k'}\langle e^{ikx-ikx(t)+ik'x'-ik'x(t')}\rangle, \\
&= \frac{1}{L^2}\sum_{k,k'} e^{ikx+ik'x'}\langle e^{-ikx(t)-ik'x(t')}\rangle, \qquad \text{(B.79)}
\end{aligned}$$

The term $e^{ikx+ik'x'}$ is like an initial position and $e^{-ikx(t)-ik'x(t')}$ the relative motion from the initial position. There is no preferential initial position that means, the integration over the initial position given the Kronecker delta $\delta(k+k')$ with $k' = -k$

$$\langle\delta(x-x_j(t))\delta(x'-x_j(t))\rangle = \frac{1}{L^2}\sum_{k} e^{ik(x-x')}\langle e^{ik(x'(t)-x(t))}\rangle. \tag{B.80}$$

$\langle e^{ik(x'(t)-x(t))}\rangle$ represents the average of the random walk starting at $x(t)$ and ending at $x'(t)$ with steps gives by the Gaussian noise distribution. It this therefore computed as:

$$\begin{aligned}\langle e^{ik(x'(t)-x(t))}\rangle_f &= e^{ik(x'(t)-x(t))}\langle \int [\mathrm{d}x][\mathrm{d}\hat{x}] e^{i\int_t \hat{x}(t)[-\gamma(\dot{x}(t)-v_0)]}\rangle_f, \\ &= \int_{\mathbb{R}} [\mathrm{d}x] e^{-ik(x(t')-x(t))-\frac{\gamma^2}{2\lambda}\int_t(\dot{x}(t)-v_0)^2}\end{aligned}$$

We discretise using the expression $x(t') - x(t) = \sum_{j=t}^{t'-\epsilon} b_j$ and have:

$$\langle e^{ik(x'(t)-x(t))}\rangle_f = \int_{\mathbb{R}} \prod_{\mathrm{j}}^{n} \mathrm{d}b_{\mathrm{j}} e^{\frac{-\epsilon\gamma^2}{2\lambda}\sum_{j=1}^{n}(\frac{b_{\mathrm{j}}}{\epsilon}-v_0)^2 - ik\sum_{j=t}^{t'-\epsilon} b_{\mathrm{j}}}. \tag{B.81}$$

We introduce a new variable $b'_{\mathrm{j}} = b_{\mathrm{j}} - \epsilon v_0$ and have:

$$\begin{aligned}\langle e^{ik(x'(t)-x(t))}\rangle_f &= \lim_{\epsilon\to 0}\int_{\mathbb{R}} \prod_{\mathrm{j}}^{n} \mathrm{d}b'_{\mathrm{j}} e^{\frac{-\epsilon\gamma^2}{2\lambda}\sum_{j=1}^{n}(\frac{b'_{\mathrm{j}}}{\epsilon})^2 - ik\sum_{\mathrm{j}}(b'_{\mathrm{j}}+\epsilon v_0)}, \\ &= \exp\left[\frac{k^2\lambda}{2\gamma^2}|t-t'| - ikv_0(t-t')\right]\end{aligned}$$

We Fourier transform and have:

$$\frac{2\sqrt{\frac{2}{\pi}}\gamma^2 k^2\lambda}{4\gamma^4\omega^2 + \lambda^2 k^4 + 4\gamma^4 k^2 v_0^2 - 8\gamma^4 k\, v_0\omega} \tag{B.82}$$

Consequently, we have for the wave vector $k \neq 0$:

$$S_{11}^{R,v_0}(x,t) = \frac{N}{2\pi L^2}\sqrt{\frac{2}{\pi}}\int_\omega \sum_{k\neq 0} \frac{2\,\lambda\,\gamma\,k^2 e^{i\omega(x-x')}e^{ik(t-t')}}{4\gamma^4(\omega - k\,v_0)^2 + \lambda^2\,k^4}. \tag{B.83}$$

In Fourier mode, we have for $k \neq 0$:

$$S_{11}^{R,v_0}(k,\omega) = \frac{2\sqrt{\frac{2}{\pi}}\gamma^3 k^2 N}{\pi\lambda^2 L^2\left(k^4 + \frac{4\gamma^4(\omega-kv_0)^2}{\lambda^2}\right)}. \tag{B.84}$$

- $S_{12}^{R,v_0}(x,t) = \langle \Delta\rho(x,t)\hat{\rho}(x',t')\rangle$:

$$\begin{aligned}
\langle \Delta\rho(x,t)\hat{\rho}(x',t')\rangle &= \langle \Delta\rho(x,t)\rangle\langle\hat{\rho}(x',t')\rangle, \\
&= \langle \sum_{j=1}^{N} \delta(x - x_{\mathrm{j}(t)}) - \rho_0 \rangle \langle \sum_{j'=1}^{N} \hat{x}_{\mathrm{j'}}(t')\, \delta(x' - x_{\mathrm{j'}(t')})\rangle, \\
&= \sum_{j\neq j'} \langle \delta(x - x_{\mathrm{j}(t)})\rangle \, \langle \hat{x}_{\mathrm{j'}}(t')\, \delta(x' - x_{\mathrm{j'}}(t'))\rangle - \rho_0 \\
&+ \sum_{j=j'} \langle \delta(x - x_{\mathrm{j}(t)})\, \hat{x}_{\mathrm{j}}(t')\, \delta(x' - x_{\mathrm{j}}(t'))\rangle, \\
&= \underbrace{\langle \rho(x,t)\, \hat{\rho}(x',t')\rangle}_{=0} - \rho_{k=0} + \frac{N}{L^2} \langle \delta(x - x_{\mathrm{j}}(t)) \hat{x}_{\mathrm{j}}(t) \delta(x' - x_{\mathrm{j}}(t'))\rangle
\end{aligned}$$

We note that have add the constraint of the causality ($\langle \hat{x}(t)\, x(t')...\rangle = 0$ if $t > t'$). For $k \neq 0$, we have:

$$\begin{aligned}
\langle \Delta\rho(x,t)\hat{\rho}(x',t')\rangle &= \frac{N}{L^2} \langle \delta(x - x_{\mathrm{j}}(t)) \hat{x}_{\mathrm{j}}(t) \delta(x' - x_{\mathrm{j}}(t'))\rangle, \\
&= \Theta(t' - t)\, \frac{N}{2\pi L^2} \sum_{k,k'\neq 0} e^{ikx + ik'x'} \langle \hat{x}(t') e^{-ikx(t) - ik'x(t')}\rangle, \\
&= \frac{N}{2\pi L^2} \begin{cases} 0 \quad \text{if} \quad t' \geqslant t, \\ \sum\limits_{k,k'\neq 0} e^{ikx + ik'x'} \langle \hat{x}(t') e^{-ikx(t) - ik'x(t')}\rangle \, \text{if}\, t' < t. \end{cases}
\end{aligned} \tag{B.85}$$

The average $\langle \hat{x}(t') e^{-ikx(t) - ik'x(t')}\rangle$ is computed using the generating functional approach. The generating function is given by the expression:

$$\begin{aligned}
Z[\hat{h}(t)] &= \left\langle \int_{\mathbb{R}} [\mathrm{d}\hat{x}][\mathrm{d}x]\, e^{i\int_t \hat{x}(t)[-\gamma(\dot{x}(t) - v_0) + f(t)] + i\int_t \hat{h}(t)\hat{x}(t)} \right\rangle_f \\
&= \aleph \int_{\mathbb{R}} [\mathrm{d}\hat{x}][\mathrm{d}x]\, e^{i\int_t \hat{x}(t)\left[-\gamma(\dot{x}(t) - v_0) + \hat{h}(t)\right] - \frac{\lambda}{2}\int_t \hat{x}^2(t)} \\
&= \aleph' \int_{\mathbb{R}} [\mathrm{d}x]\, e^{\frac{1}{2\lambda}\int_t \left[-\gamma(\dot{x}(t) - v_0) + \hat{h}(t)\right]^2}
\end{aligned} \tag{B.86}$$

We calculate the average $\langle \hat{x}(t') e^{-ikx(t) - ik'x(t')}\rangle$ by differentiate the gener-

ating functional with respect to the hat source field $\hat{h}$.

$$\begin{aligned}
\langle \hat{x}(t') e^{-ikx(t)-ik'x(t')} \rangle &= \frac{\aleph'}{i} \left[\frac{\delta}{\delta \hat{h}} \int_{\mathbb{R}} [\mathrm{d}x]\, e^{\frac{1}{2\lambda}\int_t \left[-\gamma(\dot{x}(t)-v_0)+\hat{h}(t)\right]^2} \right. \\
&\left. -ik(x(t')-x(t)) \right]_{\hat{h}=0} \Theta(t'-t) \\
&= \lim_{\epsilon\to 0} \frac{\aleph'}{i\lambda} \int_{\mathbb{R}} \prod_{j=1}^{n} [\mathrm{d}b_{\mathrm{j}}] \sum_j (\frac{-i\gamma}{\lambda})\, (\frac{b_{\mathrm{j}}}{\epsilon} - v_0)\, \Theta(t'-t) \\
&\quad e^{\frac{-\epsilon\gamma^2}{2\lambda} \sum\limits_{j=1}^{n} (\frac{b_{\mathrm{j}}}{\epsilon}-v_0)^2 - ik \sum\limits_{j=t}^{t'-\epsilon} b_{\mathrm{j}}}, \\
&= \lim_{\epsilon\to 0} \int_{\mathbb{R}} \prod_{\mathrm{j}}^{n} \mathrm{d}b'_{\mathrm{j}} \sum_j (\frac{-i\gamma}{\lambda})\, \frac{b'_{\mathrm{j}}}{\epsilon}\, \Theta(t'-t) \\
&\quad e^{\frac{-\epsilon\gamma^2}{2\lambda} \sum\limits_{j=1}^{n} (\frac{b'_{\mathrm{j}}}{\epsilon})^2 - ik \sum_{\mathrm{j}} (b'_{\mathrm{j}} + \epsilon v_0)}, \\
&= \lim_{\epsilon\to 0} (\frac{-k}{\gamma})\, \Theta(t'-t) \exp\left[\frac{k^2\lambda}{2\gamma^2}\, \epsilon\, |t-t'| - \epsilon\, i\, k\, v_0 (t-t') \right], \\
&= (\frac{-k}{\gamma})\, \Theta(t'-t) \exp\left[\frac{k^2\lambda}{2\gamma^2}\, |t-t'| - i\, k\, v_0 (t-t') \right].
\end{aligned} \tag{B.87}$$

The Fourier transform gives:

$$-\frac{\sqrt{\frac{2}{\pi}}\gamma k}{\lambda k^2 - 2i\gamma^2 (k\, v_0 - \omega)} \tag{B.88}$$

Consequently, we have for $k \neq 0$:

$$S_{12}^{R,v_0}(x,t) = \frac{N}{2\pi L^2} \int_\omega \sum_{k\neq 0} \frac{-\sqrt{\frac{2}{\pi}}\gamma k\, e^{i\omega(x-x')} e^{ik(t-t')}}{\lambda k^2 - 2i\gamma^2 (k\, v_0 - \omega)}, \tag{B.89}$$

In Fourier mode, we have:

$$S_{12}^{R,v_0}(k,\omega) = \frac{-\sqrt{\frac{2}{\pi}}\, \gamma\, k\, N}{2\, \pi\, \lambda\, L^2 \left(k^2 + \frac{2\, i\, \gamma^2 (\omega - k\, v_0)}{\lambda} \right)}. \tag{B.90}$$

In the similar way, we find

$$S_{21}^{R,v_0}(k,\omega) = \frac{\sqrt{\frac{2}{\pi}}\gamma k N}{2\pi\lambda L^2 \left(k^2 - \frac{2i\gamma^2(\omega - k v_0)}{\lambda} \right)}. \tag{B.91}$$

The other elements of the matrix are: $S_{33}^{R,v_0}(k,\omega) = S_{11}^{R,v_0}(k,\omega)$; $S_{34}^{R,v_0}(k,\omega) = S_{12}^{R,v_0}(k,\omega)$ and $S_{43}^{R,v_0}(k,\omega) = S_{21}^{R,v_0}(k,\omega)$.

The correlation matrix for the periodic ring is $G^R = B^{-1} = (i\underline{\underline{F}}_{int}^R + (\underline{\underline{S}}_0^R)^{-1})^{-1}$

The correlation function $G^R(k,\omega) = B^{-1}$ is given by:

$$\left[i \begin{pmatrix} 0 & F^{R,k}_{\text{net}} & 0 & F^{R,k}_{\text{net}} - F^{R,k}_{\text{act}} \\ F^{R,k}_{\text{net}} & 0 & F^{R,k}_{\text{net}} - F^{R,k}_{\text{act}} & 0 \\ 0 & F^{R,k}_{\text{net}} + F^{R,k}_{\text{act}} & 0 & F^{R,k}_{\text{net}} \\ F^{R,k}_{\text{net}} + F^{R,k}_{\text{act}} & 0 & F^{R,k}_{\text{net}} & 0 \end{pmatrix} + \begin{pmatrix} S^{R,v_0}_{11}(k,\omega) & S^{R,v_0}_{12}(k,\omega) & 0 & 0 \\ S^{R,v_0}_{21}(k,\omega) & 0 & 0 & 0 \\ 0 & 0 & S^{R,v_0}_{33}(k,\omega) & S^{R,v_0}_{34}(k,\omega) \\ 0 & 0 & S^{R,v_0}_{43}(k,\omega) & 0 \end{pmatrix}^{-1} \right]^{-1} \tag{B.92}$$

and the Matrix B is:

$$\begin{pmatrix} 0 & \frac{2\left(2\epsilon\eta^2 n_0 - \frac{L^3\pi\lambda\left(k^2 + \frac{2i\gamma^2(\omega - kv_0)}{\lambda}\right)}{N\gamma}\right)}{kL} & 0 & \frac{4(k\epsilon - if)\eta^2 n_0}{k^2} \\ \frac{2\pi\left(k^2\lambda - 2i\gamma^2(\omega - kv_0)\right)L^3 + 4N\gamma\epsilon\eta^2 n_0}{kLN\gamma} & \frac{8L\sqrt{2\pi}}{N} & \frac{4(k\epsilon - if)\eta^2 n_0}{k^2} & 0 \\ 0 & \frac{4(if + k\epsilon)\eta^2 n_0}{k^2} & 0 & \frac{2\left(2\epsilon\eta^2 n_0 - \frac{L^3\pi\lambda\left(k^2 + \frac{2i\gamma^2(\omega - kv_0)}{\lambda}\right)}{N\gamma}\right)}{kL} \\ \frac{4(if + k\epsilon)\eta^2 n_0}{k^2} & 0 & \frac{2\pi\left(k^2\lambda - 2i\gamma^2(\omega - kv_0)\right)L^3 + 4N\gamma\epsilon\eta^2 n_0}{kLN\gamma} & \frac{8L\sqrt{2\pi}}{N} \end{pmatrix}. \tag{B.93}$$

With $\eta = \sin[\frac{kl}{2}]$ and

B.3 Effective chain dynamics calculation

We suppose that we have a system that contains two type of chains with fixed number. N^+ and N^- are respectively the number of chains pointing to the right and to the left. We suppose for the present approximation that we randomly label one chain. The same notations as from the RPA calculation are conserved. We randomly choose to labelled one chain pointing to the + oriented chain. The Langevin equations of the system are given by:
For the labelled chain:

$$L_\ell^+ : 0 = -\gamma \dot{x}^+(t) + f^+(t) + \sum_{\alpha=1}^{N^+-1} F_{int}^R(x_\ell^+ - x_\alpha^+) + \sum_{\beta=1}^{N^-} F_{int}^R(x_\ell^+ - x_\beta^-). \quad \text{(B.94)}$$

For the (+) other chains:

$$\begin{aligned} L^+ : 0 = \sum_{\alpha=1}^{N^+-1} \Bigg[& -\gamma \dot{x}_\alpha^+(t) + f_\alpha^+(t) + \sum_{\alpha' \neq \alpha}^{N^+-1} F_{int}^R(x_\alpha^+ - x_{\alpha'}^+) \\ & + \sum_{\beta=1}^{N^-} F_{int}^R(x_\alpha^+ - x_\beta^-) + F_{int}^R(x_\alpha^+ - x_\ell^+) \Bigg]. \end{aligned} \quad \text{(B.95)}$$

For the other (-) chains:

$$\begin{aligned} L^- : 0 = \sum_{\beta=1}^{N^-} \Bigg[& -\gamma \dot{x}_\beta^-(t) + f_\beta^-(t) + \sum_{\beta' \neq \beta}^{N^-} F_{int}^R(x_\beta^- - x_{\beta'}^-) \\ & + \sum_{\alpha=1}^{N^+} F_{int}^R(x_\beta^- - x_\alpha^+) + F_{int}^R(x_\beta^- - x_\ell^+) \Bigg]. \end{aligned} \quad \text{(B.96)}$$

We perform the MSR formalism by casting the Langevin equations (B.94, B.95 and B.96) inside the generating functional:

$$\begin{aligned} Z = \frac{1}{\aleph} \int_{\mathbb{R}} & \left(\prod_{\alpha=1}^{N^+-1} [dx_\alpha^+][d\hat{x}_\alpha^+] \right) \left(\prod_{\beta=1}^{N^-} [dx_\beta^-][d\hat{x}_\beta^-] \right) [dx_\ell^+][d\hat{x}_\ell^+] \\ & \exp\left[i \int_t \hat{x}_\ell^+ L_\ell^+ + i \int_t \hat{x}_\alpha^+ L^+ + i \int_t \hat{x}_\beta^- L^- \right] \underbrace{J_{x_\ell^+} J_{x_\alpha^+} J_{x_\beta^-}}_{1}. \end{aligned} \quad \text{(B.97)}$$

After having perform the integration over the noises f_ℓ^+, f^+, f^- we have:

$$
\begin{aligned}
Z = \frac{1}{\aleph}\int_{\mathbb{R}} &\left(\prod_{\alpha=1}^{N^+-1}[dx_\alpha^+][d\hat{x}_\alpha^+]\right)\left(\prod_{\beta=1}^{N^-}[dx_\beta^-][d\hat{x}_\beta^-]\right)[dx_\ell^+][d\hat{x}_\ell^+] \\
&\exp\left[-\frac{\lambda}{2}\int_t(\hat{x}_\ell^+)^2 - i\gamma\int_t \hat{x}_L^+\dot{x}_\ell^+ + i\int_t \hat{x}_\ell^+\sum_{\alpha}^{N^+-1}F_{int}^R(x_\ell^+ - x_\alpha^+) + i\int_t \hat{x}_\ell^+\sum_{\beta=1}^{N^-}F_{int}^R(x_\ell^+ - x_\beta^-)\right] \\
&\exp\left[-\frac{\lambda}{2}\sum_{\alpha=1}^{N^+-1}\int_t(\hat{x}_\alpha^+)^2 - i\gamma\sum_{\alpha=1}^{N^+-1}\int_t \hat{x}_\alpha^+\dot{x}_\alpha^+ + i\sum_{\alpha\neq\alpha'}\int_t \hat{x}_\alpha^+F_{int}^R(x_\alpha^+ - x_{\alpha'}^+)\right. \\
&\left.+i\sum_{\alpha=1}^{N^+-1}\int_t \hat{x}_\alpha^+F_{int}^R(x_\alpha^+ - x_\ell^+) + i\sum_{\alpha,\beta}\hat{x}_\alpha^+F_{int}^R(x_\alpha^+ - x_\beta^-)\right] \\
&\exp\left[-\frac{\lambda}{2}\sum_{\beta=1}^{N^-}\int_t(\hat{x}_\beta^-)^2 - i\gamma\sum_{\beta=1}^{N^-}\int_t \hat{x}_\beta^-\dot{x}_\beta^- + i\sum_{\beta\neq\beta'}\int_t \hat{x}_\beta^-F_{int}^R(x_\beta^- - x_{\beta'}^-)\right. \\
&\left.+i\sum_{\beta=1}^{N^-}\int_t \hat{x}_\beta^-F_{int}^R(x_\beta^- - x_\ell^+) + i\sum_{\alpha,\beta}\hat{x}_\beta^-F_{int}^R(x_\beta^- - x_\alpha^+)\right] \\
&= \frac{1}{\aleph}\int_{\mathbb{R}}\left(\prod_{\alpha=1}^{N^+-1}[dx_\alpha^+][d\hat{x}_\alpha^+]\right)\left(\prod_{\beta=1}^{N^-}[dx_\beta^-][d\hat{x}_\beta^-]\right)[dx_\ell^+][d\hat{x}_\ell^+]e^{\mathcal{L}'}.
\end{aligned}
\tag{B.98}
$$

with $\mathcal{L}' = \mathcal{L}'_{int} + \mathcal{L}'_0 + \mathcal{L}'_\ell$ and

$$
\begin{aligned}
\mathcal{L}'_\ell = &-\frac{\lambda}{2}\int_t(\hat{x}_L^+)^2 - i\gamma\int_t \hat{x}_\ell^+\dot{x}_\ell^+ + i\int_t \hat{x}_\ell^+\sum_{\alpha}^{N^+-1}F_{int}^R(x_\ell^+ - x_\alpha^+) \\
&+ i\int_t \hat{x}_\ell^+\sum_{\beta=1}^{N^-}F_{int}^R(x_\ell^+ - x_\beta^-),
\end{aligned}
\tag{B.99}
$$

$$
\begin{aligned}
\mathcal{L}'_{int} = &\, i\sum_{\alpha\neq\alpha'}\int_t \hat{x}_\alpha^+F_{int}^R(x_\alpha^+ - x_{\alpha'}^+) + i\sum_{\alpha=1}^{N^+-1}\int_t \hat{x}_\alpha^+F_{int}^R(x_\alpha^+ - x_\ell^+) \\
&+ i\sum_{\alpha,\beta}\hat{x}_\alpha^+F_{int}^R(x_\alpha^+ - x_\beta^-) + i\sum_{\beta\neq\beta'}\int_t \hat{x}_\beta^-F_{int}^R(x_\beta^- - x_{\beta'}^-) \\
&+ i\sum_{\beta=1}^{N^-}\int_t \hat{x}_\beta^-F_{int}^R(x_\beta^- - x_\ell^+) + i\sum_{\alpha,\beta}\hat{x}_\beta^-F_{int}^R(x_\beta^- - x_\alpha^+),
\end{aligned}
\tag{B.100}
$$

$$\begin{aligned}\mathcal{L}'_0 = &-\frac{\lambda}{2}\sum_{\alpha=1}^{N^+-1}\int_t(\hat{x}_\alpha^+)^2 - i\gamma\sum_{\alpha=1}^{N^+-1}\int_t \hat{x}_\alpha^+\dot{x}_\alpha^+ \\ &-\frac{\lambda}{2}\sum_{\beta=1}^{N^-}\int_t(\hat{x}_\beta^-)^2 - i\gamma\sum_{\beta=1}^{N^-}\int_t \hat{x}_\beta^-\dot{x}_\beta^-.\end{aligned} \tag{B.101}$$

We introduce the collective variables:

$$\rho^+(x^+) = \sum_\alpha^{N^+-1}\delta(x^+ - x_\alpha^+(t)) \quad ; \quad \rho^-(x^-) = \sum_\beta^{N^-}\delta(x^- - x_\beta^-(t)). \tag{B.102}$$

and their complex conjugate:

$$\varphi^+(x^+) = \sum_\alpha^{N^+-1}\hat{x}_\alpha^+\delta(x^+ - x_\alpha^+(t)) \quad ; \quad \varphi^-(x^-) = \sum_\beta^{N^-}\hat{x}_\beta^-\delta(x^- - x_\beta^-(t)) \tag{B.103}$$

The actual density should be slip in its mean density $\frac{N}{L}$ (N is the total number of chains in the system and L the total length of the ring) and the density fluctuation. Using the mean field approximation, we split the density variable in its mean value and the density fluctuation. We can write: $\underline{\rho}(x,t) = \underline{\rho}_0 + \underline{\Delta\rho}(x,t)$ In Fourier space, we have: $\underline{\rho}(k,\omega) = \underline{\rho}_0 + \underline{\Delta\rho}(k,\omega)$. For the auxiliary fields, we assume that the density is equal to the fluctuation. For each density variable, we have:

$$\begin{aligned}\Delta\rho^+(k,t) &= \rho^+(k,t) - \rho_0^+, \\ \Delta\rho^-(k,t) &= \rho^-(k,t) - \rho_0^-, \\ \Delta\varphi^+(k,t) &= \varphi^+(k,t), \\ \Delta\varphi^-(k,t) &= \varphi^-(k,t),\end{aligned} \tag{B.104}$$

We define the following unity expression in term of the densities fluctuation:

$$\begin{aligned}1 = &\int_{\mathbb{R}}[\mathrm{d}\,\Delta\rho^+]\,[\mathrm{d}\,\Delta\rho^-]\,[\mathrm{d}\,\Delta\varphi^+]\,[\mathrm{d}\,\Delta\varphi^-] \\ &\int_{\mathbb{R}}[\mathrm{d}\,\widehat{\Delta}\rho^+]\,[\mathrm{d}\,\widehat{\Delta}\rho^-]\,[\mathrm{d}\,\widehat{\Delta}\varphi^+]\,[\mathrm{d}\,\widehat{\Delta}\varphi^-] \\ &\exp\Bigg[\mathrm{i}\int_{k,t}\widehat{\Delta}\rho^+\,\left(\Delta\rho^+ - \rho^+ + \rho_0^+\right) \\ &+\mathrm{i}\int_{k,t}\widehat{\Delta}\rho^-\,\left(\Delta\rho^- - \rho^- + \rho_0^-\right) \\ &+\mathrm{i}\int_{k,t}\widehat{\Delta}\varphi^+\,\left(\Delta\varphi^+ - \varphi^+\right) \\ &+\mathrm{i}\int_{k,t}\widehat{\Delta}\varphi^-\,\left(\Delta\varphi^- - \varphi^-\right)\Bigg].\end{aligned} \tag{B.105}$$

We perform a change of variables by introducing this identity expression in the generating functional equation (B.98). The Jacobian from the transformation is one. We have the following expression:

$$\begin{aligned} Z = \frac{1}{\aleph} \int_{\mathbb{R}} [\mathrm{d}x_\ell^+][\mathrm{d}\hat{x}_\ell^+] \, [\mathrm{d}\,\Delta\rho^+] \, [\mathrm{d}\,\Delta\rho^-] \, [\mathrm{d}\,\Delta\varphi^+] \, [\mathrm{d}\,\Delta\varphi^-] \\ \int_{\mathbb{R}} [\mathrm{d}\,\widehat{\Delta}\rho^+] \, [\mathrm{d}\,\widehat{\Delta}\rho^-] \, [\mathrm{d}\,\widehat{\Delta}\varphi^+] \, [\mathrm{d}\,\widehat{\Delta}\varphi^-] \\ \exp\left[\mathcal{L}'_\ell + \mathcal{L}'_0 + \mathcal{L}'_{int} + \mathcal{L}''_q + \mathcal{L}''_3\right]. \end{aligned} \tag{B.106}$$

With,

$$\mathcal{L}''_q = i \int_{k,t} \left(\widehat{\Delta}\rho^- \, \Delta\rho^- + \widehat{\Delta}\rho^- \, \Delta\rho^- + \widehat{\Delta}\varphi^- \, \Delta\varphi^- + \widehat{\Delta}\varphi^+ \, \Delta\varphi^+ \right). \tag{B.107}$$

$$\begin{aligned} \mathcal{L}''_3 = i \int_t \Delta\rho^+ \sum_\alpha^{N^+-1} \delta(x^+ - x_\alpha^+(t)) + i \int_t \Delta\rho^- \sum_\beta^{N^-} \delta(x^- - x_\beta^-(t)) \\ + \ \mathrm{i} \int_t \Delta\varphi^+ \sum_\alpha^{N^+-1} \hat{x}_\alpha^+ \, \delta(x^+ - x_\alpha^+(t)) + i \int_t \Delta\varphi^- \sum_\beta^{N^-} \hat{x}_\beta^- \, \delta(x^- - x_\beta^-(t)). \end{aligned} \tag{B.108}$$

We use the approximation : $\exp\left(\mathcal{L}''_3 + \mathcal{L}'_0\right) \simeq \exp\left[\frac{1}{2}\langle \mathcal{L}''^2_3 \rangle_0\right]$. We define two super-vectors:

$$\underline{\Delta\rho}((k,\omega)) = \left(\Delta\rho^-(k,\omega), \, \Delta\varphi^-(k,\omega), \, \Delta\rho^-(k,\omega), \, \Delta\varphi^+(k,\omega)\right), \tag{B.109}$$

and

$$\underline{\widehat{\Delta}\rho}(k,\omega) = \left(\widehat{\Delta}\rho^-(k,\omega), \widehat{\Delta}\varphi^-(k,\omega), \widehat{\Delta}\rho^+(k,\omega), \widehat{\Delta}\varphi^+(k,\omega)\right). \tag{B.110}$$

We therefore have:

$$\exp\left(\mathcal{L}''_3 + \mathcal{L}'_0\right) = \exp\left(-\frac{1}{2} \int_{\omega,\omega'} \int_{k,k'} \underline{\widehat{\Delta}\rho} \; \underline{\underline{S}}_0^R \; \underline{\widehat{\Delta}\rho}^T\right), \tag{B.111}$$

and

$$\begin{aligned} \exp\left(\mathcal{L}_{int} + \mathcal{L}_q\right) \simeq \exp\Bigg(-\frac{i}{2} \int_{\omega,\omega'} \int_{k,k'} \underline{\Delta\rho} \; \underline{\underline{F}}_{int}^R \; \underline{\Delta\rho}^T \\ + i \iint_{t,x^+} \Delta\varphi^+ F_{int}^R(x^+ - x_\ell^+) + i \iint_{t,x^-} \Delta\varphi^- \, F_{int}^R(x^- - x_\ell^+) \Bigg). \end{aligned} \tag{B.112}$$

After having perform the RPA over all the non labelled chains, we have:

$$
\begin{aligned}
Z = & \frac{1}{\aleph}\int_{\mathbb{R}}[dx_\ell^+][\mathrm{d}\hat{x}_\ell^+][\mathrm{d}\underline{\Delta\rho}][\mathrm{d}\underline{\widehat{\Delta}\rho}] \\
& \exp\left[-\frac{\lambda}{2}\int_t(\hat{x}_\ell^+)^2 - i\gamma\int_t \hat{x}_\ell^+\dot{x}_\ell^+ + i\int_t \hat{x}_\ell^+\sum_{\alpha}^{N^+-1}F_{int}^R(x_\ell^+ - x_\alpha^+) + i\int_t \hat{x}_\ell^+\sum_{\beta=1}^{N^-}F_{int}^R(x_\ell^+ - x_\beta^-)\right] \\
& \exp\left(-\frac{i}{2}\int_{\omega,\omega'}\int_{k,k'}\underline{\Delta\rho}\,\underline{\underline{F}}_{int}^R\,\underline{\Delta\rho}^T + i\iint_{t,x^+}\Delta\varphi^+F_{int}^R(x^+ - x_\ell^+) + i\iint_{t,x^-}\Delta\varphi^-\,F_{int}^R(x^- - x_\ell^+)\right. \\
& \left.-\frac{1}{2}\int_{\omega,\omega'}\int_{k,k'}\underline{\widehat{\Delta}\rho}\,\underline{\underline{S}}_0^R\,\underline{\widehat{\Delta}\rho}^T\right) \\
= & \frac{1}{\aleph}\int_{\mathbb{R}}[\mathrm{d}x_\ell^+][\mathrm{d}\hat{x}_\ell^+][\mathrm{d}\underline{\Delta\rho}]\underbrace{\exp\left(-\frac{1}{2}\int_\omega\int_k\underline{\Delta\rho}(k,\omega)\left(i\underline{\underline{F}}_{int}^R + (\underline{\underline{S}}_0^R)^{-1}\right)\underline{\Delta\rho}^T(k',\omega')\right)}_{\text{RPA}} \\
& \exp\left[-\frac{\lambda}{2}\int_t(\hat{x}_\ell^+)^2 - i\gamma\int_t\hat{x}_\ell^+\dot{x}_\ell^+\right] \\
& \exp\left[i\int_t\hat{x}_v^+\sum_{\alpha}^{N^+-1}F_{int}^R(x_\ell^+ - x_\alpha^+) + i\int_t\hat{x}_\ell^+\sum_{\beta=1}^{N^-}F_{int}^R(x_\ell^+ - x_\beta^-)\right. \\
& \left.+i\iint_{t,x^+}\Delta\varphi^+F_{int}^R(x^+ - x_\ell^+) + i\iint_{t,x^-}\Delta\varphi^-\,F_{int}^R(x^- - x_\ell^+)\right] \qquad \text{(B.113)} \\
= & \frac{1}{\aleph}\int_{\mathbb{R}}[\mathrm{d}x_\ell^+][\mathrm{d}\hat{x}_\ell^+][\mathrm{d}\underline{\Delta\rho}]\underbrace{\exp\left(-\frac{1}{2}\int_\omega\int_k\underline{\Delta\rho}(k,\omega)\,\left(i\underline{\underline{F}}_{int}^R + (\underline{\underline{S}}_0^R)^{-1}\right)\underline{\Delta\rho}^T(k',\omega')\right)}_{\text{RPA}} \\
& \exp\left[-\frac{\lambda}{2}\int_t(\hat{x}_\ell^+)^2 - i\gamma\int_t\hat{x}_\ell^+\dot{x}_\ell^+\right] \\
& \exp\left[i\int_t\int_{x^+}\hat{x}_\ell^+\Delta\rho^+F_{int}^R(x_\ell^+ - x^+) + i\int_t\int_{x^-}\hat{x}_\ell^+\Delta\rho^-F_{int}^R(x_\ell^+ - x^-)\right. \\
& \left.+i\iint_{t,x^+}\Delta\varphi^+F_{int}^R(x^+ - x_\ell^+) + i\iint_{t,x^-}\Delta\varphi^-\,F_{int}^R(x^- - x_\ell^+)\right] \\
= & \frac{1}{\aleph}\int_{\mathbb{R}}[\mathrm{d}\,x_\ell^+]\,[\mathrm{d}\,\hat{x}_\ell^+]\,[\mathrm{d}\,\underline{\Delta\rho}]\,\exp\left[-\frac{\lambda}{2}\int_t(\hat{x}_\ell^+)^2 - \,\mathrm{i}\,\gamma\int_t\hat{x}_\ell^+\,\dot{x}_\ell^+\right] \\
& \exp\left[i\iint_{k,\omega}\underline{f}(k)\,\underline{\Delta\rho}(k,\omega) + i\int_t\underline{f}(x_\ell^+)\,\underline{\rho}_0\right] \\
& \underbrace{\exp\left(-\frac{1}{2}\iint_{k,\omega}\underline{\Delta\rho}(k,\omega)\,\left(i\underline{\underline{F}}_{int}^R + (\underline{\underline{S}}_0^R)^{-1}\right)\underline{\Delta\rho}^T(k',\omega')\right)}_{\text{RPA}}.
\end{aligned}
$$

With

$$\underline{f}(x_\ell^+) = \left(\hat{x}_\ell^+ F_{int}^R(x_\ell^+ - x^-), F_{int}^R(x^- - x_\ell^+), \hat{x}_\ell^+ F_{int}^R(x_\ell^+ - x^+), F_{int}^R(x^+ - x_\ell^+)\right) \tag{B.114}$$

and the symmetry relation: $F_{int}^R(x^- - x_\ell^+) = -F_{int}^R(x_\ell^+ - x^-)$ holds.
The generating functional is therefore given by the expression:

$$\begin{aligned} Z = \frac{1}{\aleph'} \int_{\mathbb{R}} [\mathrm{d}\, x_\ell^+]\, [\mathrm{d}\, \hat{x}_\ell^+] \exp\left[-\frac{\lambda}{2} \int_t (\hat{x}_\ell^+)^2(t) \; - i\gamma \int_t \hat{x}_\ell^+ \, \dot{x}_\ell^+\right] \\ \exp\left(-\frac{\lambda}{2} \iint_{k,t} (\hat{x}_\ell^+)^2 \, a(k) \; - i\gamma \iint_{k,t} \hat{x}_\ell^+(t)\, b(k)\right. \\ \left. -i\gamma \int_t \hat{x}_\ell^+(t) \; c(t) \; + i \int_k d(k)\right). \end{aligned} \tag{B.115}$$

Where

$$\begin{aligned} \int_k a(k) = \int_k \Big[& 8\sqrt{2\pi} \, \sin^2(kl/2) \left(-f^2 \; - \; 2k^2\,\epsilon^2 \; + (f^2 \; - \; 2\,k^2\,\epsilon^2) \, \cos(kl)\right. \\ & + 2\, f^2\, k\, \epsilon \, \sin(kl)) \, n_0^2 \, (2\,k^2\,\pi^2\,\gamma^2\omega^2 + 4 \, \sin^2(kl/2) \, (-f^2 - \; 2\,k^2\,\epsilon^2 \\ & \left. + (f^2 \; - \; 2\,k^2\,\epsilon^2) \, \cos(kl) \; + 2\, f\, k^2\, \epsilon \, \sin(kl)\, n_0^2))\right] / \Big[2\,k^2\,\pi^2\,\gamma^2\,\omega^2 \\ & - 4\,k^2\,\pi\,\gamma\,\omega \, \sin(kl) n_0 \; - \; 4 \, \sin^2(kl/2) \, (-f^2 - \; 2\,k^2\,\epsilon^2 \; + \; (f^2 \; - \; 2\,k^2\,\epsilon^2) \\ & \cos(kl) + 2\, f\, k\, \epsilon \, \sin(kl)\, n_0^2) \, (2\,k^2\,\pi^2\,\gamma^2\,\omega^2 \; + \; 4\,k^2\,\pi\,\gamma\,\epsilon\,\omega \, \sin(kl)\, n_0 \\ & - 4 \, \sin^2(kl/2) \, (-f^2 \; - 2\,k^2\,\epsilon^2 \; + (f^2 \; - 2\,k^2\,\epsilon^2 + (f^2 - 2\,k^2\,\epsilon^2) \, \cos(kl) \\ & \left. + \; 2\, f\, k\, \epsilon \, \sin(kl)\, n_0^2)\Big]. \right. \end{aligned} \tag{B.116}$$

$$\int_k b(k,\omega) \quad = \int_k \frac{4\sqrt{2} n_0^2}{k^5 \pi^{3/2} \lambda} \left[-f + f\cos(kl) + k\epsilon \sin(kl)^2\right]^2. \tag{B.117}$$

$\int_k b(k) = 0$ because the integral is odd in k.

$$\begin{aligned} c(x_\ell^+, t) &= \int_x \frac{N}{L} \left(F_{int}(x_\ell^+ - x^-) + F_{int}(x_\ell^+ - x^+)\right) \\ &= \frac{N}{L} f n_0 \left(\ell - |x_\ell^+ - x^\pm|\right) \Theta(\ell - |x_\ell^+ - x^\pm|). \end{aligned} \tag{B.118}$$

We Fourier series and take for $k = 0$, we have: $\frac{fl^2 n_0 N}{L} = fl^2 n_0 \overline{\rho}_0$

$$\begin{aligned} \int_t d(x_\ell^+, t) &= \int_x -\frac{N}{L} \left(F_{int}(x_\ell^+ - x) + F_{int}(x_\ell^+ - x)\right) \\ &= -\frac{N}{L} f n_0 (\ell - |x_\ell^+ - x^\pm|) \Theta(\ell - |x_\ell^+ - x^\pm|). \end{aligned} \tag{B.119}$$

List of References

[1] J. Howards. *Mechanics of motor protein and the cytoskeleton.* Sinauer Press, Sunderland, Massachusetts, 2001.

[2] S. F. Edwards. A field theory formulation of polymer network. *J. Phys. France*, 49:1673–1682, 1988.

[3] R. Fantoni and K. K. Müller-Nedebock. Field-theoretical approach to dense polymer with an ideal binary mixture of clustering centers. *Phys. Rev. E*, 29, 2011.

[4] P. C. Martin, E. D. Siggia and H. A. Rose. Statistical dynamics of classical systems. *Phys. Rev. A*, 8(1), 1973.

[5] G. H. Fredrickson and E. Helfand. Collective dynamics of polymer solutions. *J. Chem. Phys.*, 93(3):2048–2061, 1990.

[6] M. G. Brereton and T. A. Vilgis. Compatibility and phase behavior in charged polymer systems and ionomers. *A. Chem. Soc.*, 23(7):2044–2049, 1990.

[7] K. K. Müller-Nedebock and T. A. Vilgis. Collective dynamics of random polyampholytes. *J. Chem. Phys.*, 110(4651), 1999.

[8] K. K. Müller-Nedebock and T. A. Vilgis. Dynamics of dense polyelectrolyte solutions. *A. Chem. Soc.*, 31(17):5898–5903, 1998.

[9] L. Leibler. Theory of microphase separation in block copolymers. *A. Chem. Soc. Macro. Lett.*, 13(6):1602–1617, 1980.

[10] S. Banerjee, M. C. Marchetti and K. K. Müller-Nedebock. Motor-driven dynamics of cytoskeletal filaments in motility assays. *Phys. Rev. E*, 84(87.16):011914, 2011.

[11] M. Doi. and S. F. Edwards. *The theory of polymer dynamics.* Oxford University Press, 1986.

[12] I. Teraoka. *Polymer solution: An introduction to physical properties.* Polytechnic University, Brooklyn, New York, 2002.

[13] S. Panyokov and Y. Rabin. Statistical physics of polymer gels. *Physics Reports*, 269:1–131, 1996.

[14] T. A. Vilgis. Polymer theory: path integrals and scaling. *Physics Reports*, 336(3):167 – 254, 2000.

[15] J. R. Blundell and E. M. Terentjev. The influence of disorder on deformations in semiflexible networks. *Proc. R. Soc. A*, 467:2330–2349, 2011.

[16] M. Chaichian and A. Demichev. *Path Integrals in Physics volume I Stochastic Processes and Quantum Mechanics*, volume 1. IOP Publishing, Bristol and Philadelphia, 2001.

[17] I. M. Kovalćhik. The wiener integral. *IOP Science, Russian Mathematical Surveys*, 18(1):97, 1963.

[18] L. Klaczynski. Self-consistent field theory of guest golecules in gmphiphilic lipid carriers. PhD thesis, Technische Universität Berlin, Fakultät III, 2010.

[19] R. P. Feynman. Space-time approach to non-relativistic quantum mechanics. *Rev. Mod. Phys.*, 20:367–387, Apr 1948.

[20] W. C. K Poon and D. Andelman. *Soft Condensed Matter Physics in Molecular and Cell Biology*. Taylor and Francis Group, New York , London, 2006.

[21] S. F. Edwards. The statistical mechanics of polymers with excluded volume. *Proc. Phys. Soc.*, 85(4):613, 1965.

[22] R. T. Deam and S. F. Edwards. The theory of rubber elasticity. *Philo. Trans. Roy. Soc. London Ser. A*, 280(1296):317–353, 1976.

[23] Y. Yuliand, Q. Feng and Z. Hongdong. Applications of self-consistent field theory in polymer systems. *Sci. China: Serie B Chem.*, 49(1):21–43, 2006.

[24] R. C. Ball and M. Doi and S. F. Edwards and M. Warner. Elasticity of entangled networks. *Polymer*, 22(8):1010 – 1018, 1981.

[25] S. F. Edwards and K. F. Freed. Cross linkage problems of polymers i. the method of second quantization applied to the cross linkage problem of polymers. *J. Phys. C: Solid State Physics*, 3(4):739, 1970.

[26] H. Nishimori. *Statistical Physics of Spin Glasses and Information Processing An Introduction*. Number 111. International Series of Monographs on Physics, Oxford University Press, 2001.

[27] C. De Dominicis and I. Giardina. *Random fields and spin glasses. A field theory approach*. Cambridge University Press, 2006.

[28] W. L. Vandoolaeghe and K. K. Müller-Nedebock. Polymer networks between two parallel planar surfaces. *J. Phys. A: Math. Gen.*, 36:8249–8264, 2003.

[29] R. Shlomovitz and N. S. Gov. Physical model of contractile ring initiation in dividing cells. *Biophysical J.*, 94:1155–1168, 2008.

[30] D. Marcland and J. V. Landau. The mechanism of cytokinesis: temperature-pressure studies on the cortical gel system in various marine eggs. *J. Exp. Zool.*, 125(3):507–539, 1954.

[31] A. L. Miller. The contractile ring. *National Institutes of Health*, 21(24), 2011.

[32] M. Takaine , O. Numata and K. Nakano. Anactin-myosin iii interaction is involved in maintaining the contractile ring in fission yeast. *Journal of Cell Science*, 128:2903–2918, 2015.

[33] T. D. Pollard. Progress towards understanding the mecchanism of cytokinesis in fission yeast. *Biochemical Soc.*, 36:425–430, 2008.

[34] A. Zemel and A. Mogilner. Motor-induced sliding of microtubule and actin bundles. *Phys. Chem.*, 11:4821–4833, 2009.

[35] K. Kruse and F. Jülicher. Actively contracting bundles of polar filaments. *Phys. Rev. Lett.*, 85:1778–1781, 2000.

[36] T. B. Liverpool. Anomalous fluctuations of active polar filaments. *Phys. Rev. E*, 67:031909, 2003.

[37] D. Biron, E. Alvarez-Lacalle, T. Tlusty and E. Moses. Molecular model of contractile ring. *Phys Rev Lett.*, 95(9):098102, 2005.

[38] T. E. Schroeder. The contractile ring. II. Determing its brief existence, Volumetric Changes, and Vital Role in Cleaving *Arbacia* Eggs. *J. Cell Biology*, 53:419–434, 1972.

[39] J. C. Canman and W. A. Wells. Rappaport Furrows on Our Minds: The ASCB Cytokinesis Meeting Burlington. *The Journal of Cell Biology*, 166:22–25, 2004.

[40] T. Kamasaki,M. Osumi and I. Mabuchi. Three-dimensional arrangement of f-actin in the contractile ring of fission yeast. *J. Cell Biology*, 178:765–771, 2013.

[41] M. Lenz. Geometrical origins of contractility in disordered actomyosin networks. *Phys. Rev. X*, 4:041002, 2014.

[42] I. Mendes Pinto, B. Rubinstein and R. Li. Force to divide: Structural and mechanical requirements for actomyosin ring contraction. *Biophysical J.*, 105(3):547–554, 2013.

[43] A. Zumdieck, K. Kruse, H. Bringmann, A. A. Hyman and F. Jülicher. Stress generation and filament turnover during actin ring constriction. *PloS*, 2, 2007.

[44] M. Lenz, T. Thoresen, M. L. Gardel and A. R. Dinner. Contractile units in disordered actomyosin bundles arise from f-actin buckling. *Phys. Rev. Lett.*, 108:238107, 2012.

[45] K. Kruse and F. Jülicher. Self organisation and mechanical properties of active filament bundles. *Phys. Rev. E*, 67:051913, 2003.

[46] M. Schliwa and G. Woehlke. Molecular motors. *Nature*, 522:59–769, 2003.

[47] E. M. Craig, S. Dey and A. Mogilner. The emergence of sarcomeric, graded-polarity and spindle-like patterns in bundles of short cytoskeletal polymers and two opposite molecular motors. *J. Phys.:Cond. Matt.*, 23:374102, 2011.

[48] K. Kruse, A. Zumdieck and F. Jülicher. Continum theory of contractile fibres. *Europhys. Lett.*, 64(5):716–722, 2003.

[49] H. E. Huxley. Fifty years of muscle and the sliding filament hypothesis. *Eur. J. Biochem.*, 271:1403–1415, 2004.

[50] X. Xing, B.S. Lu, F. Ye, and P. M. Goldbart. Generalized Deam-Edwards Approach to the Statistical Mechanics of Randomly Crosslinked Systems. *Phys. Rev. Lett.*, 1, 2013.

[51] S. F. Edwards. A field theoretic formalism for the entanglements of a polymer network. *Computational and Theoretical Polymer Science*, 8:247 – 252, 1998.

[52] I. K. Piechocka, K. A. Jansen, C. P. Broedersz, F. C. MacKintosh and G. H. Koenderink. Semiflexible bundle model explains the elasticity of fibrin networks. *https://arxiv.org/abs/1206.3894*, 2, 2012.

[53] C. De Dominicis and L. Peliti . Field-theory renormalization and critical dynamics above T_c: Helium, antiferromagnets, and liquid-gas systems. *Phys. Rev. B*, 18:353–376, 1978.

[54] F. Boue, S. F. Edwards and T. A. Vilgis. The entropy of a network of rod molecules. *J. Phys. France*, 49:1635–1645, 1988.

[55] S. F. Edwards and T. A. Vilgis. The tube model theory of rubber elasticity. *Rep. Prog. Phys.*, 51:243–297, 1988.

[56] P. Benetatos and S. Ulrich and A. Zippelius. Force-extension relation of cross-linked anisotropic polymer networks. *New J. Phys.*, 14(11):115011, 2012.

[57] M. Mezard, G. Parisi and M. A. Virasoro. *Spin glass theory and beyond*, volume 9. World Scientific Publishing, Singapore, New Jersey, Hong Kong, 1987.

[58] G. Migliorini, V. G. Rostiashvili and T. A. Vilgis. Polymer chain in quenched random medium slow dynamics and ergodicity breaking. *E. Phys. J. B.*, 33:61–73, 2003.

[59] M. Mateyisi. Polymer networks with mobile force-applying crosslinks. Master's thesis, Stellenbosch University, 2011.

[60] K. Möller. Dynamics of an active crosslinker on a chain and aspects of the dynamics of polymer networks. Master's thesis, Stellenbosch University, 2011.

[61] M. Mateyisi. *Particle diffusion in elastically coupled narrow parallel channels*. PhD thesis, Stellenbosch University, 2014.

[62] A. Zumdieck. *Dynamics of Active Filament Systems*. Phd thesis, Max-Planck-Institut für Physik Komplexer Systeme, 2005.

[63] R. V. Jensen. Functional intergral approach to classical statistical dynamics. *J. Stat. Phys.*, 25(2):183–210, 1981.

[64] M. Castelnovo and F. Joanny. Complexation between oppositely charged polyelectrolytes: Beyond the random phase approximation. *Eur. Phys. J. E*, 6:377–386, 2001.

[65] T. A. Vilgis and R. Borsali. Screening of interactions in homopolymer blends and diblock copolymer systems. *A. Chem. Soc.*, 23:3172–3178, 1990.

[66] M. P. Allen. Introduction to Molecular Dynamics Simulation, volume 23. John von Neumann-Institut für Computing (NIC), Jülich, 2004.

[67] M. P. Allen and D. T. Tildesley. Computer simulation of liquids. Oxford University Press, New York, 1989.

[68] N. Goga, A. J. Rzepiela, A. H. de Vries, S. J. Marrink, and H. J. C. Berendsen. Efficient algorithms for langevin and dpd dynamics. *J. Chem. Theory Comput.*, 8:3637–3649, 2012.

[69] N. Grønbech-Jensen, and O. Farago. A simple and effective verlet-type algorithm for simulating langevin dynamics. *Mol. Phys.*, 111:983, 2013.

[70] D. Frenkel and B. Smit. Understanding molecular simulation from theory to applications. Academic Press, California, 1996.